University of Sussex

Inflationary model constraints using higher-order statistics of the primordial curvature perturbation

Gemma Jayne Anderson

Submitted for the degree of Doctor of Philosophy

University of Sussex

April 2014

Declaration

I hereby declare that this thesis has not been and will not be submitted in whole or in part to another University for the award of any other degree.

The work in this thesis has been completed in collaboration with David Seery, Donough Regan and David Mulryne, and is compromised of the following papers:

- Gemma J. Anderson, Donough Regan & David Seery. 'Optimal bispectrum constraints on single-field models of inflation'. In: (2014). arXiv:1403.3403 [astro-ph.CO].
- Gemma J. Anderson, David J. Mulryne & David Seery. 'Transport equations for the inflationary trispectrum'. In: JCAP (2012) (10). p. 019. arXiv:1205.0024 [astro-ph.CO].

I have made a major contribution to all the original research presented in this thesis.

Signature:

Gemma Jayne Anderson

UNIVERSITY OF SUSSEX

GEMMA JAYNE ANDERSON, DOCTOR OF PHILOSOPHY

INFLATIONARY MODEL CONSTRAINTS USING HIGHER-ORDER STATISTICS OF THE PRIMORDIAL CURVATURE PERTURBATION

ABSTRACT

Cosmological inflation is the leading candidate for the origin of structure in the Universe. However, a huge number of inflationary models currently exist. Higher-order statistics, particularly the bispectrum and trispectrum, of the primordial curvature perturbation ζ can potentially be used to discriminate between competing models. This can provide an insight into the precise physical mechanism of inflation.

Current constraints on inflationary models using the amplitude $f_{\rm NL}$ of the *bispectrum* are quoted for specific *templates*. This results in much of the inflationary parameter space remaining unexplored. By utilizing the symmetries of the underlying quasi-de Sitter spacetime to construct a generic 'effective field theory' Lagrangian with adjustable parameters, one can encompass many *single-field* models of inflation in a unifying framework. In the first part of this thesis we perform a partial-wave decomposition of the bispectrum produced at horizon-exit by each operator in the effective Lagrangian, which we use to find the principal components using a Fisher-matrix approach. This allows us to probe much more of the parameter space. Cosmic Microwave Background bispectrum data is used to estimate the amplitude of each component, which can then translated into constraints on particular classes of single-field models. We consider the implications for DBI and ghost inflation as examples.

In the second part of this thesis we extend the transport formalism, first introduced by Mulryne, Seery and Wesley, to calculate the *trispectrum* generated during superhorizon evolution in inflationary models with *multiple fields*. We provide transport equations that track the evolution of the local trispectrum non-linearity parameters $\tau_{\rm NL}$ and $g_{\rm NL}$ throughout inflation. We compute these for several models as examples.

Acknowledgements

My first and foremost thanks go to my supervisor David Seery. I am privileged to have had such a fantastic mentor. He is a source of great understanding and infinite patience. I'd also like to thank my second supervisor Andrew Liddle, whose positive attitude to cosmology and life is truly inspiring.

The work presented in this thesis would not have been possible without my collaborators Donough Regan and David Mulryne, who were an absolute pleasure to work with. I am extremely grateful for the guidance and support they have given me.

The support I have received throughout my career has been invaluable. Particular thanks goes to my masters supervisor John McDonald, my undergraduate director of studies Gareth Hughes and Laura Kormos and my director of studies at Cambridge, Anthony Challinor.

I would also like to thank my colleagues past and present for making my Sussex experience so wonderful. Particularly Jonathan Frazer, Mafalda Dias, Vanessa Smer, Luca Porcelli, Sheng Li, Chris Byrnes, Will Watson, Antony Lewis and Antonio Vasquez.

My friends Lyn Forsyth, Julian Gibbons, Javi Garcia Laguna, Patrick Levy, Maxine Sherman, Leon Baruah, Sam Young, Ruth Pearson and Amy Campbell have been an immense source of fun, inspiration and encouragement throughout my PhD. I also have a great deal of gratitude for the help from my family, especially my mother Jane who has always believed in me every step of the way. I have been extremely lucky to have been surrounded by so much love.

I am so grateful to have been given the opportunity to study a subject I love and in such a wonderful environment. I will forever cherish the knowledge and experiences I have gained.

Contents

List of Figures

Introduction

0.1 Prelude

We are living in a very exciting time, where it is possible to probe the very beginnings of our Universe using sophisticated satellites and telescopes. The theory of inflation not only manages to iron out the creases in the Standard Model of cosmology, but also offers a simple mechanism to create the seeds of the stars and galaxies and is thought to be the source of the temperature fluctuations in the *Cosmic Microwave Background* (CMB) radiation. Very importantly, inflation makes some predictions that we are able to put to the test.

But the story doesn't end there. Inflation is a stage in which the play and actors are unknown; there are many different models of inflation, each with their own unique particles and interactions. A tremendous theoretical and observational effort is underway to understand the precise details of inflation by using even more intricate predictions to constrain these models. Not only will this help shed more light on the early Universe, but it will also give us a greater insight into particle physics at extremely high energies.

Inflationary models can be constrained using the statistics of the curvature perturbation ζ. The predictions from the various inflationary models for the statistics of this observable are met with precision measurements of the temperature and polarization of the CMB. By doing so, we aim to understand the physical mechanisms that drove inflation.

In recent years, a great deal of attention has been focussed on using the higher-order statistics of ζ to constrain the possible range of inflationary models, particularly the *bispectrum* and *trispectrum*. A reason for this is that the *power spectrum*, measuring two-point correlations of ζ, is not sufficient to discriminate between the models.

One day we hope we will be able to pinpoint a single model for the origin of structure that exactly describes our Universe. That goal is still a long way off, but in the last 20 years we have made significant progress and so there is certainly reason to be hopeful for the future.

"Each piece, or part, of the whole of nature is always merely an approximation to the complete truth, or the complete truth so far as we know it. In fact, everything we know is only some kind of approximation, because we know that we do not know all the laws as yet. Therefore, things must be learned only to be unlearned again or, more likely, to be corrected . . . The test of all knowledge is experiment. Experiment is the sole judge of scientific 'truth'." *–Richard Feynman.*

0.2 HOT BIG BANG COSMOLOGY

The Hot Big Bang (HBB) model has been so successful in describing the evolution of our Universe that it is now firmly established as the Standard Model of cosmology. Its foundations are based on the premise that the density of the Universe is homogenous and isotropic with respect to the largest scales, simply a restatement of the Cosmological Principle: that there are no preferred locations or directions in the Universe. The HBB model posits that our Universe has expanded and consequently cooled from an extremely hot, dense initial state. Underpinning this model is substantial observational evidence. The first piece of compelling evidence came to light when Slipher (1913) provided observational proof that the Universe was expanding, confirming that the Universe must have been hotter and denser in the past.[1] Objects are redshifting away from us at a rate of $\mathbf{v} = H\mathbf{r}$, where $\mathbf{v}$ is the recessional velocity, H is the Hubble parameter and $\mathbf{r}$ is the physical distance to the object. Recent measurements from the *Planck* satellite have constrained the age of the Universe to be 13.82 Gyr (Ade et al. 2013a).

The HBB model also provides a mechanism to explain the formation of light elements in the Universe, a period known as 'Big Bang Nucleosynthesis (BBN)' (Schramm and Turner 1998; Pagel and Tautvaisiene 1995). From an understanding of nuclear physics a Universe that was hot and dense at early times would have facilitated the formation of Helium and Deuterium among several other elements, but in smaller quantities. As well as providing an explanation for how the light elements were produced, it also predicts their observed abundances to a very high precision,

[1]The discovery of the redshifting of galaxies is often incorrectly attributed to Hubble. More information can be found on this page by John Peacock: http://www.roe.ac.uk/ jap/slipher/.

thereby supplying even further evidence in favour of the model. [2] The epoch of BBN is thought to have occurred during the first few minutes after the Big Bang, when the temperature of the Universe cooled sufficiently for protons and neutrons to bind into atoms.

Arguably the most successful prediction of the HBB model was the existence of 'relic radiation' (the 'afterglow' of the Big Bang) permeating the Universe with a black body spectrum, a result of photons decoupling from electrons 380,000 years after the Big Bang during an epoch known as *recombination*. This *Cosmic Microwave Background* (CMB) radiation was first discovered by Penzias and Wilson (1965) and has since been under intense study. By 1990, with the data from the NASA satellite mission COBE (Fixsen et al. 1996), it was clear that a Universe consistent with a Hot Big Bang could have produced it. The most recent measurement of its mean temperature is $T_0 = 2.7255 \pm 0.0006$ (Aghanim et al. 2013), showing impressive uniformity to one part in 10^5. The CMB has been shown to be isotropic, but assuming that we do not occupy a special vantage point in the Universe then homogeneity can also be implied. Studying the statistical properties of its temperature provides us with a wealth of data on the very early Universe. Combining this with our understanding of high-energy particle physics gives us the unique possibility to probe as far back as the very first few moments of the Universe, corresponding to huge energy scales unattainable in terrestrial experiments.

Observations of the large scale structure in our Universe from galaxy surveys show that the Universe is consistent with homogeneity and isotropy on large scales (Colless et al. 2001). These observations have instilled confidence in the HBB model and as a result, we can use it as an arena in which to conduct precision cosmology. The following section introduces the tools that are needed in subsequent chapters.

Units.—The speed of light and Planck's constant is set to unity throughout this thesis, $c = \hbar = 1$. The reduced Planck mass is defined as $M_{\rm P} = (8\pi G)^{-1/2}$, where G is Newton's constant. We adopt the metric signature $(-,+,+,+)$. Greek letters $\{\alpha, \beta, \gamma, \dots\}$ are chosen to denote spacetime indices, whereas lowercase Roman indices $\{i, j, k, \dots\}$ are used to denote solely spatial indices. An overdot denotes a derivative with respect to proper time, e.g. $\dot{a} \equiv \mathrm{d}a/\mathrm{d}t$ and a prime denotes a derivative with respect to conformal time (defined by (18)), e.g. $a' \equiv \mathrm{d}a/\mathrm{d}\eta$. In some cases we denote a partial derivative with a comma $\partial X/\partial x^\mu = \partial_\mu X = X_{,\mu}$ and a covariant derivative with a semi-colon $\nabla X_\mu = X_{;\mu}$. They are related via

$$X^\mu_{;\nu} = X^\mu_{,\nu} + \Gamma^\mu_{\nu\rho} X^\rho \tag{1}$$

[2] The first success of the Hot Big Bang model was the striking agreement between the BBN prediction for the primordial Helium abundance and observations (Burles, Nollett and Turner 2001).

where $\Gamma^{\mu}_{\nu\rho}$ is the *Christoffel symbol*, which can be defined in terms of $g_{\mu\nu}$, the metric, as

$$\Gamma^{\mu}_{\nu\rho} = \frac{1}{2} g^{\mu\sigma} (\partial_\rho g_{\nu\sigma} + \partial_\nu g_{\rho\sigma} - \partial_\sigma g_{\nu\rho}) \tag{2}$$

FLRW metric.—The background evolution of the Universe is given by the maximally-symmetric Friedmann-Lemaître-Robertson-Walker (FLRW) metric, which has the appropriate form to describe a Universe that is homogeneous and isotropic on spatial 3D hypersurfaces of constant proper time t (Weinberg 1972)

$$\mathrm{d}s^2 = -\mathrm{d}t^2 + a(t)^2 \left(\frac{\mathrm{d}r^2}{1 - Kr^2} + r^2(\mathrm{d}\theta^2 + \sin^2\theta \mathrm{d}\varphi^2) \right) \tag{3}$$

where r, θ, φ are polar co-ordinates and K is a parameter that characterizes the spatial curvature. It has the values $\{+1, 0, -1\}$ for an open, flat or closed Universe respectively. All of the time dependence is encoded in the scale factor $a(t)$, a function that increases with time due to the expansion of the Universe, which we normalize to be one at the present epoch $a(t_0) = 1$, where $t = t_0$ corresponds to the present day. The scale factor relates physical distance $\mathrm{d}\mathbf{r}$ and *comoving* (i.e. moving with the expansion) distance $\mathrm{d}\mathbf{x}$ via $\mathrm{d}\mathbf{r} = a\mathrm{d}\mathbf{x}$.

The Riemann (curvature) tensor is defined as

$$R^{\mu}{}_{\nu\beta\alpha} \equiv \partial_\alpha \Gamma^{\mu}_{\nu\beta} - \partial_\beta \Gamma^{\mu}_{\nu\alpha} + \Gamma^{\mu}_{\sigma\alpha}\Gamma^{\sigma}_{\nu\beta} - \Gamma^{\mu}_{\sigma\beta}\Gamma^{\sigma}_{\nu\alpha}. \tag{4}$$

The dynamics of gravity in the Universe is described by the Einstein-Hilbert action

$$S_{\mathrm{EH}} = \int \mathrm{d}^4x\sqrt{-g} \left(\frac{1}{2} M_{\mathrm{P}}^2 R - \Lambda \right), \tag{5}$$

where the quantity in the first square root is the determinant of the metric, $g = \det(g_{\mu\nu})$, R is the Ricci scalar, the contraction of the Ricci tensor $R_{\mu\nu}$ and Λ is called the *cosmological constant*. The Ricci tensor is itself the contraction of the Riemann curvature tensor $R_{\mu\nu} = R^{\rho}_{\mu\rho\nu}$. Including matter, described by the action $S_M = \int \mathrm{d}^4x\sqrt{-g}\mathcal{L}_M$, the full spacetime action is given by

$$S = S_{\mathrm{EH}} + S_M = \int \mathrm{d}^4x\sqrt{-g} \left(\frac{1}{2} M_{\mathrm{P}}^2 R - \Lambda + \mathcal{L}_M \right). \tag{6}$$

Einstein's field equations are derived by varying (6) with respect to the spacetime metric $g_{\mu\nu}$, yielding

$$G_{\mu\nu} \equiv R_{\mu\nu} - \frac{1}{2} g_{\mu\nu} R = \frac{1}{M_{\mathrm{P}}^2} \left(T_{\mu\nu} + \Lambda g_{\mu\nu} \right), \tag{7}$$

where $G_{\mu\nu}$ is the Einstein tensor. The energy–momentum (EM) tensor (also known as the stress-energy tensor) defined by

$$T_{\mu\nu} \equiv -2 \frac{\partial \mathcal{L}_M}{\partial g^{\mu\nu}} + g_{\mu\nu}\mathcal{L}_M, \tag{8}$$

characterizes the matter content of the Universe. The homogenous and isotropic components of the FLRW Universe can be described by a perfect fluid[3] with an EM tensor in a generic inertial

[3] A perfect fluid defines one that is isotropic in its local rest frame so that $T^{0\mathrm{i}} = 0$.

frame satisfying

$$T^{\mu\nu} = (\rho + p)U^\mu U^\nu - p g_{\mu\nu} \tag{9}$$

where ρ denotes energy density, p is the pressure and $U^\mu(\mathbf{x},t)$ is the fluid 4-velocity describing the fluid flow. The EM tensor satisfies conservation of energy

$$T^\mu_{\nu;\mu} = 0. \tag{10}$$

The first diagonal component of this equation is known as the continuity (or fluid) equation

$$\frac{\mathrm{d}\rho}{\mathrm{d}t} + 3H(1+\omega)\rho = 0, \tag{11}$$

where the equation of state is given by $\omega = p/\rho$. Integrating the continuity equation, assuming ω is constant,[4] gives

$$\rho \propto a(t)^{-3(1+\omega)}, \tag{12}$$

therefore we see that non-relativistic matter ($\omega_\mathrm{m} = 0$), which includes baryons and cold dark matter (CDM), dilutes with the expansion as the volume scale $\rho_\mathrm{m} \propto a(t)^{-3}$. The equation of state for radiation (photons and neutrinos) is $\omega_\mathrm{rad} = 1/3$ implying the energy density of radiation redshifts as $\rho_\mathrm{rad} \propto a(t)^{-4}$. A pure cosmological constant (vacuum energy), $\omega_\Lambda = -1$ results in the energy density remaining constant. Solving for the time-time component of the Einstein equations gives the Friedmann equation, essentially an evolution equation for the scale factor

$$H^2 = \frac{\rho}{3M_\mathrm{P}^2} - \frac{K}{a^2} + \frac{\Lambda}{3}, \tag{13}$$

where the Hubble parameter $H \equiv \dot{a}/a$ is the expansion rate. The present value H_0 is measured to be $H_0 = (67.4 \pm 1.4)\mathrm{km\,s^{-1}Mpc^{-1}}$ (68%; *Planck*). Integrating (13) for matter, radiation and vacuum energy domination respectively gives the solutions $a_\mathrm{m}(t) \propto t^{2/3}$, $a_\mathrm{rad}(t) \propto t^{1/2}$ and $a_\Lambda \propto \exp(Ht)$. Combining the Friedmann equation with the continuity equation results in the second Friedmann (acceleration) equation

$$\frac{\ddot{a}}{a} = -\frac{\rho}{6M_\mathrm{P}^2}(1+3\omega) + \frac{\Lambda}{3}. \tag{14}$$

We can recast the Friedmann equation in terms of a *density parameter* Ω that is a ratio of the total energy density to the critical density,

$$\Omega - 1 \equiv \frac{\rho}{3M_\mathrm{P}^2H^2} - 1 = \frac{K}{a^2H^2} \equiv \frac{\rho}{\rho_\mathrm{crit}} - 1 \tag{15}$$

where the critical density $\rho_\mathrm{crit} = 3M_\mathrm{P}^2H^2$. We can also write it as

$$\Omega(t) + \Omega_K(t) = \Omega_\mathrm{m}(t) + \Omega_\mathrm{rad}(t) + \Omega_\Lambda(t) = 1, \tag{16}$$

[4] In general, the equation of state is a time-dependent parameter.

where $\Omega_K(t) \equiv -K/(a^2H^2)$ is the curvature density parameter and $\Omega_\Lambda(t) \equiv \frac{\Lambda}{3H^2}$. For all other types of matter $\Omega_i \equiv \rho_i/\rho_{\rm crit}$. In a flat Universe, where $K = 0$, the density is given by $\rho = \rho_{\rm crit}$ and $\Omega = 1$.

The cosmological redshift z of a given epoch is defined as

$$\frac{\lambda_{\rm obs}}{\lambda_{\rm emit}} \equiv 1 + z = \frac{a(t_0)}{a(t_{\rm emit})}, \tag{17}$$

where $\lambda_{\rm emit}$ is the wavelength of light that was emitted at $t_{\rm emit}$ and $\lambda_{\rm obs}$ is the wavelength we observe the light to have now. The wavelength of light stretches with the cosmological expansion so typically $\lambda_{\rm obs} > \lambda_{\rm emit}$. Using $\mathrm{d}\mathbf{r} = a\mathrm{d}\boldsymbol{\eta}$ we can define the *comoving (particle) horizon* η as the maximum distance light could have travelled since the beginning of the Universe [5]

$$\eta \equiv \int_0^a \frac{\mathrm{d}a}{a^2H} = \int_0^t \frac{dt'}{a(t')} \tag{18}$$

where η is also often referred to as conformal time $\mathrm{d}\eta \equiv \mathrm{d}t/a$.[6]

The *number of e-foldings* N, as in the number of times the Universe expands by a factor of e, between a scale factor a_1 at t_1 and a_2 at t_2 is defined as

$$N \equiv \ln\frac{a_2}{a_1} = \int_{t_1}^{t_2} H\,\mathrm{d}t \tag{19}$$

Scales and horizons.—A physical length scale λ can be written in terms of its wavenumber k, as $\lambda = 2\pi a/k$, where k^{-1} is a comoving scale or "mode". The Hubble radius, H^{-1}, defines the boundary of causal processes because it is an estimate of how far light can travel in a Hubble time. [7] For this reason, we will use the term horizon and Hubble radius interchangeably to mean H^{-1}. [8] The region inside our horizon is often referred to as the "observable" Universe, which is part of a much larger "unobservable" Universe that we are currently unable to communicate with yet. Comoving scales that are inside the horizon are referred to as *subhorizon*, $k > aH$ and are in causal contact. Those modes that are outside the horizon are referred to as *superhorizon*, $k < aH$. "Horizon crossing" is the point when a particular comoving scale passes outside the horizon, which occurs at $k = aH$.

Despite its successes, the Hot Big Bang model leaves several important outstanding questions. We discuss these in the next section, as well as introducing a speculative, but generally well-accepted extension to the model that attempts to answer them.

[5] We have taken the beginning of the Universe to be $a = 0$. However, in practice our understanding of energy scales above the Planck mass breaks down– corresponding to energy scales above $1.2209 \times 10^{19}\mathrm{GeV}/c^2$.

[6] This coordinate is useful as it is comoving with the expansion.

[7] It can either be a distance or a time since we are using units where $c = 1$.

[8] This horizon should not be confused with the *particle horizon* (18).

0.3 Introduction to cosmological inflation

The theory of cosmological inflation, a period of quasi-exponential expansion in the very early Universe, was originally conceived by Guth (1981) as a means to resolve various puzzles regarding initial conditions that cannot be explained by the HBB model alone. A number of other authors were also working on the idea around the same time, including Brout, Englert and Gunzig (1978); Starobinsky (1980); Kazanas (1980); Sato (1981); Linde (1982); Linde (1983); Albrecht and Steinhardt (1982). This section will outline the motivations for inflation and give a brief overview of the simplest slow-roll model.

0.3.1 Motivations for inflation

Our Universe is observed to be flat, [9] corresponding to $K = 0$. From (15) this corresponds to a density parameter of $\Omega = 1$ today. However, the comoving Hubble radius $(aH)^{-1}$ increases as the Universe evolves throughout matter and radiation dominated eras, i.e. our horizon grows with time under the gravitational influence of matter satisfying the strong energy condition. Since Ω is so close to one today, (15) implies that it must have been extremely close to one at earlier times, because the $\frac{K}{(aH)^2}$ term will always serve to drive it away from one as the Universe evolves throughout the radiation and matter dominated epochs. Using the Friedmann equation (13) and (12) we can see that

$$\Omega(t) - 1 \propto Ka^{1+3\omega} \tag{20}$$

This raises several related issues that puzzled cosmologists, broadly known as the *flatness problem*. Why is the Universe so flat? Why is it flat at all? The Hot Big Bang model is unable to provide answers to these questions.

A second problem with the HBB model is known as the *horizon problem*. Two photons separated by more than the comoving horizon size, given by (18), at decoupling, which corresponds to an angular separation of about 2° on the current CMB sky if we assume the Universe has only been radiation and matter dominated previously, could *never* have been causally connected before that time. Therefore they could not have equilibrated to the same temperature before they were scattered at decoupling. Yet measurements from CMB experiments, such as the latest *Planck* mission (Aghanim et al. 2013), revealed that the entire Universe is the same temperature to an

[9] $100\Omega_K = -0.10^{+0.62}_{-0.65}$ 95% C.L. (*Planck*+lensing+WP+highL+BAO) (Ade et al. 2013b)

exceptional accuracy, with an almost perfect black body spectrum. How could two photons that have never been able to exchange thermal information have the same temperature?

There is also the problem of "missing" relic particles. These particles, which include magnetic monopoles ('t Hooft 1974), cosmic strings, topological defects, gravitinos and many others, are not detected in the Universe but are predicted by many particle physics theories, so where are they?

The temperature of the CMB is very homogeneous and isotropic, but with variations of $\mathrm{O}(10^{-5})$ from the average. These "fluctuations" are thought to be sourced from tiny perturbations in the underlying energy density of the very early Universe. Also, looking at the matter in the Universe today on the very largest scales we see that it is also very uniform, but with inhomogeneities on the (relatively) smaller scales of stars, galaxies and clusters. The same primordial perturbations that seeded the temperature fluctuations in the CMB are also believed to grow via gravitational instability into the large scale structure we see in the Universe today and their origin cannot be explained using the standard HBB model alone. Clearly, finding a theory capable of producing these cosmological density perturbations is of fundamental importance to our understanding of the Universe.

None of the aforementioned problems invalidate the HBB model and all of them can be simply included in the model as fine-tuned initial conditions. However, from a physics perspective this is unsatisfactory. The key issue is *why* do we have a Universe that is flat, devoid of relic particles and smooth on large scales with small-scale inhomogeneities? We require a dynamical mechanism capable of generating these initial conditions for the subsequent Big Bang evolution.

0.3.2 REQUIREMENTS FOR INFLATION

As Guth discovered, all of the above Big Bang issues can be elegantly resolved by inflation. It is defined simply as a brief period in the very early Universe preceding the epochs of radiation and matter domination, where the scale factor was accelerating, $\ddot{a} > 0$, causing exponential expansion. This would result in an approximately constant Hubble rate, $H \approx$ constant, and the comoving Hubble radius $(aH)^{-1}$ decreasing in time, unlike all other periods in the Universe's history where it always increases with time.

$$\ddot{a} > 0 \implies \frac{\mathrm{d}}{\mathrm{d}t}\left(\frac{1}{aH}\right) < 0 \tag{21}$$

Normal matter obeys the *strong energy condition*, which states that $\rho + 3p > 0$. From (14) it is clear that the behaviour of normal matter can only cause the scale factor to decelerate, therefore

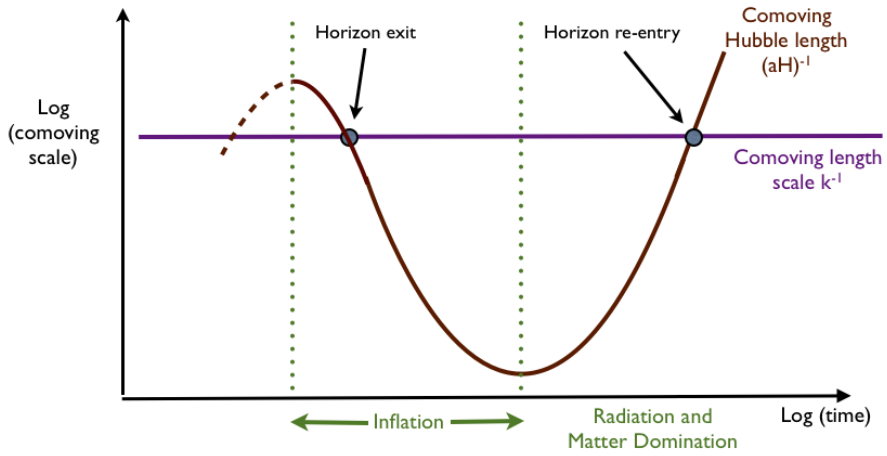

Figure 1: Behaviour of comoving scales throughout the evolution of the Universe

the substance responsible for inflation needs to have very different behaviour to ordinary matter, i.e. a fluid that violates the strong energy condition.

$$\ddot{a} > 0 \implies \rho + 3p < 0 \tag{22}$$

Assuming that density is always positive $\rho > 0$, then it is a fluid with negative pressure that is required to dominate the energy density in order to generate accelerated expansion.

By inspection of (15), one can see that an inflationary epoch can resolve the flatness problem since $\ddot{a} > 0$ and the consequent behaviour of the comoving Hubble radius will drive $\Omega(t)$ extremely close to one, making $|\Omega(t) - 1|$ an attractor solution. As long as inflation lasts for a sufficiently long time then $\Omega(t)$ will not deviate very far from one for the rest of history to the present day, therefore the current spatial curvature of the observable Universe will be very close to zero, consistent with what we observe.

Inflation also solves the horizon problem since it allows for a microscopically small, causally connected patch of the Universe, which was in thermal equilibrium before inflation, to expand to a size larger than the current observable Universe. So for example, some generic cosmological comoving scale k^{-1} that we observe to be entering our horizon now was at some time in the past inside the horizon, but the shrinking behaviour of the comoving horizon during inflation caused it to pass outside the horizon and is only just re-entering now. This can be seen in Figure 1. This means, as a result of inflation, that all the photons that we currently "see" in the observable Universe shared a causal past. Since they were in causal contact, they were able to share information about their temperature and reach thermal equilibrium. As a result, they are naturally all at the same temperature today, thus solving the horizon problem. So by invoking an epoch of inflation prior to the onset of radiation- and matter-dominated epochs we circumvent the need

to specify flatness, homogeneity and isotropy as initial conditions. Inflation can also solve the problem of missing particles: the abundances of these particles will be diluted to such an extent by the accelerated expansion during inflation that they would be difficult to detect in the present Universe. However, one must be careful because inflation can actually lead to the production of topological defects such as domain walls or particles as it ends in some models. This issue is discussed in Sakellariadou (2008). Therefore the inflationary model must be chosen such that it ensures that these particles or effects are not produced. Even though solving the problems with the HBB model was the reason inflation was invoked in the first place, inflation itself requires a degree of fine-tuning– avoiding the production of these particles being one of them. The problems with conditions for inflation will be discussed further in §0.3.4.

Later on we will see how inflation also offers a natural explanation for the origin of structure and the small anisotropies observed in the CMB. Now we are left with the task of finding a consistent model that will give us all of the above desired outcomes. Below we present the simplest model of inflation.

0.3.3 Scalar field inflation

Current observations suggest that the cosmological constant is very small. In the early Universe it will have negligible effect on the dynamics, so when considering inflation we will set $\Lambda = 0$. During inflation, the curvature redshifts away after a few e-foldings, therefore in the rest of this thesis we will also set $K = 0$. In order for inflation occur, the dominant component driving the energy density has to be a substance with an equation of state $\omega < -1/3$. An ideal candidate with this type of behaviour is a homogeneous scalar field $\varphi(t)$. The hypothetical scalar field responsible for inflation is dubbed the "inflaton". The inflaton could be embedded in some high energy theory, but for the purposes of considering the simplest case we can assume its presence and study its effects. There are many different "models" of inflation that can all exhibit the appropriate inflationary behaviour, but in some cases involve discernibly different physics. For example, different forms for the self-interacting potential energy $V(\varphi)$ of the scalar field correspond to different models of inflation. Therefore inflation can be thought of as a framework containing thousands of models that all satisfy the condition $\ddot{a} > 0$. Our aim later will be to use observables as a way to constrain these models in order to learn more about the dynamics of inflation. However, in the very simplest case, the Universe during the inflationary epoch is thought to be filled with a single scalar field

minimally[10] coupled to gravity in curved spacetime, leading to the action (Maldacena 2003)

$$S = \frac{1}{2}\int d^4x\sqrt{-g}[M_{\rm P}^2 R - (\nabla\varphi)^2 - 2V(\varphi)] + \frac{1}{8}\int_{\partial\mathcal{M}} \mathrm{d}^3x\,\sqrt{h}K, \tag{23}$$

where the expression in the square brackets is the Lagrangian density $\mathcal{L} = \mathcal{L}_{EH} + \mathcal{L}_M$. The first term corresponds to the Einstein-Hilbert term (5) and next two terms characterize the matter content, in this case assumed to be dominated by a scalar field. The last term is known as the Gibbons-Hawking-York boundary term, where the boundary of the spacetime manifold $\mathcal{M}$ is denoted $\partial\mathcal{M}$ and $h_{\mu\nu}$ is the induced metric on the boundary. The kinetic term $(\nabla\varphi)^2$ is known as a *canonical kinetic term*. Any deviation from this form for the kinetic term is known as *non-canonical*. The scalar field φ can be split into a homogeneous background value $\varphi_0(t)$, which is independent of position, with a small, spatially-varying perturbation $\delta\varphi(\mathbf{x},t)$, giving $\varphi(\mathbf{x},t) = \varphi_0(t) + \delta\varphi(\mathbf{x},t)$. The perturbations will be very important later on, but since $\delta\varphi(x,t) \ll 1$, the background evolution of the scalar field can be considered without it. By minimizing the action, $\delta S = 0$, with respect to the scalar field, we get the following equation of motion for the background component of the scalar field

$$\ddot{\varphi}_0 + 3H\dot{\varphi}_0 + \frac{\mathrm{d}V(\varphi_0)}{\mathrm{d}\varphi} = 0, \tag{24}$$

where the second term acts as *Hubble drag*, a friction term that acts to slow down the scalar field as a result of the expansion of the Universe. On the assumption that all other components of the Universe are negligible, the Friedmann equation can be written as

$$H^2 = \frac{1}{3M_{\rm P}^2}\left(\frac{1}{2}\dot{\varphi_0}^2 + V\right). \tag{25}$$

Differentiating this equation and using the field equation (24) we get an equation for the evolution of the Hubble parameter

$$\dot{H} = -\frac{\dot{\varphi_0}^2}{2M_{\rm P}^2}. \tag{26}$$

Using (8) and the Lagrangian density $\mathcal{L}_M = (\nabla\varphi)^2 - 2V(\varphi)$ we can write the energy–momentum tensor describing the scalar field as

$$T_{\mu\nu} = \partial_\mu\varphi\partial_\nu\varphi - g_{\mu\nu}\left(\frac{1}{2}(\nabla\varphi)^2 + V(\varphi)\right). \tag{27}$$

[10]There are models in which the inflaton field non-minimally couples to gravity. Models of this kind will lead to terms in the action of the form $\frac{\xi}{2}R\varphi^2$, where ξ is the coupling constant describing the strength of the interaction between the inflaton and gravity. For simplicity, the coupling is assumed to be small, so ξ is set to zero and we say that the field is minimally coupled.

0.3.4 Slow-roll conditions

Comparing the EM tensor for the scalar field (27) with the EM tensor for a perfect fluid (9) we see that the energy density and pressure of the scalar field can be expressed as

$$\rho_\varphi = \frac{1}{2}\dot{\varphi_0}^2 + V(\varphi), \tag{28}$$

$$p_\varphi = \frac{1}{2}\dot{\varphi_0}^2 - V(\varphi), \tag{29}$$

where $\dot{\varphi}^2/2$ is the kinetic term and $V(\varphi)$ is the potential energy. We can see from (29) that the scalar field will have negative pressure whenever the potential energy dominates over the kinetic energy

$$V(\varphi_0) \gg \frac{1}{2}\dot{\varphi}^2, \tag{30}$$

causing the inflaton to roll slowly, so that the kinetic term is not completely zero. This leads to quasi-exponential expansion, sometimes referred to as quasi-de Sitter expansion. It is important that the kinetic term is not exactly zero, which corresponds to a cosmological constant (a pure de Sitter spacetime), because inflation would never end. [11] We also require that the inflaton accelerates slowly in order for there to be enough inflation to solve the Big Bang problems

$$\left|\frac{\mathrm{d}V(\varphi_0)}{\mathrm{d}\varphi}\right| \gg |\ddot{\varphi}| \tag{31}$$

Thus the inflaton potential is required to be nearly constant throughout inflation. Under these approximations we can neglect the kinetic term in (25) and the $\ddot{\varphi}$ term in (24), leading to the following slow-roll equations

$$H^2 = \frac{1}{3M_\mathrm{P}^2}V, \tag{32}$$

$$3H\dot{\varphi}_0 = -\frac{\mathrm{d}V(\varphi_0)}{\mathrm{d}\varphi}, \tag{33}$$

which we can use to define the following *slow-roll* parameters

$$\epsilon_\mathrm{H} \equiv -\frac{\dot{H}}{H^2}, \tag{34}$$

and

$$\eta_\mathrm{H} \equiv \frac{\dot{\epsilon_\mathrm{H}}}{\epsilon_\mathrm{H} H}. \tag{35}$$

[11] In the case where the kinetic term is exactly zero, (28) implies that the equation of state is precisely $\omega = -1$ and therefore non-dynamical. We need the equation of state to be dynamical otherwise the Universe will continue to inflate forever.

The slow-roll approximation corresponds to $\epsilon_{\rm H} \ll {\rm O}(1)$ and $|\eta_{\rm H}| \ll {\rm O}(1)$. Inflation will occur for $\epsilon_{\rm H} < 1$. The above parameters are written in the *Hamilton-Jacobi formulation*.[12] We can also write down *potential slow-roll parameters*

$$\epsilon_{\rm V} = \frac{M_{\rm P}^2}{2}\left(\frac{V'}{V}\right)^2 \ll {\rm O}(1) \tag{37}$$

and

$$\eta_{\rm V} = M_{\rm P}^2\frac{V''}{V} \ll {\rm O}(1). \tag{38}$$

This form of the slow-roll conditions is helpful because the effect of the potential on inflation is made more apparent. We can see that $\epsilon_{\rm V}$ characterizes the slope of the potential and $\eta_{\rm V}$ characterizes the curvature. Therefore, if we assume that the inflaton is initially displaced from its potential minimum then inflation occurs if the potential is sufficiently flat for a sufficient amount of time in order to achieve enough observable inflation. In the slow-roll limit the slow-roll parameters in the two formalisms are related by $\epsilon_{\rm H} \to \epsilon_{\rm V}$ and $\eta_{\rm H} \to \eta_{\rm V} - \epsilon_{\rm V}$. Figure 2 depicts the behaviour of the potential during a period of slow-roll inflation. It is the vacuum energy that drives inflation and will result in all other particles diluted to negligible quantities. The simplest model of inflation satisfying the flatness conditions (37) and (38) has the potential

$$V \propto \varphi^n. \tag{39}$$

Models with a potential of this type are known as *chaotic inflation*, first proposed by Linde (1983). Satisfying these slow-roll conditions requires a certain degree of fine-tuning of initial conditions to ensure that the potential is flat enough that the scalar field is sufficiently displaced from its minima to give the required amount of inflation. More sophisticated models of inflation may be embedded in a high energy theory such as string theory, however, it still turns out that initial conditions need to be specified. So even though inflation provides a dynamical mechanism to generate the initial conditions for the Big Bang, it also requires us to specify initial conditions in order to obtain enough inflation to solve the problems.

[12] In single-field inflation we can think of the scalar field as the time variable, allowing us to write the Friedmann equation as

$$[H'(\varphi)]^2 - \frac{3}{2M_{\rm P}^2}H^2(\varphi) = -\frac{1}{2M_{\rm P}^4}V(\varphi), \tag{36}$$

which we now call the Hamilton-Jacobi equation. It enables us to consider the evolution of the scalar field in terms of the more geometric quantity $H(\varphi)$ instead of $V(\varphi)$. This is known as the Hamilton-Jacobi formulation (Lyth and Liddle 2009).

0.3.5 DURATION OF OBSERVABLE INFLATION

The amount of observable inflation can be characterized in terms of the number of e-folds between when a scale k^{-1}, corresponding to the largest structures we see, leaves the horizon and the end of inflation. Using the slow-roll approximation (32) we can write (19) as

$$N \simeq -\frac{8\pi}{M_{\rm P}^2}\int_{\varphi_{k^{-1}}}^{\varphi_{\rm end}}\frac{V}{V'}\,{\rm d}\varphi, \tag{40}$$

where $\varphi_{k^{-1}}$ is the field value when k^{-1} leaves the horizon and $\varphi_{\rm end}$ is the field value at the end of inflation. To solve both the flatness and horizon problems requires approximately $60-70$ e-foldings of *observable* inflation to be compatible with current cosmological observations. Inflation could have lasted longer than this, but $60-70$ e-foldings of inflation ensures that any residual spatial curvature or large-scale inhomogeneities will be on a scale well outside our current horizon H_0^{-1}, which is our largest relevant cosmological scale. Observable inflation is usually is taken to begin when the scale $k^{-1}\sim H_0^{-1}$ leaves the horizon during inflation.

0.3.6 REHEATING

Inflation ends when the slow-roll conditions are violated, $\epsilon_{\rm H}=1$. The scalar field will continue to roll down the potential until it reaches the minimum. Here, a process known as "reheating" occurs. The precise details of reheating vary depending on the model, but in all cases the aim is to recover the Hot Big Bang. The oscillatory behaviour in the reheating minimum causes the inflaton to redshift like matter. The coupling to other particles subsequently causes the inflaton to gradually decay into the Standard Model particles thereby transferring all of its energy to reheat the Universe.

0.4 COSMOLOGICAL PERTURBATIONS FROM INFLATION

The section above introduced a mechanism that causes the background to inflate, provided the potential stays sufficiently flat throughout, which solves the flatness, horizon and relic particles problems. However in this simplistic picture, there currently exist no perturbations. One of the main successes of inflation is its ability to provide a mechanism to generate the source perturbations from which structures originate. Later on we will see that predictions from models of

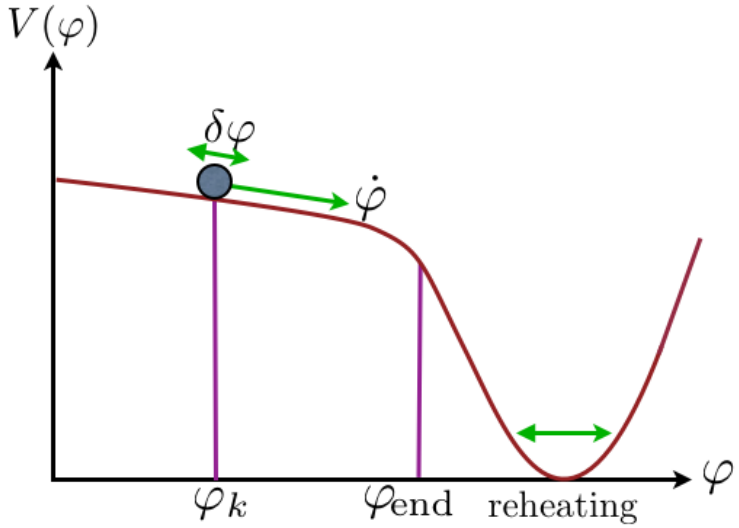

Figure 2: In single-field, slow-roll models of inflation the inflaton field φ slowly rolls down the potential with speed $\dot{\varphi}$. Observable inflation commences when scales of cosmological interest leave the horizon. However, inflation could have begun much earlier. Inflation ends when the inflaton reaches the minimum of the potential. There are small fluctuations $\delta\varphi$ about inflaton's background trajectory.

inflation can be met with precision measurements of statistical observables in the CMB. In this section we will discuss how perturbations are generated in this simplest inflationary model.

0.4.1 QUANTUM FLUCTUATIONS

One of the central points in quantum field theory is that all fundamental particles are an epiphenomenon of its associated underlying quantum field permeating the entirety of space. Quantum fluctuations correspond to a small change in energy or brief excitation of the field allowed by the uncertainty principle $\Delta E \Delta t \approx h/2\pi$. Therefore for a very brief time Δt particles with energy ΔE can pop out of the "vacuum" and will quickly disappear again so that if we averaged over a macroscopic period of time we would measure only an effect on the zero-point energy, such as in the Casimir effect. Ordinarily these transient oscillations occurring at a quantum level have no physical relevance, other than this contribution that is of the form of a cosmological constant. However, during inflation these fluctuations play a vital role in describing how the initial perturbations formed.

On a classical level inflation acts to ensure that the horizon size at the end of inflation lies well within a "smooth"[13] patch of the Universe in order to solve the problems with the Big Bang model. However, it also results in tiny quantum mechanical fluctuations $\delta\varphi$ of some particular scale k^{-1}

[13]It is smooth in the sense that it is spatially flat, in thermal equilibrium and devoid of relic particles.

in the nearly free[14] scalar field to pass outside the horizon during inflation due to the characteristic decreasing behaviour of the comoving Hubble radius.

Inside the comoving Hubble horizon $(aH)^{-1}$, the modes can oscillate. However, as inflation continues, these modes pass outside the comoving horizon. The speed at which the wavelength of the fluctuation becomes much larger than the horizon is so rapid that the fluctuation cannot propagate in order to disappear again before it is stretched out of the sphere of causality. It gets stuck with a nonzero amplitude. The modes are believed to undergo a *quantum-to-classical transition* (Lyth and Seery 2008; Lyth 1985b; Guth and Pi 1985; Polarski and Starobinsky 1996). Outside the horizon the commutator of the inflaton field φ and its conjugate momentum π goes to zero, $[\varphi,\pi] \to 0$, which is believed to be evidence for this classicalization process, allowing us to measure field correlations that have a persistent value. These modes remain superhorizon for the remainder of inflation and in the absence of other fields,[15] can no longer evolve until they are able to re-enter the horizon much later in the Universe's evolution, where their fate lies as the "primordial seeds" that then evolve under gravitational instability into the observed perturbations. It is the study of these perturbations that enables us to constrain the dynamics of inflation. The tools that particle physicists have been using for decades will enable us to make detailed predictions of inflation. The first authors that performed such calculations include Guth and Pi (1982); Bardeen, Steinhardt and Turner (1983); Sasaki (1986); Mukhanov (1985) and Lyth (1985a).

0.4.2 Perturbing the action

Now we are going to consider tiny perturbations in order to describe the small inhomogeneities that we observe. As mentioned in the previous section, we can decompose the scalar field as $\varphi(\mathbf{x},t) = \varphi_0(t) + \delta\varphi(\mathbf{x},t)$, where $\varphi_0(t)$ describes the background classical evolution of the field and $\delta\varphi(\mathbf{x},t)$ is a small perturbation. This is a fair assumption, given the very small size of the inhomogeneities observed in the CMB. In the same manner as the scalar field, we split the metric into an unperturbed and perturbed part. The unperturbed metric is just the standard FLRW metric describing a flat, homogeneous and isotropic Universe. In conformal time $\mathrm{d}t \equiv a\mathrm{d}\eta$ this can be expressed as

$$\mathrm{d}s^2 = a^2\left(-\mathrm{d}\eta^2 + \delta_{ij}\mathrm{d}x^i\mathrm{d}x^j\right) \tag{41}$$

ADM Formalism.— Due to coordinate reparametrization invariance associated with the action for

[14] A free field is non-interacting, i.e. only quadratic terms in the Lagrangian. The interaction terms, corresponding to higher-order terms in the Lagrangian are responsible for non-Gaussianity as we shall see in the next section.

[15] We will consider more complicated scenarios later.

the scalar field coupled to gravity, (23), there are other unphysical modes that can be "gauged away" by an appropriate choice of foliation and threading. Choosing a foliation corresponds to "slicing" our four-dimensional spacetime into three-dimensional hypersurfaces. The foliation and threading that proves to be most convenient in this case is a 3 + 1 decomposition of the spacetime into t = constant hypersurfaces. The threading in this case corresponds to the worldlines of possible observers (Lyth and Liddle 2009). Each hypersurface has a spatial 3-metric

$$h_{ij} \equiv a^2(t)e^{2\psi}\delta_{ij}, \tag{42}$$

where ψ is a scalar fluctuation in the metric. The proper time between slices is given by $\mathcal{N}\,\mathrm{d}t$. This is known as the Arnowitt-Deser-Misner (ADM) Hamiltonian formulation and the proper distance between coordinates (t, x^i) and $(t + \mathrm{d}t, x^i + \mathrm{d}x^i)$ on two generic hypersurfaces is given by

$$\mathrm{d}s^2 = -\mathcal{N}^2\mathrm{d}t^2 + h_{ij}(\mathrm{d}x^i + \mathcal{N}^i\mathrm{d}t)(\mathrm{d}x^j + \mathcal{N}^j\mathrm{d}t), \tag{43}$$

where $\mathcal{N}$ is the lapse function and $\mathcal{N}^i$ is the shift vector, which we can think of as Lagrange multipliers because they appear without derivatives (Arnowitt, Deser and Misner 2008a). We see in the limit that we have no perturbations, $\psi = 0$, $\mathcal{N} = 1$ and $\mathcal{N}^i = 0$, we arrive at the standard background metric (41). We can then rewrite the action (23) in the language of the ADM formalism as (Arnowitt, Deser and Misner 2008b)

$$S = \frac{1}{2}\int \sqrt{h}[\mathcal{N}R^{(3)} - 2NV + \mathcal{N}^{-1}(E_{ij}E^{ij} - E^2) + \mathcal{N}^{-1}(\dot{\varphi} - \mathcal{N}^i\partial_i\varphi)^2 - \mathcal{N}h^{ij}\partial_i\varphi\partial_j\varphi] \tag{44}$$

where $R^{(3)}$ is the Ricci scalar on the spatial hypersurfaces, $E_{ij} = \frac{1}{2}(\dot{h}_{ij} - \nabla_i\mathcal{N}_j - \nabla_j\mathcal{N}_i)$ and $E = E^i_i$. This action contains ten metric perturbations: one in $\mathcal{N}$, three in $\mathcal{N}_i$ and six in h_{ij}, and one scalar perturbation φ. However, we shall see in the next section that they are not all independent and eight can be eliminated by solving for the constraints. We will only be left with one *physical* propagating scalar degree of freedom ζ, the *curvature perturbation*. There are also two physically propagating tensor degrees of freedom that correspond to gravitational waves. They decouple from scalar perturbations at linear order so they can be ignored in this calculation. We consider tensor perturbations in §0.4.5. In principle there are also vector perturbations, but they decay rapidly in an expanding Universe in the absence of a continuous source. The scalar degree of freedom ζ is split between the scalar field perturbation $\delta\varphi$ *and* the scalar metric perturbation ψ. This is a result of the energy density being coupled to the metric via Einstein's equations, i.e. any perturbation in the density is also going to induce a perturbation (scalar gravitational "back-reaction") in the curvature of spacetime. The density and curvature are uniquely related by the gauge invariant definition (Bardeen 1980)

$$\zeta = \psi - H\frac{\delta\rho}{\dot{\rho}} \tag{45}$$

Since the scalar field φ is the dominant contribution to the energy density ρ during slow-roll inflation, this equation can be written as $\zeta = \psi - H\frac{\delta\varphi}{\dot{\varphi}}$. The curvature perturbation ζ is the true physical degree of freedom, i.e. ψ and $\delta\varphi$ don't get independent quantum fluctuations: only the combination ζ gets an independent fluctuation. It is thought that all subsequent scalar perturbations originated solely from this initial condition.[16] It therefore completely describes the vacuum fluctuations generated during inflation, which subsequently become classical perturbations after they leave the horizon. ζ enables us to track the subsequent evolution of the perturbations long after inflation ends because in single-field models it is not affected by *reheating*. When the scalar field decays, it transfers all its energy into radiation, but the gauge-invariant quantity ζ remains constant and it is *conserved* on superhorizon scales[17] (Bardeen, Steinhardt and Turner 1983; Lyth 1985b; Weinberg 2004; Lyth, Malik and Sasaki 2005; Rigopoulos and Shellard 2003).

The comoving curvature perturbation ζ is an important tool for linking theory with observation since it is possible to compare the correlation functions and other statistical observables predicted from inflation with the observed ones, using data from the *Cosmic Microwave Background*.

CONSTRAINT EQUATIONS.—Varying (44) with respect to $\mathcal{N}$ and $\mathcal{N}^i$ gives us the familiar Einstein energy and momentum constraint equations

$$\nabla_i[\mathcal{N}^{-1}(E^i_j - \delta^i_j E)] = 0 \tag{46}$$

$$R^{(3)} - 2V - \mathcal{N}^{-2}(E_{ij}E^{ij} - E^2) - \mathcal{N}^{-2}\dot{\varphi}^2 = 0 \tag{47}$$

Once we substitute these back into the action we will have successfully removed the metric perturbations associated with $\mathcal{N}$ and $\mathcal{N}_i$.[18] The constraints $\mathcal{N}$ and $\mathcal{N}_i$ will remove eight degrees of freedom in total giving us the result advertised in the last section, namely ζ is the only true physically propagating scalar degree of freedom.

[16]This is only true if the perturbations are adiabatic, i.e. the *relative* perturbation $\delta\rho_X/\dot{\rho}_X$ for all the components of the Universe is the same, where X denotes the species. An adiabatic perturbation is a perturbation in the overall energy density. Trivially this is true for single-field slow-roll inflation. However, if more than one field species was present during inflation then you can get independent perturbations in all species. In general, there can be a relative perturbation between the densities of different species, known as *isocurvature perturbations* or isocurvature modes, defined as $\mathcal{S}_{XY} \equiv 3H(\delta\rho_X/\dot{\rho}_X - \delta\rho_Y/\dot{\rho}_Y)$. Different values of $\mathcal{S}_{XY}$ label different inflationary trajectories and therefore will in general lead to different values for the final value of the curvature perturbation ζ.

[17]By the end of inflation, ζ has a coherent value over a scale of ≈ 60 Hubble volumes. Reheating is a local process and can in principle be different within each Hubble volume, therefore it would be a violation of causality for the physics within one particular Hubble volume to change the value of ζ. This implies that ζ will be conserved. We have assumed that there are no isocurvature modes present (Maldacena 2003). In the case of multiple fields, ζ will in general be time-dependent - see §0.7.2.

[18]We can do this because they are non-dynamical, i.e. they enter in the Lagrangian without derivative terms.

Choosing a Gauge.—However, we still need to fix a gauge as we still have some freedom in how we choose our foliation of spacetime, i.e. our surfaces of constant time. A gauge is simply a specification of a co-ordinate system and a gauge transformation encodes how to go from one coordinate system (gauge) to another. We can choose to either have the single scalar degree of freedom expressed in terms of the metric perturbation ψ, corresponding to spatial hypersurfaces with uniform density $\delta\rho = 0$, or in terms of a perturbation in the density $\delta\rho \neq 0$, which corresponds to *spatially-flat* hypersurfaces $\psi = 0$. In the former case, the perturbation will manifest itself as a perturbation in the intrinsic curvature $R^{(3)}$ of the spatial slices, as it is related to ψ via (Wands et al. 2000)

$$R^{(3)} = \frac{6K}{a^2} + \frac{12K}{a^2}\psi + \frac{4}{a^2}\nabla^2\psi. \tag{48}$$

It proves most physically intuitive to work in the *comoving gauge* corresponding to slices orthogonal to comoving worldlines, i.e. in the local rest frame of the observer where the momentum density T_{0i} is zero. This is physically equivalent to hypersurfaces of uniform density on superhorizon scales,[19] $\delta\rho = 0$ and 3-metric $h_{ij} = a^2(t)e^{2\zeta}\delta_{ij}$ from (45). Therefore, in the comoving gauge, $\zeta = \psi$ and so characterizes the curvature to linear order (hence its name). There are many different gauge choices, all with their own benefits. However, for the purposes of calculating observables from scalar fluctuations during inflation it suffices to consider the comoving gauge or the spatially flat gauge. Calculations in the comoving gauge can be tricky so we will sometimes find it simpler to work in the spatially flat gauge, especially when considering multiple-field models.

Second Order Action.— Choosing first the comoving gauge and by setting $\mathcal{N}_i = \partial_i\psi + \mathcal{N}_T^i$ (with $\partial_i\mathcal{N}_T^i = 0$[20]) and $\mathcal{N} = 1 + \mathcal{N}_1$ (Maldacena 2003), we can now calculate the constraints (46)-(47) to first order, resulting in (Maldacena 2003)

$$\mathcal{N}_1 = \frac{\dot\zeta}{H}, \quad \mathcal{N}_i^{(1)} = \partial_i\psi, \quad \text{where } \psi = -\frac{\zeta}{H} + a^2\frac{\dot\varphi^2}{2H^2}\partial^{-2}\dot\zeta. \tag{49}$$

Then we substitute these into (23), expand to second order, integrate by parts and use the background equation of motion, (24) to get the second order action

$$S_2 = \int \mathrm{d}t\,\mathrm{d}^3x\; ae^{\zeta}\Big[\frac{\dot\zeta}{H}\left(6H^2 - 2V - \dot\varphi^2\right) + 4\frac{\dot\varphi^2}{H^2}\left(\frac{a^3}{2}\dot\zeta^2 - \frac{a}{2}(\partial\zeta)^2\right)\Big]. \tag{50}$$

By substituting in $\zeta = -va\sqrt{2\epsilon_V}$ we arrive at the Mukhanov-Sasaki action (Mukhanov, Feldman and Brandenberger 1992)

$$S_{ms} = \frac{1}{2}\int d\eta\, d^3x\left(v'^2 - (\partial v)^2 - \frac{z''}{z}v\right), \tag{51}$$

[19]When the momentum density $T_{0i} = \dot\varphi\partial_i\varphi$ is zero it implies that $\partial_i\varphi = 0$ and so the scalar field takes a uniform value on spatial hypersurfaces. This will only be true on superhorizon scales when pressure effects no longer contribute.

[20]Here, we have decomposed $\mathcal{N}_i$ into a scalar, irrotational and vector part, divergent-free but $\mathcal{N}_i$ only has 3 degrees of freedom, so in order to write it like $\mathcal{N}_i = \partial_i\psi + \mathcal{N}_T^i$ we need this extra condition.

where $z = a\sqrt{2\epsilon_V}$.

0.4.3 Power spectrum

Now that we have the second order action, we are in a position to calculate the two-point correlator. We do this using the "in–in" formalism of quantum field theory that is discussed in more detail in Appendix 1.A. The full Hamiltonian density for this system is

$$\mathcal{H} = \pi\dot{\zeta} - \mathcal{L}, \tag{52}$$

where the canonically conjugate momentum is defined as

$$\pi = \frac{\partial \mathcal{L}}{\partial \dot{\zeta}}. \tag{53}$$

The Hamiltonian density can be split into a free part and an interacting part

$$\mathcal{H} \equiv \mathcal{H}_0 + \mathcal{H}_{\rm int} \tag{54}$$

where $\mathcal{H}_0$ is the free Hamiltonian and contains only second order terms

$$\mathcal{H}_0 = 2\epsilon_V \left[\frac{1}{2}\pi^2 + \frac{a}{2}(\partial\zeta)^2\right] \tag{55}$$

and $\mathcal{H}_{\rm int}$ involves the interaction terms. We can write $\mathcal{H}_{\rm int} = -\mathcal{L}_{\rm int}$, where $\mathcal{L}_{\rm int}$ is the Lagrangian density of the third order action, (93). Splitting the Hamiltonian in this way corresponds to the *interaction picture*. It is a hybrid of the Schrödinger picture, where states evolve in time, and the Heisenberg picture, where the operators evolve in time. The free part $\mathcal{H}_0$ describes the background which is well-understood, with $\mathcal{H}_{\rm int}$ acting as a small perturbation to the time-dependent background. It is possible to describe ζ_I, where the subscript I denotes we are now working in the interaction picture, by a superposition of harmonic oscillators[21]

$$\zeta_I(\mathbf{x},t) = \int \frac{d^3k}{(2\pi)^3}\zeta_{\mathbf{k}}(t)e^{i\mathbf{k}.\mathbf{x}} \tag{56}$$

with each harmonic oscillator, or *mode*, $\zeta_{\mathbf{k}}$ characterized by a comoving wavenumber k.

Assume that whilst the modes are far inside the horizon $k \gg aH$ and $\eta \to -\infty$, the *short-wavelength limit*, the spacetime is to a good approximation flat Minkowski. This choice of vacuum corresponds to the *Bunch-Davies vacuum* (Bunch and Davies 1978), which is annihilated by the positive frequency modes $\zeta_I^+ \mid 0\rangle = 0$. To quantize ζ_I we write

$$\zeta_I(\mathbf{x},t) = \int \frac{d^3k}{(2\pi)^3}\{a_I(\mathbf{k})u_k(t) + a_I^\dagger(-\mathbf{k})u_k^*(t)\}e^{i\mathbf{k}.\mathbf{x}} = \zeta_I^+(\mathbf{x},t) + \zeta_I^-(\mathbf{x},t), \tag{57}$$

[21]This is possible because the evolution of ζ_I is determined by $\mathcal{H}_0$ which describes a free field.

and

$$\pi_I(\mathbf{x},t) = \int \frac{d^3k}{(2\pi)^3}\{a_I(\mathbf{k})\dot{u}_k(t) + a_I^\dagger(-\mathbf{k})\dot{u}_k^*(t)\}e^{i\mathbf{k}.\mathbf{x}}, \tag{58}$$

where $a_I(\mathbf{k})$ and $a_I^\dagger(\mathbf{k})$ obey the following commutation relations

$$[a_I(\mathbf{k}), a_I(-\mathbf{k'})] = 0\,, \quad \left[a_I^\dagger(\mathbf{k}), a_I^\dagger(-\mathbf{k'})\right] = 0 \quad \left[a_I(\mathbf{k}), a_I^\dagger(-\mathbf{k'})\right] = (2\pi)^3\delta(\mathbf{k}+\mathbf{k'}). \tag{59}$$

Switching to conformal time, i.e. $\mathrm{d}\eta = 1/a\,\mathrm{d}t$, the linear order Mukhanov-Sasaki equation of motion is

$$u_k'' + \left(k^2 - \frac{z''}{z}\right)u_k = 0. \tag{60}$$

The solutions to this equation are called mode functions $u_k(\eta)$. To find the correct normalization for $u_k(\eta)$, remember the commutation relations between ζ_I and its conjugate momentum $\pi_I \equiv \partial\mathcal{H}_0/\partial\dot{\zeta} = 2\epsilon_V a^2\dot{\zeta}$ are

$$[\zeta_I(\mathbf{k},\eta), \pi_I(-\mathbf{k'},\eta)] = \frac{i}{2\epsilon_V\, a^2}\delta(\mathbf{k}+\mathbf{k'}) \tag{61}$$

where

$$\zeta_I(\mathbf{k},\eta) = a_I(\mathbf{k})u_k(\eta) + a_I^\dagger(\mathbf{k})u_k^*(\eta) \tag{62}$$

and

$$\pi_I(\mathbf{k},\eta) = \left(a_I(\mathbf{k})u_k'(\eta) + a_I^\dagger(\mathbf{k})u_k^{*\prime}(\eta)\right). \tag{63}$$

where we have transformed to conformal time and we are now working in momentum space. Therefore by computing (61), we find that the mode functions must satisfy the following *Wronskian* condition

$$2\epsilon_V\, a^2\left(u_k(\eta)u_k^{*\prime}(\eta) - u_k^*(\eta)u_k'(\eta)\right) = i. \tag{64}$$

We require oscillatory behaviour far inside the horizon when $\eta \to -\infty$. Therefore the fully normalized Bunch-Davies mode function is

$$u_k(\eta) = \frac{H}{\sqrt{4\epsilon_V k^3}}(1+ik\eta)e^{-ik\eta}. \tag{65}$$

In the limit corresponding to the Minkowski vacuum $k \gg aH$, the $\mathrm{i}k\eta$ term dominates and it can be shown that the mode function has the required oscillatory behaviour (Chen 2010)

$$u_k(\eta) = -\frac{H\eta}{\sqrt{4\epsilon_V k}}e^{-ik\eta}. \tag{66}$$

Therefore we can write the two-point correlation function of the curvature perturbation as

$$\begin{aligned}\langle 0 \mid \zeta_I(\mathbf{k}_1)\zeta_I(\mathbf{k}_2) \mid 0\rangle &\equiv \langle 0 \mid (\zeta_I^+(\mathbf{k}_1) + \zeta_I^-(\mathbf{k}_1))(\zeta_I^+(\mathbf{k}_2) + \zeta_I^-(\mathbf{k}_2)) \mid 0\rangle \\ &= \frac{H^2}{4\epsilon_V k_1^3}(2\pi)^3(1-\mathrm{i}k\eta)(1+\mathrm{i}k\eta)\delta(\mathbf{k}_1+\mathbf{k}_2) \\ &\equiv P_\zeta(k)(2\pi)^3\delta(\mathbf{k}_1+\mathbf{k}_2) \quad \text{as } \eta \to 0,\end{aligned} \tag{67}$$

where the angular brackets denote a quantum expectation value, but outside the horizon we can treat it as a classical ensemble average. The *power spectrum* of the perturbations is defined as

$$P_\zeta(k) = \frac{H^2}{4\epsilon_V k^3} \tag{68}$$

which is a measure of the variance of the fluctuations in Fourier space. It is often convenient to define a dimensionless power spectrum

$$\mathcal{P}_\zeta(k) = \frac{k^3}{2\pi^2} P_\zeta(k) = \left(\frac{H}{\dot{\varphi}_0}\right)^2 \left(\frac{H}{2\pi}\right)^2 \Bigg|_{k=k_*}. \tag{69}$$

where we used the fact that $\epsilon_V = \dot{\varphi}_0^2/2H^2$. The pivot scale k_* is arbitrary and can be chosen for convenience. The power spectrum is often parametrized by

$$\mathcal{P}_\zeta(k) = \mathcal{A}_s \left(\frac{k}{k_*}\right)^{n_s - 1 + (1/2)(\mathrm{d}n_s/\mathrm{dln}k)\ln(k/k_*)} \tag{70}$$

where n_s is the spectral tilt and $\frac{\mathrm{d}n_s}{\mathrm{dln}k}$ is the running, which are defined below. In simple inflation models, we assume we start with a vacuum state and therefore the outcome of the measurement has a Gaussian distribution (Lyth and Liddle 2009). For purely Gaussian random fields, the modes on different scales k are uncoupled and are only correlated via the reality condition $\zeta = \zeta^*$. *All* the statistical information of the perturbation is encoded in the power spectrum, which implies that all even higher order correlators are determined by (67) and the odd correlators vanish.[22] $\langle\zeta\rangle = 0$ can be chosen because it can always be absorbed into the unperturbed background.

0.4.4 Spectral tilt and running

The scalar spectral index is defined as

$$n_s - 1 \equiv \left.\frac{\mathrm{d}\ln(\mathcal{P}_\zeta(k))}{\mathrm{d}\ln k}\right|_{k=k_*} \approx -6\epsilon_V + 2\eta_V. \tag{71}$$

where the second equality was derived by Liddle and Lyth (1992). A spectrum is *scale-invariant*, corresponding to $n_s = 1$, if it is independent of wavenumber k. In this case it known as a Harrison-Zel'dovich spectrum (Harrison 1970; Zeldovich 1970). Any deviation from $n_s = 1$ describes a *tilted spectrum*. The spectrum is referred to as blue if $n_s > 1$ and red if $n_s < 1$. The simple inflationary models discussed in §0.3.3 typically produce a slightly red spectrum of perturbations.

[22] A Gaussian field can be completely specified by its mean and variance, therefore we can only ever write higher order correlators in terms of these variables. The variance corresponds to the two-point function, therefore all higher order correlators must be in terms of the two-point correlator.

The possible running of the spectral index is given by

$$\alpha_\zeta \equiv \frac{\mathrm{d}n_s}{\mathrm{dln}k} \approx -24\epsilon_\mathrm{V}^2 + 16\epsilon_\mathrm{V}\eta_\mathrm{V} - 2\xi_\mathrm{V}^2, \tag{72}$$

where ξ^2 is the second-order slow-roll parameter

$$\xi_\mathrm{V}^2 = M_\mathrm{P}^4 \frac{V'V'''}{V^2}. \tag{73}$$

0.4.5 Gravitational waves from inflation

The perturbations described in §0.4.2 are a result of quantum mechanical fluctuations in the density that have been magnified by an inflationary epoch. However, in the same manner, there will be quantum fluctuations in the gravitational field that will also be amplified by inflation. They are a key prediction of many models of inflation with Einstein gravity. The perturbed spacetime metric is

$$g_{\mu\nu} = a^2(\eta)[-\mathrm{d}\eta^2 + (\delta_{ij} + \gamma_{ij})\mathrm{d}x^i\mathrm{d}x^j] \tag{74}$$

where $|\gamma_{ij}| \ll 1$. The perturbations in the gravitational field, γ_{ij}, are known as tensor modes or "gravitational waves" and are characterized by

$$\gamma_{ij} = \gamma_+ e_{ij}^+ + \gamma_\times e_{ij}^\times. \tag{75}$$

The polarization tensors are given by $e_{ij}^{+,\times}$ and the $\gamma_{+,\times}$ are the two independent gravitational wave amplitudes.

The power spectrum of gravitational waves is given by

$$\mathcal{P}_t(k) = \frac{2}{M_\mathrm{P}^2}\frac{H^2}{\pi^2}\left(\frac{k}{aH}\right)^{n_t} \tag{76}$$

where n_t is the spectral index of the tensor perturbations

$$n_t \equiv \frac{\mathrm{dln}\mathcal{P}_t(k)}{\mathrm{dln}k} \approx -2\epsilon_\mathrm{V} \tag{77}$$

The ratio of the spectrum of gravitational waves to the scalar perturbations spectrum is referred to as the tensor-to-scalar ratio

$$r \equiv \frac{\mathcal{P}_t(k_*)}{\mathcal{P}_\zeta(k_*)} = 8M_\mathrm{P}^2\left(\frac{V'}{V}\right)^2 \approx 16\epsilon_\mathrm{H} \tag{78}$$

The consistency relation $r \approx -8n_t$ applies for slow-roll. A value of r gives us an upper bound on the energy scale of inflation since the power spectrum is only dependent on the expansion rate at that time (Linde 1983; Lyth 1984)

$$V = (1.94 \times 10^{16}\mathrm{GeV})^4(r/0.12) \tag{79}$$

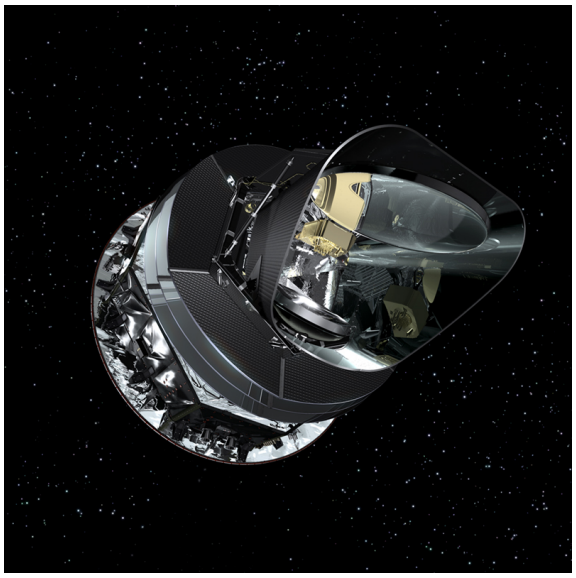

Figure 3: Artist's impression of *Planck* satellite. Credit: ESA

The amplitude of the primordial curvature perturbation $\mathcal{A}_s$, spectral index n_s, running α_s and tensor-to-scalar ratio r provide us with the necessary link between inflationary models and observations. All of these observables can be measured with exceptional accuracy using statistical information encoded in the temperature fluctuations in the CMB. The values predicted by any given model act as a "fingerprint" of that particular model and therefore allows us to constrain models of inflation using data. In the next section we outline the observational bounds on these parameters.

0.5 CURRENT OBSERVATIONAL CONSTRAINTS

The CMB is the oldest observable in our Universe. It provides a window into the Universe when it was very young and has revolutionized our understanding of early Universe cosmology, particularly inflation.

We are now well into a era of precision cosmology where we can place constraints on the observables discussed above. The successor to the COBE satellite (Bennett et al. 1996) was WMAP, which in 2012 released its final dataset after nine years of activity (Hinshaw et al. 2013) and provided a huge amount of data. The ESA funded *Planck* surveyor satellite, shown in Figure 3, provides the most precise data yet (Ade et al. 2013b). The improvement in their precision capabilities can be seen in Figure 4. Due to the degeneracies in measuring cosmological parameters, constraints are normally combined with data from other experiments, such as BOOMERanG (Balloon

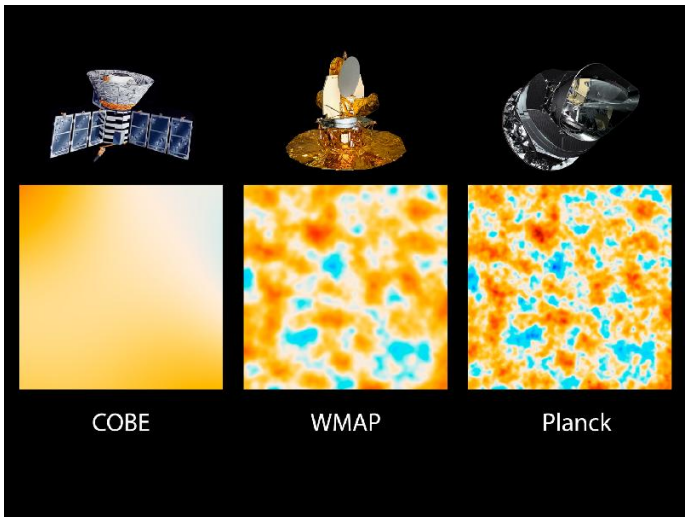

Figure 4: Focus of satellites. Credit: NASA/JPL-Caltech/ESA

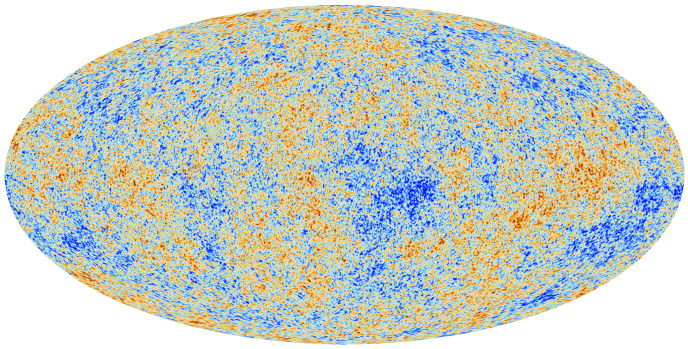

Figure 5: *Planck*. Credit: ESA

Observations Of Millimetric Extragalactic Radiation and Geophysics) experiment (Melchiorri et al. 2000; Bernardis et al. 2000), Baryon Acoustic Oscillations (BAO) in galaxy distributions (Bassett and Hlozek 2009) and supernovae surveys from the Hubble Space Telescope (HST) (Clocchiatti et al. 2006). Degeneracies occur as a result of several parameters having a similar affect on the data, therefore making an independent measurement of a parameter from another experiment can help break this degeneracy. For example, in Figure 7, we can see that the independent measurement of r has helped break the degeneracy that exists between n_s and r when only using the *Planck* data.

The things we measure in the CMB are its temperature anisotropies. The latest full-sky temperature anisotropy map from *Planck* is shown in Figure 5. The temperature fluctuations $\delta T/T$ can be expanded in spherical harmonics (Gradshteyn and Ryzhik 2007)

$$\frac{\delta T(\hat{\mathbf{n}})}{T} = \sum_{\ell=1}^{\infty} \sum_{m=-\ell}^{+\ell} a_{\ell m} Y_{\ell m}(\hat{\mathbf{n}}), \tag{80}$$

where the $a_{\ell m}$ are the multipoles measured in the CMB, $Y_{\ell m}(\hat{\mathbf{n}})$ and $\hat{\mathbf{n}}$ represents an orientation

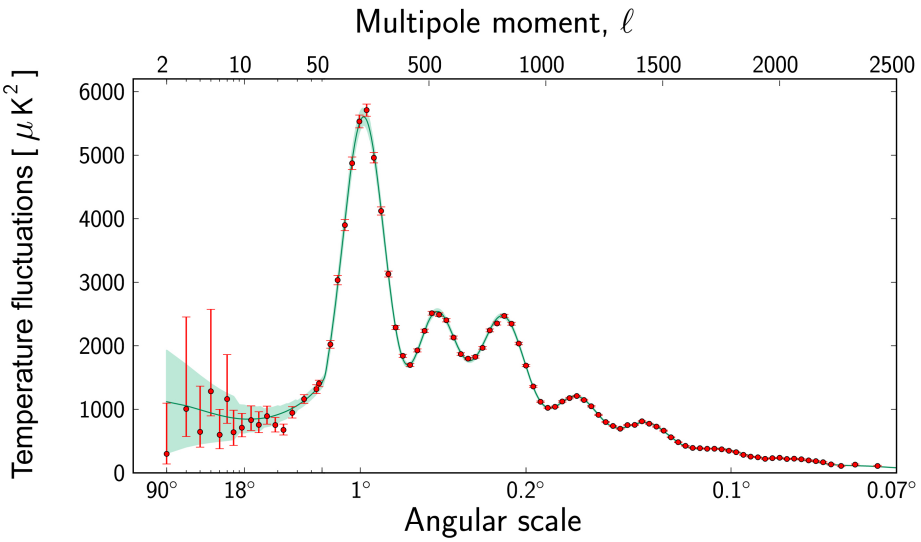

Figure 6: Power Spectrum from *Planck*. Credit: ESA

on the sky. The temperature fluctuations are thought to have originated as a result of the perturbations produced during inflation. The observed multipoles are linearly related to ζ, the primordial curvature perturbation, via

$$a_{\ell m} = 4\pi(-\mathrm{i})^{\ell} \int \frac{\mathrm{d}^3 k}{(2\pi)^3} \Delta_{\ell}(k) \zeta(\mathbf{k}) Y_{\ell m}(\hat{\mathbf{k}}), \tag{81}$$

where $\Delta_{\ell}(k)$ is a transfer function encoding the evolution of the perturbations from inflation to the surface of last scattering. Therefore by measuring statistical observables of the temperature fluctuations, we can derive strong constraints on the perturbations from inflation.

The power spectrum from *Planck*, shown in Figure 6, provides a wealth of information on the Universe.[23] Here we will only focus on the constraints relevant for inflation. The amplitude of the primordial curvature perturbation power spectrum (70) is very accurately constrained by the *Planck* satellite to be (Ade et al. 2013b)

$$\mathcal{A}_{\mathrm{s}} = (2.23 \pm 0.16) \times 10^{-9}, \tag{82}$$

with pivot scale $k_* = 0.05\mathrm{Mpc}^{-1}$. The spectral index is constrained assuming no running to be (Ade et al. 2013b)

$$n_s = 0.9603 \pm 0.0073 \ \ (68\%\,\mathrm{C.L.}), \tag{83}$$

which is a 5.4σ deviation from exact scale-invariance $n_s = 1$. The bounds quoted on the running

[23]For more information, see the *Planck* results papers, which can be found at http://www.sciops.esa.int.

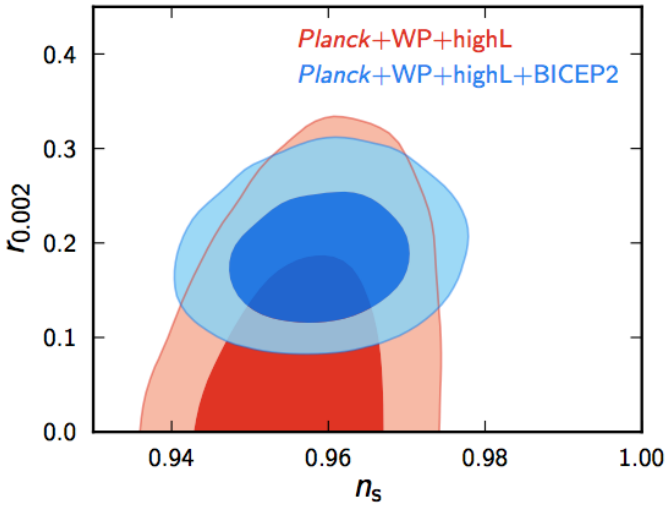

Figure 7: 1σ and 2σ confidence limits for the spectral index versus tensor-to-scalar ratio, allowing running. We define $r_{0.002}$ as the primordial tensor-to-scalar ratio (78) at a pivot scale $k_* = 0.002\text{Mpc}^{-1}$. Image credit: BICEP2 collaboration.

of the spectral index are

$$\alpha_s = -0.011 \pm 0.008 \quad (68\%\,\text{C.L.; Planck+lensing+WP+highL}). \tag{84}$$

A measurement of the tensor-to-scalar ratio r has been hailed a "smoking gun" for inflation because it is difficult to produce in non-inflationary models. It is extremely difficult to measure because the amplitude of the power spectrum of tensor modes is so much lower than the power spectrum of the scalar modes. *Planck* intends to measure $r < 0.1$. In early 2014, the Background Imaging of Cosmic Extragalactic Polarization (BICEP2) telescope (Ade et al. 2014a; Ade et al. 2014b) detected a tensor "B"-mode signal in the polarization of the CMB, measuring the tensor to scalar ratio to be

$$r = 0.2^{+0.07}_{-0.05} \tag{85}$$

disfavouring $r = 0$ at 5.9σ. *Planck* polarization data that is due to be released in late 2014 will hopefully provide a confirmation of this result.

0.6 CONTACT WITH OBSERVATIONS

To recap, the simplest model of inflation involves

- a single scalar field φ
- slowly-rolling

- minimally coupled to Einstein gravity, described by the action (23)
- canonical kinetic term
- beginning in the Bunch-Davies vacuum state (65)
- a potential of the form (39)

As well as solving the problems with the standard Big Bang model, this simple model has very clear predictions, which can be summarised as follows

- Perturbations that are *almost* scale-invariant (Bardeen, Steinhardt and Turner 1983)
- Perturbations that are adiabatic.
- The production of primordial gravitational waves
- The anticorrelation peak in the temperature-polarization (TE) cross-angular power spectrum on large angular scales ($l \sim 150$) is evidence for superhorizon fluctuations, which strongly supports an inflationary origin for the perturbations. (Bennett et al. 2003; Kogut et al. 2003; Spergel et al. 2003; Peiris et al. 2003)[24]
- Density perturbations that are Gaussian distributed

A huge success of inflation is that all but the last of the predictions above have been observationally verified. The perturbations appear to be very consistent with Gaussianity (Ade et al. 2013d), however there is still some possibility that this isn't strictly true. Gaussianity is the default and could be produced by a classical mechanism, e.g. perhaps a central-limit theorem-like effect. However, if we detected a deviation from Gaussianity, this would provide strong support for an inflationary (quantum mechanical) origin for the perturbations.

So far we have only considered the simplest inflationary model. However, there are many more models that also predict values for these observables consistent with the current bounds. Any modification to the simplest inflation model will typically result in microphysics that no longer gives rise to purely Gaussian perturbations. They may predict some amount of *non-Gaussianity*, a powerful tool that we can use to discriminate the microphysics of inflation.

Non-Gaussianity may be observed in the statistics of the CMB and therefore could potentially offer a way to break the degeneracy between these models, giving an insight into the physics that powered inflation. This will be the topic for the remainder of this thesis.

[24]During recombination, photons are interacting with free electrons via Thomson scattering. When two photons of *different* intensities scatter with an electron at 90° the outgoing radiation has a net polarization. Measurements of this polarization can be used in conjunction with the temperature data to further our understanding of inflation.

0.7 GENERALIZED INFLATIONARY SCENARIOS

For the simplest models of inflation described above, the power spectrum, spectral index, running and tensor-to-scalar ratio provides enough information to completely characterize the perturbations arising from these models. However, if we consider more complicated models,[25] where one or more of the simple inflation model requirements outlined in §0.6 is modified, the parameter space which we can probe becomes richer. Considering different models is a very important task for several reasons. As it stands, we have introduced inflation as an "add-on" to the standard Big Bang cosmological model without really understanding how it started or why. A key motivation for considering more complicated models is that they can be embedded in a high-energy theory, such as string theory. With few exceptions (e.g. Higgs inflation (Bezrukov and Shaposhnikov 2008)), all inflationary models, including the simplest scenario, involve field theory beyond the Standard Model of particle physics. Therefore inflation provides an excellent opportunity to probe physics beyond our current understanding and at energies much higher than can be reached by experiments on earth.

The simplest inflationary scenario may not necessarily be the correct one so it is important to consider every possible model allowed by the data. There are many different classes of models with wide-ranging inflationary dynamics. It is not our intention to provide an inventory of all possible models here. Lyth and Riotto have an excellent review of particle physics models of inflation (Lyth and Riotto 1999), though it is a little out of date. A slightly more recent review of developments can be found in Alabidi and Lyth (2006).

Inflation model-building has been a very active area ever since its inception. Even with constraints on the observables from the CMB slowly ruling out models, there are still swathes of viable candidates. To constrain the plethora of models on the market in a systematic way we can divide them into different *classes*. Classes of models that will not be considered here, but are equally important, include quasi-single-field models (Chen and Wang 2010), non-trivial vacua models (Chen, Huang et al. 2007; Holman and Tolley 2008; Meerburg, Schaar and Corasaniti 2009; Ashoorioon and Shiu 2011), *feature* models (Wang and Kamionkowski 2000b; Chen, Easther and Lim 2007; Chen, Easther and Lim 2008) and many, many more. Here we will consider two important classes of models important for the work presented in this thesis. The first is the class of single-field models that have non-trivial kinetic terms. The second is a class of models with an arbitrary number of fields present during the inflationary expansion known as multiple-field models. We will now

[25] Each model is essentially an effective field theory that applies during inflation.

provide a brief introduction to both in turn.

0.7.1 GENERAL SINGLE-FIELD MODELS

Models with non-canonical/higher derivative kinetic terms are abundant in the inflationary literature and have been studied by many authors. Examples that have been proposed in this category include ghost inflation (Arkani-Hamed et al. 2004), DBI (Alishahiha, Silverstein and Tong 2004), k-inflation (Armendariz-Picon, Damour and Mukhanov 1999) and many more (Chen, Huang et al. 2007). Every model has a unique Lagrangian that characterizes the inflationary dynamics that allows us to calculate their predictions in the same way as outlined for the simple model considered above.

EFFECTIVE FIELD THEORY FOR INFLATION.— It was first pointed out in Cheung et al. (2008) that many single-field inflation models can be described by one unifying effective field theory (EFT) Lagrangian. The EFT Lagrangian is constructed by allowing all possible operators that are compatible with the resulting symmetries of an inflating background spacetime. Each of these operators comes with a coefficient that will determine its relative weighting. By adjusting these coefficients we can obtain the limit corresponding to a particular existing single-field model, for example DBI or ghost inflation. However, within the general framework of EFT these coefficients are free parameters, therefore as well as encompassing models that have previously been well-studied, we also have the capacity to probe regions of the large inflationary parameter space that lie out-with these specific realizations. Therefore the effective field theory for inflation is an insightful and efficient method for studying single-field models. In Paper 1 we use the EFT approach in order to place constraints on models in this class. The EFT approach does not include models with sharp features or oscillations (Starobinsky 1992; Adams, Ross and Sarkar 1997; Adams, Cresswell and Easther 2001; Hailu and Tye 2007; Bean et al. 2008; Achucarro et al. 2011; Joy, Sahni and Starobinsky 2008; Hotchkiss and Sarkar 2010; Nakashima et al. 2011; Adshead et al. 2011). In this thesis, we will only consider the effective field theory for single-field inflation. In multiple-field models of inflation, the shift symmetry that organizes the operators in the effective field theory into an expansion in powers of energy no longer holds due to the evolution of the perturbations outside the horizon (Senatore and Zaldarriaga 2012). There are an infinite number of operators that could be important at all energies, therefore the usefulness of the EFT approach is lost.

0.7.2 Multiple-field models

Multiple-field models were first considered by Linde (1985); Kofman and Linde (1987); Silk and Turner (1987). Many high-energy physics inspired inflationary models contain multiple fields (Linde 2006; McAllister and Silverstein 2008). For example the string theory landscape (Susskind 2003) and super-gravity theories (Binetruy et al. 2004; Choi et al. 2004). In order to account for multiple fields during inflation, we can generalize the scalar field Lagrangian (23) to give (Sasaki and Stewart 1996; Nakamura and Stewart 1996)

$$S = \frac{1}{2}\int \mathrm{d}^4x\,\sqrt{-g}\,[R - \mathcal{G}_{\alpha\beta}\partial_\mu\varphi^\alpha\partial^\mu\varphi^\beta - 2V(\varphi)] \tag{86}$$

There will also be generalizations of the background equations of motions and the slow-roll equations. The new fields lead to much richer dynamics. We recall that in single-field models, ζ is conserved on superhorizon scales. Since there is only one field φ, there is only one inflationary trajectory and a generic perturbation can be characterized by small shifts along the trajectory in the 1D field space. Perturbations along the trajectory are adiabatic as they only correspond to shifts in the overall energy density. In multiple-field models it is not possible to describe a generic perturbation purely in terms of an adiabatic perturbation. In general, there will be relative perturbations between the densities of the different fields, i.e. non-adiabatic, or *isocurvature*, perturbations. As an example, consider a two-field model with fields φ and χ and field perturbations $\delta\varphi$ and $\delta\chi$ respectively. The background trajectory (shown in purple) through the inflationary field space for this model is depicted in Figure 8. It is convenient to decompose a generic perturbation into a basis with a component along the trajectory and orthogonal to it. By definition, the adiabatic perturbation $\delta\sigma_{\rm ad}$ is the component of the perturbations along the trajectory. Isocurvature perturbations $\delta\sigma_{\rm iso}$ are defined to be orthogonal to the adiabatic (curvature) perturbation. This component represents a displacement onto a different trajectory. Comparing with the earlier definition in §0.4.2, adiabatic perturbations have no relative perturbation between the fields φ and χ, $\mathcal{S}_{\varphi\chi} = 0$. Isocurvature characterizes relative perturbations between species, i.e. $\mathcal{S}_{\varphi\chi} \equiv \delta\varphi/\dot{\varphi} - \delta\chi/\dot{\chi} \neq 0$. Isocurvature modes, if present can have a large effect on the evolution of the perturbations and significant non-Gaussianities can be sourced. They can transfer power to the adiabatic mode on superhorizon scales, resulting in non-linear evolution. One also must careful to track this non-linear evolution potentially through reheating (a review of multiple fields and reheating can be found in Bassett, Tsujikawa and Wands (2006)) and beyond, as ζ may continue to evolve substantially through the post-inflationary epoch, until all isocurvature modes have decayed. This is referred to as the *adiabatic limit* (Elliston et al. 2011). *Planck* and its predecessors have found

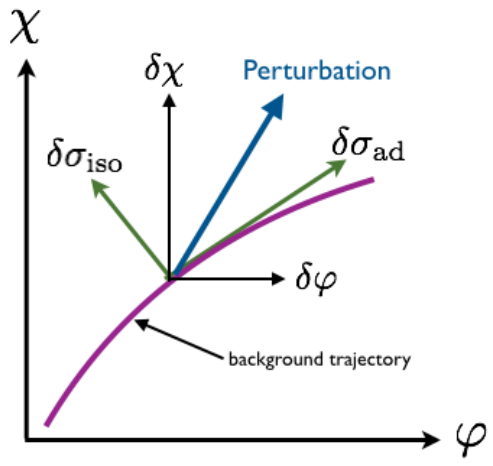

Figure 8: Phase space for a two-field inflationary model, where χ and φ correspond to the active fields. Adiabatic perturbations are defined as those tangent to the 'phase space flow', i.e. the trajectory through the phase space. Isocurvature perturbations are orthogonal to the trajectory. Adapted from Gordon et al. (2001).

no evidence for isocurvature modes at the epoch of recombination (Ade et al. 2013c) therefore all isocurvature modes must decay before that time. In Paper 2 we use non-Gaussian observables to constrain multiple-field models of inflation.

0.8 NON-GAUSSIANITY

Non-Gaussianity has received a great deal of attention in recent years due to its potential ability to break degeneracies amongst competing inflationary scenarios (Komatsu, Afshordi et al. 2009). Different models of inflation predict different levels and shapes of non-Gaussianity therefore, by making a precise measurement of it, we can potentially discriminate between them. *Planck* has been able to place very stringent constraints on non-Gaussianity (Ade et al. 2013d). A free field theory predicts a Gaussian spectrum of quantum fluctuations. A non-Gaussian signal may therefore allow us to investigate the microphysics of inflation much more thoroughly. A significant detection of primordial non-Gaussianity would rule out all canonical slow-roll, single-field models (Maldacena 2003), which would imply that much richer physical dynamics were at work during the inflationary epoch.

First introduced in Allen, Grinstein and Wise (1987) and worked on by several other authors (Falk, Rangarajan and Srednicki 1993; Gangui et al. 1994; Wang and Kamionkowski 2000a; Salopek and Bond 1990), non-Gaussianity became firmly established in the field of inflation after

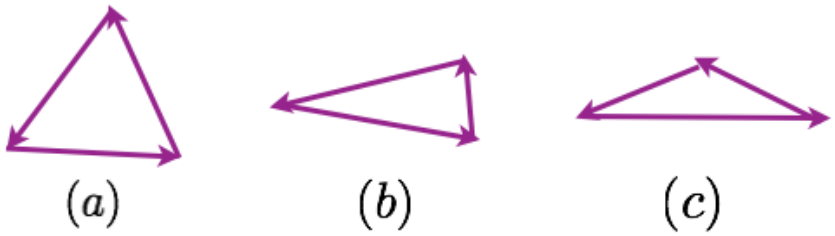

Figure 9: (a) Equilateral (b) squeezed and (c) folded shape configurations.

a ground-breaking paper by Maldacena (2003). The observationally relevant deviations are those that occur on the level of the three-point function and four-point function, known in Fourier space respectively as the bispectrum and trispectrum.

0.8.1 Bispectrum

For a Gaussian field, the three-point function vanishes by the rules of Gaussian statistics (Lyth and Liddle 2009), therefore we can use it to determine deviations from Gaussianity. It has the general form

$$\langle \zeta(\mathbf{k}_1)\zeta(\mathbf{k}_2)\zeta(\mathbf{k}_3)\rangle = (2\pi)^3\delta^3(\mathbf{k}_1+\mathbf{k}_2+\mathbf{k}_3)B_\zeta(k_1,k_2,k_3) \tag{87}$$

where the δ-function imposes the triangle closure condition. We can consider various triangular momentum configurations. Common choices are: where the momenta are all approximately equal $k_1 \approx k_2 \approx k_3$, known as the "equilateral" limit; where one of the momenta is taken to zero $k_1 \ll k_2 = k_3$, dubbed the "squeezed" (or local) limit and the limit where $k_1 \approx 2k_2 \approx 2k_3$, the so-called "folded" (or flattened) configuration. These are shown in Figure 9. However, generally there are many different *shapes* of non-Gaussianity depending on the overall dependence of $B_\zeta(k_1,k_2,k_3)$ on the momenta. We discuss shapes further in §0.8.2. For convenience when making contact with the data, standard *templates* are traditionally considered. A popular choice is the local template, given by

$$B_\zeta^{\rm local}(k_1,k_2,k_3) \equiv \frac{6}{5}f_{\rm NL}^{\rm local}\left[P_\zeta(k_1)P_\zeta(k_2) + \text{cyclic permutations.}\right], \tag{88}$$

where $f_{\rm NL}^{\rm local}$ is a non-linearity parameter associated with the bispectrum. It is essentially a number that represents the amplitude of non-Gaussianity. Non-Gaussianity of this sort peaks in the

squeezed configurations. Other choices include the equilateral template (Creminelli et al. 2006)

$$B_\zeta^{\text{equil.}}(k_1,k_2,k_3) \equiv 6A^2 f_{\text{NL}}^{\text{equi}}\Bigg(-\frac{1}{k_1^3k_2^3} - \frac{1}{k_1^3k_3^3} - \frac{1}{k_2^3k_3^3} - \frac{2}{k_1^2k_2^2k_3^2} + \left[\frac{1}{k_1k_2^2k_3^3} + 5\text{perms}\right]\Bigg), \quad (89)$$

which has its dominant contribution in equilateral configurations, the flat template (Meerburg, Schaar and Corasaniti 2009)

$$B_\zeta^{\text{flat.}}(k_1,k_2,k_3) \equiv 6A^2 f_{\text{NL}}^{\text{flat}}\Bigg(\frac{1}{k_1^3k_2^3} + \frac{1}{k_2^3k_3^3} + \frac{1}{k_3^3k_1^3} + \frac{3}{k_1^2k_2^2k_3^2} - \left[\frac{1}{k_1k_2^2k_3^3} + 5\text{perms}\right]\Bigg), \quad (90)$$

that has its maximal amplitude in the folded/flattened triangular configuration and the orthogonal template (Senatore, Smith and Zaldarriaga 2010)

$$B_\zeta^{\text{orthog.}}(k_1,k_2,k_3) \equiv 6A^2 f_{\text{NL}}^{\text{ortho}}\Bigg(-\frac{3}{k_1^3k_2^3} - \frac{3}{k_1^3k_3^3} - \frac{3}{k_2^3k_3^3} - \frac{8}{k_1^2k_2^2k_3^2} + \frac{3}{k_1k_2^2k_3^3} + 5\text{perms}\Bigg), \quad (91)$$

which peaks in the *both* the flattened and equilateral limit. Constraints on f_{NL} are typically quoted for these templates. The latest constraints are quoted later in §0.8.7. The definitions above assume that f_{NL} is scale-independent, however it could have a weak scale-dependence offering even more discriminating information. This situation is discussed in Byrnes, Gerstenlauer et al. (2010).

0.8.2 Bispectrum shapes

We can define a shape function as

$$S_\zeta(k_1,k_2,k_3) \equiv \frac{B_\zeta(k_1,k_2,k_3)}{B_{\text{ref}}(k_1,k_2,k_3)} \quad (92)$$

where $B_{\text{ref}}(k_1,k_2,k_3)$ is an arbitrary reference bispectrum. Plotting the shape of the bispectra can be a useful tool for visualising the different types of interactions occurring. In what follows we will choose the reference bispectrum to be the constant bispectrum $B^{\text{const}}(k_1,k_2,k_3) \propto 1/(k_1k_2k_3)^2$. Defining the axes $x = k_1/k_3$ and $y = k_2/k_3$ and normalising the shape function to be 1 when it resembles the equilateral configuration, the 3D function we plot is $x^2y^2B(x,y,1)/B(1,1,1)$ (Babich, Creminelli and Zaldarriaga 2004; Chen 2010). As an example we show shape plot for the equilateral template in Figure 10. The shapes can also be plotted with a different parametrization discussed in Fergusson and Shellard (2009).

0.8.3 Calculating the bispectrum: subhorizon scales

In this section we will first revisit the simplest inflationary model (single-field, slow-roll, Bunch-Davies vacuum, Einstein gravity and canonical kinetic terms) and calculate its three-point function using the approach discussed in §0.4.3 before considering more complex scenarios.

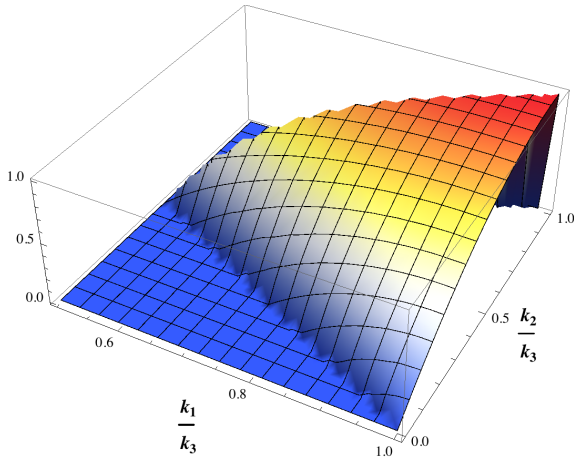

Figure 10: Shape plot of the equilateral bispectrum template (89). Shape peaks when all the k's are equal.

THIRD ORDER ACTION.—To calculate the three-point function we will first need to calculate the action to third order, which can be obtained by plugging (49)[26] into the action (44). Working in the comoving gauge the action to third order in the perturbations is given by (Maldacena 2003)

$$S_3 = \int dt\, d^3x\; a^3 \Big[\epsilon_{\rm V}^2 \zeta \dot{\zeta}^2 - 2a\epsilon_{\rm V}^2 \dot{\zeta}(\partial\zeta)(\partial\psi) + a\epsilon_{\rm V}^2 \zeta(\partial\zeta)^2 + \frac{a}{2}\epsilon_{\rm V}\dot{\eta}\zeta^2\dot{\zeta} + \frac{1}{2}\frac{\epsilon_{\rm V}}{a}\partial\zeta\partial\psi\partial^2\psi + \frac{\epsilon_{\rm V}}{4a}\partial^2\zeta(\partial\psi)^2\Big] + 2f(\zeta)\frac{\delta L_2}{\delta\zeta} \quad (93)$$

where the first order equation of motion is

$$\frac{\delta L_2}{\delta\zeta} = (a^3\epsilon_{\rm V}\dot{\zeta}) - \epsilon_{\rm V}\partial^2\zeta \quad (94)$$

and

$$f(\zeta) = \frac{\eta}{4}\zeta^2 + \frac{1}{H}\zeta\dot{\zeta} + \frac{1}{4a^2H^2}\left[-(\partial\zeta)^2 + \partial^{-2}(\partial_i\partial_j(\partial_i\zeta\partial_j\zeta))\right] + \frac{1}{2a^2H}\left[(\partial\zeta)(\partial\psi) - \partial^{-2}(\partial_i\partial_j(\partial_i\zeta\partial_j\psi))\right], \quad (95)$$

where ∂^{-2} is simply given by k^{-2} in Fourier space. We are now in a position to calculate the three-point correlator using (93). As with the calculation of the two-point function, we make use of the Schwinger-Keldysh "in–in" formalism. This procedure is detailed in Appendix 1.A where we give an explicit calculation of the bispectrum arising from the effective field theory action (Bartolo et al. 2010). Since conservation of the curvature perturbation on superhorizon scales implies that the correlation functions also remain constant, it suffices to compute the correlation functions at horizon-exit.

The final result for the three-point correlation function of the comoving curvature perturbation

[26]The higher order terms in N and N_i do not contribute, as in the second order case.

in the simplest, singe-field, slow-roll model is found to be (Maldacena 2003)

$$\begin{aligned}\langle\zeta(\mathbf{k}_1,0)\zeta(\mathbf{k}_2,0)\zeta(\mathbf{k}_3,0)\rangle =&(2\pi)^3\delta(\mathbf{k}_1+\mathbf{k}_2+\mathbf{k}_3)\frac{H^4}{M_{\rm P}^4}\frac{1}{(k_1k_2k_3)^3}\frac{1}{4\epsilon_{\rm V}^2}\\ &\left[\frac{\eta}{8}\sum k_i^3+\frac{\epsilon_{\rm V}}{8}\left(-\sum k_i^3+\sum_{i\neq j}k_ik_j^2+\frac{8}{k_t}\sum_{i\gg j}k_i^2k_j^2\right)\right],\end{aligned} \tag{96}$$

where $k_t = k_1 + k_2 + k_3$. From (68) and (88) it can be shown that this is proportional to a slow-roll parameter

$$f_{\rm NL}^{\rm local} \sim {\rm O}(\epsilon_{\rm V}, \eta_{\rm V}). \tag{97}$$

This suggests that no large non-Gaussianity can be generated in the simple inflation model (Acquaviva et al. 2003; Maldacena 2003). However, single-field models with non-canonical kinetic terms or having a violation of slow-roll for a period of time may produce detectable amounts of non-Gaussianity with a peak in the equilateral configuration. This is a result of the non-standard kinetic terms, which tend to produce large interaction terms at the horizon. Since in single-field inflation there is no significant interaction between subhorizon and superhorizon modes, the only modes that can participate in these interactions are the modes that cross the horizon at the same time, where they will have similar wavelengths $k_1 \sim k_2 \sim k_3$, corresponding to a peak in the equilateral configuration (Chen 2010).

Gauge choices.— Alternatively we can choose to calculate the correlation functions in the *spatially-flat* gauge in which we set $\psi = 0$ on the hypersurfaces of constant time. Therefore the perturbation will manifest itself as a perturbation in the scalar field, $\varphi = \varphi^{(0)} + \delta\varphi$ and the metric will just be given by the usual background 3-metric

$$h_{ij} = a^2(\delta_{ij}) \tag{98}$$

Sometimes this gauge will be more convenient, as it is technically simpler. However, it is not possible to completely specify the perturbation in terms of the scalar field without any effect on the metric. The perturbation will manifest itself as a "back-reaction" via the shift and lapse functions, N and N_i, i.e.

$$N = 1 + a(\delta\varphi) \tag{99}$$

$$N_i = b(\delta\varphi) \tag{100}$$

$$h_{ij} = a^2(t)\delta_{ij} \tag{101}$$

However, in the comoving gauge, the perturbation manifests itself as follows

$$N = 1 + c(\delta\psi) \tag{102}$$

$$N_j = d(\delta\psi) \tag{103}$$

$$h_{ij} = a^2(t)e^{2\psi}\delta_{ij}, \tag{104}$$

where a, b, c and d are functions. Therefore, in single-field inflation, in the comoving gauge we can fully describe the perturbation solely in terms of the metric without having to consider any effects in the inflaton field φ. This is a key advantage of working in the comoving gauge when considering models with only one field. However, the spatially flat gauge and the comoving gauge are related by a gauge transformation given to first order by (45) and all the results that we outlined above can also be derived in the spatially flat gauge (Maldacena 2003). The spatially flat gauge is useful when considering multiple fields because it is easier to keep track of isocurvature perturbations.

It has been shown that the non-Gaussianity generated on subhorizon scales in multiple-field models is also negligible (Seery and Lidsey 2005). However, since ζ is no longer conserved on superhorizon scales, this can lead to a significant amount of non-Gaussianity. It is possible to extend the in–in calculation for multiple-fields to later times, such as the end of inflation. However, there exist much simpler methods for calculating the level of non-Gaussianity generated on superhorizon scales that we introduce in §0.8.5.

0.8.4 Consistency condition

In the squeezed limit, $k_1 \ll k_2 \simeq k_3$, k_1 will cross the horizon much earlier than the other two modes. As described in §0.4.1, when a mode passes out of the horizon, it WKB classicalizes. Therefore it will just perturb the background and change the time the other two modes cross the horizon by $\delta t_\star = -\zeta_1/H$ since it merely amounts to a rescaling of the scale factor (Maldacena 2003). We deduce that

$$\langle\zeta(\mathbf{k}_1)\zeta(\mathbf{k}_2)\zeta(\mathbf{k}_3)\rangle \sim \langle\zeta(\mathbf{k}_1)\zeta(-\mathbf{k}_1)\rangle_{\bowtie}\frac{1}{H}\frac{\mathrm{d}}{\mathrm{d}t}\langle\zeta(\mathbf{k}_2)\zeta(\mathbf{k}_3)\rangle_\star, \tag{105}$$

where $\bowtie$ signifies evaluation when k_1 left the horizon and $\star$ signifies evaluation when k_2 and k_3 left the horizon. Using (71) and rewriting $\mathrm{d}\ln k = H\mathrm{d}t$ we can write[27]

$$n_s - 1 \equiv \frac{\mathrm{d}\ln(\mathcal{P}_\zeta(k))}{\mathrm{d}\ln k} \approx -2\eta_\mathrm{V} - 6\epsilon_\mathrm{V} = \frac{1}{H}\frac{\mathrm{d}}{\mathrm{d}t}\ln\left(\langle\zeta(k_1)\zeta(k_2)\rangle\right)\Big|^\star. \tag{106}$$

[27] $k = aH$, so $\mathrm{d}\ln k = \mathrm{d}\ln a + \mathrm{d}\ln H$, but $H \approx$ const. during inflation. Therefore we see that $\mathrm{d}\ln k = \frac{\mathrm{d}\ln a}{\mathrm{d}t}\mathrm{d}t = H\mathrm{d}t$.

Rewriting the logarithm we see that

$$\frac{1}{H}\frac{\mathrm{d}}{\mathrm{d}t}\left(\langle\zeta(k_2)\zeta(k_3)\rangle\right) = (n_s - 1)\langle\zeta(k_2)\zeta(k_3)\rangle, \tag{107}$$

and substituting this into (105) we get a *consistency condition* (Maldacena 2003)

$$\langle\zeta(\mathbf{k}_1)\zeta(\mathbf{k}_2)\zeta(\mathbf{k}_3)\rangle \sim (2\pi)^3\delta(k_1 + k_2 + k_3)(6\epsilon_{\mathrm{V}} - 2\eta_{\mathrm{V}})P_\zeta(k_1)P_\zeta(k_2). \tag{108}$$

This relation must hold for single-field inflation and rules out models with single fields if it is not satisfied. Unfortunately, observing a very long wavelength mode is severely constrained by cosmic variance.

0.8.5 CALCULATING THE BISPECTRUM: SUPERHORIZON SCALES

In multiple-field inflation there can be non-linear evolution on superhorizon scales that is *local* in space and therefore non-local in momentum space (Huston 2010), and which peaks in the squeezed configuration $k_1 \ll k_2 \simeq k_3$.

The most natural form for local non-Gaussianity is (Gangui et al. 1994; Verde et al. 2000; Wang and Kamionkowski 2000b; Komatsu and Spergel 2001)

$$\zeta = \zeta_g - \frac{3}{5}f_{\mathrm{NL}}^{\mathrm{local}} \star \zeta_g^2 \tag{109}$$

where ζ_g is Gaussian and $\star$ denotes a convolution. This comes from performing a Taylor expansion about ζ_g for superhorizon evolution in single-field inflation, where we have also assumed that the background is an attractor.[28] This form for the non-Gaussianity leads to a bispectrum of the form of (88). The factor of 3/5 is historical.

δN METHOD.— The *separate universe assumption* is a useful approach that enables us to invoke the δN formalism that we will describe in this section. It simply states that at each spatial point, the local[29] evolution can be approximately described by that of an unperturbed Universe on superhorizon scales $k \ll aH$ (Lyth 1985b). This is because once each point has been smoothed on a certain comoving scale k^{-1}, it will have negligible spatial gradients and therefore will be homogeneous. By also assuming local isotropy we are able to treat each position in the observable Universe as a *separate universe*, thereby greatly simplifying the superhorizon evolution of the perturbations (Lyth 1985a; Lyth and Rodriguez 2005b; Starobinsky 1985).

[28] This occurs when the fluctuation in π is determined by the fluctuation in φ

[29] Local refers to a region that is smaller than a certain smoothed patch, but adequately larger than the largest cosmological scale, H_0^{-1}.

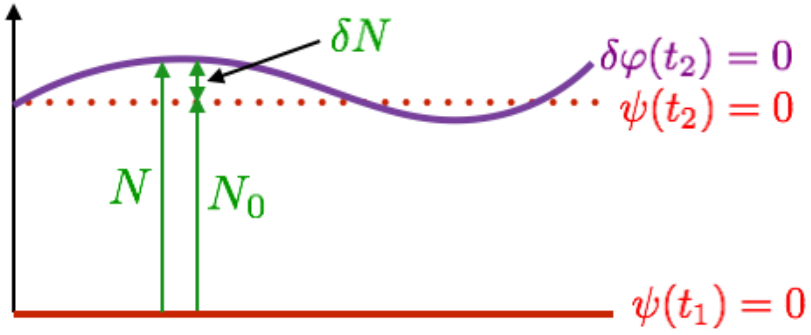

Figure 11: δN is the perturbation in the number of e-foldings from a spatially-flat slice $\psi = 0$ to a comoving slice $\delta\varphi = 0$.

Invoking the separate universe assumption, the number of e-folds N between a perturbed scalar field (spatially flat) hypersurface and a hypersurface with constant scalar field (comoving) is

$$\delta N = N(t,\mathbf{x}) - N_0(t), \tag{110}$$

where $N_0(t) \equiv \ln\left[\frac{a(t)}{a(t_{in})}\right]$. The perturbation in the number of e-folds between two generic slices $\psi(\mathbf{x},t_2)$ and $\psi(\mathbf{x},t_1)$ is

$$\delta N_{12}(\mathbf{x}) = \delta\int_{t_1}^{t_2}\frac{1}{a}\frac{da}{dt}dt = \psi(\mathbf{x},t_2) - \psi(\mathbf{x},t_1). \tag{111}$$

If we start from a spatially-flat slice $\psi(\mathbf{x},t_1) = 0$ *after* the modes of cosmological interest have crossed the horizon and choose to end on a comoving slice (where $\psi = \zeta$ from (45) since there is no perturbation in the density), then we see that

$$\zeta(\mathbf{x},t) \equiv \delta N(\mathbf{x},t) = N(\mathbf{x},t) - N_0(t), \tag{112}$$

schematically depicted in Figure 11. Expanding ζ as a Taylor series we get

$$\zeta = N_\alpha\delta\varphi_\alpha + \frac{1}{2}N_{\alpha\beta}\delta\varphi_\alpha\delta\varphi_\beta + \ldots \tag{113}$$

where $N_\alpha = (\partial N/\partial\varphi_\alpha)$ etc. The first term in this expansion is precisely the gauge transformation we encountered in (45), defined on a flat slice, namely $\zeta = N_\alpha\delta\varphi_\alpha = -H\frac{\delta\varphi_\alpha}{\dot\varphi_\alpha}$ (Wands 2010). Therefore we can write the two-point correlation function as (Chen 2010)

$$\langle\zeta(\mathbf{x}_1)\zeta(\mathbf{x}_2)\rangle = N_\alpha N_\beta\langle\delta\varphi_\alpha(\mathbf{x}_1)\delta\varphi_\beta(\mathbf{x}_2)\rangle, \tag{114}$$

Writing the three-point function in Fourier space we get (Lyth and Rodriguez 2005b; Seery and Lidsey 2005)

$$\begin{aligned}\langle\zeta(\mathbf{k}_1)\zeta(\mathbf{k}_2)\zeta(\mathbf{k}_3)\rangle =& N_\alpha N_\beta N_\gamma\langle\delta\varphi_\alpha(\mathbf{k}_1)\delta\varphi_\beta(\mathbf{k}_2)\delta\varphi_\gamma(\mathbf{k}_3)\rangle \\ &+ \frac{1}{2}N_{\alpha_1\alpha_2}N_\beta N_\gamma\langle(\delta\varphi_{\alpha_1}\star\delta\varphi_{\alpha_2})(\mathbf{k}_1)\delta\varphi_\beta(\mathbf{k}_2)\delta\varphi_\gamma(\mathbf{k}_3)\rangle + 2\text{perms.},\end{aligned} \tag{115}$$

where the first term corresponds to the intrinsic non-Gaussianities. In standard single-field inflation, the non-Gaussianity from both these contributions were of the same order (Maldacena 2003), with neither contribution generating a detectable amount. However, multiple-field inflation can generate a significantly large amount of local non-Gaussianity from superhorizon evolution due to the presence of other light fields generating non-linearities. Assuming that field perturbations on the initial slice (at horizon-exit) are Gaussian, the first term in (115) will remain negligible $\sim \mathrm{O}(\epsilon_{\mathrm{V}}, \eta_{\mathrm{V}})$ (Zaballa, Rodriguez and Lyth 2006; Vernizzi and Wands 2006). Therefore we can write the three-point correlation function as (Lyth and Rodriguez 2005a)

$$\langle\zeta(\mathbf{k}_1)\zeta(\mathbf{k}_2)\zeta(\mathbf{k}_3)\rangle = \frac{1}{2}N_{\alpha_1\alpha_2}N_\beta N_\gamma\langle(\delta\varphi_{\alpha_1}\star\delta\varphi_{\alpha_2})(\mathbf{k}_1)\delta\varphi_\beta(\mathbf{k}_2)\delta\varphi_\gamma(\mathbf{k}_3)\rangle + 2\text{perms.}. \tag{116}$$

With this assumption we can write

$$f_{\mathrm{NL}} = \frac{5}{6}\frac{N_\alpha N_\beta N^{\alpha\beta}}{(N_\gamma N^\gamma)^2}. \tag{117}$$

The δN method can only be used to compute correlation functions analytically in a few special cases such as separable potentials. In all other cases, the calculations must be performed numerically. The drawback of δN is that the calculation of the N-derivatives relies on extracting *finite differences*, which can quickly lead to large numerical errors if computing correlation functions for a large number of fields.

Transport method.— The transport method introduced by Mulryne, Seery and Wesley (2010); Mulryne, Seery and Wesley (2011) offers an alternative to computing correlation functions on superhorizon scales. The transport equations evolve the correlations of the field fluctuations $\delta\varphi$, which involve straightforward ordinary differential equations, and therefore does not suffer as much from numerical inaccuracies associated with the partial derivatives of the δN formalism. The gauge transformation to express these correlation functions in terms of ζ is then simply performed at the time we want to calculate the observables. It has a wide variety of applications. It can compute two- and three-point functions (Mulryne, Seery and Wesley 2010; Mulryne, Seery and Wesley 2011), as well as track the evolution of the spectral index (Dias and Seery 2012) and running (Dias, Frazer and Liddle 2012). It can even be extended to compute n-point functions on sub-horizon scales (Mulryne 2013). In Paper 2 we introduce the method in detail and demonstrate how it can be used to compute the trispectrum non-linearity parameters discussed below.

0.8.6 Trispectrum

As well as the bispectrum, the trispectrum can be used to quantify some deviations from Gaussianity. The four-point correlator is non-zero in the Gaussian case, but in the non-Gaussian case it will have an additional contribution (Zaldarriaga 2000)

$$\langle\zeta(\mathbf{k}_1)\zeta(\mathbf{k}_2)\zeta(\mathbf{k}_3)\zeta(\mathbf{k}_4)\rangle_c = (2\pi)^3\delta^3(\mathbf{k}_1+\mathbf{k}_2+\mathbf{k}_3+\mathbf{k}_4)T_\zeta. \tag{118}$$

where the subscript c denotes the connected part and T_ζ is the trispectrum, which for local non-Gaussianity can be written in the form

$$T_\zeta(\mathbf{k}_1,\mathbf{k}_2,\mathbf{k}_3,\mathbf{k}_4) = \tau_{\rm NL}\left[P_\zeta(k_{13})P_\zeta(k_3)P_\zeta(k_4) + 11 \text{ permutations.}\right] + \frac{54}{25}g_{\rm NL}\left[P_\zeta(k_2)P_\zeta(k_3)P_\zeta(k_4) + 3 \text{ permutations.}\right]. \tag{119}$$

where $k_{14} = \mid \mathbf{k}_1 + \mathbf{k}_4 \mid$. $\tau_{\rm NL}$ and $g_{\rm NL}$ are non-linearity parameters associated with the trispectrum. They each have a distinct k dependence.

All of the techniques introduced above for computing the primordial non-Gaussianity from the bispectrum can be extended and applied to the trispectrum.

The first full in–in single-field slow-roll calculation of the trispectrum produced at horizon-crossing was by Seery, Lidsey and Sloth (2007). They found that the trispectrum in these models was predicted to be of order $\tau_{\rm NL} < r/50$, where r is the tensor-to-scalar ratio. This is too small to ever be observed. Since ζ is conserved on superhorizon scales, no large non-Gaussianity can ever be generated in these models, as in the bispectrum case.

However, in the case of multiple-field models, non-linear superhorizon evolution of the curvature perturbation *can* generate a significant non-Gaussian signal. This can be calculated for a given model using the δN formalism (Seery and Lidsey 2007; Byrnes, Sasaki and Wands 2006). The four-point function expressed in the δN formalism is

$$\begin{aligned}\langle\zeta(\mathbf{k}_1)\zeta(\mathbf{k}_2)\zeta(\mathbf{k}_3)\zeta(\mathbf{k}_4)\rangle_c &= N_\alpha N_\beta N_\gamma N_\delta\langle\delta\varphi_\alpha(\mathbf{k}_1)\delta\varphi_\beta(\mathbf{k}_2)\delta\varphi_\gamma(\mathbf{k}_3)\delta\varphi_\delta(\mathbf{k}_4)\rangle_c \\ &+ \frac{1}{2}N_{\alpha_1\alpha_2}N_\beta N_\gamma N_\delta\left[\langle(\delta\varphi_{\alpha_1}\star\delta\varphi_{\alpha_2})(\mathbf{k}_1)\delta\varphi_\beta(\mathbf{k}_2)\delta\varphi_\gamma(\mathbf{k}_3)\delta\varphi_\delta(\mathbf{k}_4)\rangle\right. \\ &\left.+ 3 \text{ perms.}\right] \\ &+ \frac{1}{4}N_{\alpha_1\alpha_2}N_{\beta_1\beta_2}N_\gamma N_\delta\left[\langle(\delta\varphi_{\alpha_1}\star\delta\varphi_{\alpha_2})(\mathbf{k}_1)(\delta\varphi_{\beta_1}\star\delta\varphi_{\beta_2})(\mathbf{k}_2)\delta\varphi_\gamma(\mathbf{k}_3)\delta\varphi_\delta(\mathbf{k}_4)\rangle\right. \\ &\left.+ 5 \text{ perms.}\right] \\ &+ \frac{1}{3!}N_{\alpha_1\alpha_2\alpha_3}N_\beta N_\gamma N_\delta\left[\langle(\delta\varphi_{\alpha_1}\star\delta\varphi_{\alpha_2}\star\delta\varphi_{\alpha_3})(\mathbf{k}_1)\delta\varphi_\beta(\mathbf{k}_2)\delta\varphi_\gamma(\mathbf{k}_3)\delta\varphi_\delta(\mathbf{k}_4)\rangle\right. \\ &\left.+ 3 \text{ perms.}\right]\end{aligned} \tag{120}$$

In the local model (119) we can write $\tau_{\rm NL}$ and $g_{\rm NL}$ in terms of these δN coefficients

$$\tau_{\rm NL} = \frac{N_{\alpha\beta}N^{\alpha\beta}N^{\beta}N_{\gamma}}{(N_{\delta}N^{\delta})^3} \tag{121}$$

$$g_{\rm NL} = \frac{25}{54}\frac{N_{\alpha\beta\gamma}N^{\alpha}N^{\beta}N^{\gamma}}{(N_{\delta}N^{\delta})^3} \tag{122}$$

In Paper 2, we introduce the transport method to calculate $\tau_{\rm NL}$ and $g_{\rm NL}$ in multiple-field models.

0.8.7 Current constraints on non-Gaussianity

The present observational data from the *Planck* 2013 dataset (Ade et al. 2013d) impose the following constraints on the non-linearity parameters for the local, equilateral and orthogonal templates

$$f_{\rm NL}^{\rm local} = 2.7 \pm 5.8 \ (68\%\,\text{C.L.})$$

$$f_{\rm NL}^{\rm equi} = -42 \pm 75 \ (68\%\,\text{C.L.})$$

$$f_{\rm NL}^{\rm ortho} = -25 \pm 39 \ (68\%\,\text{C.L.})$$

The constraints on the non-linearity parameters associated with the trispectrum are

$$\tau_{\rm NL} < 2800 \ (95\%\,\text{C.L.};\ \text{Planck})$$

$$g_{\rm NL} = (-3.3 \pm 2.2) \times 10^5 \ (68\%\,\text{C.L.};\ \text{WMAP9})$$

Planck has not yet provided constraints for $g_{\rm NL}$, so we have used the most recent constraint from WMAP9 data (Sekiguchi and Sugiyama 2013).

There are expected to be stronger constraints on $f_{\rm NL}^{\rm local}$ in the coming years from Large Scale Structure (Bernardeau et al. 2002; Giannantonio et al. 2012), particularly from the ESA mission EUCLID (Cimatti et al. 2009) due to be launched in 2020 and the Large Synoptic Survey Telescope (LSST) (Ivezic et al. 2008). These will provide a three-dimensional data source and therefore they include more information than we are currently able to extract from the CMB. However, an added level of complexity when measuring the late-time Universe is separating the *primordial* non-Gaussianity from any non-Gaussianities that could have arisen as a result of the significant non-linear processing of the perturbations that occurred since inflation.

To be able to distinguish between the single-field slow-roll prediction for the local non-linearity parameter (97) and a very small $f_{\rm NL}^{\rm local}$, e.g. $f_{\rm NL}^{\rm local} \sim \mathrm{O}(1)$ will require more precise measurements. It is not yet clear whether these will be attainable by future missions.

0.9 OVERVIEW OF THE PAPERS

The first part of this thesis uses the bispectrum of the temperature fluctuations in the CMB to constrain generic models of single-field inflation. This is achieved by considering the EFT of inflation, introduced in §0.7.1. We calculate the bispectrum for each of the operators in the EFT Langrangian arising from subhorizon evolution using the 'in–in' formalism that was discussed in §0.8.3 and will be explained further in §1.A. We can then decompose the shape (92) of these operators into a basis of partial waves. We also perform the same decomposition on the observed CMB bispectrum (using WMAP9 data), circumventing the need to consider the templates presented in §0.8.1. We then construct a maximum likelihood estimator (MLE) for the free parameters in the EFT Lagrangian, allowing us to constrain combinations of parameters describing the most general single-field inflationary model.

The second part extends the transport formalism, introduced in §0.8.5, to compute the local trispectrum non-linearity parameters $\tau_{\rm NL}$ and $g_{\rm NL}$, defined by (119), generated by multiple field models with canonical kinetic terms on superhorizon scales. This involves working in the spatially flat gauge, tracking the evolution of the field perturbations using transport equations, which can be derived in a number of ways. In §2.B we provide a derivation of the trispectrum transport equation using a Gauss–Hermite expansion. We then provide a third-order gauge transformation in order to express the correlation functions of the field perturbations in terms of correlation functions of the observationally relevant quantity ζ, allowing us to compute the trispectrum non-linearity parameters.

REFERENCES

[1] Ana Achucarro et al. 'Features of heavy physics in the CMB power spectrum'. In: *JCAP* 1101 (2011), p. 030. arXiv: 1010.3693 [hep-ph] (cit. on p. 30).

[2] Viviana Acquaviva et al. 'Second order cosmological perturbations from inflation'. In: *Nucl.Phys.* B667 (2003), pp. 119–148. arXiv: astro-ph/0209156 [astro-ph] (cit. on p. 36).

[3] Jennifer A. Adams, Bevan Cresswell and Richard Easther. 'Inflationary perturbations from a potential with a step'. In: *Phys.Rev.* D64 (2001), p. 123514. arXiv: astro-ph/0102236 [astro-ph] (cit. on p. 30).

[4] Jennifer A. Adams, Graham G. Ross and Subir Sarkar. 'Multiple inflation'. In: *Nucl.Phys.* B503 (1997), pp. 405–425. arXiv: hep-ph/9704286 [hep-ph] (cit. on p. 30).

[5] P. A. R Ade et al. 'BICEP2 II: Experiment and Three-Year Data Set'. In: (2014). arXiv: 1403.4302 [astro-ph.CO] (cit. on p. 27).

[6] P.A.R. Ade et al. 'Planck 2013 results. I. Overview of products and scientific results'. In: (2013). arXiv: 1303.5062 [astro-ph.CO] (cit. on p. 2).

[7] P.A.R. Ade et al. 'Planck 2013 results. XVI. Cosmological parameters'. In: (2013). arXiv: 1303.5076 [astro-ph.CO] (cit. on pp. 7, 24, 26).

[8] P.A.R. Ade et al. 'Planck 2013 results. XXII. Constraints on inflation'. In: (2013). arXiv: 1303.5082 [astro-ph.CO] (cit. on p. 32).

[9] P.A.R. Ade et al. 'Planck 2013 Results. XXIV. Constraints on primordial non-Gaussianity'. In: (2013). arXiv: 1303.5084 [astro-ph.CO] (cit. on pp. 28, 32, 42).

[10] P.A.R. Ade et al. 'BICEP2 I: Detection Of B-mode Polarization at Degree Angular Scales'. In: (2014). arXiv: 1403.3985 [astro-ph.CO] (cit. on p. 27).

[11] Peter Adshead et al. 'Fast Computation of Bispectrum Features with Generalized Slow Roll'. In: *Phys.Rev.* D84 (2011), p. 043519. arXiv: 1102.3435 [astro-ph.CO] (cit. on p. 30).

[12] N. Aghanim et al. 'Planck 2013 results. XXVII. Doppler boosting of the CMB: Eppur si muove'. In: (2013). arXiv: 1303.5087 [astro-ph.CO] (cit. on pp. 3, 7).

[13] Laila Alabidi and David H. Lyth. 'Inflation models and observation'. In: *JCAP* 0605 (2006), p. 016. arXiv: astro-ph/0510441 [astro-ph] (cit. on p. 29).

[14] Andreas Albrecht and Paul J. Steinhardt. 'Cosmology for Grand Unified Theories with Radiatively Induced Symmetry Breaking'. In: *Phys.Rev.Lett.* 48 (1982), pp. 1220–1223 (cit. on p. 7).

[15] Mohsen Alishahiha, Eva Silverstein and David Tong. 'DBI in the sky'. In: *Phys.Rev.* D70 (2004), p. 123505. arXiv: hep-th/0404084 [hep-th] (cit. on p. 30).

[16] T.J. Allen, Benjamin Grinstein and Mark B. Wise. 'Nongaussian Density Perturbations in Inflationary Cosmologies'. In: *Phys.Lett.* B197 (1987), p. 66 (cit. on p. 32).

[17] Nima Arkani-Hamed et al. 'Ghost inflation'. In: *JCAP* 0404 (2004), p. 001. arXiv: hep-th/0312100 [hep-th] (cit. on p. 30).

[18] C. Armendariz-Picon, T. Damour and Viatcheslav F. Mukhanov. 'k - inflation'. In: *Phys.Lett.* B458 (1999), pp. 209–218. arXiv: hep-th/9904075 [hep-th] (cit. on p. 30).

[19] R. Arnowitt, S. Deser and C. W. Misner. 'Republication of: The dynamics of general relativity'. In: *General Relativity and Gravitation* 40 (Sept. 2008), pp. 1997–2027. eprint: arXiv:gr-qc/0405109 (cit. on p. 17).

[20] Richard L. Arnowitt, Stanley Deser and Charles W. Misner. 'The Dynamics of general relativity'. In: *Gen.Rel.Grav.* 40 (2008), pp. 1997–2027. arXiv: gr-qc/0405109 [gr-qc] (cit. on p. 17).

[21] Amjad Ashoorioon and Gary Shiu. 'A Note on Calm Excited States of Inflation'. In: *JCAP* 1103 (2011), p. 025. arXiv: 1012.3392 [astro-ph.CO] (cit. on p. 29).

[22] Daniel Babich, Paolo Creminelli and Matias Zaldarriaga. 'The Shape of non-Gaussianities'. In: *JCAP* 0408 (2004), p. 009. arXiv: astro-ph/0405356 [astro-ph] (cit. on p. 34).

[23] James M. Bardeen. 'Gauge Invariant Cosmological Perturbations'. In: *Phys.Rev.* D22 (1980), pp. 1882–1905 (cit. on p. 17).

[24] James M. Bardeen, Paul J. Steinhardt and Michael S. Turner. 'Spontaneous creation of almost scale-free density perturbations in an inflationary universe'. In: *Phys. Rev. D* 28 (4 Aug. 1983), pp. 679–693. URL: http://link.aps.org/doi/10.1103/PhysRevD.28.679 (cit. on pp. 16, 18, 28).

[25] Nicola Bartolo et al. 'Large non-Gaussianities in the Effective Field Theory Approach to Single-Field Inflation: the Bispectrum'. In: *JCAP* 1008 (2010), p. 008. arXiv: 1004.0893 [astro-ph.CO] (cit. on p. 35).

[26] Bruce A. Bassett and Renee Hlozek. 'Baryon Acoustic Oscillations'. In: (2009). arXiv: 0910.5224 [astro-ph.CO] (cit. on p. 25).

[27] Bruce A. Bassett, Shinji Tsujikawa and David Wands. 'Inflation dynamics and reheating'. In: *Rev.Mod.Phys.* 78 (2006), pp. 537–589. arXiv: astro-ph/0507632 [astro-ph] (cit. on p. 31).

[28] Rachel Bean et al. 'Duality Cascade in Brane Inflation'. In: *JCAP* 0803 (2008), p. 026. arXiv: 0802.0491 [hep-th] (cit. on p. 30).

[29] C.L. Bennett et al. 'First year Wilkinson Microwave Anisotropy Probe (WMAP) observations: Preliminary maps and basic results'. In: *Astrophys.J.Suppl.* 148 (2003), p. 1. arXiv: astro-ph/0302207 [astro-ph] (cit. on p. 28).

[30] C.L. Bennett et al. 'Four year COBE DMR cosmic microwave background observations: Maps and basic results'. In: *Astrophys.J.* 464 (1996), pp. L1–L4. arXiv: astro-ph/9601067 [astro-ph] (cit. on p. 24).

[31] F. Bernardeau et al. 'Large scale structure of the universe and cosmological perturbation theory'. In: *Phys.Rept.* 367 (2002), pp. 1–248. arXiv: astro-ph/0112551 [astro-ph] (cit. on p. 42).

[32] P. de Bernardis et al. 'A Flat universe from high resolution maps of the cosmic microwave background radiation'. In: *Nature* 404 (2000), pp. 955–959. arXiv: astro-ph/0004404 [astro-ph] (cit. on p. 25).

[33] Fedor L. Bezrukov and Mikhail Shaposhnikov. 'The Standard Model Higgs boson as the inflaton'. In: *Phys.Lett.* B659 (2008), pp. 703–706. arXiv: 0710.3755 [hep-th] (cit. on p. 29).

[34] Pierre Binetruy et al. 'Fayet-Iliopoulos terms in supergravity and cosmology'. In: *Class.Quant.Grav.* 21 (2004), pp. 3137–3170. arXiv: hep-th/0402046 [hep-th] (cit. on p. 31).

[35] R Brout, F Englert and E Gunzig. 'The creation of the universe as a quantum phenomenon'. In: *Annals of Physics* 115.1 (1978), pp. 78–106. ISSN: 0003-4916. URL: http://www.sciencedirect.com/science/article/pii/0003491678901768 (cit. on p. 7).

[36] T. S. Bunch and P. C. W. Davies. 'Quantum field theory in de Sitter space - Renormalization by point-splitting'. In: *Royal Society of London Proceedings Series A* 360 (Mar. 1978), pp. 117–134 (cit. on p. 20).

[37] Scott Burles, Kenneth M. Nollett and Michael S. Turner. 'Big bang nucleosynthesis predictions for precision cosmology'. In: *Astrophys.J.* 552 (2001), pp. L1–L6. arXiv: astro-ph/0010171 [astro-ph] (cit. on p. 3).

[38] Christian T. Byrnes, Mischa Gerstenlauer et al. 'Scale-dependent non-Gaussianity probes inflationary physics'. In: *JCAP* 1010 (2010), p. 004. arXiv: 1007.4277 [astro-ph.CO] (cit. on p. 34).

[39] Christian T. Byrnes, Misao Sasaki and David Wands. 'The primordial trispectrum from inflation'. In: *Phys.Rev.* D74 (2006), p. 123519. arXiv: astro-ph/0611075 [astro-ph] (cit. on p. 41).

[40] Xingang Chen. 'Primordial Non-Gaussianities from Inflation Models'. In: *Adv. Astron.* 2010 (2010), p. 638979. arXiv: 1002.1416 [astro-ph.CO] (cit. on pp. 21, 34, 36, 39).

[41] Xingang Chen, Richard Easther and Eugene A. Lim. 'Large Non-Gaussianities in Single Field Inflation'. In: *JCAP* 0706 (2007), p. 023. arXiv: astro-ph/0611645 [astro-ph] (cit. on p. 29).

[42] Xingang Chen, Richard Easther and Eugene A. Lim. 'Generation and Characterization of Large Non-Gaussianities in Single Field Inflation'. In: *JCAP* 0804 (2008), p. 010. arXiv: 0801.3295 [astro-ph] (cit. on p. 29).

[43] Xingang Chen, Min-xin Huang et al. 'Observational signatures and non-Gaussianities of general single field inflation'. In: *JCAP* 0701 (2007), p. 002. arXiv: hep-th/0605045 [hep-th] (cit. on pp. 29, 30).

[44] Xingang Chen and Yi Wang. 'Quasi-Single Field Inflation and Non-Gaussianities'. In: *JCAP* 1004 (2010), p. 027. arXiv: 0911.3380 [hep-th] (cit. on p. 29).

[45] Clifford Cheung et al. 'The Effective Field Theory of Inflation'. In: *JHEP* 0803 (2008), p. 014. arXiv: 0709.0293 [hep-th] (cit. on p. 30).

[46] K. Choi et al. 'Stability of flux compactifications and the pattern of supersymmetry breaking'. In: *JHEP* 0411 (2004), p. 076. arXiv: hep-th/0411066 [hep-th] (cit. on p. 31).

[47] A. Cimatti et al. 'Euclid Assessment Study Report for the ESA Cosmic Visions'. In: (2009). arXiv: 0912.0914 [astro-ph.CO] (cit. on p. 42).

[48] A. Clocchiatti et al. 'Hubble Space Telescope and Ground-Based Observations of Type Ia Supernovae at Redshift 0.5: Cosmological Implications'. In: *Astrophys.J.* 642 (2006), pp. 1–21. arXiv: astro-ph/0510155 [astro-ph] (cit. on p. 25).

[49] Matthew Colless et al. 'The 2dF Galaxy Redshift Survey: Spectra and redshifts'. In: *Mon.Not.Roy.Astron.Soc.* 328 (2001), p. 1039. arXiv: astro-ph/0106498 [astro-ph] (cit. on p. 3).

[50] Paolo Creminelli et al. 'Limits on non-gaussianities from wmap data'. In: *JCAP* 0605 (2006), p. 004. arXiv: astro-ph/0509029 [astro-ph] (cit. on p. 34).

[51] Mafalda Dias, Jonathan Frazer and Andrew R. Liddle. 'Multifield consequences for D-brane inflation'. In: (2012). arXiv: 1203.3792 [astro-ph.CO] (cit. on p. 40).

[52] Mafalda Dias and David Seery. 'Transport equations for the inflationary spectral index'. In: *Phys.Rev.* D85 (2012), p. 043519. arXiv: 1111.6544 [astro-ph.CO] (cit. on p. 40).

[53] Joseph Elliston et al. 'Evolution of $f_{\rm NL}$ to the adiabatic limit'. In: *JCAP* 1111 (2011), p. 005. arXiv: 1106.2153 [astro-ph.CO] (cit. on p. 31).

[54] Toby Falk, Raghavan Rangarajan and Mark Srednicki. 'The Angular dependence of the three point correlation function of the cosmic microwave background radiation as predicted by inflationary cosmologies'. In: *Astrophys.J.* 403 (1993), p. L1. arXiv: astro-ph/9208001 [astro-ph] (cit. on p. 32).

[55] J.R. Fergusson and E.P.S. Shellard. 'The shape of primordial non-Gaussianity and the CMB bispectrum'. In: *Phys.Rev.* D80 (2009), p. 043510. arXiv: 0812.3413 [astro-ph] (cit. on p. 34).

[56] D.J. Fixsen et al. 'The Cosmic Microwave Background spectrum from the full COBE FIRAS data set'. In: *Astrophys.J.* 473 (1996), p. 576. arXiv: astro-ph/9605054 [astro-ph] (cit. on p. 3).

[57] Alejandro Gangui et al. 'The Three point correlation function of the cosmic microwave background in inflationary models'. In: *Astrophys.J.* 430 (1994), pp. 447–457. arXiv: astro-ph/9312033 [astro-ph] (cit. on pp. 32, 38).

[58] Tommaso Giannantonio et al. 'Constraining primordial non-Gaussianity with future galaxy surveys'. In: *Mon.Not.Roy.Astron.Soc.* 422 (2012), pp. 2854–2877. arXiv: 1109.0958 [astro-ph.CO] (cit. on p. 42).

[59] Christopher Gordon et al. 'Adiabatic and entropy perturbations from inflation'. In: *Phys.Rev.* D63 (2001), p. 023506. arXiv: astro-ph/0009131 [astro-ph] (cit. on p. 32).

[60] I. S. Gradshteyn and I. M. Ryzhik. *Table of integrals, series, and products*. Seventh. Translated from the Russian, Translation edited and with a preface by Alan Jeffrey and Daniel Zwillinger, With one CD-ROM (Windows, Macintosh and UNIX). Elsevier/Academic Press, Amsterdam, 2007, pp. xlviii+1171. ISBN: 978-0-12-373637-6; 0-12-373637-4 (cit. on p. 25).

[61] Alan H. Guth. 'Inflationary universe: A possible solution to the horizon and flatness problems'. In: *Phys. Rev. D* 23 (2 Jan. 1981), pp. 347–356. URL: http://link.aps.org/doi/10.1103/PhysRevD.23.347 (cit. on p. 7).

[62] Alan H. Guth and So-Young Pi. 'Fluctuations in the New Inflationary Universe'. In: *Phys. Rev. Lett.* 49 (15 Oct. 1982), pp. 1110–1113. URL: http://link.aps.org/doi/10.1103/PhysRevLett.49.1110 (cit. on p. 16).

[63] Alan H. Guth and So-Young Pi. 'The Quantum Mechanics of the Scalar Field in the New Inflationary Universe'. In: *Phys.Rev.* D32 (1985), pp. 1899–1920 (cit. on p. 16).

[64] Girma Hailu and S.-H. Henry Tye. 'Structures in the Gauge/Gravity Duality Cascade'. In: *JHEP* 0708 (2007), p. 009. arXiv: hep-th/0611353 [hep-th] (cit. on p. 30).

[65] E. R. Harrison. 'Fluctuations at the Threshold of Classical Cosmology'. In: *Phys. Rev. D* 1 (10 May 1970), pp. 2726–2730. URL: http://link.aps.org/doi/10.1103/PhysRevD.1.2726 (cit. on p. 22).

[66] G. Hinshaw et al. 'Nine-Year Wilkinson Microwave Anisotropy Probe (WMAP) Observations: Cosmological Parameter Results'. In: *Astrophys.J.Suppl.* 208 (2013), p. 19. arXiv: 1212.5226 [astro-ph.CO] (cit. on p. 24).

[67] R. Holman and Andrew J. Tolley. 'Enhanced Non-Gaussianity from Excited Initial States'. In: *JCAP* 0805 (2008), p. 001. arXiv: 0710.1302 [hep-th] (cit. on p. 29).

[68] Shaun Hotchkiss and Subir Sarkar. 'Non-Gaussianity from violation of slow-roll in multiple inflation'. In: *JCAP* 1005 (2010), p. 024. arXiv: 0910.3373 [astro-ph.CO] (cit. on p. 30).

[69] Ian Huston. 'Constraining Inflationary Scenarios with Braneworld Models and Second Order Cosmological Perturbations'. In: (2010). arXiv: 1006.5321 [astro-ph.CO] (cit. on p. 38).

[70] Z. Ivezic et al. 'LSST: from Science Drivers to Reference Design and Anticipated Data Products'. In: (2008). arXiv: 0805.2366 [astro-ph] (cit. on p. 42).

[71] Minu Joy, Varun Sahni and Alexei A. Starobinsky. 'A New Universal Local Feature in the Inflationary Perturbation Spectrum'. In: *Phys.Rev.* D77 (2008), p. 023514. arXiv: 0711.1585 [astro-ph] (cit. on p. 30).

[72] D. Kazanas. 'Dynamics of the Universe and Spontaneous Symmetry Breaking'. In: *Astrophys.J.* 241 (1980), pp. L59–L63 (cit. on p. 7).

[73] L.A. Kofman and A.D. Linde. 'Generation of density perturbations in inflationary cosmology'. In: *Nuclear Physics B* 282 (1987), pp. 555–588. ISSN: 0550-3213. URL: http://www.sciencedirect.com/science/article/pii/0550321387906985 (cit. on p. 31).

[74] A. Kogut et al. 'Wilkinson Microwave Anisotropy Probe (WMAP) first year observations: TE polarization'. In: *Astrophys.J.Suppl.* 148 (2003), p. 161. arXiv: astro-ph/0302213 [astro-ph] (cit. on p. 28).

[75] E. Komatsu, N. Afshordi et al. 'Non-Gaussianity as a Probe of the Physics of the Primordial Universe and the Astrophysics of the Low Redshift Universe'. In: (2009). arXiv: 0902.4759 [astro-ph.CO] (cit. on p. 32).

[76] Komatsu and Spergel. 'Acoustic signatures in the primary microwave background bispectrum'. In: *Phys.Rev.* D63 (2001), p. 063002. arXiv: astro-ph/0005036 [astro-ph] (cit. on p. 38).

[77] Andrew R. Liddle and David H. Lyth. 'COBE, gravitational waves, inflation and extended inflation'. In: *Phys.Lett.* B291 (1992), pp. 391–398. arXiv: astro-ph/9208007 [astro-ph] (cit. on p. 22).

[78] Andrei D. Linde. 'A New Inflationary Universe Scenario: A Possible Solution of the Horizon, Flatness, Homogeneity, Isotropy and Primordial Monopole Problems'. In: *Phys.Lett.* B108 (1982), pp. 389–393 (cit. on p. 7).

[79] Andrei D. Linde. 'Chaotic Inflation'. In: *Phys.Lett.* B129 (1983), pp. 177–181 (cit. on pp. 7, 13, 23).

[80] Andrei D. Linde. 'Generation of Isothermal Density Perturbations in the Inflationary Universe'. In: *Phys.Lett.* B158 (1985), pp. 375–380 (cit. on p. 31).

[81] Andrei D. Linde. 'Inflation and string cosmology'. In: *Prog.Theor.Phys.Suppl.* 163 (2006), pp. 295–322. arXiv: hep-th/0503195 [hep-th] (cit. on p. 31).

[82] D. H. Lyth. 'Large-scale energy-density perturbations and inflation'. In: *Phys. Rev. D* 31 (8 Apr. 1985), pp. 1792–1798. URL: http://link.aps.org/doi/10.1103/PhysRevD.31.1792 (cit. on pp. 16, 38).

[83] D. H. Lyth and A. R. Liddle. *The Primordial Density Perturbation*. Ed. by Lyth, D. H. & Liddle, A. R. 2009 (cit. on pp. 13, 17, 22, 33).

[84] David H. Lyth, Karim A. Malik and Misao Sasaki. 'A General proof of the conservation of the curvature perturbation'. In: *JCAP* 0505 (2005), p. 004. arXiv: astro-ph/0411220 [astro-ph] (cit. on p. 18).

[85] David H. Lyth and Antonio Riotto. 'Particle physics models of inflation and the cosmological density perturbation'. In: *Phys.Rept.* 314 (1999), pp. 1–146. arXiv: hep-ph/9807278 [hep-ph] (cit. on p. 29).

[86] David H. Lyth and Yeinzon Rodriguez. 'Non-gaussianity from the second-order cosmological perturbation'. In: *Phys. Rev.* D71 (2005), p. 123508. arXiv: astro-ph/0502578 (cit. on p. 40).

[87] David H. Lyth and Yeinzon Rodriguez. 'The Inflationary prediction for primordial non-Gaussianity'. In: *Phys.Rev.Lett.* 95 (2005), p. 121302. arXiv: astro-ph/0504045 [astro-ph] (cit. on pp. 38, 39).

[88] David H. Lyth and David Seery. 'Classicality of the primordial perturbations'. In: *Phys.Lett.* B662 (2008), pp. 309–313. arXiv: astro-ph/0607647 [astro-ph] (cit. on p. 16).

[89] D.H. Lyth. 'A Bound on Inflationary Energy Density From the Isotropy of the Microwave Background'. In: *Phys.Lett.* B147 (1984), p. 403 (cit. on p. 23).

[90] D.H. Lyth. 'Large Scale Energy Density Perturbations and Inflation'. In: *Phys.Rev.* D31 (1985), pp. 1792–1798 (cit. on pp. 16, 18, 38).

[91] Juan Martin Maldacena. 'Non-Gaussian features of primordial fluctuations in single field inflationary models'. In: *JHEP* 05 (2003), p. 013. arXiv: astro-ph/0210603 (cit. on pp. 11, 18, 19, 32, 33, 35–38, 40).

[92] Liam McAllister and Eva Silverstein. 'String Cosmology: A Review'. In: *Gen.Rel.Grav.* 40 (2008), pp. 565–605. arXiv: 0710.2951 [hep-th] (cit. on p. 31).

[93] Pieter Daniel Meerburg, Jan Pieter van der Schaar and Pier Stefano Corasaniti. 'Signatures of Initial State Modifications on Bispectrum Statistics'. In: *JCAP* 0905 (2009), p. 018. arXiv: 0901.4044 [hep-th] (cit. on pp. 29, 34).

[94] A. Melchiorri et al. 'A measurement of omega from the North American test flight of BOOMERANG'. In: *Astrophys.J.* 536 (2000), pp. L63–L66. arXiv: astro-ph/9911445 [astro-ph] (cit. on p. 25).

[95] Viatcheslav F. Mukhanov. 'Gravitational Instability of the Universe Filled with a Scalar Field'. In: *JETP Lett.* 41 (1985), pp. 493–496 (cit. on p. 16).

[96] Viatcheslav F. Mukhanov, H.A. Feldman and Robert H. Brandenberger. 'Theory of cosmological perturbations. Part 1. Classical perturbations. Part 2. Quantum theory of perturbations. Part 3. Extensions'. In: *Phys.Rept.* 215 (1992), pp. 203–333 (cit. on p. 19).

[97] David J. Mulryne. 'Transporting non-Gaussianity from sub to super-horizon scales'. In: *JCAP* 1309 (2013), p. 010. arXiv: 1302.3842 [astro-ph.CO] (cit. on p. 40).

[98] David J. Mulryne, David Seery and Daniel Wesley. 'Moment transport equations for non-Gaussianity'. In: *JCAP* 1001 (2010), p. 024. arXiv: 0909.2256 [astro-ph.CO] (cit. on p. 40).

[99] David J. Mulryne, David Seery and Daniel Wesley. 'Moment transport equations for the primordial curvature perturbation'. In: *JCAP* 1104 (2011). * Temporary entry *, p. 030. arXiv: 1008.3159 [astro-ph.CO] (cit. on p. 40).

[100] Takahiro T. Nakamura and Ewan D. Stewart. 'The Spectrum of cosmological perturbations produced by a multicomponent inflaton to second order in the slow roll approximation'. In: *Phys.Lett.* B381 (1996), pp. 413–419. arXiv: astro-ph/9604103 [astro-ph] (cit. on p. 31).

[101] Masahiro Nakashima et al. 'The effect of varying sound velocity on primordial curvature perturbations'. In: *Prog.Theor.Phys.* 125 (2011), pp. 1035–1052. arXiv: 1009.4394 [astro-ph.CO] (cit. on p. 30).

[102] B. E. J. Pagel and G. Tautvaisiene. 'Chemical evolution of primary elements in the Galactic disc: an analytical model'. In: *mnras* 276 (Sept. 1995), pp. 505–514 (cit. on p. 2).

[103] H.V. Peiris et al. 'First year Wilkinson Microwave Anisotropy Probe (WMAP) observations: Implications for inflation'. In: *Astrophys.J.Suppl.* 148 (2003), p. 213. arXiv: astro-ph/0302225 [astro-ph] (cit. on p. 28).

[104] Arno A. Penzias and Robert Woodrow Wilson. 'A Measurement of excess antenna temperature at 4080-Mc/s'. In: *Astrophys.J.* 142 (1965), pp. 419–421 (cit. on p. 3).

[105] David Polarski and Alexei A. Starobinsky. 'Semiclassicality and decoherence of cosmological perturbations'. In: *Class.Quant.Grav.* 13 (1996), pp. 377–392. arXiv: gr-qc/9504030 [gr-qc] (cit. on p. 16).

[106] G.I. Rigopoulos and E.P.S. Shellard. 'The separate universe approach and the evolution of nonlinear superhorizon cosmological perturbations'. In: *Phys.Rev.* D68 (2003), p. 123518. arXiv: astro-ph/0306620 [astro-ph] (cit. on p. 18).

[107] Mairi Sakellariadou. 'Production of Topological Defects at the End of Inflation'. In: *Lect.Notes Phys.* 738 (2008), pp. 359–392. arXiv: hep-th/0702003 [hep-th] (cit. on p. 10).

[108] D.S. Salopek and J.R. Bond. 'Nonlinear evolution of long wavelength metric fluctuations in inflationary models'. In: *Phys.Rev.* D42 (1990), pp. 3936–3962 (cit. on p. 32).

[109] Misao Sasaki. 'Large Scale Quantum Fluctuations in the Inflationary Universe'. In: *Progress of Theoretical Physics* 76.5 (1986), pp. 1036–1046. eprint: http://ptp.oxfordjournals.org/content/76/5/1036.full.pdf+html. URL: http://ptp.oxfordjournals.org/content/76/5/1036.abstract (cit. on p. 16).

[110] Misao Sasaki and Ewan D. Stewart. 'A General analytic formula for the spectral index of the density perturbations produced during inflation'. In: *Prog.Theor.Phys.* 95 (1996), pp. 71–78. arXiv: astro-ph/9507001 [astro-ph] (cit. on p. 31).

[111] K. Sato. 'First Order Phase Transition of a Vacuum and Expansion of the Universe'. In: *Mon.Not.Roy.Astron.Soc.* 195 (1981), pp. 467–479 (cit. on p. 7).

[112] David N. Schramm and Michael S. Turner. 'Big bang nucleosynthesis enters the precision era'. In: *Rev.Mod.Phys.* 70 (1998), pp. 303–318. arXiv: astro-ph/9706069 [astro-ph] (cit. on p. 2).

[113] David Seery and James E. Lidsey. 'Primordial non-gaussianities from multiple-field inflation'. In: *JCAP* 0509 (2005), p. 011. arXiv: astro-ph/0506056 (cit. on pp. 37, 39).

[114] David Seery and James E. Lidsey. 'Non-Gaussianity from the inflationary trispectrum'. In: *JCAP* 0701 (2007), p. 008. arXiv: astro-ph/0611034 [astro-ph] (cit. on p. 41).

[115] David Seery, James E. Lidsey and Martin S. Sloth. 'The inflationary trispectrum'. In: *JCAP* 0701 (2007), p. 027. arXiv: astro-ph/0610210 [astro-ph] (cit. on p. 41).

[116] Toyokazu Sekiguchi and Naoshi Sugiyama. 'Optimal constraint on g_{NL} from CMB'. In: *JCAP* 1309 (2013), p. 002. arXiv: 1303.4626 [astro-ph.CO] (cit. on p. 42).

[117] Leonardo Senatore, Kendrick M. Smith and Matias Zaldarriaga. 'Non-Gaussianities in Single Field Inflation and their Optimal Limits from the WMAP 5-year Data'. In: *JCAP* 1001 (2010), p. 028. arXiv: 0905.3746 [astro-ph.CO] (cit. on p. 34).

[118] Leonardo Senatore and Matias Zaldarriaga. 'The Effective Field Theory of Multifield Inflation'. In: *JHEP* 1204 (2012), p. 024. arXiv: 1009.2093 [hep-th] (cit. on p. 30).

[119] Joseph Silk and Michael S. Turner. 'Double inflation'. In: *Phys. Rev. D* 35 (2 Jan. 1987), pp. 419–428. URL: http://link.aps.org/doi/10.1103/PhysRevD.35.419 (cit. on p. 31).

[120] V. M. Slipher. 'The radial velocity of the Andromeda Nebula'. In: *Lowell Observatory Bulletin* 2 (1913), pp. 56–57 (cit. on p. 2).

[121] D.N. Spergel et al. 'First year Wilkinson Microwave Anisotropy Probe (WMAP) observations: Determination of cosmological parameters'. In: *Astrophys.J.Suppl.* 148 (2003), pp. 175–194. arXiv: astro-ph/0302209 [astro-ph] (cit. on p. 28).

[122] Alexei A. Starobinsky. 'A New Type of Isotropic Cosmological Models Without Singularity'. In: *Phys.Lett.* B91 (1980), pp. 99–102 (cit. on p. 7).

[123] Alexei A. Starobinsky. 'Multicomponent de Sitter (Inflationary) Stages and the Generation of Perturbations'. In: *JETP Lett.* 42 (1985), pp. 152–155 (cit. on p. 38).

[124] Alexei A. Starobinsky. 'Spectrum of adiabatic perturbations in the universe when there are singularities in the inflation potential'. In: *JETP Lett.* 55 (1992), pp. 489–494 (cit. on p. 30).

[125] Leonard Susskind. 'The Anthropic landscape of string theory'. In: (2003). arXiv: hep-th/0302219 [hep-th] (cit. on p. 31).

[126] Gerard 't Hooft. 'Magnetic Monopoles in Unified Gauge Theories'. In: *Nucl.Phys.* B79 (1974), pp. 276–284 (cit. on p. 8).

[127] Licia Verde et al. 'Large scale structure, the cosmic microwave background, and primordial non-gaussianity'. In: *Mon.Not.Roy.Astron.Soc.* 313 (2000), pp. L141–L147. arXiv: astro-ph/9906301 [astro-ph] (cit. on p. 38).

[128] Filippo Vernizzi and David Wands. 'Non-gaussianities in two-field inflation'. In: *JCAP* 0605 (2006), p. 019. arXiv: astro-ph/0603799 [astro-ph] (cit. on p. 40).

[129] David Wands. 'Local non-Gaussianity from inflation'. In: *Class. Quant. Grav.* 27 (2010), p. 124002. arXiv: 1004.0818 [astro-ph.CO] (cit. on p. 39).

[130] David Wands et al. 'A New approach to the evolution of cosmological perturbations on large scales'. In: *Phys.Rev.* D62 (2000), p. 043527. arXiv: astro-ph/0003278 [astro-ph] (cit. on p. 19).

[131] Limin Wang and Marc Kamionkowski. 'Cosmic microwave background bispectrum and inflation'. In: *Phys. Rev. D* 61 (6 Feb. 2000), p. 063504. URL: http://link.aps.org/doi/10.1103/PhysRevD.61.063504 (cit. on p. 32).

[132] Wang and Kamionkowski. 'The Cosmic microwave background bispectrum and inflation'. In: *Phys.Rev.* D61 (2000), p. 063504. arXiv: astro-ph/9907431 [astro-ph] (cit. on pp. 29, 38).

[133] Steven Weinberg. *Gravitation and Cosmology*. John Wiley & Sons, 1972 (cit. on p. 4).

[134] Steven Weinberg. 'Must cosmological perturbations remain non-adiabatic after multi-field inflation?' In: *Phys.Rev.* D70 (2004), p. 083522. arXiv: astro-ph/0405397 [astro-ph] (cit. on p. 18).

[135] Ignacio Zaballa, Yeinzon Rodriguez and David H. Lyth. 'Higher order contributions to the primordial non-Gaussianity'. In: *JCAP* 0606 (2006), p. 013. arXiv: astro-ph/0603534 [astro-ph] (cit. on p. 40).

[136] Matias Zaldarriaga. 'Lensing of the CMB: Non-Gaussian aspects'. In: *Phys.Rev.* D62 (2000), p. 063510. arXiv: astro-ph/9910498 [astro-ph] (cit. on p. 41).

[137] Ya.B. Zeldovich. 'Gravitational instability: An Approximate theory for large density perturbations'. In: *Astron.Astrophys.* 5 (1970), pp. 84–89 (cit. on p. 22).

Paper 1

Optimal bispectrum constraints on single-field models of inflation

Gemma J. Anderson, Donough Regan and David Seery

We use WMAP 9-year bispectrum data to constrain the free parameters of an 'effective field theory' describing fluctuations in single-field inflation. The Lagrangian of the theory contains a finite number of operators associated with unknown mass scales. Each operator produces a fixed bispectrum shape, which we decompose into partial waves in order to construct a likelihood function. Based on this likelihood we are able to constrain four linearly independent combinations of the mass scales. As an example of our framework we specialize our results to the case of 'Dirac–Born–Infeld' and 'ghost' inflation and obtain the posterior probability for each model, which in Bayesian schemes is a useful tool for model comparison. Our results suggest that DBI-like models with two or more free parameters are disfavoured by the data by comparison with single-parameter models in the same class.

1.1 INTRODUCTION

Successive microwave-background surveys have accumulated some evidence for the inflationary paradigm, in which structure in the universe was seeded by quantum fluctuations during an epoch preceding the hot, dense phase where nucleosynthesis occurred (Ade et al. 2013; Hinshaw et al. 2013). But despite broad support for the overall framework, attempts to identify the precise degrees of freedom whose quantum fluctuations were relevant have met with less success. Whatever microphysics underlay the putative inflationary epoch remains mysterious.

In scattering experiments, an abundance of observables—including, among others, branching ratios, decay rates, and differential dependence on energy or angles—allow indirect access to microphysical information through reconstruction of the correlation functions, or 'n-point functions'. These measure interference between quantum fluctuations and encode information about the dynamics of the theory. It is the rich information which can be obtained from reconstruction of the correlation functions which makes measurements in particle physics so constraining.

In cosmology our observables are more limited and so is the degree to which the n-point functions can be reconstructed. Over a narrow range of scales, the n-point functions of the cosmic microwave background ('CMB') anisotropies are sensitive to the n-point functions of the primordial 'curvature perturbation', which is a calculable, model-dependent mix of the fluctuations imprinted on the light fields of the inflationary epoch. This correspondence has been used for many years to place restrictions on the inflationary model space from measurements of the CMB temperature and polarization two-point functions. But if a *three*-point function of the CMB anisotropies could be measured it would provide access to more nuanced and discriminating microphysical information. Ideally we would like to observe systematic relationships between the n-point functions which would point clearly to a quantum mechanical origin for the fluctuations. This is important because it is unclear whether we could ever rule out a non-quantum origin (perhaps associated with new but non-inflationary physics at early times) using only the two-point function.[1]

Measurements of the CMB temperature anisotropy have now reached sufficient accuracy that it is feasible to estimate the three-point temperature autocorrelation function. The most precise constraints come from the Planck2013 dataset (Ade et al. 2013). But despite the quality of the measurements, the signal-to-noise for any particular combination of wavenumbers is still too low

[1]If the fluctuations were produced by a classical process, e.g. a thermal process, then, as a result of the central-limit theorem, they would be random in nature. We would therefore not expect the correlation functions to have detailed momentum dependences that are produced by quantum fluctuations.

to allow the three-point function to be reconstructed directly. Instead, measurements are made by picking an Ansatz or 'template' for the way in which the correlations change with wavenumber. By comparing this template with the CMB data over many different combinations of wavenumber it is possible to attain reasonable signal-to-noise. This comparison carries a considerable computational burden, so constraints from the data are typically reported as amplitudes for just a handful of well-known templates, such as the 'local', 'equilateral' and 'orthogonal' shapes. These amplitudes are often written $\hat{f}_{\rm NL}^{\rm local}$, $\hat{f}_{\rm NL}^{\rm equi}$, $\hat{f}_{\rm NL}^{\rm ortho}$, and so on.[2]

A specific inflationary model will be characterized by a number N_λ of adjustable parameters λ_i, $1 \leqslant i \leqslant N_\lambda$. These may include Lagrangian parameters which are analogues of masses and couplings, but in multiple-field models may also include a specification of the initial conditions in field-space. To apply constraints from $\hat{f}_{\rm NL}^{\rm local}$, $\hat{f}_{\rm NL}^{\rm equi}$, $\hat{f}_{\rm NL}^{\rm ortho}$, ..., to such a model its three-point function must be computed and projected on to each of these templates. This generates predictions for each of the amplitudes $f_{\rm NL}^{\rm local}(\lambda_i)$, $f_{\rm NL}^{\rm equi}(\lambda_i)$, $f_{\rm NL}^{\rm ortho}(\lambda_i)$, ... The results obtained by a microwave background survey can then be converted into constraints on the underlying parameters λ_i.

This approach is perfectly reasonable, but there are reasons to expect that it may not be optimal. First, if the set of templates does not cover the entire range of three-point correlations which can be produced by adjusting the parameters λ_i then we are not making efficient use of the data: we should measure the amplitude of more templates in order to obtain better constraints. But, as many authors have pointed out, it is not clear *a priori* how large a range of templates is required, or how they should be chosen.

Second, if our templates are chosen injudiciously then there will come a point of diminishing returns at which no new information is gained because the shapes we are fitting are strongly correlated with shapes which have been tried before. This is a reflection of a more general problem: the error bars reported for any set of amplitudes will typically be correlated, with the correlation described by some covariance matrix. Without knowledge of these covariances we risk underestimating the uncertainties associated with our reconstruction of the parameters λ_i.

In this paper we take a different approach. We investigate the construction of maximum-likelihood estimators for the Lagrangian parameters λ_i directly from the data. (Because noise maps for the Planck2013 data release are not yet available, we use the WMAP 9-year dataset.) To decide which templates to use, we catalogue the different types of correlation which can be produced in a well-specified class of models: those whose fluctuations are described the the effective field theory of inflation (Cheung, Creminelli et al. 2008). We construct the Fisher matrix associated with these correlations and use it to determine the principal directions whose amplitudes can

[2]Here and throughout the remainder of the paper we distinguish quantities estimated from data by a hat.

be measured efficiently. We account for the covariance between measurements of these amplitudes and use them to place constraints on the underlying Lagrangian parameters.

Summary.—In §1.2 we briefly review the effective field theory approach to single-field inflation and catalogue the operators arising from a general single-field action. In §1.3 we discuss the calculation of bispectra corresponding to these operators, and point out a number of subtleties which must be borne in mind when interpreting our results. In §1.4 we assemble the formalism which is used to extract constraints from the CMB map: in §1.4.1 we construct the Fisher matrix and use it to determine the principal directions which can be constrained efficiently, and in §2.6 we report our measurements of their amplitudes from the 9-year WMAP dataset. §1.5 translates these general constraints into the language of specific models, and §1.6 uses the framework of Bayesian model comparison to gain some qualitative information regarding the type of model favoured by the data. We conclude in §2.7. A short appendix tabulates the three-point functions used in the main text.

Notation.—We use units in which $c = \hbar = 1$, and define the reduced Planck mass $M_{\rm P}$ to be $M_{\rm P}^{-2} = 8\pi G$. Our index and summation conventions are explained in the main text.

1.2 Overview of the effective field theory of inflation

In this paper we focus on single-field models of inflation which terminate in a unique minimum, which we refer to as the 'reheating minimum'. In multiple-field models there are complications associated with our freedom to set initial conditions. These determine the average field-space trajectory followed by the region of the universe we choose to study. In a single-field model there is a unique trajectory which terminates in the reheating minimum.

In both single- and multiple-field cases it is quantum fluctuations around this average field-space trajectory which are inherited by the large-scale density perturbation, but where there is no unique trajectory the calculation of these fluctuations is a serious computational challenge. Their evolution must be followed until an 'adiabatic limit' has been reached, at which all isocurvature modes become exhausted (Weinberg 2003; Weinberg 2004a; Weinberg 2004b; Meyers and Sivanandam 2011; Elliston, Mulryne et al. 2011). Normally this will require numerical methods. In contrast, the fluctuations produced in single-field inflation—or, more precisely, 'single-clock' inflation (only one relevant degree of freedom)—typically do not evolve and can be computed analytically under certain circumstances. Below, we discuss the precise conditions which

are required.

Model parametrization.—Our aim is to estimate the Lagrangian parameters which characterize a single-field inflationary model. How many such parameters are needed? The answer depends on the range of behaviour which we allow. Cheung et al. gave an argument based on nonlinearly realized Lorentz invariance which, under certain conditions, constrains the possible three-body interactions between scalar perturbations on a smooth inflationary background (Cheung, Creminelli et al. 2008). This is the 'effective field theory of inflation'. In this section we briefly review their construction.

The effective field theory is not used to describe the background cosmology, but only fluctuations around it. Therefore it is agnostic regarding the precise mechanism of inflation. The background is assumed to be described by a Robertson–Walker metric

$$\mathrm{d}s^2 = -\mathrm{d}t^2 + a^2(t)\,\mathrm{d}\mathbf{x}^2, \tag{1.1}$$

where $a(t)$ is the scale factor, t is cosmic time and $H(t) = \dot{a}/a$ is the Hubble rate. Since the background is evolving it spontaneously breaks time-translation invariance (and therefore manifest Lorentz invariance), but because the spatial slices are homogeneous and isotropic the background remains manifestly invariant under spatial coordinate transformations. We will use the terminology 'coordinate transformations' and 'diffeomorphisms' interchangeably.

Knowledge of the background evolution is equivalent to specifying $H(t)$ as a smooth function of t. The condition that the universe is 'single-clock' is that a coordinate system exists in which only the metric carries fluctuations; in this coordinate system all fields needed to describe the matter sector are homogeneous, depending only on the time t. By analogy with similar constructions in particle physics, Cheung et al. called this coordinate system the *unitary gauge*. Where the matter sector is described by a single scalar field ϕ it corresponds to the gauge where fluctuations $\delta\phi$ vanish, but this is not necessary.

To describe dynamics we require a Lagrangian. A Lagrangian which is manifestly invariant under the unbroken (linearly-realized) group of purely spatial coordinate transformations will be a function F which transforms as a scalar under these diffeomorphisms. Cheung et al. argued that the most general such Lagrangian could be constructed as a scalar function of the metric and the intrinsic and extrinsic curvature tensors on the spatial slices, together with their covariant derivatives (Cheung, Creminelli et al. 2008). These may appear in arbitrary combinations with t and the metric function g^{00}, which are both invariant under spatial coordinate transformations. Therefore,

$$S_{\mathrm{gen}} = \int \mathrm{d}^4x\, \sqrt{-g}\, F(R_{\mu\nu\rho\sigma}, K_{\mu\nu}, \nabla_\mu, g^{00}, t). \tag{1.2}$$

By itself, this Lagrangian can describe fluctuations around any cosmological background with linearly-realized spatial diffeomorphism invariance. Specializing it to the background $H(t)$ fixes the background and linear terms,

$$S = \int \mathrm{d}^4x\ \sqrt{-g}\Big(\frac{M_{\rm P}^2}{2}R + M_{\rm P}^2\dot{H}g^{00} - M_{\rm P}^2(3H^2+\dot{H}) + \sum_{n\geqslant 2} F_n(\delta R_{\mu\nu\rho\sigma}, \delta K_{\mu\nu}, \nabla_\mu, \delta g^{00}, t)\Big), \quad (1.3)$$

where $\delta R_{\mu\nu\rho\sigma}$ and $\delta K_{\mu\nu}$ are, respectively, perturbations in the intrinsic and extrinsic curvature tensors, and $\delta g^{00} = g^{00} + 1$ is the perturbation in the time–time metric function or 'lapse'. The arbitrary functions F_n are homogeneous polynomials of order n, and therefore the leading correction to the first three terms appearing in (1.3) is quadratic.

We have not yet made use of the requirement that the full theory is invariant under time reparametrizations, $t \to t' = t + \xi(\mathbf{x})$, where the translation ξ may be a function of position.[3] On an expanding cosmological background this symmetry is spontaneously broken. Nevertheless, once a choice of spatially-invariant operators has been made in Eq. (1.3), the broken time-translation symmetry is strong enough to fix the interactions of one scalar mode. To determine these interactions we construct a new action by formally performing a time translation $t \to t' = t - \pi$. If we promote π to a dynamical field which shifts linearly under time translations (that is, $\pi \to \pi' = \pi - \xi$ when $t \to t' = t + \xi$) then the total action becomes manifestly invariant. The field π represents a scalar degree of freedom in the system, but its interactions are fixed uniquely by the combination of tensors appearing in the F_n, the background cosmology $H(t)$, and the time translation symmetry (Creminelli, Luty et al. 2006; Cheung, Creminelli et al. 2008; Cheung, Fitzpatrick et al. 2008; Weinberg 2008; Senatore, Smith and Zaldarriaga 2010)

For this formalism to be useful it must be possible to calculate each amplitude of interest using states which contain no more than a handful of π particles, or π-lines in diagrammatic terms. This is not generally true. But if all background fields are time-independent then rigid time translations $t \mapsto t' = t + \xi$ (with ξ a constant) are a *global* symmetry of the theory, no matter what transformation law we ascribe to π. Therefore π must behave as a Goldstone boson: where it appears in the action it must be accompanied by at least one derivative. In a process which takes place at a well-defined characteristic energy scale E, each derivative will translate to a power of E. The justification for neglecting diagrams which contain a large number of π-lines is then the same as any effective field theory of Goldstone modes, enabling a perturbative expansion in powers of E/M where M is some large mass scale characterizing the strength of the interactions. The mass scale M characterizes the energy scale of the fundamental theory and therefore is necessarily much larger than the energy scale at which we would like to calculate.

[3] An arbitrary action of the form (1.3) can describe theories with this symmetry, in addition to others which do not.

For applications to inflation the background fields are not constant but slowly varying, so rigid time translations are only an approximate symmetry. Therefore terms involving undifferentiated powers of π may appear in the action, although suppressed by dimensionless factors which measure the degree to which the global symmetry is broken. These generate effects which are unaccompanied by powers of E/M and therefore may be important at all energies.[4] However, provided the approximate symmetry is sufficiently good that corrections to it are at least as small as the first neglected power of E/M it is still possible to carry out a consistent calculation. During inflation we are interested in the type of correlations induced by each operator between modes of the quantized field near the epoch of Hubble exit, so the scale E will be of order the Hubble scale H.

At sufficiently high energies $E > E_{\rm mix}$ the Goldstone mode decouples from the remaining degrees of freedom in $\delta R_{\mu\nu\rho\sigma}$ and $\delta K_{\mu\nu}$. (The notation '$E_{\rm mix}$' was introduced by Cheung, Creminelli et al. (2008), who emphasized that below $E_{\rm mix}$ the mixing with gravitational degrees of freedom cannot be ignored.) If the decoupling scale $E_{\rm mix}$ is at least modestly smaller than $E = H$ then it is possible to study how each operator generates correlations without including gravitational fluctuations. In this paper we will work exclusively in the decoupling limit. With this assumption, Bartolo et al. (2010a); Bartolo et al. (2010b) gave an effective action up to cubic terms,

$$\begin{aligned} S_{\rm EFT} = \int {\rm d}^4x\,\sqrt{-g}\Big\{ & M_{\rm P}^2\dot H(\partial_\mu\pi)^2 + 2M_2^4\Big[\dot\pi^2 - \dot\pi\frac{(\partial\pi)^2}{a^2}\Big] - \frac{4}{3}M_3^4\dot\pi^3 \\ & - \frac{\bar M_1^3}{2a^2}\Big[-2H(\partial\pi)^2 + \frac{(\partial\pi)^2\partial^2\pi}{a^2}\Big] \\ & - \frac{\bar M_2^2}{2a^4}\Big[(\partial^2\pi)(\partial^2\pi) + H(\partial^2\pi)(\partial\pi)^2 + 2\dot\pi\partial^2\partial_j\pi\partial_j\pi\Big] \\ & - \frac{\bar M_3^2}{2a^4}\Big[(\partial^2\pi)(\partial^2\pi) + 2H\partial^2\pi(\partial\pi)^2 + 2\dot\pi\partial^2\partial_j\pi\partial_j\pi\Big] \\ & - \frac{2\bar M_4^3}{3a^2}\dot\pi^2\partial^2\pi + \frac{\bar M_5^2}{3a^4}\dot\pi(\partial^2\pi)^2 + \frac{\bar M_6^2}{3a^4}\dot\pi(\partial_i\partial_j\pi)^2 - \frac{\bar M_7}{3!\cdot a^6}(\partial^2\pi)^3 \\ & - \frac{\bar M_8}{3!\cdot a^6}\partial^2\pi(\partial_i\partial_j\pi)^2 - \frac{\bar M_9}{3!\cdot a^6}\partial_i\partial_j\pi\partial_j\partial_k\pi\partial_k\partial_i\pi\Big\}. \end{aligned} \tag{1.4}$$

Our notation has been chosen to match Bartolo et al. (2010a) and Bartolo et al. (2010b). The mass scales M_2, M_3 and $\bar M_1,\ldots,\bar M_9$ characterize the model under consideration.[5] Terms dec-

[4] It is these terms which cause superhorizon evolution of the perturbations in multiple-field models. Their importance at all scales is reflected in the fact that they remain relevant even when k/aH is very soft.

[5] To aid intuition, the powers of the M_i and $\bar M_i$ appearing in Eq. (1.4) have been chosen so that the M_i and $\bar M_i$ all have dimensions of mass when using natural units in which $c = \hbar = 1$. In some cases this means that positive integer powers of masses appear, such as M_3^4, which can only be positive if M_3 is real. In reality there is an undetermined sign which we are suppressing, so that M_3^4 should be regarded as an object which can be either positive or negative. The associated mass scale is $|M_3^4|^{1/4}$.

orated with a bar are associated with operators involving the extrinsic curvature $\delta K_{\mu\nu}$, whereas unbarred terms correspond to powers of δg^{00}. In writing Eq. (1.4), Bartolo et al. did not include all possible operators: they neglected higher-derivative operators containing derivatives of the form $\nabla_\mu \delta g^{00}$ and $\nabla_\lambda K_{\mu\nu}$, and from the lowest-derivative combinations for each M_i or $\bar{M}_i$ they retained only terms which gave a parametrically large contribution to the three-point function. We can expect the higher-derivative operators to be small provided the mass scales M_i, $\bar{M}_i$ are sufficiently large, which is already the condition that the EFT is predictive. Therefore, although (1.4) does not represent the most general set of interactions, it is reasonable to speculate that it may approximate the most general set of *observable* interactions for a smooth background $H(t)$. In this paper we only consider backgrounds which satisfy this smoothness requirement. The properties of fluctuations over backgrounds which are not sufficiently smooth require a separate analysis; for example, see Bartolo, Cannone and Matarrese (2013) and Adshead, Hu and Miranda (2013).

When is the decoupling approximation valid? Estimates for the scale $E_{\rm mix}$ were given by Cheung, Creminelli et al. (2008), but strictly this scale can be determined only when the M_i and $\bar{M}_i$ are known and therefore it must be checked *a posteriori*. As an example, in canonical single-field inflation, Cheung et al. argued that $E_{\rm mix} \sim \epsilon^{1/2} H$, where $\epsilon \equiv -\dot{H}/H^2$ is a measure of the degree to which the global symmetry of rigid time translations is broken. If $\epsilon \ll 1$ then a decoupling regime can exist near the Hubble scale.

The scales M_i and $\bar{M}_i$ can be adjusted to reproduce the results of well-known models including canonical single-field inflation, Dirac–Born–Infeld inflation (Alishahiha, Silverstein and Tong 2004) and Ghost Inflation (Arkani-Hamed et al. 2004). Alternatively they may be allowed to float. The action (1.4) then explores a range of interactions for fluctuations on a quasi-de Sitter background with nonlinearly realized Lorentz invariance, subject to the proviso (as described above) that only the dominant term for each M_i and $\bar{M}_i$ has been retained. In principle these mass scales depend on time, but because we are taking the time-dependence of background quantities to be very weak we will treat them as constants.

1.3 Calculation of the bispectrum

In this paper our aim is to estimate the parameters M_i, $\bar{M}_i$ by using observations to indirectly reconstruct the two- and three-point functions $\langle \pi\pi \rangle$ and $\langle \pi\pi\pi \rangle$. By itself, π is not an observable and neither are its correlations: the measurable quantity is the temperature fluctuation $\delta T/T$ as a

function of angular position on the sky. Typically this is decomposed into harmonics, generating corresponding amplitudes $a_{\ell m}$,

$$\frac{\delta T(\hat{\mathbf{n}})}{T} = \sum_{\ell m} a_{\ell m} Y_{\ell m}(\hat{\mathbf{n}}), \tag{1.5}$$

where $\hat{\mathbf{n}}$ represents an orientation on the sky and $Y_{\ell m}(\hat{\mathbf{n}})$ is a conventionally-normalized spherical harmonic. The amplitude $a_{\ell m}$ can be predicted in terms of primordial quantities using the formula[6]

$$a_{\ell m} = 4\pi(-\mathrm{i})^{\ell} \int \frac{\mathrm{d}^3 k}{(2\pi)^3} \Delta_{\ell}(k) \zeta(\mathbf{k}) Y_{\ell m}(\hat{\mathbf{k}}), \tag{1.6}$$

where the 'curvature perturbation' $\zeta = \delta \ln a(\mathbf{x}, t)$ represents a fluctuation in the local scale factor $a(\mathbf{x}, t)$. It can be related to π via $\zeta = -H\pi$ up to terms which vanish on superhorizon scales, i.e. in the limit $k/aH \to 0$, where k is the Fourier mode under consideration and aH is the comoving wavenumber associated with the Hubble length.

In writing (1.6) we have assumed that, for each relevant Fourier mode, $\zeta(\mathbf{k})$ attains a practically time-independent value by some time during the radiation era. The transfer function $\Delta_{\ell}(k)$ describes the subsequent process by which this time-independent seed perturbation is taken up by fluctuations in the primordial plasma and propagated to the surface of last scattering, where it constitutes a temperature fluctuation δT. Under these circumstances, Eq. (1.6) shows that the n-point functions of the $a_{\ell m}$ can be linearly related to the n-point functions of $\zeta(\mathbf{k})$, and therefore $\pi(\mathbf{k})$, provided we evaluate the curvature perturbation in (1.6) at a time when the $\mathrm{O}(k/aH)$ corrections in the relationship between π and ζ are negligible.

Correlation functions of ζ.—Therefore, we must estimate the correlation functions of ζ at the time they achieve their constant values. It is this requirement which makes the study of multiple-field models challenging (Elliston, Mulryne et al. 2011; Dias, Ribeiro and Seery 2013), because it is difficult to predict in advance when the time-independent epoch will occur. In single-field models the situation is simpler because the approximate global symmetry under rigid time translations (together with certain technical assumptions) is sufficient to prove the operator statement $\dot{\zeta} = 0$ in the limit $k/aH \to 0$ (Assassi, Baumann and Green 2013; Senatore and Zaldarriaga 2010; Senatore and Zaldarriaga 2011; Senatore and Zaldarriaga 2012; Baumann and Green 2011; Baumann, Senatore and Zaldarriaga 2011). Therefore all correlation functions of ζ are constant on superhorizon scales, where $|k/aH|$ is negligible. An important consequence of this result is that subleading terms in the effective action (1.4) map to subleading terms in each n-point function (Dias, Ribeiro and Seery 2013), so to obtain a lowest-order result there is no need to consider corrections to (1.4) due to our neglect of time dependence in the M_i, $\bar{M}_i$.

[6] We have absorbed a conventional factor of $3/5$ into the normalization of the transfer function.

In perturbation theory, a three- or higher n-point function is computed by integrating the reaction rate for an n-body interaction together with factors representing the available interaction volume and the probability for suitable particles to be present. These techniques were first applied to inflation by Maldacena (2003) and later refined by various authors (Creminelli 2003; Alishahiha, Silverstein and Tong 2004; Seery and Lidsey 2005b; Seery and Lidsey 2005a; Weinberg 2005; Chen et al. 2007; Burrage, Ribeiro and Seery 2011; Elliston, Seery and Tavakol 2012). We refer to this literature for technical details. In this section we wish to emphasize that, in the context of a general effective field theory, there are subtleties associated with computation of the field mode functions. These represent the amplitude for single-particle excitations of the vacuum. Therefore their properties significantly influence the n-point functions because they determine the probability for particles to be present in the interaction region.

Bartolo et al. noted that the scales M_1, $\bar{M}_1$, $\bar{M}_2$ and $\bar{M}_3$ in Eq. (1.4) are correlated with contributions to the second-order effective action, and of these $\bar{M}_2$ and $\bar{M}_3$ generate kinetic terms involving fourth-order derivatives. Kinetic terms of this type had previously been encountered in the 'Ghost Inflation' scenario proposed by Arkani-Hamed et al. (2004). Such terms are problematic because they imply that the mode functions can no longer be expressed in terms of elementary functions. This obstructs analytic integration of the interaction rate and hence each n-point function. In scenarios which require these high-order kinetic terms, exact results for the correlation functions typically require numerical calculation.

Bartolo et al. gave an explicit formula for the mode functions including the contribution of fourth-order terms, expressed in terms of hypergeometric functions and generalized Laguerre polynomials (Bartolo et al. 2010a), and performed an analysis of its influence on each n-point function (Bartolo et al. 2010a; Bartolo et al. 2010b). They concluded that the fourth-order terms could significantly modify propagation deep within the horizon, but produced qualitatively similar results near the epoch of horizon exit. Since the correlations we are seeking to study are exponentially dominated by interactions occurring near this epoch, this implies that an acceptable estimate of the bispectrum *shape* can be obtained using a simpler mode function which does not account for fourth-order contributions. The penalty for this approximation is an uncertainty in the amplitude, which arises from a difference in *normalization* between the mode functions with and without the inclusion of fourth-order terms. For more details we refer to the discussion in Bartolo et al. (2010a) and Bartolo et al. (2010b).

In this paper we follow Bartolo et al. and estimate each bispectrum shape by neglecting the influence of fourth-order terms. This means that our results must be interpreted with some care:

1. When applied to a model for which $\bar{M}_2 = \bar{M}_3 = 0$, our results are exact within the approx-

imations which have already been discussed. In this case, we expect both our qualitative and quantitative conclusions to be reliable.

2. When applied to a model for which at least one of $\bar{M}_2$ or $\bar{M}_3$ is nonzero, the normalization of our bispectra will be incorrect for the reasons just explained. This uncertainty in normalization affects the bispectrum for each operator in Eq. (1.4), not just those associated with the scales $\bar{M}_2$ and $\bar{M}_3$—but we expect that it should be approximately the same for all of them. In this scenario, our quantitative estimates for the mass scales M_i, $\bar{M}_i$ are not reliable. However, qualitative conclusions regarding the relative importance of each operator should be unaffected because ratios of these mass scales divide out any uncertainty in normalization.

   To obtain reliable quantitative estimates of the mass scales when at least one of $\bar{M}_2$ or $\bar{M}_3$ is nonzero, it would be necessary to substitute numerical calculations of the bispectra in our analysis. In addition, the likelihood function to be discussed in §1.4 would no longer be approximately Gaussian and the analysis to follow should be replaced by a more sophisticated numerical exploration of the likelihood surface.

   These modifications significantly increase the complexity of the analysis. They would certainly be required if observations provided pressure to include an $\bar{M}_2$ or $\bar{M}_3$ term in the effective Lagrangian. At present, our view is that such a step in complexity is not justified by the data.

1.4 ESTIMATING THE EFT MASS SCALES

BISPECTRUM OF CURVATURE PERTURBATION.—Under the approximations discussed in §1.3, the shapes of the bispectra generated by each operator in Eq. (1.4) were plotted in Bartolo et al. (2010a). We tabulate analytical results for the corresponding three-point functions (which were not given explicitly in Bartolo et al. (2010a)) in Appendix 1.A. The total three-point function for ζ should be obtained by summing these contributions, weighted by an appropriate mass scale M_i or $\bar{M}_i$.

In what follows it will be convenient to collect these mass scales, together with other normalization factors, into dimensionless combinations λ_α given in Table 1.1. There are eleven independent mass scales and therefore eleven independent λ_α. We use Greek indices α, β, ..., to label these scales and the corresponding Lagrangian operators, which we write abstractly as O^α. Each index ranges over the values A, B, ..., K, and the effective action is the combination

$S_{\rm EFT} = \int \mathrm{d}^4x\,\sqrt{-g}\,\sum_\alpha \lambda_\alpha O^\alpha$. We position indices so that the normal rules of the Einstein summation convention are respected, but for clarity we will usually write summations over these indices explicitly. With these choices, we find

$$B_\zeta(k_1,k_2,k_3) = \frac{3}{5}\sum_\alpha \lambda_\alpha B^\alpha(k_1,k_2,k_3), \tag{1.7}$$

where B labels the bispectrum, defined so that (for example)

$$\langle\zeta(\mathbf{k}_1)\zeta(\mathbf{k}_2)\zeta(\mathbf{k}_3)\rangle = (2\pi)^3\delta(\mathbf{k}_1+\mathbf{k}_2+\mathbf{k}_3)B_\zeta(k_1,k_2,k_3), \tag{1.8}$$

and similarly for the π three-point function, which produces a bispectrum B^α for each operator O^α. In Eq. (1.7) the normalization of each λ_α has been adjusted so that the B^α satisfy

$$\frac{B^\alpha(k,k,k)}{6P_\zeta(k)^2} = 1, \tag{1.9}$$

where $P_\zeta(k) = 2\pi^2\mathcal{A}_\mathrm{s}/k^3$ is the power spectrum and $\mathcal{A}_\mathrm{s}$ is the scalar amplitude. Each bispectrum is evaluated at the equilateral point and in principle depends on the side length k. However, because the n-point functions we study are nearly scale invariant (which for the bispectra implies $B^\alpha(k,k,k) \sim k^{-6}$), the precise choice of scale used to fix this normalization is unimportant. For a precisely local bispectrum, our convention (1.9) would make the corresponding λ_α equal to the conventional nonlinearity parameter $f_{\rm NL}^{\rm local}$. In general, however, the B^α will not be local and although each nonlinearity parameter such as $f_{\rm NL}^{\rm local}$, $f_{\rm NL}^{\rm equi}$, etc., will be a linear combination of the λ_α, the coefficients in these combinations need not be simple.

Projection to the CMB bispectrum.—Eq. (1.6) shows that measurements of the microwave background anisotropies do not furnish information about B_ζ directly, but only via correlation functions of the $a_{\ell m}$. The first such correlation function which contains accessible information regarding B_ζ is the three-point function $\langle a_{\ell_1 m_1} a_{\ell_2 m_2} a_{\ell_3 m_3}\rangle$. It is conventional to extract a combinatorical factor $\mathcal{G}^{l_1 l_2 l_3}_{m_1 m_2 m_3}$—the so-called 'Gaunt integral'—which is nonzero only for allowed combinations of the ℓ_i and m_i. The remainder of the correlation function is written as a 'reduced bispectrum' $b_{\ell_1\ell_2\ell_3}$,

$$\langle a_{\ell_1 m_1} a_{\ell_2 m_2} a_{\ell_3 m_3}\rangle = b_{\ell_1\ell_2\ell_3}\mathcal{G}^{\ell_1\ell_2\ell_3}_{m_1 m_2 m_3}. \tag{1.10}$$

Our task is to determine $b_{\ell_1\ell_2\ell_3}$ given B_ζ. A strategy for doing so was developed by Fergusson, Liguori and Shellard (2010); Fergusson, Liguori and Shellard (2012); Fergusson, Regan and Shellard (2012); Fergusson, Regan and Shellard (2010); Regan, Shellard and Fergusson (2010) and extended by other authors (Byun and Bean 2013; Battefeld and Grieb 2011). We briefly recount the steps in this strategy, using the notation of Regan, Mukherjee and Seery (2013) and

Parameter	**expressed as a mass scale**	
	in terms of H	H eliminated
λ_A	$-\frac{65}{20736}\frac{1}{\pi^4\epsilon^3 c_\mathrm{s}^4\mathcal{A}_\mathrm{s}^2}\frac{\bar{M}_1^3H^3}{M_\mathrm{P}^6}$	$-\frac{65}{648\sqrt{2}}\frac{1}{\pi\epsilon^{3/2}c_\mathrm{s}^{5/2}\mathcal{A}_\mathrm{s}^{1/2}}\frac{\bar{M}_1^3}{M_\mathrm{P}^3}$
λ_B	$-\frac{85}{10368}\frac{1}{\pi^4\epsilon^3 c_\mathrm{s}^2\mathcal{A}_\mathrm{s}^2}\frac{M_2^4H^2}{M_\mathrm{P}^6}$	$-\frac{85}{1296}\frac{1}{\pi^2\epsilon^2 c_\mathrm{s}\mathcal{A}_\mathrm{s}}\frac{M_2^4}{M_\mathrm{P}^4}$
λ_C	$-\frac{325}{62208}\frac{1}{\pi^4\epsilon^3 c_\mathrm{s}^4\mathcal{A}_\mathrm{s}^2}\frac{\bar{M}_2^2H^4}{M_\mathrm{P}^6}$	$-\frac{325}{972}\frac{1}{\epsilon c_\mathrm{s}^2}\frac{\bar{M}_2^2}{M_\mathrm{P}^2}$
λ_D	$\frac{5}{3888}\frac{1}{\pi^4\epsilon^3\mathcal{A}_\mathrm{s}^2}\frac{M_3^4H^2}{M_\mathrm{P}^6}$	$\frac{5}{486}\frac{c_\mathrm{s}}{\pi^2\epsilon^2\mathcal{A}_\mathrm{s}}\frac{M_3^4}{M_\mathrm{P}^4}$
λ_E	$-\frac{65}{7776}\frac{1}{\epsilon^3 c_\mathrm{s}^4\mathcal{A}_\mathrm{s}^2}\frac{\bar{M}_3^2H^4}{M_\mathrm{P}^6}$	$-\frac{130}{243}\frac{1}{\epsilon c_\mathrm{s}^2}\frac{\bar{M}_3^2}{M_\mathrm{P}^2}$
λ_F	$\frac{5}{3888}\frac{1}{\pi^4\epsilon^3 c_\mathrm{s}^2\mathcal{A}_\mathrm{s}^2}\frac{\bar{M}_4^3H^3}{M_\mathrm{P}^6}$	$\frac{5\sqrt{2}}{243}\frac{1}{\pi\epsilon^{3/2}c_\mathrm{s}^{1/2}\mathcal{A}_\mathrm{s}^{1/2}}\frac{\bar{M}_4^3}{M_\mathrm{P}^3}$
λ_G	$-\frac{65}{46656}\frac{1}{\pi^4\epsilon^3 c_\mathrm{s}^4\mathcal{A}_\mathrm{s}^2}\frac{\bar{M}_5^2H^4}{M_\mathrm{P}^6}$	$-\frac{65}{729}\frac{1}{\epsilon c_\mathrm{s}^2}\frac{\bar{M}_5^2}{M_\mathrm{P}^2}$
λ_H	$-\frac{65}{186624}\frac{1}{\pi^4\epsilon^3 c_\mathrm{s}^4\mathcal{A}_\mathrm{s}^2}\frac{\bar{M}_6^2H^4}{M_\mathrm{P}^6}$	$-\frac{65}{2916}\frac{1}{\epsilon c_\mathrm{s}^2}\frac{\bar{M}_6^2}{M_\mathrm{P}^2}$
λ_I	$\frac{115}{69984}\frac{1}{\pi^4\epsilon^3 c_\mathrm{s}^6\mathcal{A}_\mathrm{s}^2}\frac{\bar{M}_7H^5}{M_\mathrm{P}^6}$	$\frac{460\sqrt{2}}{2187}\frac{\pi\mathcal{A}_\mathrm{s}^{1/2}}{\epsilon^{1/2}c_\mathrm{s}^{7/2}}\frac{\bar{M}_7}{M_\mathrm{P}}$
λ_J	$\frac{115}{279936}\frac{1}{\pi^4\epsilon^3 c_\mathrm{s}^6\mathcal{A}_\mathrm{s}^2}\frac{\bar{M}_8H^5}{M_\mathrm{P}^6}$	$\frac{115\sqrt{2}}{2187}\frac{\pi\mathcal{A}_\mathrm{s}^{1/2}}{\epsilon^{1/2}c_\mathrm{s}^{7/2}}\frac{\bar{M}_8}{M_\mathrm{P}}$
λ_K	$-\frac{115}{559872}\frac{1}{\pi^4\epsilon^3 c_\mathrm{s}^6\mathcal{A}_\mathrm{s}^2}\frac{\bar{M}_9H^5}{M_\mathrm{P}^6}$	$-\frac{115}{2187\sqrt{2}}\frac{\pi\mathcal{A}_\mathrm{s}^{1/2}}{\epsilon^{1/2}c_\mathrm{s}^{7/2}}\frac{\bar{M}_9}{M_\mathrm{P}}$

Table 1.1: Parameters λ_α in terms of the coefficients in the Lagrangian. The speed of sound of the fluctuations is denoted by c_s and $\mathcal{A}_\mathrm{s}$ is the amplitude of the power spectrum defined in (82).

Regan, Gosenca and Seery (2013). First, for each bispectrum B^α one defines a corresponding dimensionless 'shape function' S^α using a fixed reference bispectrum $B_{\rm ref}$,

$$S^\alpha(k_1,k_2,k_3) \equiv \frac{B^\alpha(k_1,k_2,k_3)}{B_{\rm ref}(k_1,k_2,k_3)}. \tag{1.11}$$

In principle, our final predictions do not depend on the choice of $B_{\rm ref}$. In practice we will be forced to make approximations, some of which may introduce a residual dependence on $B_{\rm ref}$. For this reason it is helpful to choose a form which has good numerical properties; often it is a good choice to fix a $B_{\rm ref}$ which shares features similar to the B^α. In this paper we will use the 'constant' bispectrum (Fergusson and Shellard 2009),

$$B_{\rm ref}(k_1,k_2,k_3) = 6\left(\frac{2\pi^2\mathcal{A}_{\rm s}}{k_1k_2k_3}\right)^2. \tag{1.12}$$

Second, one chooses a set of functions $\mathcal{R}^n$ which furnish at least an approximate basis for the functions S^α. We define coefficients α^α_n so that

$$S^\alpha(k_1,k_2,k_3) \approx \sum_n \alpha^\alpha_n \mathcal{R}^n(k_1,k_2,k_3). \tag{1.13}$$

In practice it is only possible to retain a finite number of the $\mathcal{R}^n$,[7] so they should be chosen to give an acceptable approximation for each S^α using only a small number of modes. For details regarding the construction of suitable $\mathcal{R}^n$ we refer to the literature (Fergusson, Regan and Shellard 2010; Byun and Bean 2013; Battefeld and Grieb 2011). Our implementation uses 80 basis functions and achieves correlations of greater than 99% for each template S^α. It follows that, to a good approximation, the ζ bispectrum can be written

$$B_\zeta(k_1,k_2,k_3) \approx \frac{3}{5}B_{\rm ref}(k_1,k_2,k_3)\sum_n\sum_\alpha \lambda_\alpha\alpha^\alpha_n\mathcal{R}^n(k_1,k_2,k_3). \tag{1.14}$$

The map from $\zeta(\mathbf{k})$ to $a_{\ell m}$ expressed by Eq. (1.6) is linear, and therefore the observable quantity $b_{\ell_1\ell_2\ell_3}$ must be proportional to a linear combination of the coefficients $\sum_\alpha \lambda_\alpha\alpha^\alpha_n$. Therefore we can write

$$b_{\ell_1\ell_2\ell_3} = \sum_{n,m}\Gamma_n{}^m b^n_{\ell_1\ell_2\ell_3}\sum_\alpha\lambda_\alpha\alpha^\alpha_m = \sum_\alpha \lambda_\alpha b^\alpha_{\ell_1\ell_2\ell_3}, \tag{1.15}$$

where $b^\alpha_{\ell_1\ell_2\ell_3}$ is the reduced angular bispectrum associated with the operator O^α,

$$b^\alpha_{\ell_1\ell_2\ell_3} \equiv \sum_{n,m}\alpha^\alpha_m\Gamma_n{}^m b^n_{\ell_1\ell_2\ell_3}, \tag{1.16}$$

and the basis functions $b^n_{\ell_1\ell_2\ell_3}$ are defined in Fergusson, Liguori and Shellard (2010) and Regan, Mukherjee and Seery (2013). They do not depend on any details of the cosmological model, which

[7] The error associated with this truncation is one place where residual dependence on the reference bispectrum $B_{\rm ref}$ can appear.

is carried only by the 'transfer matrix' ${\Gamma_n}^m$. This can be expressed as an integral over the linear transfer function $\Delta_\ell(k)$. The virtue of the approach of Fergusson, Shellard et al. is that calculation of ${\Gamma_n}^m$ is numerically more tractable than calculation of an arbitrary bispectrum. Explicit formulae for the $b^n_{\ell_1\ell_2\ell_3}$ and ${\Gamma_n}^m$ were given in Regan, Mukherjee and Seery (2013) and Regan, Gosenca and Seery (2013). To compress notation we define $\bar{\alpha}^\alpha_n \equiv \sum_m {\Gamma_n}^m \alpha^\alpha_m$ and $\bar{\beta}_n = \sum_\alpha \lambda_\alpha \bar{\alpha}^\alpha_n$, from which it follows that

$$b_{\ell_1\ell_2\ell_3} \approx \sum_n \bar{\beta}_n b^n_{\ell_1\ell_2\ell_3}. \tag{1.17}$$

This projection procedure introduces correlations between the observable bispectra $b^\alpha_{\ell_1\ell_2\ell_3}$ produced by different Lagrangian operators, even if the corresponding primordial bispectra $B^\alpha(k_1, k_2, k_3)$ are nearly uncorrelated. We will return to this issue in §1.4.1 below.

COMPARISON WITH DATA.—It follows from Eq. (1.17) that information about the observable bispectrum from a microwave background survey can be reduced to estimates of the $\bar{\beta}_n$ and their covariances. We denote these estimates $\hat{\beta}_n$ and write their covariance matrix $\hat{C}_{mn}$,

$$\hat{C}_{mn} \approx \langle \Delta\hat{\beta}_m \Delta\hat{\beta}_n \rangle, \tag{1.18}$$

where $\Delta\hat{\beta}_n$ is the deviation of the observed $\hat{\beta}_n$ from its expected value, $\Delta\hat{\beta}_n \equiv \hat{\beta}_n - \bar{\beta}_n$. The standard methods of linear algebra can be used to obtain an orthonormal combination of bispectra from a Cholesky decomposition of this matrix (Fergusson, Liguori and Shellard 2010; Fergusson, Liguori and Shellard 2012; Fergusson, Regan and Shellard 2012; Fergusson, Regan and Shellard 2010; Regan, Shellard and Fergusson 2010; Regan, Mukherjee and Seery 2013; Regan, Gosenca and Seery 2013). In the interests of simplicity we assume this has been done, which makes $\hat{C}_{mn}$ equal (for the rotated bispectra) to the identity matrix.[8]

For a set of measurements $\hat{\beta}_n$, the likelihood function $\mathscr{L}$ represents the probability that these values would be observed given a particular model for their origin—in this case, the effective

[8]We estimate $\hat{C}_{mn}$ from the covariance matrix of the cubic needlet statistic, after changing basis to the $\mathcal{R}_n$ as described in §II.B of Regan, Mukherjee and Seery (2013). (See also Regan, Gosenca and Seery (2013).) The signal-to-noise for the bispectrum (1.18) is roughly

$$\left(\frac{\mathrm{S}}{\mathrm{N}}\right)^2 \approx -2\ln\mathscr{L} \approx \sum_{mn} \bar{\beta}_m (\hat{C}^{-1})^{mn} \bar{\beta}_n, \tag{1.19}$$

making $\hat{C}_{mn}$ a Fisher estimate of the covariance for the $\bar{\beta}_n$. Under the assumption that the bispectrum is small we assume that this covariance matrix is a reasonable approximation to $\langle \Delta\beta_m \Delta\beta_n \rangle$.

To compute $\hat{C}_{mn}$ we use a suite of 50,000 Gaussian simulations, and for the change-of-basis coefficients we use a suite of 1,000 non-Gaussian simulations. These simulations incorporate the effect of the WMAP beam and mask for each channel, including noise with variance-per-pixel determined by the WMAP 9-year data release. In the rotated basis, where we choose $\hat{C}_{mn} = \delta_{mn}$, all these details are transferred to the definition of the $\hat{\beta}_n$.

Lagrangian (1.4) with parameters λ_α. Assuming that the non-Gaussianity is sufficiently weak that the $\hat{\beta}_n$ are Gaussian distributed, this probability can be written

$$\mathscr{L}(\hat{\beta}_n|\lambda_\alpha) = \frac{1}{\sqrt{2\pi \det \hat{C}}} \exp\Big(-\frac{1}{2} \sum_{m,n} (\hat{C}^{-1})^{mn} \Delta\hat{\beta}_m \Delta\hat{\beta}_n \Big). \tag{1.20}$$

MAXIMUM LIKELIHOOD ESTIMATOR.—It is now simple to construct a maximum likelihood estimator for the λ_α by finding the combination which has the greatest likelihood given the data. This gives the estimate

$$\hat{\lambda}_\alpha = \sum_\beta \hat{b}^\beta (\hat{\mathcal{F}}^{-1})_{\beta\alpha}, \tag{1.21}$$

where $\hat{b}^\alpha$ is defined by

$$\hat{b}^\alpha = \sum_{m,n} \hat{\beta}_m (\hat{C}^{-1})^{mn} \bar{\alpha}^\alpha_n. \tag{1.22}$$

The matrix $\hat{\mathcal{F}}$ is the Fisher matrix associated with the likelihood (1.20),

$$\hat{\mathcal{F}}^{\alpha\beta} = -\frac{\partial^2 \ln \mathscr{L}}{\partial\lambda_\alpha \partial\lambda_\beta} = \sum_{m,n} \bar{\alpha}^\alpha_m (\hat{C}^{-1})^{mn} \bar{\alpha}^\beta_n. \tag{1.23}$$

Truncating at the quadratic level, its inverse is formally the covariance matrix of the $\hat{\lambda}_\alpha$,

$$\langle (\hat{\lambda}_\alpha - \lambda_\alpha)(\hat{\lambda}_\beta - \lambda_\beta) \rangle = (\hat{\mathcal{F}}^{-1})_{\alpha\beta}. \tag{1.24}$$

In the rotated basis, where $\hat{C}_{mn}$ is defined to be the unit matrix, Eq. (1.23) makes $\hat{\mathcal{F}}^{\alpha\beta}$ the square of the matrix $\bar{\alpha}^\alpha_n$ which expresses the decomposition of the angular bispectrum corresponding to the operator O^α. In practice the Fisher formalism and Eq. (1.24) are likely to be trustworthy only in the limit of sufficiently high signal-to-noise.[9]

The maximum likelihood estimator is an essentially frequentist concept, as is its variance (1.24). In a Bayesian framework one should instead interpret $(\hat{\mathcal{F}}^{-1})_{\alpha\beta}$ as the covariance of the posterior probability distribution of the parameters λ_α, constructed from a single set of measurements $\hat{\beta}_n$, assuming that any prior probabilities for the λ_α are flat over the range of interest.

1.4.1 How many independent shapes?

This analysis applies provided the matrix $\hat{\mathcal{F}}^{\alpha\beta}$ is invertible. However, invertibility may fail if two linear combinations of the operators O^α produce nearly degenerate angular bispectra. This would imply that $\hat{\mathcal{F}}^{\alpha\beta}$ has an approximate null eigenvector.

[9] In the limit of high signal-to-noise the maximum likelihood estimator satisfies the Cramér-Rao bound and therefore coincides with the Fisher result (Vallisneri 2008).

The appearance of exact or approximate null eigenvectors implies that the likelihood function is a singular Gaussian distribution: it does not vary along directions in parameter space which correspond to the null eigenvectors. Therefore the variance of the maximum likelihood estimator (1.24) is formally infinite for all $\hat{\lambda}_\alpha$. To deal with this one should first discard those combinations of parameters which are unconstrained by the likelihood function. This is necessary even in the case of an approximate null eigenvector, because although the Fisher matrix may be formally invertible it will usually be ill-conditioned. Therefore we should trust a numerical inversion only if it is possible to compute $\hat{\mathcal{F}}^{\alpha\beta}$ to very high accuracy. Typically this cannot be done because the accuracy with which we know $\hat{\mathcal{F}}^{\alpha\beta}$ is limited by our ability to estimate $\hat{C}_{mn}$, and by the numerical integrations required to compute $\bar{\alpha}^\alpha_n$. For a discussion of the issues involved in handling singular Fisher matrices, see (for example) Vallisneri (2008).

MEASURES OF CORRELATION.—Two operators will produce degenerate bispectra if their decomposition coefficients α^α_m or $\bar{\alpha}^\alpha_m$ are nearly the same. These two measures do not have to agree, because (as explained on p. 70) the projection from α^α_m to $\bar{\alpha}^\alpha_m$ can change the degree of correlation. The Fisher matrix $\hat{\boldsymbol{\mathcal{F}}}$ is constructed from angular bispectra, and therefore—as a point of principle—the problematic degeneracies are those which occur for the $\bar{\alpha}^\alpha_m$. But in practice, for computation reasons, it is sometimes more practical to use the α^α_m as a proxy.

To measure the correlation between two primordial bispectra B_1 and B_2 we introduce an inner product, defined by

$$\langle\!\langle S^1, S^2 \rangle\!\rangle \equiv \int_{\mathcal{V}} \mathrm{d}v \; S_1(k_1,k_2,k_3) S_2(k_1,k_2,k_3) \omega(k_1,k_2,k_3), \tag{1.25}$$

where S_1 and S_2 are the corresponding shape functions, $\mathrm{d}v$ is an element of volume on the integration domain $\mathcal{V}$ (which corresponds to allowable triangular configurations of the momenta $\mathbf{k}_i$), and ω is a weight function which can be chosen to suit our convenience. For a more detailed discussion of Eq. (1.25) we refer to the literature (Fergusson, Liguori and Shellard 2010). We normalize the $\mathcal{R}^n$ so that $\langle\!\langle \mathcal{R}^m, \mathcal{R}^n \rangle\!\rangle = \delta^{mn}$ and therefore (1.13) implies

$$\langle\!\langle S^1, S^2 \rangle\!\rangle = \sum_n \alpha^1_m \alpha^2_m. \tag{1.26}$$

When measuring correlations between angular bispectra it is helpful to account for the ability of the WMAP instrument to distinguish between different shapes. This ability is measured by the matrix $(\hat{C}^{-1})^{mn}$ discussed in footnote 8 on p. 70. We define

$$\langle\!\langle b^1_{\ell_1,\ell_2,\ell_3}, b^2_{\ell_1,\ell_2,\ell_3} \rangle\!\rangle = \sum_{m,n} \bar{\alpha}^1_m (\hat{C}^{-1})^{mn} \bar{\alpha}^2_n. \tag{1.27}$$

Note that we write the inner product $\langle\!\langle \cdot, \cdot \rangle\!\rangle$ for both the primordial and angular bispectra, but they are *not* equal; the definition is different depending whether it is taken between primordial or angular bispectra. In either case it is conventional to measure the correlation between shapes by defining a 'cosine',

$$\cos(1,2) = \frac{\langle\!\langle 1,2 \rangle\!\rangle}{\langle\!\langle 1 \rangle\!\rangle^{1/2} \langle\!\langle 2 \rangle\!\rangle^{1/2}}, \tag{1.28}$$

where '1' and '2' should be substituted by the appropriate angular or primordial bispectrum.

Principal directions.—To factor out the degenerate directions we diagonalize $\hat{\boldsymbol{\mathcal{F}}}$, finding a new orthogonal matrix $\mathbf{U}$ and a nonnegative-definite diagonal matrix $\boldsymbol{\Sigma}$ so that $\hat{\boldsymbol{\mathcal{F}}} = \mathbf{U}\boldsymbol{\Sigma}\mathbf{U}^{\mathrm{t}}$ where a superscript 't' denotes matrix transposition.[10] The matrix $\mathbf{U}$ can be regarded as a rotation from the operators O^{α} to a new set of operators $O^{\alpha'}$ which satisfy $O^{\alpha'} = \sum_{\alpha} O^{\alpha} U_{\alpha}{}^{\alpha'}$, and likewise a new set of dimensionless coefficients $\lambda_{\alpha'} = \sum_{\alpha} \lambda_{\alpha} U^{\alpha}{}_{\alpha'}$. The Lagrangian $\sum_{\alpha} \lambda_{\alpha} O^{\alpha} = \sum_{\alpha'} \lambda_{\alpha'} O^{\alpha'}$ is invariant under a rigid rotation of this kind.

The presence of degeneracies means that the eigenvalues of $\hat{\boldsymbol{\mathcal{F}}}$ vary significantly in magnitude. The largest eigenvalues are

$$2.23 \times 10^{-3},\ 1.70 \times 10^{-4},\ 7.17 \times 10^{-7},\ 1.22 \times 10^{-9},\ \text{and}\ 1.20 \times 10^{-14}, \tag{1.29}$$

with the remaining eigenvalues being of order 10^{-15} or smaller. We retain the first four, which corresponds to a hierarchy between largest and smallest eigenvalues of $\sim 10^{6}$.[11] The corresponding eigenvectors in parameter space yield four linear combinations λ_1, λ_2, λ_3, λ_4 which can be constrained. It should be remembered that because the covariance matrix $\hat{C}_{mn}$ defined in (1.18) depends on details of the WMAP experiment (including the masks, beam and noise properties as described in footnote 8 on p. 70), the Fisher matrix and therefore the shapes corresponding to these leading eigenvalues also depend on these details. They may vary between experiments, depending on the varying sensitivity of each experiment to different regions of multipole-space. The precise specification of the leading shapes given in Table 1.3, and we plot the shapes of the corresponding primordial bispectra in Fig. 1.1.

Shapes of principal directions.—These shapes can be given an approximate interpretation in terms of the standard templates. Fig. 1.1a is associated with the largest eigenvalue, and is therefore the

[10] In practice, it can happen that numerical inaccuracies cause $\hat{\boldsymbol{\mathcal{F}}}$ to develop very small negative eigenvalues which spoil simple diagonalization strategies. Where this occurs we perform a singular value decomposition, which corresponds to finding (possibly complex) unitary matrices $\mathbf{U}$, $\mathbf{V}$ and a nonnegative-definite diagonal matrix $\boldsymbol{\Sigma}$ so that $\hat{\boldsymbol{\mathcal{F}}} = \mathbf{U}\boldsymbol{\Sigma}\mathbf{V}^{\mathrm{t}}$. We discard complex directions and check that the results are stable under exchange of $\mathbf{U}$ and $\mathbf{V}$.

[11] The hierarchy is too large to allow the numerical inversion of the rotated Fisher matrix $\Sigma_{\alpha'\beta'}$ when keeping any more than the first 4 principal components.

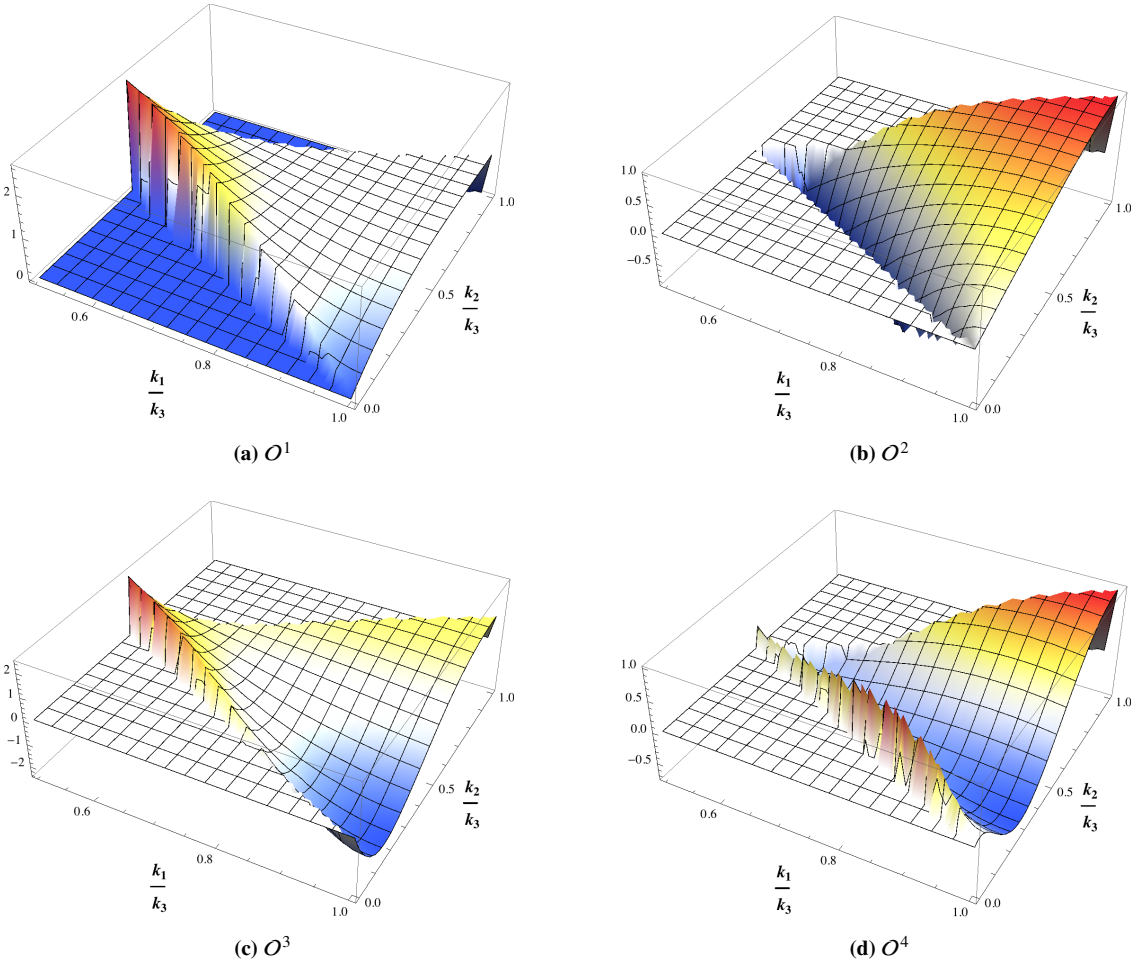

Figure 1.1: Bispectrum shapes generated by the operators $O^{\alpha'}$ corresponding to the constrainable parameter combinations $\lambda_{\alpha'}$. These plots follow the conventions of Babich, Creminelli and Zaldarriaga (2004). For each $O^{\alpha'}$ the plotted quantity is $x^2y^2B_{\alpha'}(x, y, 1)/B_{\alpha'}(1, 1, 1)$ where $x = k_1/k_3$ and $y = k_2/k_3$ (no sum on α').

best-measured shape. It exhibits significant correlations for $x = y = 0.5$, which corresponds the 'folded' configuration (Meerburg, Schaar and Corasaniti 2009). Fig. 1.1b exhibits significant correlations in the equilateral limit $x = y = 1$, and some anticorrelation in the folded configuration. It can be regarded as an approximate 'orthogonal' shape (Senatore, Smith and Zaldarriaga 2010). Together, a linear combination of these two configurations can be used to produce an approximate 'equilateral' shape. These results are consistent with the forecast of Byun and Bean (2013), who suggested that (neglecting the local shape), the highest signal-to-noise should be achieved for shapes similar to the folded and orthogonal templates. Note that Byun & Bean's analysis was based on a survey with Planck-like masks, beams and noise rather than the WMAP9 characteristics adopted here.

Fig. 1.1c has an interior node, where—without our choice of signs—anti-correlations have a local maximum in the interior of the allowed triangular region. This is quite different to the be-

haviour of Figs. 1.1a–1.1b, in which local maxima only occur for extreme configurations on the boundary of the allowed region. The shape of Fig. 1.1c is similar to a shape produced in a Galileon theory by Creminelli, D'Amico et al. (2011), and later reproduced in a general Horndeski Lagrangian by Burrage, Ribeiro and Seery (2011) and Ribeiro and Seery (2011). Finally, Fig. 1.1d is a complex shape containing an interior node together with substantial correlations in the equilateral configuration. It represents something different from the shape of Fig. 1.1c, but it will be seen in §2.6 below that it is rather weakly constrained by the data.

These results are consistent with the conclusions of Ribeiro and Seery (2011), who found that in a very general single-field model[12] it could be possible to produce a measurable signal in a mode similar to that of Fig. 1.1c, or equivalently the Creminelli et al. shape (Creminelli, D'Amico et al. 2011), but that further orthogonal shapes would be difficult to measure.

Correlation of shapes.—We tabulate the correlation between these shapes in Table 1.2, and also between these shapes and the standard CMB templates. The correlation is computed for the primordial bispectra using (1.25). In particular we note that, although the angular bispectra for the $O^{\alpha'}$ are orthogonal by construction, mapping back to the primordial bispectrum introduces some correlation; for example, $\cos(O^3, O^4) = -0.62$. This degradation is expected, because the increasing covariance represented by (1.29) will cause noise to dominate over signal. Therefore the linear relationship between the primordial and CMB n-point functions, implied by Eq. (1.6), is no longer satisfied.

One can regard these results as a reflection of the fact that the first three operators O^1, O^2 and O^3 are reasonably well-measured, whereas the fourth operator O^4 is only weakly constrained.

1.4.2 Results

A framework for estimating the $\hat{\beta}_n$ from a CMB temperature map using wavelet or needlet methods was developed by Regan, Mukherjee and Seery (2013); Regan, Gosenca and Seery (2013). and we refer to these papers for more details on the implementation of the estimator. Wavelets (and needlets) offer several advantages as a means to decompose a CMB map due to their localization in both scale and position. In addition, they allow for considerable data compression without impairing the optimality of the estimator. For example, Curto, Martinez-Gonzalez and Barreiro (2010) found that optimality could be achieved using only 15 wavelet scales, corresponding to 680

[12]Ribeiro et al. worked with a model for the fluctuations which is equivalent to the fluctuations in a general Horndeski action. Although very permissive, this model is still less general than the full effective field theory (1.4).

	O^1	O^2	O^3	O^4
O^1	1.00	−0.03	−0.11	−0.01
O^2	−0.03	1.00	0.17	0.24
O^3	−0.11	0.17	1.00	−0.62
O^4	−0.01	0.24	−0.62	1.00
constant	−0.95	−0.21	−0.09	0.00
equilateral	−0.80	−0.57	0.03	−0.16
flat	−0.73	0.19	−0.38	0.31
local	−0.54	0.00	−0.29	0.02
orthogonal	0.36	−0.79	0.27	−0.35

Table 1.2: Cosines of the shapes appearing in Fig. 1.1 between themselves and the standard CMB templates. Inner products are computed using (1.25) and the constant bispectrum as a reference.

triples. In this paper we also fix 15 such scales.

We apply these methods to 9-year data from the WMAP satellite (Hinshaw et al. 2013; Bennett et al. 2013). After diagonalizing our Fisher matrix $\hat{\boldsymbol{\mathcal{F}}} = \mathbf{U}\boldsymbol{\Sigma}\mathbf{V}^{\mathrm{t}}$, we can rewrite Eq. (1.21) as

$$\sum_{\alpha'}\left(\sum_{\alpha}\hat{\lambda}_{\alpha}U_{\alpha}^{\alpha'}\right)\Sigma_{\alpha'\beta'} = \sum_{\beta}\hat{b}_{\beta}U_{\beta}^{\beta'}, \tag{1.30}$$

which has the same functional form as (1.21), with rotated coefficients $\hat{\lambda}_{\alpha'} = \sum_{\alpha}\hat{\lambda}_{\alpha}U_{\alpha}^{\alpha'}$ and $\hat{b}_{\beta'} = \sum_{\beta}\hat{b}_{\beta}U_{\beta}^{\beta'}$. The Fisher matrix for the constrainable parameters $\lambda_{\alpha'}$ is given by $\Sigma_{\alpha'\beta'}$, which is the diagonal matrix of the first 4 principal eigenvalues listed in Eq. (1.29). Therefore we can constrain 4 rotated parameters $\lambda_{\alpha'}$ (corresponding to 4 linear combinations of the original parameters λ_{α}), with covariance matrix $\langle(\hat{\lambda}_{\alpha'} - \lambda_{\alpha'})(\hat{\lambda}_{\beta'} - \lambda_{\beta'})\rangle = (\Sigma^{-1})_{\alpha'\beta'}$. For the constrainable parameters $\{\lambda_{\alpha'}\} = \{\lambda_1, \lambda_2, \lambda_3, \lambda_4\}$ we find

	Estimate
$\hat{\lambda}_1$	−22.9 ± 20.9
$\hat{\lambda}_2$	94.9 ± 76.7
$\hat{\lambda}_3$	−956 ± 1180
$\hat{\lambda}_4$	42400 ± 28600

The quoted errors are 1σ and marginalized over the other $\lambda_{\alpha'}$. Contour plots for the best-fit values of the parameters are shown in Fig. 1.3.

Senatore, Smith and Zaldarriaga (2010) obtained constraints on the amplitude of the 'equilateral' and 'orthogonal' bispectrum templates from the 5-year WMAP data, and used these to constrain a subset of terms in the effective Lagrangian (1.4). They concluded that each shape included in their analysis could be approximately described by a linear combination of these two templates, up to $\sim 90\%$ correlation. However, they included only two of the operators in Eq. (1.4). Our analysis demonstrates that it is possible to increase the number of linearly independent operators from two to four, although the estimate $\hat{\lambda}_4 = 42400 \pm 28600$ shows that that sensitivity is already decreasing markedly for the fourth parameter.

1.5 Constraints on models

In §1.4 we obtained constraints on certain linear combinations of the EFT scales M_i, $\bar{M}_i$. The remaining linear combinations formally have infinite uncertainties because of degeneracies. Together, these results summarize the information which can be recovered from the WMAP9 bispectrum, but to apply them to specific models we must first match the mass scales M_i, $\bar{M}_i$. In this section we give two examples of this programme for models of observational interest: the Dirac–Born–Infeld model ('DBI inflation') and 'Ghost inflation'.

Once the M_i, $\bar{M}_i$ are known, the results of §1.4 would give four constraints on different combinations of these scales. Depending how many scales are needed to parametrize an individual model, it may be possible to estimate some or all of them, or they may even be over-constrained. The latter possibility indicates that the model is a poor fit for the data. Where more than four mass scales are needed to characterize a model, the constraints pick out an observationally-allowed subspace which is consistent with the CMB bispectrum measurements.

Methodology.— To map our four constraints for $\{\lambda_1, \lambda_2, \lambda_3, \lambda_4\}$ onto a subset of the original parameter space M_i, $\bar{M}_i$ we minimize the value

$$X^2 = \sum_{\alpha'=1}^{4} \frac{[\lambda_{\alpha'}(M_i, \bar{M}_i) - \hat{\lambda}_{\alpha'}]^2}{\Sigma^{-1}_{\alpha'\alpha'}}, \tag{1.31}$$

where $\Sigma_{\alpha'\beta'}$ is the diagonal matrix of principal eigenvalues listed in Eq. (1.29); $\lambda_{\alpha'}(M_i, \bar{M}_i)$ represents the value of the linear combination $\lambda_{\alpha'}$ which would be predicted given a fixed choice of mass scales M_i, $\bar{M}_i$; and $\hat{\lambda}_{\alpha'}$ represents the value estimated from the data in §1.4. With four

	λ_A	λ_B	λ_C	λ_D	λ_E	λ_F	λ_G	λ_H	λ_I	λ_J	λ_K
λ_1	−0.173206	−0.193711	−0.221619	−0.260354	−0.203464	−0.260354	−0.256692	−0.507151	−0.24732	−0.446539	0.350338
λ_2	−0.240889	−0.222667	−0.200172	−0.163445	−0.215441	−0.163445	−0.165617	0.060200	−0.171386	0.048317	−0.830493
λ_3	0.269654	0.191121	0.050094	−0.064110	0.132429	−0.064110	0.006499	−0.782966	0.226131	0.379275	−0.233301
λ_4	−0.219333	−0.233381	−0.193386	−0.279000	−0.203131	−0.279000	−0.120479	0.176132	0.481877	0.541142	0.304148

Table 1.3: Linear combinations of the λ_α parameters which can be constrained using the WMAP9 bispectrum data. The unrotated parameters are labelled λ_A, λ_B, …, and correspond to those defined in Table 1.1 in terms of the EFT mass scales. The rotated parameters are labelled λ_1, λ_2, ….

constraints on the $\lambda_{\alpha'}$ we can constrain up to four of the M_i, $\bar{M}_i$. In general, this approach will allow us to find approximate estimates even in the case that a model is over-constrained.

We take X^2 to be χ^2-distributed with four degrees of freedom. The $\lambda_{\alpha'}$ are constructed from a linear combination of the $\hat{\beta}_n$, and we assume that the experimental error for each $\hat{\beta}_n$ is independent and Gaussian-distributed. Because the $\lambda_{\alpha'}$ are chosen to be orthogonal, the experimental errors on each $\hat{\lambda}_{\alpha'}$ will be obtained from a nearly uncorrelated sum of Gaussians, and will therefore also be nearly independent. This makes X^2 approximately equal to a sum of four approximately independent, unit Gaussians, and hence roughly χ^2-distributed.

Confidence intervals for the M_i, $\bar{M}_i$ could be determined by searching for suitable critical values of the χ^2 distribution. Alternatively, assuming that the $\hat{\lambda}_{\alpha'}$ have uncorrelated Gaussian errors, we could expand X^2 to second order around the maximum likelihood point,

$$\begin{aligned} X^2 &= X^2|_{\text{MLE}} + \sum_{\alpha'\beta'} \left.\frac{\partial^2 X^2}{\partial\lambda_{\alpha'}\partial\lambda_{\beta'}}\right|_{\text{MLE}} (\lambda_{\alpha'} - \lambda_{\alpha'}|_{\text{MLE}})(\lambda_{\beta'} - \lambda_{\beta'}|_{\text{MLE}}) + \cdots \\ &= X^2|_{\text{MLE}} + \Delta X^2, \end{aligned} \tag{1.32}$$

and construct confidence contours at the n^{th}-σ level by searching for critical values where $\Delta X^2 = n^2$. In principle these methods agree if the $\hat{\lambda}_{\alpha'}$ are Gaussian and uncorrelated. We find that the agreement is not quite exact, which we ascribe to a small residual correlation between the errors on the $\hat{\lambda}_{\alpha'}$. The single-parameter constraints reported below are obtained using the second-order expansion (1.32), which reproduces the Fisher-matrix estimates. For two or more parameters we report constraints extracted from critical values of the full χ^2-distribution with 4 degrees of freedom.

DBI INFLATION.—The first example we consider is the 'Dirac–Born–Infeld' or 'DBI' inflationary model.

The Dirac–Born–Infeld action describes fluctuations of a membrane moving in a warped transverse space, or 'throat'. Under certain circumstances it can describe an inflationary epoch in which inflaton perturbations propagate at less than the speed of light from the perspective of a brane-based observer, due to constraints imposed by the extradimensional covering theory. The small sound speed means that these models can produce significant nongaussianities in the equilateral mode.

Fluctuations in a single-field DBI model can be described by the effective action (1.4), retaining only the B and D operators (Cheung, Creminelli et al. 2008),

$$\lambda_B O^B \propto M_2^4 \frac{1}{a^2}\dot{\pi}(\partial\pi)^2 \tag{1.33a}$$

$$\lambda_D O^D \propto M_3^4 \dot{\pi}^3. \tag{1.33b}$$

This model does not involve the problematic scales $\bar{M}_2$, $\bar{M}_3$ which lead to normalization inaccuracies for the single-particle mode functions and therefore we expect our estimates to be quantitatively reliable.

The original DBI model had a single free parameter and therefore M_2 and M_3 cannot be chosen independently but are correlated as described below. Alternatively, one can consider a larger family of DBI-like models which retain only these operators but allow M_2 and M_3 to vary. Following Senatore et al., constraints are typically expressed using the parameters

$$\frac{1}{c_s^2} = 1 - \frac{2M_2^4}{M_P^2\dot{H}} = 1 - \frac{324}{85}\lambda_B, \tag{1.34a}$$

$$\tilde{c}_3\Big(\frac{1}{c_s^2} - 1\Big) = \frac{2M_3^4 c_s^2}{M_P^2\dot{H}} = -\frac{243}{10}\lambda_D. \tag{1.34b}$$

Causality requires the speed of sound c_s to be less than or equal to unity. Since $\dot{H} < 0$ during inflation it follows that M_2^4 must be positive (see footnote 5 on p. 62). If $M_2^4 \gtrsim M_P^4|\dot{H}|$ then a significant bispectrum can be generated. The reason for expressing constraints in terms of these parameters is that it is not possible to determine M_2 and M_3 without simultaneously specifying $\dot{H}$. The original DBI model imposes the constraint $\tilde{c}_3 = 3(1 - c_s^2)/2$.

We estimate the *joint* constraints on λ_B and λ_D to be

$$\lambda_B = -1151 \pm 760 \tag{1.35a}$$

$$\lambda_D = \quad 946 \pm 584. \tag{1.35b}$$

The Planck collaboration expressed their constraints in terms of f_{NL}-like parameters f_{NL}^{EFT1} and f_{NL}^{EFT2}. In our notation these correspond, respectively, to λ_B under the assumption $\lambda_D = 0$ and λ_D under the assumption $\lambda_B = 0$. Using the 2013 dataset, the Planck collaboration reported the bounds $f_{NL}^{EFT1} = 8 \pm 73$ and $f_{NL}^{EFT2} = 19 \pm 57$ (Ade et al. 2013). Using the same notation, we find

$$f_{NL}^{EFT1} = 68.3 \pm 103 \tag{1.36a}$$

$$f_{NL}^{EFT2} = 69.3 \pm 79. \tag{1.36b}$$

The Planck2013 errors represent an improvement of order 30%.

Alternatively, each bound can be expressed in terms of c_s and $\tilde{c}_3$. To compare with the constraints reported by the Planck collaboration we consider three possibilities. First, marginalizing over $\tilde{c}_3$ gives a conservative lower bound on c_s,

$$c_s \geqslant 0.010 \quad \text{at } 95\% \text{ confidence.} \tag{1.37a}$$

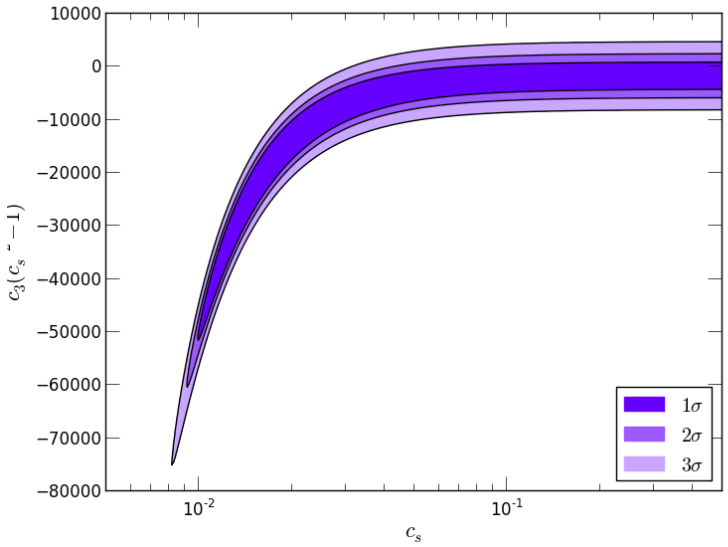

Figure 1.2: Constraints on the DBI-like parameters c_s, $\tilde{c}_3$.

For comparison, Planck2013 found $c_s \geqslant 0.02$ (Ade et al. 2013) at the same confidence level. Second, imposing $\tilde{c}_3 = 0$ gives

$$c_s \geqslant 0.044 \quad \text{at } 95\% \text{ confidence.} \tag{1.37b}$$

Finally, assuming the strict DBI relation between c_s and $\tilde{c}_3$ leaves c_s as a single free parameter. We find

$$c_s \geqslant 0.051 \quad \text{at } 95\% \text{ confidence.} \tag{1.37c}$$

Planck2013 obtained $c_s \geqslant 0.07$ (Ade et al. 2013), also at 95% confidence. Eq. (1.37c) can also be expressed as an $f_{\rm NL}$ parameter for the DBI shape. This gives

$$f_{\rm NL}^{\rm DBI} = 69.6 \pm 97.4. \tag{1.38}$$

Finally, allowing both c_s and $\tilde{c}_3$ to vary results in a lower bound for c_s and relatively weak constraints for $\tilde{c}_3$, plotted in Fig. 1.2.

Similar bounds were reported by Senatore, Smith and Zaldarriaga (2010). Our construction ensures that the bounds reported above correspond to the most accurate constraints which can be achieved using this data set, because the shapes are explored using four rather than two orthogonal directions in the likelihood (1.31). For example, using only the leading principal component to construct the likelihood yields the constraint $c_s > 0.061$ in the DBI model. This bound unduly weights the component of the DBI shape along this principal direction, giving an overly optimistic constraint when compared with the four-component result (1.37c).

Ghost inflation.—Our second example is the 'Ghost inflation' model proposed by Arkani-Hamed et al. (2004), in which inflation is driven by a so-called 'ghost condensate' which spontaneously breaks Lorentz invariance in the background. The ghost condensate is described by a scalar field ϕ whose time derivative gains a nonvanishing vacuum expectation value, $\langle\dot{\phi}^2\rangle = M^2 \neq 0$. This expectation value is time-independent and is not diluted as inflation proceeds.

In the effective theory, fluctuations around the background correspond to nonzero $\bar{M}_2^2$ and $\bar{M}_3^2$, and the limit $\dot{H} \to 0$. This limit sets the quadratic spatial-derivative terms in (1.4) to zero, so that the speed of sound is formally zero. The fluctuations are nevertheless propagating modes because higher-order spatial derivative terms are present in the Lagrangian. The relevant EFT operators are

$$\lambda_C O^C \propto \frac{\bar{M}_2^4}{a^5}\Big(\frac{H}{2}\partial^2\pi(\partial\pi)^2 + \dot{\pi}\partial^2\partial_i\pi\partial_i\pi\Big) \tag{1.39a}$$

$$\lambda_E O^E \propto \frac{\bar{M}_3^2}{a^4}\Big(H\partial^2\pi(\partial\pi)^2 + \dot{\pi}\partial^2\partial_i\pi\partial_i\pi\Big). \tag{1.39b}$$

The arrangement of derivatives is identical up to a relative factor of 2 in the first term. In terms of the mass scales $\bar{M}_2$ and $\bar{M}_3$ we have

$$\lambda_C = -\frac{325}{972c_s^2\epsilon}\frac{\bar{M}_2^2}{M_P^2}, \tag{1.40a}$$

$$\lambda_E = -\frac{130}{243c_s^2\epsilon}\frac{\bar{M}_3^2}{M_P^2}. \tag{1.40b}$$

The inclusion of factors of c_s and ϵ is purely formal, since this model technically involves the limits $c_s \to 0$ and $\epsilon \to 0$. Proceeding as for the DBI model we obtain the maximum-likelihood estimates

$$\lambda_C = -3680 \pm 2280 \tag{1.41a}$$

$$\lambda_E = 3900 \pm 2450. \tag{1.41b}$$

Bartolo et al. observed that the operators (1.39a)–(1.39b) are nearly the same and chose to aggregate them into a single term operator by introducing a common mass scale $\bar{M}_0$, satisfying by $\bar{M}_0^2 \equiv 2\bar{M}_3^2/3 \equiv -2\bar{M}_2^2$. The λ corresponding to this aggregate operator [still defined to satisfy the normalization condition (1.9)] represents an estimate of the amplitude of the ghost-inflation bispectrum, and we label it $\lambda^{\rm ghost}$. As explained in §1.3, the ghost inflation model involves fourth-order kinetic terms whose details we do not capture, and therefore the precise normalization of this estimate is uncertain. We find

$$\lambda^{\rm ghost} = -68.4 \pm 100.5. \tag{1.42}$$

For comparison, the Planck collaboration reported the constraint $f_{\rm NL}^{\rm ghost} = -23 \pm 88$. Both estimates agree that the bispectrum in this channel is consistent with zero within 1σ. In addition, this comparison shows that, even in a case where the normalization uncertainty is important, our result matches an exact calculation within a factor of order unity.

1.6 Model comparison using the bispectrum

The analyses of §§1.4–1.5 determine best-fit values for the λ_α, essentially in a frequentist sense, assuming a fixed model for the underlying microphysical fluctuations. Therefore our conclusions up to this point are restricted to *parameter estimation*.

Within this framework it is not possible to address questions such as whether the best-fit combination for DBI inflation, Eqs. (1.35a)–(1.35b), represents a better description of the data than the best-fit combination for Ghost inflation, Eqs. (1.41a)–(1.41b). These broader questions constitute the province of *model comparison*. Recent work has addressed the issue of inflationary model comparison based on measurements of the two-point function of the temperature anisotropy (Martin et al. 2013). It is much more challenging to perform a similar analysis based on the three-point function. In this section we take some steps towards this objective within the framework described in §§1.2–1.4.

For computational reasons we must impose limitations on the meaning of the term 'model'. Conceptually this should include whatever information is necessary to specify the value of each observable. For example, the transfer matrix ${\Gamma_n}^m$ depends on the post-inflationary cosmological history and in a global analysis the parameters which specify this history should be varied in addition to the inflationary parameters M_i, $\bar{M}_i$. However, this generates a large parameter space which is expensive to search because calculation of ${\Gamma_n}^m$ is time-consuming. In this analysis we will fix the transfer matrix using standard best-fit values for the post-inflationary history and address the more restricted question of which inflationary model yields a better fit for the three-point function given these assumptions.

Evidence for a model.—There is no single metric which unambiguously quantifies the evidence for or against a particular model. One popular choice is the 'Bayes factor'. For a particular set of observations D and a pair of models M_1 and M_2, this is defined to be the ratio of likelihoods,

$$K_{12} = \frac{P(D|M_1)}{P(D|M_2)} = \frac{\int P(D|\lambda_1, M_1) P(\lambda_1|M_1)\, \mathrm{d}\lambda_1}{\int P(D|\lambda_2, M_2) P(\lambda_2|M_2)\, \mathrm{d}\lambda_2}. \tag{1.43}$$

We use λ_1, λ_2 to schematically denote two different choices of the parameters λ_α which characterize a particular model. Because M_1 and M_2 are different they may require a different number of parameters.

The probabilities $P(\lambda_i|M_i)$ represent the prior probability, for each model, that a particular parameter choice occurs. They must be chosen by hand. Where meaningful prior information exists (for example, previous measurements of a parameter) this can be encoded using these probabilities.

Empirical scales are used to give meaning to the Bayes factor. Commonly used examples are due to Jeffreys or Kass and Raftery (1995). In Kass & Raftery's prescription, $\ln K$ in the range $(1,3)$ is considered evidence in favour of M_1, whereas $\ln K$ in the range $(3,5)$ is considered strong evidence and larger values of K are considered decisive. Ratios for which $|\ln K| < 1$ are uninformative.

CHOICE OF PRIORS.—In our case the λ_α represent Lagrangian coefficients. Some prior estimates exist, but the datasets from which these were obtained are not independent of the 9-year WMAP data used in this analysis. For this reason we disregard these prior constraints, and therefore some other way must be found to justify the functional form of each prior.

If we insist that perturbation theory is valid then the λ_α should not be too large. This requirement is convenient but not obviously necessary. However, for the purpose of performing a concrete calculation we shall adopt it in what follows. In that case, the requirement that the bispectrum generated by the operator O^α does not overwhelm the power spectrum $\mathcal{P}_\zeta$ is roughly $|\lambda_\alpha|\mathcal{P}_\zeta^{1/2} \lesssim 1$, and therefore $|\lambda_\alpha| \lesssim 10^4$. This limit is helpful but gives no guidance regarding the functional form of $P(\lambda_\alpha|M)$. To explore the range of outcomes we consider two possibilities:

- The 'Jeffries prior' $P(\lambda_\alpha) \propto |\lambda_\alpha|^{-1}$. This choice assigns equal probability for each decade of $|\lambda_\alpha|$: that is, for λ_α to be between 1 and 10, 10 and 100, and so on. The Jeffries prior makes it relatively likely for $|\lambda_\alpha|$ to be near zero, and therefore can be regarded as conservative.[13]

- The flat prior, for which $P(\lambda_\alpha)$ is constant. This choice assigns equal probability to each

[13]Strictly, the Jeffries prior has a divergence at $\lambda_\alpha = 0$. We regularize this by cutting out the region $|\lambda_\alpha| < 1$ and taking $P(\lambda_\alpha)$ to be zero within it. We have checked that our results are robust to modest changes of the boundary value. The choice of cutoff at unity is, of course, somewhat arbitrary. However, motivated by the fact that in the single parameter case λ_α corresponds to the conventionally defined $f_{\rm NL}$ parameter, we note that error bars on $f_{\rm NL}$ for single field inflationary models are at best expected to achieve values of order unity. Therefore, we shall regard $\lambda_\alpha = 1$ as a 'natural' cutoff, but shall also consider the dependency of the results on the cutoff, by presenting results with cutoff at 0.01, i.e. at a value of order of the slow roll parameters.

value of λ_α, and therefore makes it relatively more likely for $|\lambda_\alpha|$ to be large. It is less conservative than the Jeffries prior in the sense that that it enhances the probability for the Lagrangian (1.4) to predict observably large nongaussianities.

Examples

- First, consider the comparison between a trivial Gaussian model (M_1) for which $\lambda_\alpha = 0$ and a DBI-like model (M_2) with free parameter $\lambda_B \neq 0$.

  Adopting the Jeffries prior, the Bayes factor between these models is

  $$K_{21} = \frac{1}{I} \exp\Big(\frac{\chi^2(\lambda_B = 0)}{2}\Big) \int_{-10^4}^{10^4} \exp\Big(-\frac{\chi^2(\lambda_B)}{2}\Big) \frac{\mathrm{d}\lambda_B}{|\lambda_B|}. \tag{1.44}$$

  The normalization factor I formally satisfies $I = \int_{-10^4}^{10^4} \mathrm{d}\lambda_B/|\lambda_B|$, although it is regularized as described in footnote 13. We find $\ln K_{21} \approx 0.63$ which gives no preference for either model. Note that there is an 'Ockham's razor' penalty implicit in (1.44), because the parameter λ_B is allowed to float over a relatively large interval. For a flat prior this Ockham penalty strongly disfavours the DBI model, producing $\ln K_{21} = -4.23$. We conclude that the data are not sufficient to overcome the ambiguity in specifying a prior.

  The Bayes factor K_{21} is only one of a number of metrics which can be used to assess goodness of fit. Another is the Akaike 'information criterion', defined by $\mathrm{AIC} = \chi^2_{\mathrm{MLE}} + 2k$, where k measures the number of parameters in the model and is a proxy for the 'Ockham razor' penalty of Eq. (1.43). The model with smallest AIC is preferred. We find $\mathrm{AIC}_1 - \mathrm{AIC}_2 = -1.56$, which implies a preference for the trivial Gaussian model M_1 in comparison to a model with nonzero λ_B. The same preference is found if we allow any other single Lagrangian parameter to be nonzero.

- Next, consider a third DBI-like model M_3 in which the two parameters λ_B and λ_D (or, equivalently, the parameters c_s and $\tilde{c}_3$ in the notation of §1.5) are allowed to float. We find

		Jeffries prior	
	AIC difference	$\lvert\ln K\rvert$, cutoff=1	$\lvert\ln K\rvert$, cutoff=0.01
M_1 vs. M_3	−0.94	1.26	0.75
M_2 vs. M_3	0.62	0.64	0.38

  The Akaike information criterion prefers M_1 to M_3, but M_3 to M_2. Therefore the trivial Gaussian model M_1 is preferred overall, but if we discard this option then the information criterion prefers a two-parameter fit (M_3) to a single-parameter fit (M_2).

The Bayes factors are inconclusive, but it could be argued that they show a weak preference for the opposite conclusion. We compute the Bayes factor using two different choices for the regularization of the Jeffries prior; see footnote 13 on p. 84. A *smaller* cutoff increases the weight of probability for the λ_α to be near zero, and therefore *decreases* the probability that the model generates an observable signature. As we increase the lower limit for the parameters λ_α to the 'natural' level $\lambda_\alpha = 1$, the Bayes factor does not strongly discriminate between a two- or three-parameter fit. However, it does marginally begin to disfavour a two-parameter fit (M_3) compared to the trivial model (M_1). Therefore it appears that a fit for a DBI-like model using more than two parameters becomes mildly in tension with the data for 'natural' choices of the dimensionless scales λ_α.

The apparent discrepancy with the Akaike information criterion should be ascribed to a stronger 'Ockham' or complexity penalty in the Bayes factor. The information criterion down-weights each model by a fixed amount depending on the number of parameters, whereas the Bayes factor attempts to account for the increased volume of parameter space which becomes available. For example, using a flat prior instead of the Jeffries prior very strongly disfavours the models M_2 and M_3.

1.7 Discussion and conclusions

The availability of high-quality maps of the CMB temperature anisotropy from the WMAP and Planck missions means that it has become feasible to search for primordial three-point correlations. Such correlations are typically predicted by any scenario in which the fluctuations have an inflationary origin, due to microphysical three-body interactions among the light, active degrees of freedom of the inflationary epoch. If detected, their precise form could provide decisive evidence in favour of the inflationary hypothesis.

Unfortunately, due to issues of computational complexity, it is not yet possible to perform a blind search for these primordial three-point correlations. Instead, we must search for signals which we have some prior reason to believe may be present in the data. Therefore the amount of information we manage to extract depends on which signals we choose to look for.

In this paper we have made a systematic search of the 9-year WMAP data for correlations which could be produced in a very general model of single-field inflation, under the assumption that the background evolution is smooth, yielding corresponding smooth and nearly scale-invariant

correlation functions. This excludes models which contain sharp features or oscillations (Starobinsky 1992; Adams, Ross and Sarkar 1997; Adams, Cresswell and Easther 2001; Hailu and Tye 2007; Bean et al. 2008; Achucarro et al. 2011; Joy, Sahni and Starobinsky 2008; Hotchkiss and Sarkar 2010; Nakashima et al. 2011; Adshead, Hu, Dvorkin et al. 2011). It also excludes models in which significant three-point correlations are generated by differences of evolution between regions of the universe separated by super-Hubble distances. Correlations generated by this mechanism are generally most significant in the 'squeezed' or soft limit, where the correlation is between fluctuations on very disparate scales. Such correlations have been disfavoured by analysis of the Planck2013 data release (Ade et al. 2013). By comparison, the 9-year WMAP data achieve a smaller signal-to-noise for such configurations. The difference between the 9-year WMAP and Planck2013 datasets is less pronounced for the momentum configurations which we probe, with for example 1σ error bars on $f_{\rm NL}^{\rm equil}$ improving from 117 to 75.

The essential steps of our analysis were assembled in §§1.2–1.4. We begin with an effective field theory which parametrizes the unknown details of three-body interactions between inflaton fluctuations, but preserves nonlinearly realized Lorentz invariance. The effective theory is agnostic regarding the physical mechanism which underlies inflation. We compute the bispectrum generated by each operator in the effective theory, and break these into principal components using a Fisher-matrix approach. The amplitude of each principal component is recovered from the data, after which the results can be translated into constraints on the mass scales which appeared in the original effective theory. We find that no significant deviation from Gaussianity has been detected in any region of the inflationary parameter space. This conclusion is consistent with previous analyses of the 9-year WMAP and Planck2013 datasets.

Our principal components are similar to those obtained by Byun & Bean, who forecast the constraints which could be obtained from a Planck-like survey (Byun and Bean 2013). We find that the best-constrained principal direction exhibits similarities to (in order) the flattened, orthogonal and 'Galileon' templates. A fourth principal direction is more complex, but at best weakly constrained.

The large space of models which fit into the class of single-field scenarios invites attempts to identify best-fitting regions. To approach this problem we use the framework of Bayesian model comparison. The results are at best weakly significant, but tend to disfavour models with more parameters when compared to simpler cases with zero or one parameter. This is not surprising given that the amplitude of each principal direction is consistent with zero. However, it should be borne in mind that our analysis is restricted to smooth and nearly scale-invariant bispectra. It is possible that a significant signal of a different type is hidden in the data. In some cases, n-point

functions of this type can be described within the framework of effective field theory (Bartolo, Cannone and Matarrese 2013). The analysis developed in §§1.2–1.4 could be applied immediately to such scenarios given a suitable choice of basis functions $\mathcal{R}_n$.

ACKNOWLEDGEMENTS

It is a pleasure to thank Andrew Liddle for many helpful discussions and useful comments on an advance draft of this manuscript. We are also grateful to Raquel Ribeiro and Sébastien Renaux-Petel for discussions which helped motivate the approach we developed in this work.

Some numerical presented in this paper were obtained using the COSMOS supercomputer, which is funded by STFC, HEFCE and SGI. Other numerical computations were carried out on the Sciama High Performance Compute (HPC) cluster which is supported by the ICG, SEPNet and the University of Portsmouth. DR and DS acknowledge support from the Science and Technology Facilities Council [grant number ST/I000976/1]. GJA is supported by STFC grant ST/I506029/1. DS also acknowledges support from the Leverhulme Trust. The research leading to these results has received funding from the European Research Council under the European Union's Seventh Framework Programme (FP/2007–2013) / ERC Grant Agreement No. [308082].

1.A THREE-POINT FUNCTIONS FOR THE EFT OPERATORS

This appendix has been expanded from the version in the original paper to include more details of the calculation of the three-point functions corresponding to each operator in the effective Lagrangian (1.4). The principal tool is Schwinger's formulation of 'in–in' expectation values and the corresponding expansion into diagrams due to Keldysh (Schwinger 1961; Bakshi and Mahanthappa 1963a; Bakshi and Mahanthappa 1963b; Keldysh 1964). The technique was applied to general relativity by Jordan, who used it to study the effective equations of motion obtained by integrating out quantum fluctuations (Jordan 1986). It was imported into cosmology by Calzetta and Hu (1987) and applied to inflation by Maldacena (2003) and subsequent authors (Weinberg 2005; Weinberg 2006).

IN–IN CALCULATIONS.—Calculating inflationary correlation functions corresponds to computing an expectation value of an operator $\mathcal{O}$ at a fixed time t_*, usually taken to be the end of inflation, given

some 'in'-state at very early times. So what we want to construct in this case are averages over all subsequent field histories of the in-states, because in cosmology we have no prior information on the out-states. Therefore we need to do an "in-in" calculation, instead of the usual "in-out" calculations that are used in calculating transition amplitudes in standard scattering calculations, where the "in" state at past infinity becomes an "out" state at future infinity. This expectation can be computed in a couple of ways. The calculations of the propagator and bispectrum for the simple inflation model in §0.4.3 and §0.8.3 were conducted using the Hamiltonian formulation (Maldacena 2003). In this appendix we will use the path integral formalism (Seery and Lidsey 2005b) to calculate the bispectrum contributions arising from the EFT operators. Both ways are entirely equivalent. This expectation value is

$$\langle \mathcal{O} \rangle_* \equiv \langle \mathrm{in} | \mathcal{O}(t_*) | \mathrm{in} \rangle, \tag{1.45}$$

where the subscript '$*$' is used to denote evaluation of $\mathcal{O}$ at time t_*. In the present case, $\mathcal{O}$ will correspond to a product of field operators evaluated at the same time but at distinct spatial positions.

Inserting a complete set of intermediate states labelled by the three-dimensional field configuration $\pi(\mathbf{x},T)$ at some arbitrary time $T > t_*$

$$\int [\mathrm{d}\pi(\mathbf{x},T)] \;\; |\pi(\mathbf{x},T)\rangle\langle\pi(\mathbf{x},T)| = \mathbf{1}, \tag{1.46}$$

we conclude

$$\langle \mathcal{O} \rangle_* = \int [\mathrm{d}\pi(\mathbf{x},T)] \, \langle \mathrm{in} | \pi(\mathbf{x},T)\rangle\langle\pi(\mathbf{x},T) | \mathcal{O}(t_*) | \mathrm{in} \rangle, \tag{1.47}$$

where the measure $[\mathrm{d}\pi(\mathbf{x},T)]$ denotes integration over all field configurations (Peskin and Schroeder 1995). Each overlap in (1.47) can be written as a conventional Feynman path integral,

$$\langle \pi(\mathbf{x},T) | \mathrm{in} \rangle = \int [\mathrm{d}\pi]_{\mathrm{in}}^{\pi(\mathbf{x},T)} \, \exp\left[\mathrm{i} S(\pi) \right] \tag{1.48}$$

with the integration running over all field *histories* $\pi(\mathbf{x},t)$ which are consistent with the in-state $|\mathrm{in}\rangle$ in the far past, and which coincide with the configuration $\pi(\mathbf{x},T)$ at time T. The result is the 'closed time path' integral

$$\langle \mathcal{O}(t_*) \rangle = \int [\mathrm{d}\pi_+ \, \mathrm{d}\pi_-] \, \mathcal{O}(t_*) \, \exp\left[\mathrm{i} S(\pi_+) - \mathrm{i} S(\pi_-) \right] \delta[\pi_+(T) - \pi_-(T)], \tag{1.49}$$

with the independent integrations π_+, π_- running over field histories which are compatible with the in-state but are unrestricted at late times. This is shown in Figure. 1.4.

The action now implicitly contains $\mathrm{i}\epsilon$ terms that implement the $|\mathrm{in}\rangle$ vacuum as described in Weinberg (2005). Eq. (1.49) admits an expansion into diagrams in which the Green's functions connecting only '+' or only '−' fields obey the usual Feynman boundary conditions, but are

augmented by Green's functions which mix the '+' and '−' labels and whose boundary conditions are determined by the δ-function. For further details, see Weinberg (2005).

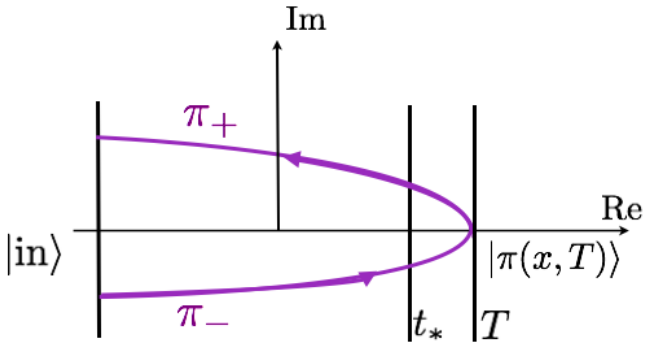

Figure 1.4: Schwinger's closed time path integral.

Mode functions.—It was explained in §1.3 that we approximate the mode functions as Hankel functions of order 3/2. Analytically, this corresponds to building Green's functions from the mode function

$$u(\tau,\mathbf{k}) = \frac{\mathrm{i}H}{\sqrt{4\epsilon\tilde{c}_\mathrm{s}k^3}}(1+\mathrm{i}k\tilde{c}_\mathrm{s}\tau)e^{-\mathrm{i}k\tilde{c}_\mathrm{s}\tau}, \tag{1.50}$$

and its complex conjugate. In this formula, $\tau = -\int_t^\infty \mathrm{d}t'/a(t')$ is the conformal time and $\tilde{c}_\mathrm{s}$ is a 'generalized' speed of sound. This will also contain $\mathrm{i}\epsilon$ terms, but they can be accounted for by rotating the contour of integration over the action at $-\infty$, which we will denote in future equations by $-\infty^+$. The procedure is analogous to performing a Wick rotation $\tau \to \mathrm{i}\tau$ in Minkowski space (Peskin and Schroeder 1995). In a model without fourth-derivative kinetic terms this will usually be the phase velocity, determined from the ratio of coefficients of the spatial and temporal kinetic terms. In other cases it may bear less relation to what would normally be thought of as a phase velocity. Our notation coincides with that of Bartolo et al. (2010a) and Bartolo et al. (2010b), to which we refer for further details; see especially the discussion below Eq. (2.6) in Bartolo et al. (2010b). In writing Eq. (1.50) we have assumed that the in-state $|\mathrm{in}\rangle$ contains zero particles, corresponding to the 'Bunch–Davies' vacuum (Bunch and Davies 1978).

The general expression for the propagator (67) can be written as

$$\langle\zeta(k_1,\tau)\zeta(k_2,\eta)\rangle = (2\pi)^3\delta(k_1+k_2)\times\begin{cases}u(k_1,\tau)u^*(k_2,\eta) & \tau<\eta\\ u^*(k_1,\tau)u^*(k_2,\eta) & \tau>\eta\end{cases} \tag{1.51}$$

Calculating three-point correlation functions amounts to setting the operator $\mathcal{O}(t_*)$ appearing in (1.49) to be the product of three copies of the field π evaluated at a common time τ_*, but

with different wave numbers

$$\langle \pi_{\mathbf{k}_1}\pi_{\mathbf{k}_2}\pi_{\mathbf{k}_3}\rangle = \int [\mathrm{d}\pi]\, \pi(\mathbf{k}_1,\tau_*)\pi(\mathbf{k}_2,\tau_*)\pi(\mathbf{k}_3,\tau_*)\, \exp\Big[\mathrm{i}S(\pi)\Big], \tag{1.52}$$

The action can be expanded order by order as follows $S = S_2 + S_3 + \ldots$, where S_2 is the second order "Gaussian" action and S_3 is the interaction action (1.4). Performing a Taylor expansion of $\exp\Big[\mathrm{i}S_3(\pi)\Big]$ and keeping only the leading order non-zero contribution gives [14]

$$\langle \pi_{\mathbf{x}_1}\pi_{\mathbf{x}_2}\pi_{\mathbf{x}_3}\rangle = \int [\mathrm{d}\pi]\, \exp\Big[\mathrm{i}S_2(\pi)\Big]\, \pi(\mathbf{k}_1,\tau_*)\pi(\mathbf{k}_2,\tau_*)\pi(\mathbf{k}_3,\tau_*)\, \Big[\mathrm{i}S_3(\pi)\Big], \tag{1.53}$$

where the "external" momenta $\mathbf{k}_i$ are associated with the time of observation τ_*. The three-point function contribution from each operator in the EFT action (1.4) is computed by substituting the operator into this equation. As an example we will detail the calculation of the three-point function arising from $O_D = -4M_3^4\dot{\pi}^3/3$. Transforming to conformal time and using $\zeta = -H\pi$ to write the correlation functions in terms of the observationally relevant quantity ζ we can use (1.53) to write this operators contribution to the three-point function as

$$\begin{aligned}\langle \zeta_{\mathbf{k}_1}\zeta_{\mathbf{k}_2}\zeta_{\mathbf{k}_3}\rangle = &\int [\mathrm{d}\zeta]\, \exp\Big[\mathrm{i}S_2(\pi)\Big]\, \zeta(\mathbf{k}_1,\tau_*)\zeta(\mathbf{k}_2,\tau_*)\zeta(\mathbf{k}_3,\tau_*)\\ &\int_{-\infty+}^{\tau_*}\mathrm{d}\eta \int \mathrm{d}^3x \frac{4}{3}M_3(t)^4\frac{1}{H^4\eta}\int \Pi_i\Big[\frac{\mathrm{d}^3q_i}{(2\pi)^3}\Big]\zeta'(\mathbf{q}_1,\eta)\zeta'(\mathbf{q}_2,\eta)\zeta'(\mathbf{q}_3,\eta)\\ &\exp\big[-\mathrm{i}(\mathbf{q}_1+\mathbf{q}_2+\mathbf{q}_3)\cdot\mathbf{x}\big],\end{aligned} \tag{1.54}$$

where we written O_D in Fourier space and have also used the fact that $a = -1/H\eta$. The "internal" momenta $\mathbf{q}_i$ are associated with early times. Performing the d^3x and $[\mathrm{d}\zeta]$ integrals we find

$$\begin{aligned}\langle \zeta_{\mathbf{k}_1}\zeta_{\mathbf{k}_2}\zeta_{\mathbf{k}_3}\rangle = &\int_{-\infty+}^{\tau_*}\mathrm{d}\eta \int \mathrm{d}^3x \frac{4}{3}M_3(t)^4\frac{1}{H^4\eta}\int \Pi_i\Big[\frac{\mathrm{d}^3q_i}{(2\pi)^3}(2\pi)^3\Big]\delta(\mathbf{q}_1+\mathbf{q}_2+\mathbf{q}_3)\\ &\langle\zeta(\mathbf{k}_1,\tau_*)\zeta'(\mathbf{q}_1,\eta)\rangle\langle\zeta(\mathbf{k}_2,\tau_*)\zeta'(\mathbf{q}_2,\eta)\rangle\langle\zeta(\mathbf{k}_3,\tau_*)\zeta'(\mathbf{q}_3,\eta)\rangle\\ &+\text{perms.}+\text{c.c.},\end{aligned} \tag{1.55}$$

where we used Wick's theorem to break up the correlation function into three copies of the propagator (1.51) connecting internal and external momenta, where the permutations arise from all the different ways to connect the internal momentum lines associated with the interaction with the external physical momenta.

Using (1.51) and (1.50) it is straightforward to show that this reduces to

$$\begin{aligned}\langle \zeta_{\mathbf{k}_1}\zeta_{\mathbf{k}_2}\zeta_{\mathbf{k}_3}\rangle = &-\frac{1}{24}\mathrm{i}(2\pi)^3\delta(\mathbf{k}_1+\mathbf{k}_2+\mathbf{k}_3)M_3(t)^4H_\star\left(\frac{\tilde{c}_\mathrm{s}}{\epsilon}\right)^3\\ &(1+\mathrm{i}\tilde{c}_\mathrm{s}k_1\tau_*)(1+\mathrm{i}\tilde{c}_\mathrm{s}k_2\tau_*)(1+\mathrm{i}\tilde{c}_\mathrm{s}k_3\tau_*)\exp[-\mathrm{i}\tilde{c}_\mathrm{s}k_t\tau_*]\\ &\int_{-\infty+}^{\tau_*}\mathrm{d}\eta\ \eta^2\exp[\mathrm{i}\tilde{c}_\mathrm{s}k_t\eta]+\text{perms.},\end{aligned} \tag{1.56}$$

[14] The first term in the Taylor expansion will be zero as a consequence of the Gaussian measure. Higher order terms in $S_3(\pi)$ will be negligible as they will be down by a factor of slow-roll compared to the tree-level contribution.

We are performing the calculations at horizon-crossing and the Hubble parameter is approximately constant during inflation so $H \approx H_\star$. The integral can be computed by performing many integrations by parts. The result is

$$\int_{-\infty+}^{\tau_*} \mathrm{d}\eta\ \eta^2 \mathrm{e}^{\mathrm{i}\tilde{c}_s k_t \eta} = \Big[\frac{\mathrm{i}}{\tilde{c}_s k_t}\tau_*^2 + \frac{2}{\tilde{c}_s^2 k_t^2}\tau_* + \frac{2\mathrm{i}}{\tilde{c}_s^3 k_t^3}\Big]\, \mathrm{e}^{\mathrm{i}\tilde{c}_s k_t \tau_*} \tag{1.57}$$

where the contour rotation at $-\infty$ means that there are no boundary contributions from $-\infty$ as we expect. Substituting this back into (1.56) and ignoring terms $\mathrm{O}(\tau_*)$ or higher because they will be subleading around horizon-crossing, the final result is

$$\langle \zeta_{\mathbf{k}_1}\zeta_{\mathbf{k}_2}\zeta_{\mathbf{k}_3}\rangle = -\frac{1}{4}(2\pi)^3\delta(\mathbf{k}_1+\mathbf{k}_2+\mathbf{k}_3)M_3(t)^4\frac{H_\star^2}{\epsilon^3 k_\beta^3}\frac{1}{k_t^3} \tag{1.58}$$

with $k_t = k_1 + k_2 + k_3$ and $k_\beta^3 = k_1 k_2 k_3$. Performing similar calculations for the other terms, the three-point function contributions corresponding to the EFT operators in (1.4) are:

- $O_A = -\bar{M}_1^3(\partial\pi)^2\partial^2\pi/2a^4$

$$B_\zeta(k_1,k_2,k_3) \supseteq \frac{1}{16}\bar{M}_1^3\frac{H_\star^3}{\epsilon^3 c_s^4\prod_i k_i^3}\, k_1^2\ \mathbf{k}_2\cdot\mathbf{k}_3\ \mathcal{A}_1 + 1\to 2 + 1\to 3\,, \tag{1.59}$$

- $O_B = -2M_2^4\dot{\pi}(\partial\pi)^2/a^2$

$$B_\zeta(k_1,k_2,k_3) \supseteq \frac{1}{8}M_2^4\frac{H_\star^2}{\epsilon^3 c_s^2\prod_i k_i^3}k_1^2\,\mathbf{k}_2\cdot\mathbf{k}_3\left(\frac{1}{k_t}+\frac{k_2+k_3}{k_t^2}+\frac{2k_2k_3}{k_t^3}\right) + 1\to 2 + 1\to 3\,, \tag{1.60}$$

- $O_C = -\bar{M}_2^2\left[H(\partial^2\pi)(\partial\pi)^2/2 + \dot{\pi}\partial^2\partial_j\pi\partial_j\pi\right]/a^4$

$$B_\zeta(k_1,k_2,k_3) \supseteq \frac{1}{16}\bar{M}_2^2\frac{H_\star^4}{\epsilon^3 c_s^4\prod_i k_i^3}\, k_1^2\ \mathbf{k}_2\cdot\mathbf{k}_3\left[\mathcal{A}_1 + (k_2^2+k_3^2)\ \mathcal{A}_2\right] + 1\to 2 + 1\to 3\,, \tag{1.61}$$

- $O_D = -4M_3^4\dot{\pi}^3/3$

$$B_\zeta(k_1,k_2,k_3) \supseteq \frac{1}{2}M_3^4\frac{H_\star^2}{\epsilon^3\prod_i k_i}\frac{1}{k_t^3}\,, \tag{1.62}$$

- $O_E = -\bar{M}_3^2\left[H(\partial\pi)^2\partial^2\pi + \dot{\pi}\partial^2\partial_j\pi\partial_j\pi\right]/a^4$

$$B_\zeta(k_1,k_2,k_3) \supseteq \frac{1}{8}\bar{M}_3^2\frac{H_\star^4}{\epsilon^3 c_s^4\prod_i k_i^3}\, k_1^2\ \mathbf{k}_2\cdot\mathbf{k}_3\ \left(\mathcal{A}_1 + \frac{k_2^2+k_3^2}{2}\mathcal{A}_2\right) + 1\to 2 + 1\to 3\,, \tag{1.63}$$

- $O_F = -2\bar{M}_4^3\dot{\pi}^2\partial^2\pi/3a^2$

$$B_\zeta(k_1,k_2,k_3) \supseteq \frac{1}{2}\bar{M}_4^3\frac{H_\star^3}{\epsilon^3 c_s^2\prod_i k_i}\frac{1}{k_t^3}\,, \tag{1.64}$$

- $O_G = \bar{M}_5^2\dot{\pi}(\partial^2\pi)^2/3a^4$

$$B_\zeta(k_1,k_2,k_3) \supseteq -\frac{1}{8}\bar{M}_5^2\frac{H_\star^4}{\epsilon^3 c_s^4\prod_i k_i}\,\frac{1}{k_t^3}\left(3+\frac{4k_\alpha^2}{k_t^2}\right), \tag{1.65}$$

- $O_H = \bar{M}_6^2\dot{\pi}(\partial_i\partial_j\pi)^2/3a^4$

$$B_\zeta(k_1,k_2,k_3) \supseteq -\frac{1}{24}\bar{M}_6^2\frac{H_\star^4}{\epsilon^3 c_s^4\prod_i k_i^3}\,k_1^2\;(\mathbf{k}_2\cdot\mathbf{k}_3)^2\;\mathcal{A}_2\;+1\to2+1\to3\,, \tag{1.66}$$

- $O_I = -\bar{M}_7(\partial^2\pi)^3/3!a^6$

$$B_\zeta(k_1,k_2,k_3) \supseteq \frac{1}{4}\bar{M}_7\frac{H_\star^5}{\epsilon^3 c_s^6\prod_i k_i}\;\mathcal{A}_3\,, \tag{1.67}$$

- $O_J = -\bar{M}_8\partial^2\pi(\partial_j\partial_k\pi)^2/3!a^6$

$$B_\zeta(k_1,k_2,k_3) \supseteq \frac{1}{12}\bar{M}_8\frac{H_\star^5}{\epsilon^3 c_s^6\prod_i k_i^3}\,k_1^2\;(\mathbf{k}_2\cdot\mathbf{k}_3)^2\;\mathcal{A}_3+1\to2+1\to3\,, \tag{1.68}$$

- $O_K = -\bar{M}_9\partial_i\partial_j\pi\partial_j\partial_k\pi\partial_k\partial_i\pi/3!a^6$

$$B_\zeta(k_1,k_2,k_3) \supseteq \frac{1}{4}\bar{M}_9\frac{H_\star^5}{\epsilon^3 c_s^6\prod_i k_i^3}\;(\mathbf{k}_1\cdot\mathbf{k}_2)(\mathbf{k}_1\cdot\mathbf{k}_3)(\mathbf{k}_2\cdot\mathbf{k}_3)\;\mathcal{A}_3\,, \tag{1.69}$$

where $1\to2$ etc. denotes permutations.

$$\mathcal{A}_1 = \left(\frac{1}{k_t}+\frac{k_\alpha^2}{k_t^3}+\frac{3k_\beta^3}{k_t^4}\right),\quad \mathcal{A}_2 = \left(\frac{1}{k_t^3}+\frac{3(k_2+k_3)}{k_t^4}+\frac{12k_2k_3}{k_t^5}\right),\quad \mathcal{A}_3 = \left(\frac{1}{k_t^3}+\frac{3k_\alpha^2}{k_t^5}+\frac{15k_\beta^3}{k_t^6}\right),$$

with $k_\alpha^2 = k_1k_2+k_1k_3+k_2k_3$.

REFERENCES

[1] Ana Achucarro et al. 'Features of heavy physics in the CMB power spectrum'. In: *JCAP* 1101 (2011), p. 030. arXiv: 1010.3693 [hep-ph] (cit. on p. 87).

[2] Jennifer A. Adams, Bevan Cresswell and Richard Easther. 'Inflationary perturbations from a potential with a step'. In: *Phys.Rev.* D64 (2001), p. 123514. arXiv: astro-ph/0102236 [astro-ph] (cit. on p. 87).

[3] Jennifer A. Adams, Graham G. Ross and Subir Sarkar. 'Multiple inflation'. In: *Nucl.Phys.* B503 (1997), pp. 405–425. arXiv: hep-ph/9704286 [hep-ph] (cit. on p. 87).

[4] P.A.R. Ade et al. 'Planck 2013 Results. XXIV. Constraints on primordial non-Gaussianity'. In: (2013). arXiv: 1303.5084 [astro-ph.CO] (cit. on pp. 57, 80, 81, 87).

[5] Peter Adshead, Wayne Hu, Cora Dvorkin et al. 'Fast Computation of Bispectrum Features with Generalized Slow Roll'. In: *Phys.Rev.* D84 (2011), p. 043519. arXiv: 1102.3435 [astro-ph.CO] (cit. on p. 87).

[6] Peter Adshead, Wayne Hu and Vinícius Miranda. 'Bispectrum in Single-Field Inflation Beyond Slow-Roll'. In: *Phys.Rev.* D88 (2013), p. 023507. arXiv: 1303.7004 [astro-ph.CO] (cit. on p. 63).

[7] Mohsen Alishahiha, Eva Silverstein and David Tong. 'DBI in the sky'. In: *Phys.Rev.* D70 (2004), p. 123505. arXiv: hep-th/0404084 [hep-th] (cit. on pp. 63, 65).

[8] Nima Arkani-Hamed et al. 'Ghost inflation'. In: *JCAP* 0404 (2004), p. 001. arXiv: hep-th/0312100 [hep-th] (cit. on pp. 63, 65, 82).

[9] Valentin Assassi, Daniel Baumann and Daniel Green. 'Symmetries and Loops in Inflation'. In: *JHEP* 1302 (2013), p. 151. arXiv: 1210.7792 [hep-th] (cit. on p. 64).

[10] Daniel Babich, Paolo Creminelli and Matias Zaldarriaga. 'The Shape of non-Gaussianities'. In: *JCAP* 0408 (2004), p. 009. arXiv: astro-ph/0405356 [astro-ph] (cit. on p. 74).

[11] Pradip M. Bakshi and Kalyana T. Mahanthappa. 'Expectation value formalism in quantum field theory. 1.' In: *J.Math.Phys.* 4 (1963), pp. 1–11 (cit. on p. 88).

[12] Pradip M. Bakshi and Kalyana T. Mahanthappa. 'Expectation value formalism in quantum field theory. 2.' In: *J.Math.Phys.* 4 (1963), pp. 12–16 (cit. on p. 88).

[13] Nicola Bartolo, Dario Cannone and Sabino Matarrese. 'The Effective Field Theory of Inflation Models with Sharp Features'. In: *JCAP* 1310 (2013), p. 038. arXiv: 1307.3483 [astro-ph.CO] (cit. on pp. 63, 88).

[14] Nicola Bartolo et al. 'Large non-Gaussianities in the Effective Field Theory Approach to Single-Field Inflation: the Bispectrum'. In: *JCAP* 1008 (2010), p. 008. arXiv: 1004.0893 [astro-ph.CO] (cit. on pp. 62, 65, 66, 90).

[15] Nicola Bartolo et al. 'Large non-Gaussianities in the Effective Field Theory Approach to Single-Field Inflation: the Trispectrum'. In: *JCAP* 1009 (2010), p. 035. arXiv: 1006.5411 [astro-ph.CO] (cit. on pp. 62, 65, 90).

[16] Thorsten Battefeld and Jan Grieb. 'Anatomy of bispectra in general single-field inflation – modal expansions'. In: *JCAP* 1112 (2011), p. 003. arXiv: 1110.1369 [astro-ph.CO] (cit. on pp. 67, 69).

[17] Daniel Baumann and Daniel Green. 'Equilateral Non-Gaussianity and New Physics on the Horizon'. In: *JCAP* 1109 (2011), p. 014. arXiv: 1102.5343 [hep-th] (cit. on p. 64).

[18] Daniel Baumann, Leonardo Senatore and Matias Zaldarriaga. 'Scale-Invariance and the Strong Coupling Problem'. In: *JCAP* 1105 (2011), p. 004. arXiv: 1101.3320 [hep-th] (cit. on p. 64).

[19] Rachel Bean et al. 'Duality Cascade in Brane Inflation'. In: *JCAP* 0803 (2008), p. 026. arXiv: 0802.0491 [hep-th] (cit. on p. 87).

[20] C.L. Bennett et al. 'Nine-Year Wilkinson Microwave Anisotropy Probe (WMAP) Observations: Final Maps and Results'. In: *Astrophys.J.Suppl.* 208 (2013), p. 20. arXiv: 1212.5225 [astro-ph.CO] (cit. on p. 76).

[21] T. S. Bunch and P. C. W. Davies. 'Quantum field theory in de Sitter space - Renormalization by point-splitting'. In: *Royal Society of London Proceedings Series A* 360 (Mar. 1978), pp. 117–134 (cit. on p. 90).

[22] Clare Burrage, Raquel H. Ribeiro and David Seery. 'Large slow-roll corrections to the bispectrum of noncanonical inflation'. In: *JCAP* 1107 (2011), p. 032. arXiv: 1103.4126 [astro-ph.CO] (cit. on pp. 65, 75).

[23] Joyce Byun and Rachel Bean. 'Non-Gaussian Shape Recognition'. In: *JCAP* 1309 (2013), p. 026. arXiv: 1303.3050 [astro-ph.CO] (cit. on pp. 67, 69, 74, 87).

[24] E. Calzetta and B.L. Hu. 'Closed Time Path Functional Formalism in Curved Space-Time: Application to Cosmological Back Reaction Problems'. In: *Phys.Rev.* D35 (1987), p. 495 (cit. on p. 88).

[25] Xingang Chen et al. 'Observational signatures and non-Gaussianities of general single field inflation'. In: *JCAP* 0701 (2007), p. 002. arXiv: hep-th/0605045 [hep-th] (cit. on p. 65).

[26] Clifford Cheung, Paolo Creminelli et al. 'The Effective Field Theory of Inflation'. In: *JHEP* 0803 (2008), p. 014. arXiv: 0709.0293 [hep-th] (cit. on pp. 58, 60–63, 79).

[27] Clifford Cheung, A. Liam Fitzpatrick et al. 'On the consistency relation of the 3-point function in single field inflation'. In: *JCAP* 0802 (2008), p. 021. arXiv: 0709.0295 [hep-th] (cit. on p. 61).

[28] Paolo Creminelli. 'On non-Gaussianities in single-field inflation'. In: *JCAP* 0310 (2003), p. 003. arXiv: astro-ph/0306122 [astro-ph] (cit. on p. 65).

[29] Paolo Creminelli, Guido D'Amico et al. 'Galilean symmetry in the effective theory of inflation: new shapes of non-Gaussianity'. In: *JCAP* 1102 (2011), p. 006. arXiv: 1011.3004 [hep-th] (cit. on p. 75).

[30] Paolo Creminelli, Markus A. Luty et al. 'Starting the Universe: Stable Violation of the Null Energy Condition and Non-standard Cosmologies'. In: *JHEP* 0612 (2006), p. 080. arXiv: hep-th/0606090 [hep-th] (cit. on p. 61).

[31] A. Curto, E. Martinez-Gonzalez and R.B. Barreiro. 'On the optimality of the spherical Mexican hat wavelet estimator for the primordial non-Gaussianity'. In: (2010). arXiv: 1007.2181 [astro-ph.CO] (cit. on p. 75).

[32] Mafalda Dias, Raquel H. Ribeiro and David Seery. 'The Î´N formula is the dynamical renormalization group'. In: *JCAP* 1310 (2013), p. 062. arXiv: 1210.7800 [astro-ph.CO] (cit. on p. 64).

[33] Joseph Elliston, David J. Mulryne et al. 'Evolution of $f_{\rm NL}$ to the adiabatic limit'. In: *JCAP* 1111 (2011), p. 005. arXiv: 1106.2153 [astro-ph.CO] (cit. on pp. 59, 64).

[34] Joseph Elliston, David Seery and Reza Tavakol. 'The inflationary bispectrum with curved field-space'. In: *JCAP* 1211 (2012), p. 060. arXiv: 1208.6011 [astro-ph.CO] (cit. on p. 65).

[35] J.R. Fergusson, M. Liguori and E.P.S. Shellard. 'General CMB and Primordial Bispectrum Estimation I: Mode Expansion, Map-Making and Measures of f_{NL}'. In: *Phys.Rev.* D82 (2010), p. 023502. arXiv: 0912.5516 [astro-ph.CO] (cit. on pp. 67, 69, 70, 72).

[36] J.R. Fergusson, M. Liguori and E.P.S. Shellard. 'The CMB Bispectrum'. In: *JCAP* 1212 (2012), p. 032. arXiv: 1006.1642 [astro-ph.CO] (cit. on pp. 67, 70).

[37] J.R. Fergusson, D.M. Regan and E.P.S. Shellard. 'Optimal Trispectrum Estimators and WMAP Constraints'. In: (2010). arXiv: 1012.6039 [astro-ph.CO] (cit. on pp. 67, 69, 70).

[38] J.R. Fergusson, D.M. Regan and E.P.S. Shellard. 'Rapid Separable Analysis of Higher Order Correlators in Large Scale Structure'. In: *Phys.Rev.* D86 (2012), p. 063511. arXiv: 1008.1730 [astro-ph.CO] (cit. on pp. 67, 70).

[39] J.R. Fergusson and E.P.S. Shellard. 'The shape of primordial non-Gaussianity and the CMB bispectrum'. In: *Phys.Rev.* D80 (2009), p. 043510. arXiv: 0812.3413 [astro-ph] (cit. on p. 69).

[40] Girma Hailu and S.-H. Henry Tye. 'Structures in the Gauge/Gravity Duality Cascade'. In: *JHEP* 0708 (2007), p. 009. arXiv: hep-th/0611353 [hep-th] (cit. on p. 87).

[41] G. Hinshaw et al. 'Nine-Year Wilkinson Microwave Anisotropy Probe (WMAP) Observations: Cosmological Parameter Results'. In: *Astrophys.J.Suppl.* 208 (2013), p. 19. arXiv: 1212.5226 [astro-ph.CO] (cit. on pp. 57, 76).

[42] Shaun Hotchkiss and Subir Sarkar. 'Non-Gaussianity from violation of slow-roll in multiple inflation'. In: *JCAP* 1005 (2010), p. 024. arXiv: 0910.3373 [astro-ph.CO] (cit. on p. 87).

[43] R.D. Jordan. 'Effective Field Equations for Expectation Values'. In: *Phys.Rev.* D33 (1986), pp. 444–454 (cit. on p. 88).

[44] Minu Joy, Varun Sahni and Alexei A. Starobinsky. 'A New Universal Local Feature in the Inflationary Perturbation Spectrum'. In: *Phys.Rev.* D77 (2008), p. 023514. arXiv: 0711.1585 [astro-ph] (cit. on p. 87).

[45] Robert E. Kass and Adrian E. Raftery. 'Bayes Factors'. In: *Journal of the American Statistical Association* 90.430 (1995), pp. 773–795. eprint: http://amstat.tandfonline.com/doi/pdf/10.1080/01621459.1995.10476572. URL: http://amstat.tandfonline.com/doi/abs/10.1080/01621459.1995.10476572 (cit. on p. 84).

[46] L.V. Keldysh. 'Diagram technique for nonequilibrium processes'. In: *Zh.Eksp.Teor.Fiz.* 47 (1964), pp. 1515–1527 (cit. on p. 88).

[47] Juan Martin Maldacena. 'Non-Gaussian features of primordial fluctuations in single field inflationary models'. In: *JHEP* 05 (2003), p. 013. arXiv: astro-ph/0210603 (cit. on pp. 65, 88, 89).

[48] Jerome Martin et al. 'The Best Inflationary Models After Planck'. In: (2013). arXiv: 1312.3529 [astro-ph.CO] (cit. on p. 83).

[49] Pieter Daniel Meerburg, Jan Pieter van der Schaar and Pier Stefano Corasaniti. 'Signatures of Initial State Modifications on Bispectrum Statistics'. In: *JCAP* 0905 (2009), p. 018. arXiv: 0901.4044 [hep-th] (cit. on p. 74).

[50] Joel Meyers and Navin Sivanandam. 'Non-Gaussianities in Multifield Inflation: Superhorizon Evolution, Adiabaticity, and the Fate of fnl'. In: *Phys.Rev.* D83 (2011), p. 103517. arXiv: 1011.4934 [astro-ph.CO] (cit. on p. 59).

[51] Masahiro Nakashima et al. 'The effect of varying sound velocity on primordial curvature perturbations'. In: *Prog.Theor.Phys.* 125 (2011), pp. 1035–1052. arXiv: 1009.4394 [astro-ph.CO] (cit. on p. 87).

[52] Michael E. Peskin and Dan V. Schroeder. *An Introduction To Quantum Field Theory (Frontiers in Physics)*. Westview Press, 1995. ISBN: 0201503972. URL: http://www.amazon.com/Introduction-Quantum-Theory-Frontiers-Physics/dp/0201503972?SubscriptionId=13CT5CVB80YFWJEPWS02&tag=ws&linkCode=xm2&camp=2025&creative=165953&creativeASIN=0201503972 (cit. on pp. 89, 90).

[53] D.M. Regan, E.P.S. Shellard and J.R. Fergusson. 'General CMB and Primordial Trispectrum Estimation'. In: *Phys.Rev.* D82 (2010), p. 023520. arXiv: 1004.2915 [astro-ph.CO] (cit. on pp. 67, 70).

[54] Donough Regan, Mateja Gosenca and David Seery. 'Constraining the WMAP9 bispectrum and trispectrum with needlets'. In: (2013). arXiv: 1310.8617 [astro-ph.CO] (cit. on pp. 69, 70, 75).

[55] Donough Regan, Pia Mukherjee and David Seery. 'General CMB bispectrum analysis using wavelets and separable modes'. In: (2013). arXiv: 1302.5631 [astro-ph.CO] (cit. on pp. 67, 69, 70, 75).

[56] Raquel H. Ribeiro and David Seery. 'Decoding the bispectrum of single-field inflation'. In: *JCAP* 1110 (2011), p. 027. arXiv: 1108.3839 [astro-ph.CO] (cit. on p. 75).

[57] Julian S. Schwinger. 'Brownian motion of a quantum oscillator'. In: *J.Math.Phys.* 2 (1961), pp. 407–432 (cit. on p. 88).

[58] David Seery and James E. Lidsey. 'Primordial non-gaussianities from multiple-field inflation'. In: *JCAP* 0509 (2005), p. 011. arXiv: astro-ph/0506056 (cit. on p. 65).

[59] David Seery and James E. Lidsey. 'Primordial non-gaussianities in single field inflation'. In: *JCAP* 0506 (2005), p. 003. arXiv: astro-ph/0503692 (cit. on pp. 65, 89).

[60] Leonardo Senatore, Kendrick M. Smith and Matias Zaldarriaga. 'Non-Gaussianities in Single Field Inflation and their Optimal Limits from the WMAP 5-year Data'. In: *JCAP* 1001 (2010), p. 028. arXiv: 0905.3746 [astro-ph.CO] (cit. on pp. 61, 74, 77, 81).

[61] Leonardo Senatore and Matias Zaldarriaga. 'On Loops in Inflation'. In: *JHEP* 1012 (2010), p. 008. arXiv: 0912.2734 [hep-th] (cit. on p. 64).

[62] Leonardo Senatore and Matias Zaldarriaga. 'A Naturally Large Four-Point Function in Single Field Inflation'. In: *JCAP* 1101 (2011), p. 003. arXiv: 1004.1201 [hep-th] (cit. on p. 64).

[63] Leonardo Senatore and Matias Zaldarriaga. 'The Effective Field Theory of Multifield Inflation'. In: *JHEP* 1204 (2012), p. 024. arXiv: 1009.2093 [hep-th] (cit. on p. 64).

[64] Alexei A. Starobinsky. 'Spectrum of adiabatic perturbations in the universe when there are singularities in the inflation potential'. In: *JETP Lett.* 55 (1992), pp. 489–494 (cit. on p. 87).

[65] Michele Vallisneri. 'Use and abuse of the Fisher information matrix in the assessment of gravitational-wave parameter-estimation prospects'. In: *Phys.Rev.* D77 (2008), p. 042001. arXiv: gr-qc/0703086 [GR-QC] (cit. on pp. 71, 72).

[66] Steven Weinberg. 'Adiabatic modes in cosmology'. In: *Phys.Rev.* D67 (2003), p. 123504. arXiv: astro-ph/0302326 [astro-ph] (cit. on p. 59).

[67] Steven Weinberg. 'Can non-adiabatic perturbations arise after single-field inflation?' In: *Phys.Rev.* D70 (2004), p. 043541. arXiv: astro-ph/0401313 [astro-ph] (cit. on p. 59).

[68] Steven Weinberg. 'Must cosmological perturbations remain non-adiabatic after multi-field inflation?' In: *Phys.Rev.* D70 (2004), p. 083522. arXiv: astro-ph/0405397 [astro-ph] (cit. on p. 59).

[69] Steven Weinberg. 'Quantum contributions to cosmological correlations'. In: *Phys.Rev.* D72 (2005), p. 043514. arXiv: hep-th/0506236 [hep-th] (cit. on pp. 65, 88–90).

[70] Steven Weinberg. 'Quantum contributions to cosmological correlations. II. Can these corrections become large?' In: *Phys.Rev.* D74 (2006), p. 023508. arXiv: hep-th/0605244 [hep-th] (cit. on p. 88).

[71] Steven Weinberg. 'Effective Field Theory for Inflation'. In: *Phys.Rev.* D77 (2008), p. 123541. arXiv: 0804.4291 [hep-th] (cit. on p. 61).

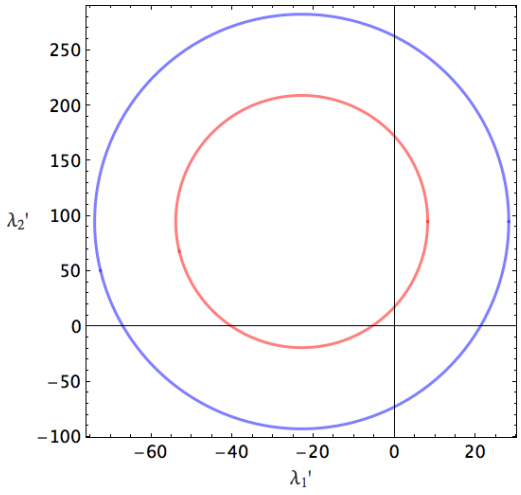

(a) λ_1' versus λ_2'

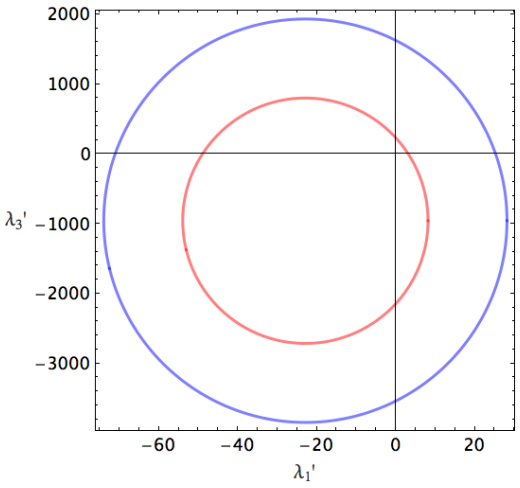

(b) λ_1' versus λ_3'

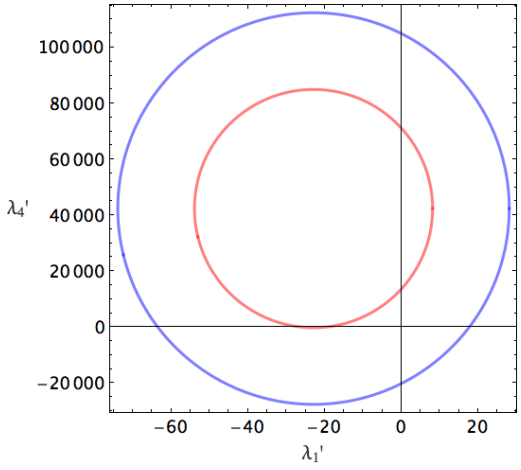

(c) λ_1' versus λ_4'

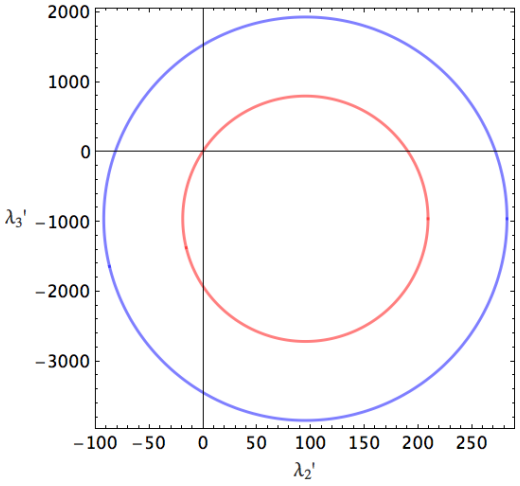

(d) λ_2' versus λ_3'

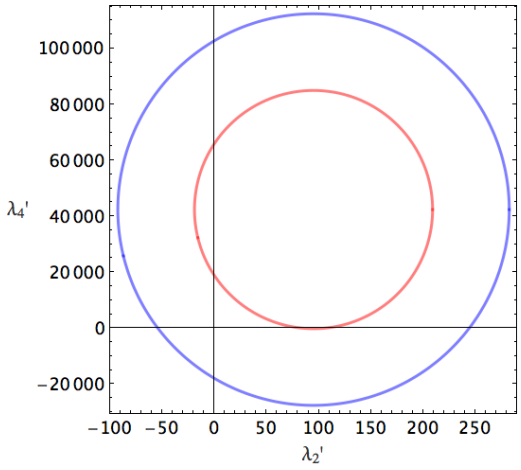

(e) λ_2' versus λ_4'

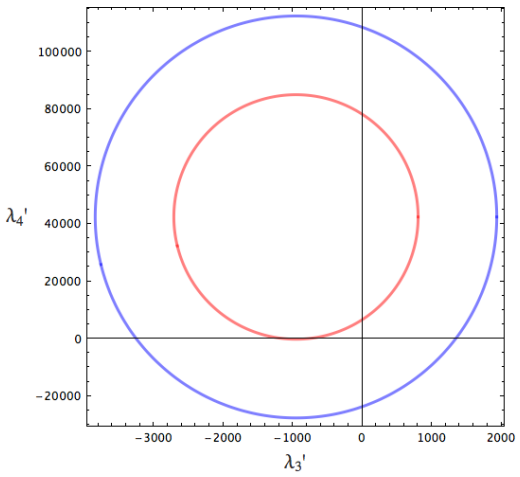

(f) λ_3' versus λ_4'

Figure 1.3: 1σ (red) 2σ (blue) confidence regions for two out of four principal components $\hat{\lambda}_{\alpha'}$ constrained by 9-year WMAP data. The results show consistency with zero magnitude generally within $1 - 1.5\sigma$, suggesting no strong evidence of nongaussianity in the single field inflationary parameter space.

Paper 2

Transport equations for the inflationary trispectrum

Gemma J. Anderson, David J. Mulryne and David Seery

We use transport techniques to calculate the trispectrum produced in multiple-field inflationary models with canonical kinetic terms. Our method allows the time evolution of the local trispectrum parameters, $\tau_{\rm NL}$ and $g_{\rm NL}$, to be tracked throughout the inflationary phase. We illustrate our approach using examples. We give a simplified method to calculate the super-horizon part of the relation between field fluctuations on spatially flat hypersurfaces and the curvature perturbation on uniform density slices, ζ, and obtain its third-order part for the first time. We clarify how the 'backwards' formalism of Yokoyama et al. relates to our analysis and other recent work. We supply explicit formulae which enable each inflationary observable to be computed in any canonical model of interest, using a suitable first-order ODE solver.

2.1 INTRODUCTION

Cosmological inflation predicts the generation of a primordial perturbation, ζ, believed to have seeded the temperature anisotropy of the cosmic microwave background ("CMB") and the galaxy density field. This fluctuation is sensitive to the physics that created it, and therefore different models of inflation typically generate perturbations with distinct statistical properties. These properties can be observed by measuring their correlation functions. We expect this approach to provide the most important observational constraints on an era of early-universe inflation.

What information is encoded in these correlation functions? The two-point function is nearly determined by the symmetries of the background, rather than the choice of microphysics, although useful information may be extracted from its scale dependence. The higher n-point functions are much less constrained, but only the three- and four-point functions (the "bispectrum" and "trispectrum") are likely to be measured in the near future. Canonical single field inflation predicts a bi- and trispectrum which will be undetectable by present-day or near-future experiments (Maldacena 2003; Lyth and Rodriguez 2005; Seery and Lidsey 2005; Seery, Lidsey and Sloth 2007; Seery and Lidsey 2007; Seery, Sloth and Vernizzi 2009). But if more than one field is active during inflation, or noncanonical interactions are present, the three- and four-point functions can be measured and their properties can discriminate between these possibilities.

Because of their observational relevance and constraining power, these "nongaussian" effects have received considerable attention. During inflation, each comoving k-mode of a light scalar field receives a perturbation when the corresponding physical scale crosses outside the horizon. Once outside, causality forbids any exchange between neighbouring regions and therefore ζ must be generated by reprocessing the local fluctuations. Where only a single degree of freedom ζ_g is relevant, this gives (Starobinsky 1985; Sasaki and Stewart 1996; Lyth and Rodriguez 2005)

$$\zeta(\mathbf{x}) = \zeta_g(\mathbf{x}) + \frac{3}{5} f_{\mathrm{NL}} (\zeta_g^2(\mathbf{x}) - \langle \zeta_g^2 \rangle) + \frac{9}{25} g_{\mathrm{NL}} \zeta_g^3(\mathbf{x}) + \cdots , \tag{2.1}$$

where all quantities are evaluated at the same time, and $\mathbf{x}$ labels a coarse-grained spatial position with sub-horizon details smoothed out. This local character gives each correlation function a very distinctive momentum dependence. At leading-order the bispectrum has only one possibility, generated by the quadratic term in (2.1). Its amplitude is parametrized by the number f_{NL} (Verde et al. 2000; Komatsu and Spergel 2001), which may depend weakly on the smoothing scale. But the trispectrum has two possibilities, generated respectively by the cubic term and the square of the quadratic term. These are conventionally parametrized by the numbers τ_{NL} and g_{NL} (Sasaki,

Väliviita and Wands 2006; Boubekeur and Lyth 2006; Alabidi and Lyth 2006; Seery and Lidsey 2007; Byrnes, Sasaki and Wands 2006). In the single-field case, τ_{NL} does not appear in (2.1) and can be expressed in terms of f_{NL}; the precise relation is $\tau_{\mathrm{NL}} = (6f_{\mathrm{NL}}/5)^2$. Where more than one light degree of freedom is present, they may all appear in Eq. (2.1) and this relation is weakened to the Suyama–Yamaguchi inequality $\tau_{\mathrm{NL}} \geqslant (6f_{\mathrm{NL}}/5)^2$ (Suyama and Yamaguchi 2008; Smith, LoVerde and Zaldarriaga 2011). The role of such relations in diagnosing the active particle spectrum during inflation was recently emphasized by Assassi, Baumann and Green (2012).

TRANSPORT METHODS.—In this paper we explain how the non-linearity parameters τ_{NL} and g_{NL} can be calculated using "transport" methods.

Such calculations can already be carried out within the "δN formalism" (Starobinsky 1985; Sasaki and Stewart 1996; Lyth and Rodriguez 2005), which requires a Taylor expansion of the background solution in small displacements from a chosen initial condition. An expression for τ_{NL} was given in this formalism by Alabidi and Lyth (2006). A comparable result for g_{NL} was provided by Sasaki, Väliviita and Wands (2006) in the context of a curvaton model, and later generalized to an arbitrary number of light fields in Seery and Lidsey (2007). The "δN" Taylor expansion leads to concise and attractive analytic results. But it is not ideally suited to numerical implementation, because it relies on extracting small variations which can easily be swamped by numerical noise.

In Seery, Mulryne et al. (2012) it was explained that the Taylor expansion can be understood as a variational method to compute Jacobi fields for the flow of inflationary trajectories in phase space. These fields can be used to explore local properties of any flow, and were introduced by Jacobi in his reformulation of Hamiltonian mechanics into what is now Hamilton–Jacobi theory. In inflation, they represent the geometrical structure which underlies perturbation theory in the long wavelength limit. They recur in many areas of physics (see, e.g., Hawking and Ellis (1973) and Visser (1993)), and have been much-studied in WKB approximations to the path integral (DeWitt-Morette 1976; DeWitt-Morette and Zhang 1983; DeWitt-Morette, Zhang and Nelson 1983).

The Jacobi fields are the necessary ingredient to compute τ_{NL} and g_{NL}, but it is not necessary to use variational techniques to compute them. Their evolution can be determined equally well using an ordinary differential equation—the 'Jacobi equation' (Jacobi 1837). The equivalence was emphasized by DeWitt-Morette (1976). The Jacobi equation is usually preferable for numerical implementation. It can be solved using conventional ODE techniques and is usually much more stable against numerical noise. Jacobi methods are widely used in other applications, including gravitational lensing (Lewis and Challinor 2006; Lewis 2012).

With this motivation, one can ask whether it is possible to replace the "δN" Taylor expansion with an approach based on the Jacobi equation. To do so, one gives an evolution equation for each n-point function. Such equations were introduced in Mulryne, Seery and Wesley (2010) and Mulryne, Seery and Wesley (2011) and were originally framed in real space.[1] Real-space methods are adequate if one wishes to extract only the local part of the three-point function. But if one wishes to include more general momentum-dependence or study n-point functions for $n \geqslant 4$, where it is necessary to distinguish between "squeezed" and "collapsed" momentum configurations, one must revert to Fourier space as it is not possible to do so in real space. In Seery, Mulryne et al. (2012) it was explained how to formulate evolution equations for the full $\mathbf{k}$-space correlation functions, which can be integrated using an approach similar to the "line of sight integral" used to simplify solution of the Boltzmann equation. In Seery, Mulryne et al. (2012) this was used to give formal but explicit expressions for the n-point functions in terms of the Jacobi fields and their derivatives, and hence to demonstrate equivalence with the variational "δN formalism" up the three-point function.

In this paper we specialize this method to the trispectrum. We write a transport equation for the four-point function of field fluctuations $\delta\varphi_\alpha$ defined on spatially flat slices. As in Seery, Mulryne et al. (2012), this can be integrated in terms of Jacobi fields and reproduces the variational formulae discussed above. In a second step, we express the correlation functions of ζ in terms of those of the $\delta\varphi_\alpha$. At this point the required values of τ_{NL} and g_{NL} can be extracted. However, our method is not limited to obtention of the ζ correlation functions and can be deployed to determine the correlation functions of both ζ and any isocurvature modes.

OUTLINE.—In §2.2 we introduce the transport framework and extend it to third order. In §2.2.2 we write down the full $\mathbf{k}$-dependent equation which evolves the four-point function on superhorizon scales. By studying the momentum-dependence of this equation, we can extract (in §2.2.3) the coefficients of the "squeezed" and "collapsed" configurations. We give separate evolution equations for these.

In §2.3 we demonstrate that the transport (Jacobi) method is equivalent to the familiar Taylor expansion of the separate universe formalism. We use our evolution equation to derive ordinary differential equations which evolve the separate-universe Taylor coefficients *forward* in time, and which supply the basis of an efficient numerical implementation. In §2.4 we finish the task of

[1] A similar formalism had been introduced earlier by Yokoyama, Suyama and Tanaka (2007); Yokoyama, Suyama and Tanaka (2008), who gave evolution equations for the Taylor coefficients of the δN formalism rather than the n-point functions directly. It was shown in Seery, Mulryne et al. (2012) that these formalisms are equivalent up to the 3-point function. In §§2.3–2.5 we extend this equivalence to the 4-point function.

extracting $\tau_{\rm NL}$ and $g_{\rm NL}$ by computing the relationship between ζ and the field fluctuations $\delta\varphi_\alpha$. Our final expressions are given in §2.4.2. We supply explicit expressions which enable each inflationary observable to be computed in any canonical model of interest, using a suitable first-order ODE solver.

In §2.5 we describe the alternative *backwards* transport method introduced by Yokoyama et al., and extend it to accommodate the trispectrum parameters. We briefly comment on the relative advantages of each formulation. In §2.6 we discuss some representative numerical results. Finally, we conclude with a short discussion in §2.7.

NOTATION AND CONVENTIONS.—We set $c = \hbar = 1$ and work in terms of the reduced Planck mass, $M_{\rm P}^2 = (8\pi G)^{-1}$ where G is Newton's constant. The species of light scalar fields are indexed by Greek labels $\alpha, \beta, \ldots, .$

2.2 TRANSPORT EQUATIONS

After smoothing on a length scale $k^{-1} \gg (aH)^{-1}$, the field value in each smoothed region of the universe ("patch") will evolve independently, as though it were in a homogeneous and isotropic *separate universe*. Making use of the slow-roll approximation, and assuming that all fields are canonically normalized and minimally coupled to Einstein gravity, Eq. (32) implies each smoothed field φ_α evolves according to (Mulryne, Seery and Wesley 2010; Mulryne, Seery and Wesley 2011; Seery, Mulryne et al. 2012)

$$\frac{{\rm d}\varphi_\alpha}{{\rm d}N} = -M_{\rm P}^2 \frac{\partial \ln V(\varphi)}{\partial\varphi_\alpha} \equiv u_\alpha, \tag{2.2}$$

up to gradient-suppressed corrections. In writing (2.2) we have used the e-folding number ${\rm d}N = H\,{\rm d}t$ as a time variable, and t is cosmic time. The index α labels the species of light scalar fields and u_α can be interpreted as a flow vector describing the trajectory of the smoothed field in phase space. In this paper we will take these indices to be contracted using the flat metric $\delta_{\alpha\beta}$, so that index placement is immaterial.

If desired the slow-roll approximation could be abandoned by passing to a Hamiltonian formulation. The resulting transport equations are structurally identical, requiring only specification of suitable initial conditions. This method was described in Mulryne, Seery and Wesley (2011) and Seery, Mulryne et al. (2012) and later implemented by Dias, Frazer and Liddle (2012) for the purpose of studying D-brane models of inflation. In this paper we will restrict ourselves to

the slow-roll approximation, but our evolution equations are unchanged by this choice and can be extended immediately to the full phase space.

2.2.1 JACOBI EQUATION

The field value varies between coarse-grained patches. Picking a fiducial patch labelled by the spatial position $\mathbf{x}$, the field in a neighbouring patch at relative position $\mathbf{r}$ will be displaced by a small amount $\delta\varphi_\alpha$,

$$\varphi_\alpha(\mathbf{x}+\mathbf{r}) \approx \varphi_\alpha(\mathbf{x}) + \delta\varphi_\alpha(\mathbf{r}). \tag{2.3}$$

At a generic position, and provided the region under consideration is not too large, we can expect $|\delta\varphi_\alpha|$ to be small in comparison with $|\varphi_\alpha|$. With these assumptions the evolution of $\delta\varphi_\alpha$ can be obtained by making a Taylor expansion of the velocity u_α in the neighbourhood of the fiducial trajectory. Hence,

$$\begin{aligned}\frac{\mathrm{d}\delta\varphi_\alpha(\mathbf{r})}{\mathrm{d}N} = {} & u_{\alpha\beta}[\varphi(\mathbf{x})]\delta\varphi_\beta(\mathbf{r}) + \frac{1}{2!}u_{\alpha\beta\gamma}[\varphi(\mathbf{x})]\delta\varphi_\beta(\mathbf{r})\delta\varphi_\gamma(\mathbf{r}) \\ & + \frac{1}{3!}u_{\alpha\beta\gamma\delta}[\varphi(\mathbf{x})]\delta\varphi_\beta(\mathbf{r})\delta\varphi_\gamma(\mathbf{r})\delta\varphi_\delta(\mathbf{r}) + \cdots,\end{aligned} \tag{2.4}$$

where $u_{\alpha\beta}[\varphi(\mathbf{x})] \equiv \partial_\beta u_\alpha$, $u_{\alpha\beta\gamma}[\varphi(\mathbf{x})] \equiv \partial_\gamma u_{\alpha\beta}$ and $u_{\alpha\beta\gamma\delta}[\varphi(\mathbf{x})] \equiv \partial_\delta u_{\alpha\beta\gamma}$. We now exchange $\mathbf{r}$ for a Fourier space description. To keep the resulting equations compact we employ the 'primed' DeWitt index convention introduced in Seery, Mulryne et al. (2012). In this notation, a compound index such as α' includes a field label α and a momentum label $\mathbf{k}_\alpha$, and also indicates evaluation at some common time of interest N. The summation convention applied to α' implies integration over momentum with measure $\mathrm{d}^3\mathbf{k}_\alpha/(2\pi)^3$, and summation over the species α. In this notation we find

$$\begin{aligned}\frac{\mathrm{d}\delta\varphi_{\alpha'}}{\mathrm{d}N} = {} & u_{\alpha'\beta'}\delta\varphi_{\beta'} + \frac{1}{2!}u_{\alpha'\beta'\gamma'}\Big(\delta\varphi_{\beta'}\delta\varphi_{\gamma'} - \langle\delta\varphi_{\beta'}\delta\varphi_{\gamma'}\rangle\Big) \\ & + \frac{1}{3!}u_{\alpha'\beta'\gamma'\delta'}\Big(\delta\varphi_{\beta'}\delta\varphi_{\gamma'}\delta\varphi_{\delta'} - \langle\delta\varphi_{\beta'}\delta\varphi_{\gamma'}\delta\varphi_{\delta'}\rangle\Big) + \cdots.\end{aligned} \tag{2.5}$$

Eq. (2.5) is the nonlinear Jacobi equation. We have subtracted a zero-mode to ensure the equation of motion preserves $\langle\delta\phi\rangle = 0$ throughout the evolution. This amounts to discarding disconnected terms in the correlation functions. The disconnected terms are ones that can be written as products of lower correlation functions. The u-matrices contained in (2.5) inherit a dependence on the fiducial region $\mathbf{x}$ through their dependence on the background fields, but the resulting connected correlation functions depend only on statistical properties of the ensemble of smoothed fields.

Explicitly, we find

$$u_{\alpha'\beta'} \equiv (2\pi)^3\delta(\mathbf{k}_\alpha - \mathbf{k}_\beta)u_{\alpha\beta}[\varphi(\mathbf{x})] \tag{2.6}$$

$$u_{\alpha'\beta'\gamma'} \equiv (2\pi)^3\delta(\mathbf{k}_\alpha - \mathbf{k}_\beta - \mathbf{k}_\gamma)u_{\alpha\beta\gamma}[\varphi(\mathbf{x})] \tag{2.7}$$

$$u_{\alpha'\beta'\gamma'\delta'} \equiv (2\pi)^3\delta(\mathbf{k}_\alpha - \mathbf{k}_\beta - \mathbf{k}_\gamma - \mathbf{k}_\delta)u_{\alpha\beta\gamma\delta}[\varphi(\mathbf{x})]. \tag{2.8}$$

2.2.2 Evolution of correlation functions

The Jacobi equation (2.5) summarizes evolution in the ensemble of smoothed patches. The u-matrices can be calculated using any suitable method, such as the long-wavelength limit of cosmological perturbation theory or the separate-universe approximation. However they are obtained, they control not only the evolution of physical field fluctuations but also their correlation functions.

To show this we note that for any classical observable O not explicitly depending on time, the time derivative of its expectation value satisfies $\mathrm{d}\langle O\rangle/\mathrm{d}N = \langle \mathrm{d}O/\mathrm{d}N\rangle$, provided probability is conserved.[2] It also applies quantum-mechanically if O is a Heisenberg picture field. Transport equations for the quantum case, similar to those we will develop here, were given by Andrews (1985) and developed by Ballentine (1998). The classical limit was studied by Hepp (1974).

We define the two-point function $\Sigma_{\alpha'\beta'}$ to satisfy

$$\Sigma_{\alpha'\beta'} \equiv \langle \delta\varphi_{\alpha'}\delta\varphi_{\beta'}\rangle. \tag{2.9}$$

Recall that our index convention implies that each quantity on the right-hand side is evaluated at the common time of interest, N. Differentiating this expression, and moving the time derivative inside the expectation value as discussed above, we obtain an evolution equation for $\Sigma_{\alpha'\beta'}$,

$$\frac{\mathrm{d}\Sigma_{\alpha'\beta'}}{\mathrm{d}N} = \left\langle \frac{\mathrm{d}\delta\varphi_{\alpha'}}{\mathrm{d}N}\delta\varphi_{\beta'} + \delta\varphi_{\alpha'}\frac{\mathrm{d}\delta\varphi_{\beta'}}{\mathrm{d}N}\right\rangle. \tag{2.10}$$

Use of Eq. (2.5) allows the right-hand side to be rewritten in terms of u-matrices and correlation functions. Working to the lowest relevant order,[3] we conclude

$$\frac{\mathrm{d}\Sigma_{\alpha'\beta'}}{\mathrm{d}N} = u_{\alpha'\gamma'}\Sigma_{\gamma'\beta'} + u_{\beta'\gamma'}\Sigma_{\gamma'\alpha'} + [\geqslant 3\text{p.f.}], \tag{2.11}$$

where "$[\geqslant 3\text{p.f.}]$" denotes terms containing higher-order correlation functions which have been omitted, beginning with the three-point function. Eq. (2.11) will be a good approximation whenever

[2] Technically, the probability distribution P must vanish sufficiently rapidly on the boundary of phase space that $u_\alpha P \to 0$ there, and therefore integration by parts inside the expectation value does not generate any boundary terms.

[3] Retaining higher-order contributions would reproduce the 'loop corrections' of the δN formalism; see Boubekeur and Lyth (2006); Lyth and Seery (2008); Seery (2010).

these higher-order correlation functions are negligible, which will usually be satisfied during an epoch of quasi-exponential inflation. In that case, the correlation functions typically order their amplitudes in powers of H^2 (Jarnhus and Sloth 2008) making the relative error after translation to ζ of order $(H/M_{\rm P})^2 \ll 1$. A similar procedure gives the evolution of the three-point function. We define

$$\alpha_{\alpha'\beta'\gamma'} \equiv \langle \delta\varphi_{\alpha'} \delta\varphi_{\beta'} \delta\varphi_{\gamma'} \rangle, \tag{2.12}$$

and the corresponding transport equation is

$$\frac{\mathrm{d}\alpha_{\alpha'\beta'\gamma'}}{\mathrm{d}N} = u_{\alpha'\lambda'}\alpha_{\lambda'\beta'\gamma'} + u_{\alpha'\lambda'\mu'}\Sigma_{\lambda'\beta'}\Sigma_{\mu'\gamma'} + \text{cyclic} + [\geqslant 4\text{p.f.}], \tag{2.13}$$

where "cyclic" denotes the two cyclic permutations of each term, and "$[\geqslant 4\text{p.f.}]$" again denotes terms involving higher-order correlation functions which have been discarded, beginning with the four-point function. As for the two-point function, Eq. (2.13) will be a good approximation whenever these are negligible in comparison with the terms which have been retained.

FOUR-POINT FUNCTION.—Eqs. (2.11) and (2.13) were given in Seery, Mulryne et al. (2012). In this section, for the first time, we give the corresponding transport equation for the four-point function. To do so, we must distinguish carefully between the connected and disconnected contributions. The disconnected contributions are always present, even in the case of purely Gaussian statistics, and therefore provide no new information. But if the perturbations develop some *intrinsic* nongaussianity during their evolution, this is encoded in the *connected* part of the four-point function. To obtain it we subtract the disconnected terms from the full four-point function, and define

$$\beta_{\alpha'\beta'\gamma'\delta'} \equiv \langle \delta\varphi_{\alpha'} \delta\varphi_{\beta'} \delta\varphi_{\gamma'} \delta\varphi_{\delta'} \rangle - \Sigma_{\alpha'\beta'}\Sigma_{\gamma'\delta'} - \Sigma_{\alpha'\gamma'}\Sigma_{\beta'\delta'} - \Sigma_{\alpha'\delta'}\Sigma_{\beta'\gamma'}. \tag{2.14}$$

In statistical language, the four-point function $\langle \delta\varphi_{\alpha'} \delta\varphi_{\beta'} \delta\varphi_{\gamma'} \delta\varphi_{\delta'} \rangle$ is the moment, and the connected part $\beta_{\alpha'\beta'\gamma'\delta'}$ is the cumulant.

The transport equation for $\beta_{\alpha'\beta'\gamma'\delta'}$ is

$$\begin{aligned}\frac{\mathrm{d}\beta_{\alpha'\beta'\gamma'\delta'}}{\mathrm{d}N} = &\left(u_{\alpha'\lambda'}\beta_{\lambda'\beta'\gamma'\delta'} + 3 \text{ cyclic}\right) + \left(u_{\alpha'\lambda'\mu'}\alpha_{\lambda'\beta'\gamma'}\Sigma_{\mu'\delta'} + 11 \text{ cyclic}\right) \\ &+ \left(u_{\alpha'\lambda'\mu'\nu'}\Sigma_{\lambda'\beta'}\Sigma_{\mu'\gamma'}\Sigma_{\nu'\delta'} + 3 \text{ cyclic}\right) + [\geqslant 5\text{p.f.}].\end{aligned} \tag{2.15}$$

It can be obtained by various methods, including the Gauss–Hermite cumulant expansion used in Mulryne, Seery and Wesley (2010), the method of generating functions used in Mulryne, Seery and Wesley (2011) and the approach described above. We derive this equation in 2.B using the Gauss–Hermite approach.

2.2.3 SEPARATION OF LOCAL SHAPES

The transport equations (2.11), (2.13) and (2.15) evolve each correlation function in its entirety. Although they are first order ordinary differential equations, they are not trivial to solve because they couple the correlation functions associated with different **k**- and species labels.[4] Indeed, the coupled system can be regarded as simply a form of Boltzmann hierarchy. Like the hierarchy used to compute CMB anisotropies it must be truncated—by discarding higher-order correlation functions—if it is to be turned into a practical computational tool. We will see in §2.3 that it admits a similar kind of formal solution. But if we wish only to track the evolution of the local momentum shapes, then we can extract simpler "flavour" equations which do not involve the continuum of **k**-modes. These are ordinary differential equations for a finite number of variables and their numerical solution is straightforward.

Eqs. (2.11), (2.13) and (2.15) show that (at least to this order), each correlation function is sourced by the correlation functions of *lower* order. Hence, we proceed inductively: if the **k**-dependence of the two-point function is known, then it can be used to determine the local **k**-dependence inherited by the three-point function and subsequently the four-point function.

TWO-POINT FUNCTION.—Since we anticipate approximate scale-invariance, we write the two-point function as

$$\Sigma_{\alpha'\beta'} = (2\pi)^3 \delta(\mathbf{k}_\alpha + \mathbf{k}_\beta) \frac{\Sigma_{\alpha\beta}}{k_\alpha^3}, \tag{2.16}$$

where $\Sigma_{\alpha\beta}$ has dimension of $[\text{mass}]^2$ but is nearly independent of $k_\alpha = k_\beta$. It is this k_α^{-3} dependence which will be inherited by all higher n-point functions. The possible ways in which this inheritance can happen correspond to the possible local ("squeezed" and "collapsed") momentum shapes.

We first require a transport equation for $\Sigma_{\alpha\beta}$. As described above, this is a flavour-only matrix, carrying indices for the species of scalar fields but not momentum labels. Substituting (2.16) into (2.11), we conclude

$$\frac{\mathrm{d}\Sigma_{\alpha\beta}}{\mathrm{d}N} = u_{\alpha\lambda}\Sigma_{\lambda\beta} + u_{\beta\lambda}\Sigma_{\lambda\alpha}. \tag{2.17}$$

This is symbolically the same equation as the full **k**-space transport equation, Eq. (2.11), with primed indices exchanged for unprimed ones.

[4] For example, the four-point function with momentum labels $\mathbf{k}_1$, $\mathbf{k}_2$, $\mathbf{k}_3$ and $\mathbf{k}_4$ couples to other correlation functions with momenta $\mathbf{k}_1 + \mathbf{k}_2$, and so on. Had we retained loop corrections, these would make the hierarchy considerably more complex because each correlation function no longer couples only to a few other isolated **k**-modes, but to the whole phase space of soft superhorizon modes. Handling this is a computational challenge. For one approach see, eg., Huston and Malik (2011).

In practice, $\Sigma_{\alpha\beta}$ carries a small dependence on the k-scale at which it is evaluated. This k-dependence, typically characterized by a spectral index, can also be calculated by transport methods; see Dias and Seery (2012). Recently Dias, Frazer & Liddle extended this method to obtain the scale-dependence of the spectral index, or "running" (Dias, Frazer and Liddle 2012).

THREE-POINT FUNCTION.—Examination of the transport equation for the three-point function, Eq. (2.13), shows that in a small time interval δN, the change to $\alpha_{\alpha'\beta'\gamma'}$ is of the schematic form $\delta\alpha \sim (u'\alpha + u''\Sigma\Sigma)\delta N$, where a prime $'$ applied to u indicates one of the field-space derivatives which generate the index structure for the u-matrices. The $u'\alpha$ terms generate a change $\delta\alpha$ which is proportional to the momentum-dependence already carried by α. Therefore this term can reorganize the amplitudes of these shapes, but introduces no new types of momentum dependence. New shapes are sourced only by the $\Sigma\Sigma$ terms.

Eq. (2.16) shows that the product $\Sigma\Sigma$ must generate a shape of the form $k_\alpha^{-3}k_\beta^{-3}$, and therefore the most general structure which can be *sourced* during the evolution has the form

$$\alpha_{\alpha'\beta'\gamma'} \supseteq (2\pi)^3\delta(\mathbf{k}_\alpha + \mathbf{k}_\beta + \mathbf{k}_\gamma)\left(\frac{a_{\alpha|\beta\gamma}}{k_\beta^3 k_\gamma^3} + \frac{a_{\beta|\alpha\gamma}}{k_\alpha^3 k_\gamma^3} + \frac{a_{\gamma|\alpha\beta}}{k_\alpha^3 k_\beta^3}\right), \tag{2.18}$$

where we use the notation "$\supseteq$" to indicate that the three-point function contains this term together with others which have not been written. The matrices $a_{\alpha|\beta\gamma}$ carry information about the "flavour", but do not evolve the $\mathbf{k}$-dependence. They are symmetric under exchange of $\beta \leftrightarrow \gamma$, but need not possess further symmetries. The full three-point function corresponds to the sourced contribution (2.18) plus an *unsourced* term appearing as its initial condition. The unsourced piece is generated by quantum interference effects operating around the epoch of horizon exit, and typically has a very complicated momentum dependence (Seery and Lidsey 2005). However, its amplitude is small in the canonical models to which we restrict attention in this paper (Lyth and Zaballa 2005; Vernizzi and Wands 2006).

After substitution of (2.18) into the transport equation (2.13), we obtain an evolution equation for $a_{\alpha|\beta\gamma}$,

$$\frac{\mathrm{d}a_{\alpha|\beta\gamma}}{\mathrm{d}N} = u_{\alpha\lambda}a_{\lambda|\beta\gamma} + u_{\beta\lambda}a_{\alpha|\lambda\gamma} + u_{\gamma\lambda}a_{\alpha|\beta\lambda} + u_{\alpha\lambda\mu}\Sigma_{\lambda\beta}\Sigma_{\mu\gamma}. \tag{2.19}$$

Eq. (2.19) strictly applies only when the momenta entering the correlation function are not too dissimilar in magnitude. This is usually an acceptable approximation for CMB experiments, but a more refined analysis might be required where larger hierarchies of scale exist. This issue is not confined to the transport framework; it applies to results obtained using any method, including the familiar δN Taylor expansion.

FOUR-POINT FUNCTION.—Eqs. (2.17) and (2.19) were given in Seery, Mulryne et al. (2012). The

same analysis applied to the four-point function shows that, in a small time interval δN, the change in the connected part of the correlation function has the schematic form

$$\delta\beta \sim (u'\beta + u''\alpha\Sigma + u'''\Sigma\Sigma\Sigma)\delta N. \tag{2.20}$$

As for the three-point function, the term $u'\beta$ is simply a shift in the amplitude of shapes already present in β. The sourced contributions are now $u''\alpha\Sigma$ and $u'''\Sigma\Sigma\Sigma$. Of these, the $\Sigma\Sigma\Sigma$ term must generate a shape of the form $k_\alpha^{-3}k_\beta^{-3}k_\gamma^{-3}$, which can be recognized as a g_{NL}-type contribution (Byrnes, Sasaki and Wands 2006).

The $\alpha\Sigma$ term is more complex, because the momentum δ-function in u'' [see Eq. (2.7)] reorganizes the momenta appearing in the denominators of the three-point function (2.18). Written out explicitly, this term is

$$\begin{aligned} u_{\alpha'\lambda'\mu'}\alpha_{\lambda'\beta'\gamma'}\Sigma_{\mu'\delta'} = (2\pi)^3 \int \mathrm{d}^3k_\lambda\, \mathrm{d}^3k_\mu\, \delta(\mathbf{k}_\alpha - \mathbf{k}_\lambda - \mathbf{k}_\mu)\delta(\mathbf{k}_\lambda + \mathbf{k}_\beta + \mathbf{k}_\gamma)\delta(\mathbf{k}_\mu + \mathbf{k}_\delta) \\ \times u_{\alpha\lambda\mu}\frac{\Sigma_{\mu\delta}}{k_\delta^3}\Big(\frac{a_{\lambda|\beta\gamma}}{k_\beta^3 k_\gamma^3} + \frac{a_{\beta|\lambda\gamma}}{k_\lambda^3 k_\gamma^3} + \frac{a_{\gamma|\beta\lambda}}{k_\beta^3 k_\lambda^3}\Big), \end{aligned} \tag{2.21}$$

plus the nontrivial permutations of α', β', γ' and δ'. The first term in round brackets, $\sim k_\beta^{-3}k_\gamma^{-3}$, has the form of a g_{NL}-type contribution. But the remaining terms involve k_λ^{-3}, and the δ-functions in (2.21) show that $\mathbf{k}_\lambda = \mathbf{k}_\alpha + \mathbf{k}_\delta$. Therefore this term generates a *different* momentum shape; it is the "collapsed" configuration, which corresponds to a τ_{NL}-type contribution (Byrnes, Sasaki and Wands 2006). It follows that the most general structure sourced by time evolution can be written

$$\beta_{\alpha'\beta'\gamma'\delta'} = (2\pi)^3\delta(\mathbf{k}_\alpha+\mathbf{k}_\beta+\mathbf{k}_\gamma+\mathbf{k}_\delta)\Big(\frac{g_{\alpha|\beta\gamma\delta}}{k_\beta^3k_\gamma^3k_\delta^3} + 3\text{ cyclic} + \frac{\tau_{\alpha\beta|\gamma\delta}}{k_\alpha^3k_\beta^3|\mathbf{k}_\alpha+\mathbf{k}_\gamma|^3} + 11\text{ cyclic}\Big), \tag{2.22}$$

where the "cyclic" pieces refer to the cyclic permutations of the preceding terms. The matrix $g_{\alpha|\beta\gamma\delta}$ is symmetric under any exchange of β,γ,δ, but has no symmetries under permutations involving α. The matrix $\tau_{\alpha\beta|\gamma\delta}$ is symmetric under the simultaneous exchanges $\alpha \leftrightarrow \beta$ and $\gamma \leftrightarrow \delta$, giving 12 independent elements.

Substitution of (2.22) into the transport equation (2.15) enables us to extract individual evolution equations for $g_{\alpha|\beta\gamma\delta}$ and $\tau_{\alpha\beta|\gamma\delta}$. They are

$$\begin{aligned} \frac{\mathrm{d}g_{\alpha|\beta\gamma\delta}}{\mathrm{d}N} &= u_{\alpha\lambda}g_{\lambda|\beta\gamma\delta} + u_{\beta\lambda}g_{\alpha|\lambda\gamma\delta} + u_{\gamma\lambda}g_{\alpha|\beta\lambda\delta} + u_{\delta\lambda}g_{\alpha|\beta\gamma\lambda} \\ &\quad + u_{\alpha\lambda\mu}a_{\lambda|\beta\gamma}\Sigma_{\mu\delta} + u_{\alpha\lambda\mu}a_{\lambda|\beta\delta}\Sigma_{\mu\gamma} + u_{\alpha\lambda\mu}a_{\lambda|\gamma\delta}\Sigma_{\mu\beta} + u_{\alpha\lambda\mu\nu}\Sigma_{\lambda\beta}\Sigma_{\mu\gamma}\Sigma_{\nu\delta} \end{aligned} \tag{2.23}$$

$$\begin{aligned} \frac{\mathrm{d}\tau_{\alpha\beta|\gamma\delta}}{\mathrm{d}N} &= u_{\alpha\lambda}\tau_{\lambda\beta|\gamma\delta} + u_{\beta\lambda}\tau_{\alpha\lambda|\gamma\delta} + u_{\gamma\lambda}\tau_{\alpha\beta|\lambda\delta} + u_{\delta\lambda}\tau_{\alpha\beta|\gamma\lambda} \\ &\quad + u_{\gamma\lambda\mu}\Sigma_{\mu\alpha}a_{\delta|\lambda\beta} + u_{\delta\lambda\mu}\Sigma_{\mu\beta}a_{\gamma|\lambda\alpha}. \end{aligned} \tag{2.24}$$

Note that the a-dependent source terms in the second line of (2.24) preserve the symmetry under simultaneous exchange of the index pairs (α, β) and (γ, δ). We have dropped the initial value of $\alpha_{\alpha'\beta'\gamma'}$, even though it appears in (2.15) as a source term and, as a matter of principle, could appear in $\beta_{\alpha'\beta'\gamma'\delta'}$ with a non-negligible coefficient. In 2.A we show that this will usually be an acceptable approximation in models with canonically normalized scalar fields; the initial value of $\alpha_{\alpha'\beta'\gamma'}$ remains negligible provided $|r f_{\rm NL}| \lesssim 1$ throughout the evolution where $r < 1$ is the tensor-to-scalar ratio. On the other hand, in non-canonical models where the initial value need *not* be negligible it is important to retain this term (Renaux-Petel 2009).

2.3 EQUIVALENCE TO TAYLOR EXPANSION METHOD

Eqs. (2.23)–(2.24) enable us to follow the evolution of the sourced, local-mode contributions to the trispectrum. As we will explain in §2.4, after changing variable to ζ they allow us to calculate the observable quantities $\tau_{\rm NL}$ and $g_{\rm NL}$. However, they are quite different in appearance to the familiar expressions of the "δN formalism",[5] which take the form of a Taylor expansion in the initial conditions (Lyth and Rodriguez 2005).

The connexion between these methods was explored in Seery, Mulryne et al. (2012). By formally integrating the transport equations, in a similar way to the "line of sight" integral used when solving the Boltzmann equation, it is possible to demonstrate equality with the "δN" expressions. In Seery, Mulryne et al. (2012) this analysis was given for the two- and three-point functions. Here we extend it to include the four-point function.

INTEGRATING FACTOR.—The "line of sight integral" naturally expresses each correlation function in terms of the underlying Jacobi fields. We briefly recapitulate the argument of Seery, Mulryne et al. (2012). Without loss of generality, we write the two-point function in the form

$$\Sigma_{\alpha'\beta'} = \Gamma_{\alpha' i'} \Gamma_{\beta' j'} \Sigma_{i' j'} . \tag{2.25}$$

A suitable choice for $\Gamma_{\alpha' i'}$ means it will function as an integrating factor. In writing (2.25) we have introduced a new type of primed Latin index (i', j', ...). This has the same interpretation as the primed Greek indices: i' carries a flavour index i and a momentum label $\mathbf{k}_i$, which range over the same values as α and $\mathbf{k}_\alpha$. However, it indicates evaluation at a different time N_0, as follows.

[5]Here and below, we use the term "δN formalism" to mean a Taylor expansion in the initial conditions, even if the quantity being expanded is not N.

Substitution of Eq. (2.25) in (2.11) shows that the terms involving $u_{\alpha'\beta'}$ can be removed if Γ is chosen to satisfy

$$\frac{\mathrm{d}\Gamma_{\alpha' i'}}{\mathrm{d}N} = u_{\alpha'\beta'}\Gamma_{\beta' i'}. \tag{2.26}$$

Comparison with Eqs (2.4)–(2.5) shows that $\Gamma_{\alpha' i'}$ has an interpretation as a differential coefficient,

$$\Gamma_{\alpha' i'} = \frac{\partial\varphi_{\alpha'}}{\partial\varphi_{i'}} = \frac{\partial\varphi_\alpha(\mathbf{k}_\alpha, N)}{\partial\varphi_i(\mathbf{k}_i, N_0)} = \delta(\mathbf{k}_\alpha - \mathbf{k}_i)\frac{\partial\varphi_\alpha(N)}{\partial\varphi_i(N_0)} \tag{2.27}$$

Eq. (2.27) is sometimes described as the "Jacobi map". It has a formal solution in terms of a path-ordered exponential

$$\Gamma_{\alpha' i'} = (2\pi)^3\delta(\mathbf{k}_\alpha - \mathbf{k}_i)\,\mathsf{P}\exp\left(\int_{N_0}^{N}\mathrm{d}N'\; u_{\alpha i}(N')\right). \tag{2.28}$$

In this expression, P denotes the path-ordering operator which rewrites its argument in order of position on the trajectory: objects evaluated early on the trajectory appear to the right of objects evaluated later. This path-ordered exponential is related to the inverse of the van Vleck matrix, which is equivalent to the matrix of Jacobi fields. Reference to Eqs. (2.13) and (2.15) shows that, in each transport equation, this choice for Γ will absorb the terms proportional to the n-point function itself. Returning to the two-point function and discarding higher-order contributions, it follows that the "kernel" $\Sigma_{i'j'}$ can be obtained as an integral over the source terms. It is this integral over sources which can be compared to the "line of sight" integral for the Boltzmann equation.

With these choices, and working to leading order, there are *no* sources for the kernel $\Sigma_{i'j'}$. Therefore it is constant, and equal to its initial condition set at horizon crossing. We write this constant value $\mathcal{S}_{i'j'}$.

THREE-POINT FUNCTION.—When this method is applied to the three-point function, it transpires that the kernel *is* sourced. Again without loss of generality, we write

$$\alpha_{\alpha'\beta'\gamma'} = \Gamma_{\alpha' i'}\Gamma_{\beta' j'}\Gamma_{\gamma' k'}A_{i'j'k'}. \tag{2.29}$$

We define $\tilde{u}_{i'j'k'} \equiv \Gamma^{-1}_{i'\alpha'}u_{\alpha'\beta'\gamma'}\Gamma_{\beta' j'}\Gamma_{\gamma' k'}$ and obtain

$$A_{i'j'k'} = \mathcal{A}_{i'j'k'} + \left[\int_{N_0}^{N}\mathrm{d}N'\;\tilde{u}_{i'm'n'}(N')\mathcal{S}_{m'j'}\mathcal{S}_{n'k'} + 2\text{ cyclic}\right] + \mathrm{O}(H^6). \tag{2.30}$$

The integration constant $\mathcal{A}_{i'j'k'}$ is the unsourced initial condition which was neglected above, and the estimate $\mathrm{O}(H^6)$ for the terms we have omitted assumes that the correlation functions order themselves in increasing powers of H^2 as described by Jarnhus and Sloth (2008). Defining

$$\begin{aligned}\Gamma_{\alpha' i' j'} = \Gamma_{\alpha' m'}\int_{N_0}^{N}\tilde{u}_{m' i' j'}(N')\,\mathrm{d}N' &= (2\pi)^3\delta(\mathbf{k}_\alpha - \mathbf{k}_i - \mathbf{k}_j)\Gamma_{\alpha m}\int_{N_0}^{N}\tilde{u}_{mij}(N')\,\mathrm{d}N',\\ &= (2\pi)^3\delta(\mathbf{k}_\alpha - \mathbf{k}_i - \mathbf{k}_j)\Gamma_{\alpha ij},\end{aligned} \tag{2.31}$$

we conclude

$$\alpha_{\alpha'\beta'\gamma'} = \Gamma_{\alpha' i'}\Gamma_{\beta' j'}\Gamma_{\gamma' k'}\mathcal{A}_{i'j'k'} + \Big(\Gamma_{\alpha' i' j'}\Gamma_{\beta' k'}\Gamma_{\gamma'\ell'}\mathcal{S}_{i'k'}\mathcal{S}_{j'\ell'} + 2 \text{ cyclic}\Big) + \text{loops}. \tag{2.32}$$

It can be shown that the quantity $\Gamma_{\alpha ij}$ appearing on the right-hand side of (2.31) is equal to[6]

$$\Gamma_{\alpha ij} = \frac{\partial\Gamma_{\alpha i}}{\partial\varphi_j(N_0)} = \frac{\partial^2\phi_\alpha(N)}{\partial\varphi_i(N_0)\partial\varphi_j(N_0)}, \tag{2.33}$$

from which it follows that Eq. (2.32) is equivalent to the Lyth–Rodríguez Taylor expansion formula for the three-point function (Lyth and Rodriguez 2005). Moreover, differentiation of (2.31) shows that $\Gamma_{\alpha ij}$ satisfies the evolution equation

$$\frac{\mathrm{d}\Gamma_{\alpha ij}}{\mathrm{d}N} = u_{\alpha\beta}\Gamma_{\beta ij} + u_{\alpha\beta\gamma}\Gamma_{\beta i}\Gamma_{\gamma j}. \tag{2.34}$$

FOUR-POINT FUNCTION.—The analysis for the four-point function is similar. We introduce the integrating factor $\Gamma_{\alpha' i'}$,

$$\beta_{\alpha'\beta'\gamma'\delta'} = \Gamma_{\alpha' i'}\Gamma_{\beta' j'}\Gamma_{\gamma' k'}\Gamma_{\delta'\ell'}B_{i'j'k'\ell'}. \tag{2.35}$$

The kernel $B_{i'j'k'\ell'}$ is given by an integral over sources, as before, which are drawn from the lower-order n-point functions. In this case they are the two- and three-point functions. Keeping only leading-order terms, we find

$$\begin{aligned} B_{i'j'k'\ell'} = \mathcal{B}_{i'j'k'\ell'} &+ \Big(\int_{N_0}^{N}\mathrm{d}N'\ \tilde{u}_{i'p'q'}(N')A_{p'j'k'}(N')\mathcal{S}_{q'\ell'} + 11 \text{ cyclic}\Big) \\ &+ \Big(\int_{N_0}^{N}\mathrm{d}N'\ \tilde{u}_{i'q'r's'}(N')\mathcal{S}_{q'j'}\mathcal{S}_{r'k'}\mathcal{S}_{s'\ell'} + 3 \text{ cyclic}\Big) + \mathrm{O}(H^8), \end{aligned} \tag{2.36}$$

where we have defined $\tilde{u}_{i'j'k'\ell'} = \Gamma^{-1}_{i'\alpha'}u_{\alpha'\beta'\gamma'\delta'}\Gamma_{\beta' j'}\Gamma_{\gamma' k'}\Gamma_{\delta'\ell'}$. The integration constant $\mathcal{B}_{i'j'k'\ell'}$ is the initial value of the four-point function at time $N = N_0$, as for the three-point function. Taking the four $\mathbf{k}$-modes entering the four-point function to have a similar time of horizon exit, and the initial time N_0 to be around this epoch, the initial condition was shown in Seery, Lidsey and Sloth (2007) and Seery, Sloth and Vernizzi (2009) to be dominated by the correlations induced by decay of gravitational waves into scalar quanta. It is negligible when the amplitude of the four-point function is sufficiently large to be observable. On the other hand, the initial value of the three-point function appears in the kernel $A_{p'j'k'}$ which forms part of the source integral (2.36), and need not be entirely negligible. However, as discussed below Eqs. (2.23)–(2.24), and in more detail in 2.A, its contribution to τ_{NL} or g_{NL} is likely no more than O(1) for models with acceptable $|f_{\mathrm{NL}}|$.

[6]Direct differentiation of Eq. (2.28) is subtle, because of the path-ordered exponential. It is simpler to differentiate the Jacobi equation, Eq. (2.26), and then solve it using $\Gamma_{\alpha i}$ as an integrating factor.

To relate (2.36) to the expressions produced by the Taylor expansion algorithm we must express $A_{p'j'k'}$ purely in terms of correlations at the initial time N_0. Combining (2.30) and (2.36) we find

$$\int_{N_0}^{N} \mathrm{d}N'\, \tilde{u}_{i'p'q'}(N') A_{p'j'k'}(N') = \int_{N_0}^{N} \mathrm{d}N'\, \tilde{u}_{i'p'q'}(N') \Big\{ \mathcal{A}_{p'j'k'} + \int_{N_0}^{N'} \mathrm{d}N''\, \tilde{u}_{p'r's'}(N'') \mathcal{S}_{r'j'} \mathcal{S}_{s'k'} + \int_{N_0}^{N'} \mathrm{d}N''\, \tilde{u}_{j'r's'}(N'') \mathcal{S}_{r'p'} \mathcal{S}_{s'k'} + \int_{N_0}^{N'} \mathrm{d}N''\, \tilde{u}_{k'r's'}(N'') \mathcal{S}_{r'p'} \mathcal{S}_{s'j'} \Big\} \tag{2.37}$$

The term involving $\mathcal{A}_{p'j'k'}$ presents no difficulties. It makes a contribution to $\beta_{\alpha'\beta'\gamma'\delta'}$ of the form

$$\beta_{\alpha'\beta'\gamma'\delta'} \supseteq \Gamma_{\alpha'p'q'} \Gamma_{\beta'j'} \Gamma_{\gamma'k'} \Gamma_{\delta'\ell'} \mathcal{A}_{p'j'k'} \mathcal{S}_{q'\ell'} + 11 \text{ cyclic}, \tag{2.38}$$

where, as above, the symbol "$\supseteq$" indicates that the four-point function contains this contribution among others. The other terms in (2.37) are nested integrals, and divide into two groups. One involves a contraction between the two u-matrices, of the form $\tilde{u}_{i'p'q'} \tilde{u}_{p'r's'}$. We first focus on the other two, which involve no contraction. After summing over permutations there are twenty-four such terms. Consider the specific choice $\tilde{u}_{i'p'q'} \tilde{u}_{j'r's'}$ which appears in (2.37). In combination with one of the terms generated by simultaneously exchanging $i' \leftrightarrow j'$ and $k' \leftrightarrow \ell'$ this generates

$$\int_{N_0}^{N} \mathrm{d}N' \int_{N_0}^{N} \mathrm{d}N''\, \tilde{u}_{i'p'q'}(N') \tilde{u}_{j'r's'}(N'') \mathcal{S}_{r'p'} \mathcal{S}_{s'k'} \mathcal{S}_{q'\ell'} + \int_{N_0}^{N} \mathrm{d}N' \int_{N_0}^{N} \mathrm{d}N''\, \tilde{u}_{j'r's'}(N') \tilde{u}_{i'p'q'}(N'') \mathcal{S}_{p'r'} \mathcal{S}_{q'\ell'} \mathcal{S}_{s'k'}, \tag{2.39}$$

where we have relabelled the dummy indices $p' \leftrightarrow r'$ and $q' \leftrightarrow s'$. Now we can combine the terms

$$\int_{N_0}^{N} \mathrm{d}N' \int_{N_0}^{N} \mathrm{d}N''\, \left[\Theta(N'' \leqslant N') + \Theta(N'' \geqslant N')\right] \times \tilde{u}_{i'p'q'}(N') \tilde{u}_{j'r's'}(N'') \mathcal{S}_{r'p'} \mathcal{S}_{s'k'} \mathcal{S}_{q'\ell'}. \tag{2.40}$$

The Heaviside functions inside the square-brackets is equal to 1,[7] so the combination can be written as

$$\int_{N_0}^{N} \mathrm{d}N' \int_{N_0}^{N} \mathrm{d}N''\, \tilde{u}_{i'p'q'}(N') \tilde{u}_{j'r's'}(N'') \mathcal{S}_{r'p'} \mathcal{S}_{s'k'} \mathcal{S}_{q'\ell'}, \tag{2.41}$$

[7]This is not strictly true. At the point $N' = N''$ this term gives a value of 2, but an integral does not depend on the value of the integrand at any particular point and therefore for the purposes of doing the integral we can replace it with 1 everywhere.

in which the integrals are no longer nested. Pairing all such terms in this way generates the 12 cyclic permutations of indices in (2.41). The corresponding contribution to the four-point function is

$$\beta_{\alpha'\beta'\gamma'\delta'} \supseteq \Gamma_{\alpha' p' q'}\Gamma_{\beta' r' s'}\Gamma_{\gamma' k'}\Gamma_{\delta'\ell'}\mathcal{S}_{p' r'}\mathcal{S}_{s' k'}\mathcal{S}_{q'\ell'} + 11 \text{ cyclic}. \tag{2.42}$$

Now focus on the contracted terms $\tilde{u}_{i' p' q'}\tilde{u}_{p' r' s'}$. Summing over the permutations $\ell' \to \{j', k'\}$ is equivalent to symmetrization over $\{q', r', s'\}$. Therefore this term can be combined with the $\tilde{u}_{i' q' r' s'}$ source in (2.36), giving a total contribution to the four-point function of the form

$$\beta_{\alpha'\beta'\gamma'\delta'} \supseteq \Gamma_{\alpha' q' r' s'}\Gamma_{\beta' j'}\Gamma_{\gamma' k'}\Gamma_{\delta'\ell'}\mathcal{S}_{q' j'}\mathcal{S}_{r' k'}\mathcal{S}_{s'\ell'} + 3 \text{ cyclic}, \tag{2.43}$$

where we have defined $\Gamma_{\alpha' q' r' s'}$ to satisfy

$$\begin{aligned}\Gamma_{\alpha' q' r' s'} = \Gamma_{\alpha' i'} \int_{N_0}^{N} \mathrm{d}N'\, \tilde{u}_{i' q' r' s'}(N') \\ + \Big(\Gamma_{\alpha' i'} \int_{N_0}^{N} \mathrm{d}N'\, \tilde{u}_{i' p' q'}(N') \int_{N_0}^{N'} \mathrm{d}N''\, \tilde{u}_{p' r' s'}(N'') + [q' \to \{r', s'\}]\Big).\end{aligned} \tag{2.44}$$

As with the previous examples of Γ-matrices, the momentum dependence of $\Gamma_{\alpha' q' r' s'}$ is a pure δ-function. It can be converted to a pure flavour matrix by the rule

$$\Gamma_{\alpha' q' r' s'} = (2\pi)^3\delta(\mathbf{k}_\alpha - \mathbf{k}_q - \mathbf{k}_r - \mathbf{k}_s)\Gamma_{\alpha q r s}. \tag{2.45}$$

By explicit differentiation and back-substitution, it can be shown that this flavour matrix satisfies the ordinary differential equation

$$\frac{\mathrm{d}\Gamma_{\alpha q r s}}{\mathrm{d}N} = u_{\alpha\beta}\Gamma_{\beta q r s} + \Big(u_{\alpha\beta\gamma}\Gamma_{\beta q r}\Gamma_{\gamma s} + 2 \text{ cyclic}\Big) + u_{\alpha\beta\gamma\delta}\Gamma_{\beta q}\Gamma_{\gamma r}\Gamma_{\delta s}. \tag{2.46}$$

We have already seen that the lower-order Taylor coefficients $\Gamma_{\alpha i}$ and $\Gamma_{\alpha i j}$ are determined by the evolution equations (2.26) (with primed indices exchanged for unprimed ones) and (2.34); for an extended discussion, see Seery, Mulryne et al. (2012). These equations provide an efficient means to compute the "δN coefficients" numerically.

Returning to the four-point function, we must also include the initial condition

$$\beta_{\alpha'\beta'\gamma'\delta'} \supseteq \Gamma_{\alpha' i'}\Gamma_{\beta' j'}\Gamma_{\gamma' k'}\Gamma_{\delta'\ell'}\mathcal{B}_{i' j' k'\ell'}. \tag{2.47}$$

Repeating the steps described above, it can be shown that

$$\Gamma_{\alpha q r s} = \frac{\partial\Gamma_{\alpha q r}}{\partial\varphi_s(N_0)} = \frac{\partial^3\varphi_\alpha(N)}{\partial\varphi_q(N_0)\partial\varphi_r(N_0)\partial\varphi_s(N_0)}. \tag{2.48}$$

Therefore we have reproduced the usual Taylor expansion formulae for the trispectrum. Specifically, Eq. (2.47) matches (8) of Seery, Lidsey and Sloth (2007), and Eqs. (2.38), (2.42) and (2.43) match (73), (74) and (75) of the same reference. These expressions were later given in slightly more generality by Byrnes, Sasaki and Wands (2006). In the formulation given by these authors, Eqs. (2.38), (2.42), (2.43) and (2.47) of this paper match (36) of Byrnes, Sasaki and Wands (2006).

2.4 TRANSFORMATION TO THE CURVATURE PERTURBATION

We now have the transport equations which evolve the n-point functions of the scalar field perturbations during inflation, up to and including $n = 4$. These can be obtained either by solving the "shape equations", Eqs. (2.23)–(2.24), or using Eq. (2.46) to evolve the Γ-matrices. For the latter case, the initial conditions are $\Gamma_{\alpha i} = \delta_{\alpha i}$ at $N = N_0$, with all other Γ-matrices zero there.

2.4.1 CURVATURE PERTURBATION AT THIRD ORDER

The scalar field fluctuations are not observable by themselves. At present we have observational evidence only for a single primordial fluctuation—the density fluctuation, which is a nonlinear and model-dependent combination of the field fluctuations. The appropriate combination can be deduced from the displacement δN (measured in e-folds) between a fixed spatially-flat hypersurface and an adjacent uniform-density hypersurface with which it coincides on average. This displacement is determined by the field configuration on the spatially flat hypersurface. Therefore $\zeta = \delta N = \delta[N(\varphi_\alpha)]$, yielding

$$\zeta = N_\alpha \delta\varphi_\alpha + \frac{1}{2!} N_{\alpha\beta} (\delta\varphi_\alpha \delta\varphi_\beta - \langle \delta\varphi_\alpha \delta\varphi_\beta \rangle) + \frac{1}{3!} N_{\alpha\beta\gamma} (\delta\varphi_\alpha \delta\varphi_\beta \delta\varphi_\gamma - \langle \delta\varphi_\alpha \delta\varphi_\beta \delta\varphi_\gamma \rangle) + \cdots , \quad (2.49)$$

where $N_\alpha = \partial N / \partial \varphi_\alpha$ and similarly for the higher derivatives. Note that these are ordinary partial derivatives, with all quantities evaluated at the same time: they are not the nonlocal variational derivatives which appear in the Lyth–Rodríguez Taylor expansion. In particular, we are not using the δN formula (2.49) to account for any time dependence of the correlation functions; this is handled by the transport equations. Eq. (2.49) is used solely to obtain the relationship between the $\delta\varphi_\alpha$ and ζ. There are various other ways in which this could be obtained. Malik and Wands (2009) gave a comprehensive discussion from the viewpoint of traditional cosmological perturbation theory. Another approach was used by Maldacena (2003). Eq. (2.49) has the advantage that it computes the transformation only in the superhorizon limit $k/aH \to 0$, which is all we require.

Calculation of the derivatives N_α, $N_{\alpha\beta}$ and $N_{\alpha\beta\gamma}$ is tedious, although straightforward in principle. Seery, Mulryne et al. (2012) used a raytracing method which gave the relation a geometrical meaning. It would be interesting to apply this technique at third order, but it is helpful primarily for analytic and geometric intuition rather than numerical optimization. Mulryne, Seery and Wesley (2010) exploited the fact that any potential is separable for first order displacements to set up constants of the motion, as originally done by Garcia-Bellido and Wands (1996); Vernizzi and

Wands (2006). However, this method is relatively lengthy even for the second-order coefficient $N_{\alpha\beta}$. Here we employ a simpler alternative.

We first focus on a *single* trajectory and measure the number of e-folds N accumulated along it. During any period where the density decreases monotonically we may measure N as a function of ρ. Consider the number of e-folds ΔN which elapse between some arbitrary point on the trajectory (the "starting point") and a nearby hypersurface of fixed density ρ_c. Under the slow-roll approximation, the density at the starting point is simply the potential energy evaluated there. Therefore we may express ΔN as a Taylor expansion in the difference $\Delta\rho = \rho_c - V$,

$$\Delta N = N(V + \Delta\rho) - N(V) = \frac{\mathrm{d}N}{\mathrm{d}\rho}\Delta\rho + \frac{1}{2!}\frac{\mathrm{d}^2N}{\mathrm{d}\rho^2}\Delta\rho^2 + \frac{1}{3!}\frac{\mathrm{d}^3N}{\mathrm{d}\rho^3}\Delta\rho^3 + \cdots . \tag{2.50}$$

Note that the differential coefficients are *ordinary* derivatives taken along the trajectory. In Eq. (2.50) they are evaluated at the starting point.

We now perturb the starting point by an amount $\delta\varphi_\alpha$ while keeping the final hypersurface fixed. In general $\delta\varphi_\alpha$ will not be aligned with the inflationary trajectory used to construct the ρ-derivatives in Eq. (2.50), which therefore vary. The same is true for the displacement $\Delta\rho$. Accounting for both these effects changes the total elapsed e-folds by an amount $\delta(\Delta N)$. Finally, to study fluctuations around the hypersurface $\rho = \rho_c$ we take the limit $\Delta\rho \to 0$, after which $\delta(\Delta N) \to \zeta$. The advantage of this method is that it uses the handful of low-order derivatives appearing in Eq. (2.50) to isolate the limited information we require regarding local properties of the transformation: higher-order information is discarded at the outset. This contrasts with the constants-of-motion approach used in Mulryne, Seery and Wesley (2010), where high-order information is implicitly kept through the majority of the computation, although it is never used.

Under a shift of the starting point we conclude

$$\delta(\Delta\rho) = -V_\alpha\delta\varphi_\alpha - \frac{1}{2!}V_{\alpha\beta}\delta\varphi_\alpha\delta\varphi_\beta - \frac{1}{3!}V_{\alpha\beta\gamma}\delta\varphi_\alpha\delta\varphi_\beta\delta\varphi_\gamma - \cdots . \tag{2.51}$$

By retaining contributions to ρ from the kinetic energy, and evaluating the differential coefficients in (2.50) without use of the slow-roll approximation, this approach could be extended to provide the transformation from the full phase space variables $\delta\varphi_\alpha$, $\delta\dot{\varphi}_\alpha$ to ζ. This was done in Dias, Frazer and Liddle (2012).

Invoking the slow-roll approximation, we may calculate the derivative $\mathrm{d}N/\mathrm{d}\rho$,

$$\left.\frac{\mathrm{d}N}{\mathrm{d}\rho}\right| = \frac{\mathrm{d}N}{\mathrm{d}t}\left.\frac{\mathrm{d}t}{\mathrm{d}V}\right|_\gamma = -\frac{3H^2}{V_\alpha V_\alpha} = -\frac{1}{M_{\mathrm{P}}^2}\frac{V}{V_\alpha V_\alpha}, \tag{2.52}$$

where $\mathrm{d}V/\mathrm{d}t$ is to be computed along the trajectory γ. Higher derivatives can be obtained in the same way, by repeated differentiation with respect to t and use of the chain rule to convert these

into derivatives with respect to ρ. We obtain

$$\left.\frac{\mathrm{d}^2N}{\mathrm{d}\rho^2}\right| = -\frac{1}{M_{\rm P}^2}\left(\frac{1}{V_\lambda V_\lambda} - 2\frac{VV_\alpha V_\beta V_{\alpha\beta}}{(V_\lambda V_\lambda)^3}\right), \tag{2.53}$$

$$\left.\frac{\mathrm{d}^3N}{\mathrm{d}\rho^3}\right| = \frac{1}{M_{\rm P}^2}\left(4\frac{V_\alpha V_\beta V_{\alpha\beta}}{(V_\lambda V_\lambda)^3} - 12\frac{V(V_\alpha V_\beta V_{\alpha\beta})^2}{(V_\lambda V_\lambda)^5} + 4\frac{VV_\alpha V_{\alpha\beta}V_{\beta\gamma}V_\gamma}{(V_\lambda V_\lambda)^4} + 2\frac{VV_{\alpha\beta\gamma}V_\alpha V_\beta V_\gamma}{(V_\lambda V_\lambda)^4}\right). \tag{2.54}$$

The first and second-order variations are

$$N_\alpha = -\left.\frac{\mathrm{d}N}{\mathrm{d}\rho}\right| V_\alpha, \tag{2.55}$$

$$N_{\alpha\beta} = -\left.\frac{\mathrm{d}N}{\mathrm{d}\rho}\right| V_{\alpha\beta} + \left.\frac{\mathrm{d}^2N}{\mathrm{d}\rho^2}\right| V_\alpha V_\beta + \frac{1}{M_{\rm P}^2}(V_\alpha A_\beta + V_\beta A_\alpha), \tag{2.56}$$

which agree with existing expressions in the literature. (See below for the definition of A_α.) At third order we find

$$\begin{aligned} N_{\alpha\beta\gamma} = &-\left.\frac{\mathrm{d}^3N}{\mathrm{d}\rho^3}\right| V_\alpha V_\beta V_\gamma + \left(\left.\frac{\mathrm{d}^2N}{\mathrm{d}\rho^2}\right| V_\alpha V_{\beta\gamma} + \text{cyclic}\right) - \left.\frac{\mathrm{d}N}{\mathrm{d}\rho}\right| V_{\alpha\beta\gamma} \\ &+ \frac{1}{M_{\rm P}^2}\left(A_\alpha V_{\beta\gamma} + \text{cyclic}\right) + \frac{1}{M_{\rm P}^2}\left(B_{\alpha\beta}V_\gamma + \text{cyclic}\right) + \frac{1}{M_{\rm P}^2}\left(C_\alpha V_\beta V_\gamma + \text{cyclic}\right). \end{aligned} \tag{2.57}$$

The tensors A_α, $B_{\alpha\beta}$ and C_α have been defined to satisfy

$$A_\alpha = \frac{V_\alpha}{V_\lambda V_\lambda} - 2\frac{VV_\kappa V_{\kappa\alpha}}{(V_\lambda V_\lambda)^2} \tag{2.58}$$

$$B_{\alpha\beta} = \frac{V_{\alpha\beta}}{V_\lambda V_\lambda} - 2\frac{V_\kappa V_{\kappa\alpha}V_\beta + V_\kappa V_{\kappa\beta}V_\alpha}{(V_\lambda V_\lambda)^2} + 8\frac{VV_\kappa V_{\kappa\alpha}V_\epsilon V_{\epsilon\beta}}{(V_\lambda V_\lambda)^3} - 2\frac{VV_{\kappa\alpha}V_{\kappa\beta}}{(V_\lambda V_\lambda)^2} - 2\frac{VV_\kappa V_{\kappa\alpha\beta}}{(V_\lambda V_\lambda)^2} \tag{2.59}$$

$$C_\alpha = \frac{V_{\alpha\beta}}{V_\lambda V_\lambda} + 2\frac{V_\alpha V_\kappa V_{\kappa\epsilon}V_\epsilon}{(V_\lambda V_\lambda)^3} - 12\frac{VV_\kappa V_{\kappa\epsilon}V_\epsilon V_\rho V_{\rho\alpha}}{(V_\lambda V_\lambda)^3} + 4\frac{VV_\kappa V_{\kappa\epsilon}V_{\epsilon\alpha}}{(V_\lambda V_\lambda)^3} + 2\frac{VV_\kappa V_{\kappa\epsilon\alpha}V_\epsilon}{(V_\lambda V_\lambda)^3} \tag{2.60}$$

2.4.2 Inflationary observables

Finally, we must assemble all these contributions to obtain expressions for $\tau_{\rm NL}$ and $g_{\rm NL}$. We find

$$P_\zeta = N_\alpha N_\beta \Sigma_{\alpha\beta} \tag{2.61}$$

$$\frac{6}{5}f_{\rm NL} = \frac{N_\alpha N_\beta N_\gamma \alpha_{\alpha|\beta\gamma} + N_{\alpha\beta}N_\gamma N_\delta \Sigma_{\alpha\gamma}\Sigma_{\beta\delta}}{(N_\omega N_\zeta \Sigma_{\omega\zeta})^2} \tag{2.62}$$

$$\tau_{\rm NL} = \frac{N_\alpha N_\beta N_\gamma N_\delta \tau_{\alpha\beta|\gamma\delta} + 2N_\alpha N_\beta N_\gamma N_{\lambda\mu}a_{\alpha|\beta\lambda}\Sigma_{\gamma\mu} + N_{\alpha\beta}N_{\gamma\delta}N_\lambda N_\mu \Sigma_{\alpha\gamma}\Sigma_{\beta\lambda}\Sigma_{\delta\mu}}{(N_\omega N_\zeta \Sigma_{\omega\zeta})^3} \tag{2.63}$$

$$\frac{54}{25}g_{\rm NL} = \frac{N_\alpha N_\beta N_\gamma N_\delta g_{\alpha|\beta\gamma\delta} + 3N_\alpha N_\beta N_\gamma N_{\lambda\mu}a_{\lambda|\alpha\beta}\Sigma_{\gamma\mu} + N_{\alpha\beta\gamma}N_\delta N_\lambda N_\mu \Sigma_{\alpha\delta}\Sigma_{\beta\lambda}\Sigma_{\gamma\mu}}{(N_\omega N_\zeta \Sigma_{\omega\zeta})^3}. \tag{2.64}$$

2.5 ALTERNATIVE APPROACHES

In this paper, our approach to calculating the statistics of the curvature perturbation has been to develop transport equations for objects such as the n-point functions [Eqs. (2.11), (2.13) and (2.15)], or their shape tensors [Eqs. (2.17), (2.19) and (2.23)–(2.24)]. The results of §2.3 show that this is equivalent to the Lyth–Rodríguez Taylor expansion

$$\delta\varphi_\alpha = \Gamma_{\alpha i}\delta\varphi_i + \frac{1}{2!}\Gamma_{\alpha ij}\delta\varphi_i\delta\varphi_j + \frac{1}{3!}\Gamma_{\alpha ijk}\delta\varphi_i\delta\varphi_j\delta\varphi_k + \cdots, \tag{2.65}$$

where we recall that objects with Greek indices are evaluated at time N, and those with Latin indices at some earlier time N_0, which is usually taken as the common time of horizon exit for the $\mathbf{k}$-modes under consideration.[8]

'FORWARD' AND 'BACKWARD' METHODS.—To solve these equations we must supply a boundary condition at $N = N_0$, but we are free to choose how this is done: we may start either with N_0 at the initial epoch and evolve N *forward* to the time of interest, or fix N at this time and evolve N_0 *backwards*. These approaches are distinct but equally valid, because (at least during inflation) there is no obstacle to computing the relevant initial conditions at any time of our choosing. The transport equations we have described in this paper are of the forwards variety.

Eq. (2.65) shows explicitly what must be computed in order to completely characterize the fluctuations $\delta\varphi_\alpha$ at any given order. At first order in a d-field slow-roll model, we require the d^2 independent components of the Jacobi map $\Gamma_{\alpha i}$. At second order there are d^3 components of $\Gamma_{\alpha ij}$, reduced to $d^2(d+1)/2$ after accounting for symmetries. Finally, at third order there are d^4 components of $\Gamma_{\alpha ijk}$, which reduce to $d^2(d+1)(d+2)/6$ independent components after symmetries. We conclude that to compute all two-point functions in such a model requires solution of $\mathrm{O}(d^2)$ differential equations. Likewise, all three-point functions requires $\mathrm{O}(d^3)$ equations, and all four-point functions requires $\mathrm{O}(d^4)$ equations. This is to be expected, because there are $\mathrm{O}(d^m)$ independent m-point functions.

AUTOCORRELATION FUNCTIONS OF ζ ONLY.—Sometimes we do not require all correlation functions, but only the autocorrelation functions of ζ. In such cases it would be advantageous if an autonomous set of transport equations could be set up for the Taylor coefficients of ζ rather than $\delta\varphi_\alpha$,

$$\delta N = N_i\delta\varphi_i + \frac{1}{2!}N_{ij}\delta\varphi_i\delta\varphi_j + \frac{1}{3!}N_{ijk}\delta\varphi_i\delta\varphi_j\delta\varphi_k. \tag{2.66}$$

[8]Indeed, one can verify that inserting (2.65) into (2.5) and equating coefficients order-by-order reproduces the Γ-matrix evolution equations with unprimed indices [Eqs. (2.26), (2.34) and (2.46)].

This would require the solution of only $\mathrm{O}(d^{m-1})$ independent equations to obtain the m-point function of ζ. This saving could be helpful in models with a large number of fields. There is currently no *forwards* formulation of this type but a set of *backwards* equations were given by Yokoyama, Suyama and Tanaka (2007); Yokoyama, Suyama and Tanaka (2008), and later extended to the trispectrum (Yokoyama, Suyama and Tanaka 2009).

The Taylor coefficients for N can be expressed in terms of the Γ-matrices,

$$N_i = N_\alpha \Gamma_{\alpha i} \tag{2.67}$$

$$N_{ij} = N_\alpha \Gamma_{\alpha ij} + N_{\alpha\beta}\Gamma_{\alpha i}\Gamma_{\beta j} \tag{2.68}$$

$$N_{ijk} = N_\alpha \Gamma_{\alpha ijk} + N_{\alpha\beta\gamma}\Gamma_{\alpha i}\Gamma_{\beta j}\Gamma_{\gamma k} + \left(N_{\alpha\beta}\Gamma_{\beta i}\Gamma_{\alpha jk} + 2 \text{ cyclic}\right). \tag{2.69}$$

We could attempt to obtain forward transport equations by direct differentiation with respect to time followed by use of the Γ-matrix evolution equations. But this does not generate a closed set of autonomous equations because derivatives of the $N_{\alpha\ldots}$ also appear, which obstruct an attempt to eliminate the Γ-matrices in favour of their N counterparts.

Instead, the backwards equations of Yokoyama et al. can be derived as follows. As described above, we fix N to be the late time of interest and aim to evolve N_0 backwards. The backwards evolution of $\Gamma_{\alpha i}$ can be obtained very simply by differentiating (2.65) while keeping $\delta\varphi_\alpha$ fixed, or alternatively by differentiating (2.28) with respect to N_0. Whichever method is chosen, we find $\mathrm{d}\Gamma_{\alpha i}/\mathrm{d}N_0 = -\Gamma_{\alpha j}u_{ji}$. Subsequently differentiating (2.67) with respect to N_0 and using this relation, we obtain an autonomous set of equations for N_i,

$$\frac{\mathrm{d}N_i}{\mathrm{d}N_0} = -N_j u_{ji}. \tag{2.70}$$

This technique can be extended to higher orders, giving evolution equations for N_{ij} and N_{ijk}.[9] We find

$$\frac{\mathrm{d}N_{ij}}{\mathrm{d}N_0} = -N_k u_{kij} - N_{ik}u_{kj} - N_{jk}u_{ki}, \tag{2.73}$$

and

$$\frac{\mathrm{d}N_{ijk}}{\mathrm{d}N_0} = -N_\ell u_{\ell ijk} - \left(N_{i\ell}u_{\ell jk} + N_{jk\ell}u_{\ell i} + 2 \text{ cyclic}\right). \tag{2.74}$$

The first of these was given in Seery, Mulryne et al. (2012). Here we have extended the method to include N_{ijk}, which enables trispectrum quantities to be calculated. These equations should be

[9] The evolution equations for $\Gamma_{\alpha ij}$ and $\Gamma_{\alpha ijk}$, which are required to obtain these results, are

$$\frac{\mathrm{d}\Gamma_{\alpha ij}}{\mathrm{d}N_0} = -\Gamma_{\alpha m}u_{mij} - \Gamma_{\alpha im}u_{mj} - \Gamma_{\alpha mj}u_{mi} \tag{2.71}$$

$$\frac{\mathrm{d}\Gamma_{\alpha ijk}}{\mathrm{d}N_0} = -\Gamma_{\alpha m}u_{mijk} - \left(\Gamma_{\alpha im}u_{mjk} + \Gamma_{\alpha mjk}u_{mi} + 2 \text{ cyclic}\right). \tag{2.72}$$

solved with initial conditions chosen so that N_i, N_{ij} and N_{ijk} equal the transformation matrices N_α, $N_{\alpha\beta}$ and $N_{\alpha\beta\gamma}$, respectively, at $N_0 = N$.

If we require only the bispectrum of ζ and are prepared to take the field fluctuations at time N_0 to be Gaussian and uncorrelated with each other, then more is possible. Under these circumstances, Yokoyama et al. showed that the $\mathrm{O}(d^2)$ equations for N_{ij} could be replaced by only $\mathrm{O}(d)$ equations for an auxiliary quantity $\Theta_\alpha = \Gamma_{\alpha i} N_i$ (Yokoyama, Suyama and Tanaka 2008; Yokoyama, Suyama and Tanaka 2007).

Constraint for first-order coefficients.—There is a further simplification which can be made for the N_i system. Using the flow equation $\mathrm{d}\phi_i = u_i \, \mathrm{d}N$, it follows that the displacement $\mathrm{d}\phi_i = u_i$ precisely tangent to the trajectory generates a change in the e-foldings required to reach the final uniform density slice corresponding to

$$\delta N = u_i N_i = -1. \tag{2.75}$$

This implies that *one* of the N_i can be determined algebraically in terms of the others, without solving a separate differential equation. Therefore, in a two-field model, the Yokoyama et al. equations (2.70) can be decoupled,

$$\frac{\mathrm{d}N_\phi}{\mathrm{d}N_0} = \left(\frac{u_\phi}{u_\chi} u_{\chi\phi} - u_{\phi\phi} \right) N_\phi + \frac{u_{\chi\phi}}{u_\chi}, \tag{2.76}$$

where we have labelled the fields ϕ and χ. A similar equation can be given for N_χ, but it is unnecessary because (2.75) can be used to obtain N_χ once N_ϕ is known. Although the possibility of decoupling these equations is interesting, it confers no particular advantages.

A variation of the Yokoyama et al. formulation was recently given by Mazumdar and Wang (2012) in which they pointed out the possibility of this decoupling in the two-field case, although without making explicit use of the constraint (2.75). Their analysis is equivalent to the one presented here, and in Appendix A of Seery, Mulryne et al. (2012). Mazumdar & Wang ascribed the possibility of decoupling to the choice of coordinates used in their derivation. However, the evolution equation (2.70) can be derived using any convenient method and is independent of such choices. The argument above shows that decoupling is a consequence of the constraint (2.75), and is a special feature of the two-field system. In a general d-field model, the best that can be obtained is a coupled system of $d - 1$ equations.

2.6 NUMERICAL RESULTS

We now illustrate the transport approach using a number of concrete models. For each model, we numerically solve Eqs. (2.17), (2.19) and (2.23)–(2.24), and use Eqs. (2.62)–(2.64) to determine the values of $f_{\rm NL}$, $\tau_{\rm NL}$ and $g_{\rm NL}$ from horizon crossing onwards. We label the number of e-folds of inflation from $N = 0$ at horizon exit.

2.6.1 NUMERICAL EXAMPLES

D-BRANE MODEL.—Our first example was studied by Dias, Frazer and Liddle (2012). It is an approximation to inflation driven by the motion of a D-brane in a warped throat, allowing for angular degrees of freedom. In that study, the authors employed the transport approach to calculate the distribution of observable parameters over a large number of realizations of their model. However, they restricted attention to the spectrum and local-type bispectrum. Here we present the evolution of the local-type trispectrum parameters for one typical realization.

The potential is given by

$$V = \alpha_0 + \alpha_1\phi_1 + \alpha_3\phi_1^3 + \beta\phi_2, \tag{2.77}$$

which contains an inflexion point in the ϕ_1 direction. The ϕ_1 and ϕ_2 directions of the brane correspond to the radial and angular directions respectively. Inflation occurs close to this inflexion point. We choose $\alpha_0 = 100M^2M_{\rm P}^2$, $\alpha_1 = M^2M_{\rm P}$, $\alpha_3 = 5M^2/M_{\rm P}$, $\beta = 5M^2M_{\rm P}$, $\phi_{1\rm exit} = 0.5M_{\rm P}$, and $\phi_{2\rm exit} = 0.5M_{\rm P}$, where the subscript 'exit' indicates these are the initial values of the fields at horizon exit. M is an overall normalisation, which can be fixed to match the WMAP normalization of the power spectrum. These initial conditions have been chosen to give 60-efolds of inflation, taking inflation to end when $\epsilon = 1$. Allowing the system to evolve past this point would lead to erroneous results because we are employing slow-roll equations of motion. As explained in §2.2 this could be resolved by writing transport equations in the full phase-space. However, for simplicity, we do not do so here. In Fig. 2.1 we give the evolution of $\tau_{\rm NL}$, $g_{\rm NL}$, and $(6f_{\rm NL}/5)^2$ for this choice of parameters and initial conditions.

For single-field models we recall that $\tau_{\rm NL} = (6f_{\rm NL}/5)^2$, which is relaxed to an inequality in multiple-field models (Suyama and Yamaguchi 2008; Smith, LoVerde and Zaldarriaga 2011). The use of the relative magnitude of $\tau_{\rm NL}$ and $(6f_{\rm NL}/5)^2$ as a diagnostic of the spectrum of active fields during inflation was emphasized by Smidt et al. (2010), who made a forecast of observational

prospects. Very recently, Assassi, Baumann and Green (2012) gave precise formulae in terms of the spectrum of single-particle states. This signature of multiple active fields is clearly visible in Fig. 2.1, although in this realization the nongaussian parameters are too small to be observable. (As a point of principle an inflexion point potential may give rise to a large local bispectrum (Elliston et al. 2011a) and trispectrum (Elliston, Alabidi et al. 2012), via the hilltop mechanism suggested by Kim, Liddle and Seery (2010). However, an observable signal can usually be obtained only for finely tuned initial conditions and parameter choices.)

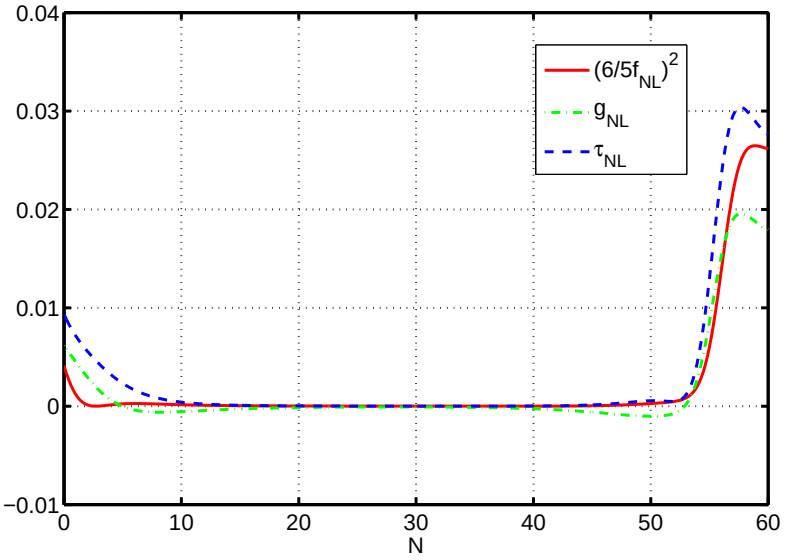

Figure 2.1: Evolution of $\tau_{\rm NL}$, $g_{\rm NL}$ and $(6/5f_{\rm NL})^2$ for the inflexion-point potential (2.77). Initial conditions and parameter choices are described in the main text.

QUADRATIC-EXPONENTIAL MODEL.—Our second example was constructed by Byrnes, Choi and Hall (2008) as an example of a product-separable model which could give rise to a large $f_{\rm NL}$ for finely-tuned initial conditions. It was later studied by Elliston et al. (2011b) and Huston and Christopherson (2012).

The potential is

$$V = M^4\phi_1^2 e^{-\lambda\phi_2^2}. \tag{2.78}$$

We choose the parameter values and initial conditions $\lambda = 0.05/M_{\rm P}^2$, $\phi_{1\rm exit} = 16M_{\rm P}$, and $\phi_{2\rm exit} = 0.001M_{\rm P}$, and fix M as before to match the WMAP normalization. These initial values also give 60-efolds of inflation. They have been chosen to select a background trajectory which gives rise to significant nongaussianity. In Fig. 2.2, we present the evolution of the $\tau_{\rm NL}$ and $g_{\rm NL}$ parameters in this model for the first time. The $g_{\rm NL}$ parameter in this model is significantly smaller (though non-zero) than $f_{\rm NL}$ and $\tau_{\rm NL}$, which could not have been predicted in advance. We also show the

evolution of $(6f_{\rm NL}/5)^2$. However, although the $f_{\rm NL}$ and $\tau_{\rm NL}$ parameters are large at the end of inflation, it is important to note that the fluctuations are still evolving at this time. Therefore the model is not predictive by itself: it must be supplemented by post-inflationary evolution, which tracks the fluctuations until the surface of last scattering, or explains how all isocurvature modes eventually decay.

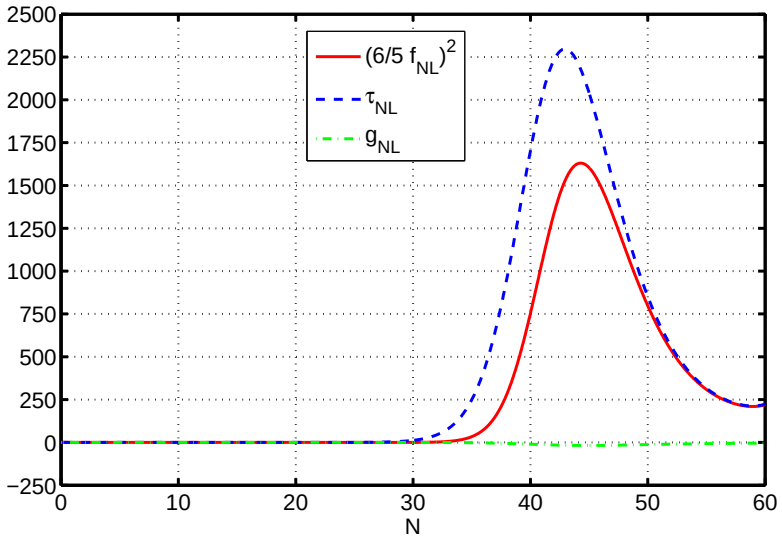

Figure 2.2: Evolution of $\tau_{\rm NL}$, $g_{\rm NL}$ and $(6/5f_{\rm NL})^2$ for the potential (2.78). Initial conditions and parameter choices are described in the main text.

NON-SEPARABLE HYBRID MODEL.—Finally, we present results for a hybrid-type potential in the large field regime studied by Mulryne, Orani and Rajantie (2011). This is an example of a non-separable potential. For general initial conditions, no analytic estimate is known for any of $f_{\rm NL}$, $\tau_{\rm NL}$ or $g_{\rm NL}$, even assuming slow-roll. Therefore numerical methods, such as our implementation of the transport equations, become essential. The potential contains a hilltop region, and parameter choices and initial conditions can be chosen so that the model is of the type discussed by Kim, Liddle and Seery (2010). This gives rise to large nongaussianity for initial conditions sufficiently close to the hilltop.

The potential satisfies

$$V = M^4\left[\frac{1}{2}m^2\phi_1^2 + \frac{1}{2}g^2\phi_1^2\phi_2^2 + \frac{\lambda}{4}\left(\phi_2^2 - v^2\right)^2\right], \tag{2.79}$$

and we choose the parameter values $g^2 = v^2/\phi_{\rm crit}^2$, $m^2 = v^2$, $v = 0.2M_{\rm P}$, $\phi_{\rm crit} = 20M_{\rm P}$ and $\lambda = 5$. The initial conditions are $\phi_{1\rm exit} = 15.5M_{\rm P}$ and $\phi_{2\rm exit} = 0.0015M_{\rm P}$. As above, these initial values give 60-efolds of inflation and have been adjusted to produce significant nongaussianity. M is adjusted as before. In Fig. 2.3, we present the evolution of the $\tau_{\rm NL}$ and $g_{\rm NL}$ parameters in this

model for the first time. In contrast to the previous example, the statistics here approach constant values before the end of inflation, reflecting the fact that isocurvature modes decay. We also give the evolution of $(6f_{\rm NL}/5)^2$.

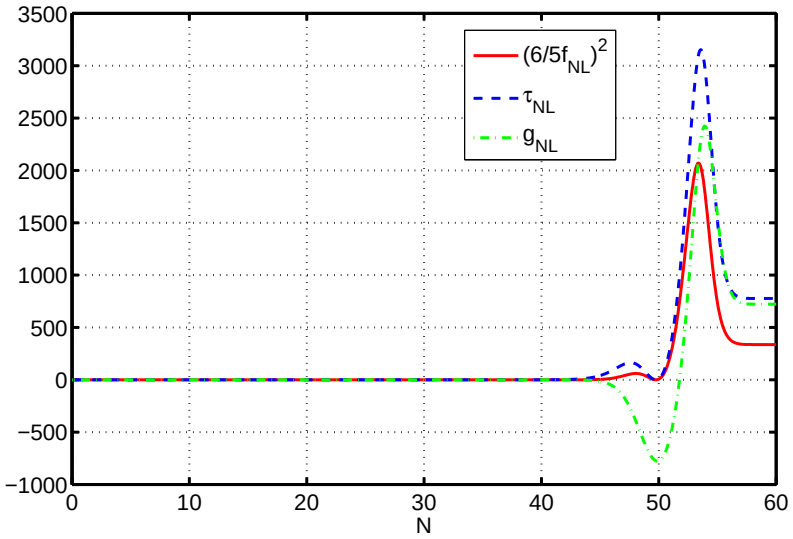

Figure 2.3: Evolution of $\tau_{\rm NL}$, $g_{\rm NL}$ and $(6/5f_{\rm NL})^2$ for the potential (2.79). Initial conditions and parameter choices are described in the main text.

2.7 Discussion and Conclusions

In this paper we have provided transport equations to evolve the four-point functions of a collection of light scalar fields during an inflationary phase. The transport system can be thought of as a form of Boltzmann hierarchy, and can be solved by similar methods. Since inflationary fluctuations are typically close to Gaussian, connected correlation functions of increasing order are typically decreasing in amplitude. Therefore only a few low-order functions are important in sourcing those of higher order. Truncating the hierarchy to include only these sources generates the local-type "squeezed" and "collapsed" configurations. We parametrize the amplitude of these configurations with "shape tensors" for which we have supplied evolution equations. Expressing the correlation functions of ζ in terms of those of the $\delta\varphi_\alpha$, it is possible to extract $\tau_{\rm NL}$ and $g_{\rm NL}$. This analysis was given in §2.2.

This method of integrating the transport hierarchy expresses the correlation functions in terms of the Jacobi fields generated by the underlying phase space flow, and their derivatives. One can regard this as a statement of the separate universe approximation. The "Jacobi map" relates these

fields to the variation of a general solution of the equations of motion with respect to its constants of integration. Using this equivalence, we have shown that the result reproduces the familiar Taylor expansion used by Lyth & Rodríguez. The procedure can be viewed as an application of classical Hamilton–Jacobi theory.

Our equations supply a toolkit which can be used to study the evolution of inflationary observables in any multi-field model of interest, provided all fields possess canonical kinetic terms. There are two equivalent approaches. First, one can solve Eqs. (2.17), (2.19), (2.23) and (2.24) for the shape tensors corresponding to the two-, three- and four-point functions, using suitable initial conditions. Eqs. (2.61)–(2.63) can then be used to extract observables. Alternatively, one can solve the evolution equations (2.26) (after exchanging primed for unprimed indices), (2.34) and (2.46) for the Taylor coefficients of the "δN formalism", applied to the field fluctuations. Once these are known, Eqs. (2.67)–(2.69) can be used to exchange them for the Taylor coefficients of N itself. The usual formulae then allow observables to be computed. If the spectral index or its running are required, they can be extracted using the methods described by Dias and Seery (2012); Dias, Frazer and Liddle (2012).

Assuming slow-roll, either method requires the solution of $\mathrm{O}(d^m)$ equations to obtain the m-point functions of a d-field model. Since there are $\mathrm{O}(d^m)$ independent correlation functions it will not be possible to reduce this asymptotic complexity. But if only the autocorrelation functions of ζ are required, then it may be advantageous to use the 'backwards' formalism introduced by Yokoyama, Suyama & Tanaka, in which one can reduce the number of equations to be solved to $\mathrm{O}(d^{m-1})$ by forfeiting the possibility of obtaining correlation functions with insertions of isocurvature modes. [For clarity, we emphasize that the formalism of Yokoyama et al. correctly accounts for the influence of these isocurvature modes on the evolution of the ζ correlation functions. But it is not possible to determine mixed correlation functions, such as $\langle \zeta s \rangle$, where s is a field space direction orthogonal to ζ.] Unfortunately, it is often necessary to know something about such correlation functions to determine whether unquenched isocurvature modes remain, which could change the inflationary prediction by transferring their energy to the curvature fluctuation during or after reheating. (We refer to Seery, Mulryne et al. (2012) for a more comprehensive discussion.) But in some cases this may not be a concern, and where this is true our extension of the formalism of Yokoyama et al. allows trispectrum parameters to be obtained.

2.8 Acknowledgements

GJA was supported by the Science and Technology Facilities Council [grant number ST/I506029/1]. DJM acknowledges support from the Science and Technology Facilities Council [grant number ST/J001546/1]. DS acknowledges support from the Science and Technology Facilities Council [grant number ST/I000976/1] and the Leverhulme Trust. We would like to thank Lingfei Wang and Antony Lewis for helpful discussions.

2.A Appendix: Contributions to the four-point function from the initial condition of the three-point function

In this appendix we verify the claim made in §2.2.3, that the arbitrary initial condition for the three-point function makes a negligible contribution to the sourced component of the four-point function. In the text, this was used to conclude that the initial value need not be retained in Eqs. (2.23)–(2.24).

It was first proved by Lyth & Zaballa that the initial condition for the three-point function could be neglected in comparison with the sourced contribution whenever the sum of the two was large enough to be observed (Lyth and Zaballa 2005). Their argument was later simplified by Vernizzi and Wands (2006). The same result for the four-point function follows from the analysis of Seery, Lidsey and Sloth (2007) and Seery, Sloth and Vernizzi (2009). However, we are unaware of a similar demonstration for the question addressed in this appendix—the contribution of initial value of the *three*-point function to the sourced component of the *four*-point function.

We work with the variational formulation of the separate universe approximation, as discussed by Lyth and Rodriguez (2005). We write

$$\zeta = N_i \delta\varphi_i + \frac{1}{2!} N_{ij} \delta\varphi_i \delta\varphi_j + \cdots , \tag{2.80}$$

where the Latin indices i, j, …, have the same meaning as in the main text. We define the trispectrum T_ζ to be the four-point function with its momentum-conservation δ-function stripped away,

$$\langle \zeta(\mathbf{k}_1)\zeta(\mathbf{k}_2)\zeta(\mathbf{k}_3)\zeta(\mathbf{k}_4)\rangle = (2\pi)^3 \delta(\mathbf{k}_1 + \mathbf{k}_2 + \mathbf{k}_3 + \mathbf{k}_4) T_\zeta . \tag{2.81}$$

Using the initial value of the three-point function computed in Seery and Lidsey (2005), the corresponding contribution to the sourced part of T_ζ can be written

$$T_\zeta \supseteq N_i N_j N_k N_{mn} \Bigg\{ \delta^{im} \frac{H_*^2}{2k_1^3} \frac{H_*^4}{8k_2^3 k_3^3 k_{14}^3} \sum_{\text{perms}} \frac{\dot\varphi_j \delta_{kn}}{2H_*} \Big(-3\frac{k_3^2 k_{14}^2}{k_t} - \frac{k_3^2 k_{14}^2}{k_t^2}(k_2 + 2k_{14}) + \frac{k_2^3}{2} - k_2 k_3^2 \Big) + [\mathbf{k}_1 \to \{\mathbf{k}_2, \mathbf{k}_3\}] \Bigg\} + \text{cyclic permutations } \mathbf{k}_4 \to \{\mathbf{k}_1, \mathbf{k}_2, \mathbf{k}_3\} \tag{2.82}$$

where "$*$" denotes evaluation at horizon exit, $k_t = k_1 + k_2 + k_{14}$, the summation is over all simultaneous permutations of the index set $\{\beta, \gamma, \epsilon\}$ and the momenta $\{\mathbf{k}_2, \mathbf{k}_3, \mathbf{k}_{14}\}$, and we have defined $k_{14} = |\mathbf{k}_1 + \mathbf{k}_4|$.

This contribution can be divided into an effective g_{NL}, an effective τ_{NL}, and an 'equilateral-type' term which does not fit naturally into either of the local-type shapes. The effective g_{NL} can be written

$$\Delta g_{\mathrm{NL}} = \frac{25}{72} \frac{N_i N_{ij} \dot\varphi_j / H_*}{(N_k N_k)^2} \tag{2.83}$$

(the placement of indices is immaterial in this and other expressions, since contraction occurs under the Kronecker-δ), and the effective τ_{NL} is

$$\Delta \tau_{\mathrm{NL}} = -\frac{1}{2} \frac{N_i N_{ij} N_j}{(N_k N_k)^3}. \tag{2.84}$$

These expressions can be simplified. Introducing the scalar-to-tensor ratio r and the spectral index n_s, we find

$$\Delta g_{\mathrm{NL}} = \frac{25}{1152} r(n_s - 1 + 2\epsilon_*) \ll 1 \tag{2.85}$$

$$\Delta \tau_{\mathrm{NL}} = -\frac{3}{35} r f_{\mathrm{NL}}, \tag{2.86}$$

where f_{NL} is the sourced local-mode contribution to the three-point function. The g_{NL} contribution is clearly negligible. The τ_{NL} contribution is negligible provided $|r f_{\mathrm{NL}}| \lesssim 1$. Taking the bound on r to be roughly $r \lesssim 0.1$, this term can be observationally relevant only if $|f_{\mathrm{NL}}| \gtrsim 50$. This is already on the verge of being ruled out by experiment, so the τ_{NL} contribution is likely to be no more than O(1) in most acceptable models. It could perhaps be kept if very accurate estimates are required.

Finally, the equilateral-type term is

$$T_\zeta \supseteq \frac{H_*^6}{8k_1^3k_2^3k_3^3k_{14}^3}\left(N_iN_{ij}\frac{\dot\varphi_j}{4H_*}(N_kN_k)\left(-\frac{8k_2^2k_3^2}{k_t}-k_{14}(k_2^2+k_3^2)\right)\right.$$
$$\left.-\frac{N_iN_{ij}N_j}{4}\left(-8\frac{k_{14}^2}{k_t}(k_2^2+k_3^2)-k_{14}^2(k_2+k_3)-k_2k_3(k_2+k_3)\right)\right) \qquad (2.87)$$
$$+[\mathbf{k}_1\to\{\mathbf{k}_2,\mathbf{k}_3\}]+(\text{cyclic }\mathbf{k}_4\to\{\mathbf{k}_1,\mathbf{k}_2,\mathbf{k}_3\})$$

The coefficients of these contributions are related to those of Eqs. (2.83) and (2.84), and will therefore not typically be large.

2.B Appendix: Gauss–Hermite expansion method

The transport equation for the trispectrum given in this paper can be derived in a number of ways. In this appendix we adopt a *cumulant expansion* procedure (Juszkiewicz et al. 1995; Bouchet and Juszkiewicz 1993; Bouchet 1995; Fosalba, Gaztanaga and Elizalde 1999). This was the approach taken in Mulryne, Seery and Wesley (2010) and Mulryne, Seery and Wesley (2011) to derive the transport equation for the bispectrum. Here we extend the calculation to derive the transport equation for the trispectrum.

2.B.1 Cumulant expansion

In each smoothed patch of the universe the value of the scalar field φ is described by a unique probability density function $P(\varphi)$. From inflation we expect that any non-Gaussianity will be small, and therefore it is a justifiable approximation that the higher-order moments will be a small correction to a Gaussian probability density function (pdf). In this case we can use a Gauss–Hermite expansion method to perturb a Gaussian probability distribution function $P_g(\varphi)$. This approach has also been used by Taylor and Watts (2000) and also Juszkiewicz et al. (1995); Bouchet and Juszkiewicz (1993); Bouchet (1995); Fosalba, Gaztanaga and Elizalde (1999); Matarrese, Verde and Jimenez (2000); Amendola (2002); Watts and Coles (2003); Amendola (1996); Lam and Sheth (2009); Seery and Hidalgo (2006); LoVerde et al. (2008).

To consider non-Gaussianity on the level of the trispectrum we perturb the pdf to fourth order to give

$$P(\varphi)=P_g(\varphi)\left[1+\frac{\alpha^z_{\alpha'\beta'\gamma'}}{3!}H_{\alpha'\beta'\gamma'}(\mathbf{z})+\frac{\beta^z_{\alpha'\beta'\gamma'\delta'}}{4!}H_{\alpha'\beta'\gamma'\delta'}(\mathbf{z})+\ldots\right], \qquad (2.88)$$

where

$$P_g(\varphi) \equiv \frac{1}{(\det 2\pi\Sigma)^{1/2}} \exp\left(-\frac{\mathbf{z}^2}{2}\right). \tag{2.89}$$

The covariance matrix Σ is the two-point function for the field perturbations, reproduced here for convenience, is given by

$$\begin{aligned} \Sigma_{\alpha'\beta'} &\equiv \langle(\varphi_{\alpha'} - \Phi_{\alpha'})(\varphi_{\beta'} - \Phi_{\beta'})\rangle \\ &= \langle \delta\varphi_{\alpha'} \delta\varphi_{\beta'} \rangle \end{aligned} \tag{2.90}$$

which we can decompose as $\Sigma = \mathbf{A}\mathbf{A}^{\mathrm{T}}$, with $\mathbf{A}^{\mathrm{T}}$ denoting the matrix transpose of $\mathbf{A}$. We can use this matrix to define a new variable $z_{\alpha'}(\delta\varphi_{\alpha'}) = A^{-1}_{\alpha'\beta'}\delta\varphi_{\alpha'}$. The objects $\alpha^z_{\alpha'\beta'\gamma'} = \langle z_{\alpha'} z_{\beta'} z_{\gamma'}\rangle$ and $\beta^z_{\alpha'\beta'\gamma'\delta'} = \langle z_{\alpha'} z_{\beta'} z_{\gamma'} z_{\delta'}\rangle$ characterise the deviations from Gaussianity. They are respectively the third and fourth order moments of the $z_{\alpha'}$, corresponding to the skewness and kurtosis of the pdf, shown in Figure. 2.4.

Figure 2.4: Plot showing a Gaussian (blue), Gaussian with skew (purple) and Gaussian with kurtosis (gold). Image credit: Sam Young.

Their relation to the three- and four-point functions of the fields is

$$\alpha_{\alpha'\beta'\gamma'} = A_{\alpha'\delta'} A_{\beta'\mu'} A_{\gamma'\nu'} \alpha^z_{\delta'\mu'\nu'} \tag{2.91}$$

$$\beta_{\alpha'\beta'\gamma'\delta'} = A_{\alpha'\delta'} A_{\beta'\mu'} A_{\gamma'\nu'} A_{\delta'\kappa'} \beta^z_{\delta'\mu'\nu'\kappa'} \tag{2.92}$$

where

$$\alpha_{\alpha'\beta'\gamma'} \equiv \langle \delta\varphi_{\alpha'} \delta\varphi_{\beta'} \delta\varphi_{\gamma'}\rangle \tag{2.93}$$

$$\beta_{\alpha'\beta'\gamma'\delta'} \equiv \langle \delta\varphi_{\alpha'} \delta\varphi_{\beta'} \delta\varphi_{\gamma'} \delta\varphi_{\delta'}\rangle. \tag{2.94}$$

$H_{\nu'}$ is the ν'^{th} Hermite polynomial defined by

$$H_{\alpha'\beta'\ldots\gamma'}(\mathbf{z}) = (-1)^{\nu'}\exp\left(\frac{z_{\mu'}z_{\mu'}}{2}\right)\frac{\partial^{\nu'}}{\partial z_{\alpha'}\partial z_{\beta'}\ldots\partial z_{\gamma'}}\exp\left(-\frac{z_{\mu'}z_{\mu'}}{2}\right) \tag{2.95}$$

obeying the following normalisation condition

$$\int_{-\infty}^{\infty}\frac{1}{\sqrt{2\pi}}e^{-\varphi^2/2}H_{\nu'}(\mathbf{z})H_{\mu'}(\mathbf{z})\,dz = \nu'!\,\delta_{\mu'\nu'}. \tag{2.96}$$

First multiplying (2.95) by $z_{\mu'}$ and using integration by parts we can write

$$\begin{aligned} z_{\mu'}H_{\alpha'\beta'\ldots\gamma'} &= (-1)^{\nu'}\exp\left(\frac{z_{\lambda'}z_{\lambda'}}{2}\right)\frac{\partial}{\partial z_{\alpha'}}\left(z_{\mu'}\frac{\partial^{\nu'-1}}{\partial z_{\beta'}\ldots\partial z_{\gamma'}}\exp\left(-\frac{z_{\lambda'}z_{\lambda'}}{2}\right)\right) \\ &\quad -(-1)^{\nu'}\exp\left(\frac{z_{\lambda'}z_{\lambda'}}{2}\right)\delta_{\alpha'\mu'}\left(z_{\mu'}\frac{\partial^{\nu'-1}}{\partial z_{\beta'}\ldots\partial z_{\gamma'}}\exp\left(-\frac{z_{\lambda'}z_{\lambda'}}{2}\right)\right) \end{aligned} \tag{2.97}$$

Pushing the $z_{\mu'}$ in the first term through the rest of the gradient terms we get

$$\begin{aligned} z_{\mu'}H_{\alpha'\beta'\ldots\gamma'} &= \delta_{\alpha'\mu'}H_{\beta'\ldots\gamma'} + \delta_{\beta'\mu'}H_{\alpha'\ldots\gamma'} + \cdots + \delta_{\gamma'\mu'}H_{\alpha'\beta'\ldots} \\ &+ (-1)^{\nu'}\mathrm{e}^{\mathbf{z}^2/2}\frac{\partial^{\nu'}}{\partial z_{\alpha'}\partial z_{\beta'}\ldots\partial z_{\gamma'}}\left(z_{\mu'}\mathrm{e}^{-\mathbf{z}^2/2}\right) \end{aligned} \tag{2.98}$$

and using

$$\frac{\partial}{\partial z_{\mu'}}\mathrm{e}^{-\mathbf{z}^2/2} = -z_{\mu'}\mathrm{e}^{-\mathbf{z}^2/2} \tag{2.99}$$

to rewrite the last term we have derived the following identity that we will make use of in our calculation

$$z_{\mu'}H_{\alpha'\beta'\ldots\gamma'} = H_{\alpha'\beta'\ldots\gamma'\mu'} + \delta_{\alpha'\mu'}H_{\beta'\ldots\gamma'} + \delta_{\beta'\mu'}H_{\alpha'\ldots\gamma'} + \cdots + \delta_{\gamma'\mu'}H_{\alpha'\beta'\ldots}. \tag{2.100}$$

Differentiating $H_{\alpha'\beta'\ldots\gamma'}$ with respect to $z_{\mu'}$ gives

$$\begin{aligned} \frac{\partial H_{\alpha'\beta'\ldots\gamma'}}{\partial z_{\mu'}} &= (-1)^{\nu'}z_{\mu'}\mathrm{e}^{\mathbf{z}^2/2}\left(\frac{\partial^{\nu'}}{\partial z_{\alpha'}\partial z_{\beta'}\ldots\partial z_{\gamma'}}\mathrm{e}^{-\mathbf{z}^2/2}\right) \\ &\quad +(-1)^{\nu'}\mathrm{e}^{\mathbf{z}^2/2}\left(\frac{\partial^{\nu'+1}}{\partial z_{\alpha'}\partial z_{\beta'}\ldots\partial z_{\gamma'}\partial z_{\mu'}}\mathrm{e}^{-\mathbf{z}^2/2}\right) \end{aligned} \tag{2.101}$$

Using (2.100) to rewrite the first term we arrive at another important identity

$$\frac{\partial H_{\alpha'\beta'\ldots\gamma'}}{\partial z_{\mu'}} = \delta_{\alpha'\mu'}H_{\beta'\ldots\gamma'} + \delta_{\beta'\mu'}H_{\alpha'\ldots\gamma'} + \cdots + \delta_{\gamma'\mu'}H_{\alpha'\beta'\ldots} \tag{2.102}$$

The derivative of $z_{\alpha'}$ is given by

$$\begin{aligned} \frac{\partial z_{\alpha'}}{\partial t} &= \frac{\partial A^{-1}_{\alpha'\beta'}}{\partial t}(\varphi_{\beta'} - \Phi_{\beta'}) - A^{-1}_{\alpha'\beta'}\frac{\partial \Phi_{\beta'}}{\partial t} \\ &= \frac{\partial A^{-1}_{\alpha'\beta'}}{\partial t}A_{\beta'\gamma'}z_{\gamma'} - A^{-1}_{\alpha'\beta'}\frac{\partial \Phi_{\beta'}}{\partial t} \end{aligned} \tag{2.103}$$

Therefore

$$\frac{\partial H_{\alpha'\beta'\ldots\nu'}}{\partial t} = \left(\delta_{\alpha'\mu'}H_{\beta'\ldots\nu'} + \delta_{\beta'\mu'}H_{\alpha'\ldots\nu'} + \cdots + \delta_{\nu'\mu'}H_{\alpha'\beta'\ldots}\right)\left(\frac{\partial A^{-1}_{\mu'\delta'}}{\partial t}A_{\delta'\nu'}z_{\nu'} - A^{-1}_{\mu'\delta'}\frac{\partial \Phi_{\delta'}}{\partial t}\right) \tag{2.104}$$

and

$$\frac{\partial \det\Sigma}{\partial t} = (\det\Sigma)\Sigma^{-1}_{\mu'\nu'}\frac{\partial \Sigma_{\nu'\mu'}}{\partial t} \tag{2.105}$$

2.B.2 Transport equation for the pdf

The probability density function evolves via the following transport equation

$$\frac{\partial P}{\partial t} + \frac{\partial}{\partial \varphi}\Big[uP\Big] = 0, \tag{2.106}$$

where the velocity field is defined in (2.2), reproduced here for convenience

$$u \equiv \frac{\mathrm{d}\varphi}{\mathrm{d}N} = -M_{\rm P}^2\frac{\partial \ln V(\varphi)}{\partial \varphi}, \tag{2.107}$$

where $\mathrm{d}N = H\mathrm{d}t$. Expanding u_i around the instantaneous centroid we get

$$\begin{aligned} u_{\alpha'} &= u_{\alpha'0} + u_{\alpha'\beta'}(\varphi_{\beta'} - \Phi_{\beta'}) + \frac{1}{2}u_{\alpha'\beta'\gamma'}(\varphi_{\beta'} - \Phi_{\beta'})(\varphi_{\gamma'} - \Phi_{\gamma'}) + \ldots \qquad (2.108)\\ &= u_{\alpha'0} + u_{\alpha'\beta'}A_{\beta'\gamma'}z_{\gamma'} + \frac{1}{2}u_{\alpha'\beta'\gamma'}A_{\beta'\delta'}A_{\gamma'\mu'}z_{\delta'}z_{\mu'}\\ &\quad + \frac{1}{3!}u_{\alpha'\beta'\gamma'\delta'}A_{\beta'\kappa'}A_{\gamma'\lambda'}A_{\delta'\rho'}z_{\kappa'}z_{\lambda'}z_{\rho'}\\ &\quad + \frac{1}{4!}u_{\alpha'\beta'\gamma'\delta'\mu'}A_{\beta'\kappa'}A_{\gamma'\lambda'}A_{\delta'\rho'}A_{\mu'\sigma'}z_{\kappa'}z_{\lambda'}z_{\rho'}z_{\sigma'} \qquad (2.109)\end{aligned}$$

To solve this equation, we will first calculate $\frac{\partial P}{\partial N}$ and then calculate $\frac{\partial}{\partial \varphi}[uP]$, by using the tools introduced in §2.B.1

2.B.3 Calculating $\frac{\partial P}{\partial t}$

By differentiating the probability density function, (2.88), with respect to time t we get

$$\begin{aligned}\frac{\partial P}{\partial t} &= \frac{\partial P_g}{\partial t}\left(1 + \frac{\alpha^z_{\alpha'\beta'\gamma'}}{3!}H_{\alpha'\beta'\gamma'} + \frac{\beta^z_{\alpha'\beta'\gamma'\delta'}}{4!}\right) + \frac{1}{3}\alpha^z_{\alpha'\beta'\gamma'}\frac{\partial H_{\alpha'\beta'\gamma'}}{\partial t} + \frac{1}{3!}\frac{\partial \alpha^z_{\alpha'\beta'\gamma'}}{\partial t}H_{\alpha'\beta'\gamma'}\\ &+ \frac{1}{4!}\frac{\partial \beta^z_{\alpha'\beta'\gamma'\delta'}}{\partial t}H_{\alpha'\beta'\gamma'\delta'} + \frac{1}{4!}\beta^z_{\alpha'\beta'\gamma'\delta'}\frac{\partial H_{\alpha'\beta'\gamma'\delta'}}{\partial t} \qquad (2.110)\end{aligned}$$

Using (2.105) and (2.103), the derivative of P_g can be written as

$$\frac{\partial P_g}{\partial t} = P_g\left[-\frac{1}{2}\Sigma^{-1}_{\mu'\nu'}\frac{\partial \Sigma_{\mu'\nu'}}{\partial t} - z_{\mu'}\left(\frac{\partial A^{-1}_{\mu'\nu'}}{\partial t}A_{\nu'\rho'}z_{\rho'} - A^{-1}_{\mu'\nu'}\frac{\partial \Phi_{\nu'}}{\partial t}\right)\right] \tag{2.111}$$

Substituting this into (2.110) and using (2.104) to rewrite the Hermite derivative terms gives

$$\begin{aligned}
\frac{\partial P}{\partial t} &= P_g\Bigg[-\frac{1}{2}\Sigma^{-1}_{\mu'\nu'}\frac{\partial \Sigma_{\mu'\nu'}}{\partial t}\left(1+\frac{\alpha^z_{\alpha'\beta'\gamma'}}{3!}H_{\alpha'\beta'\gamma'}+\frac{\beta^z_{\alpha'\beta'\gamma'\delta'}}{4!}H_{\alpha'\beta'\gamma'\delta'}\right)\\
&- z_{\mu'}\left(\frac{\partial A^{-1}_{\mu'\nu'}}{\partial t}A_{\nu'\rho'}z_{\rho'}-A^{-1}_{\mu'\nu'}\frac{\partial \Phi_{\nu'}}{\partial t}\right)\left(1+\frac{\alpha^z_{\alpha'\beta'\gamma'}}{3!}H_{\alpha'\beta'\gamma'}+\frac{\beta^z_{\alpha'\beta'\gamma'\delta'}}{4!}H_{\alpha'\beta'\gamma'\delta'}\right)\\
&+ \frac{1}{3!}\alpha^z_{\alpha'\beta'\gamma'}(\delta_{\alpha'\mu'}H_{\beta'\gamma'}+\delta_{\beta'\mu'}H_{\alpha'\gamma'}+\delta_{\gamma'\mu'}H_{\alpha'\beta'})\left(\frac{\partial A^{-1}_{\mu'\lambda'}}{\partial t}A_{\lambda'\rho'}z_{\rho'}-A^{-1}_{\mu'\lambda'}\frac{\partial \Phi_{\lambda'}}{\partial t}\right)\\
&+ \frac{1}{4!}\beta^z_{\alpha'\beta'\gamma'\delta'}(\delta_{\alpha'\mu'}H_{\beta'\gamma'\delta'}+\delta_{\beta'\mu'}H_{\alpha'\gamma'\delta'}+\delta_{\gamma'\mu'}H_{\alpha'\beta'\delta'}+\delta_{\delta'\mu'}H_{\alpha'\beta'\gamma'})\\
&\quad\left(\frac{\partial A^{-1}_{\mu'\lambda'}}{\partial t}A_{\lambda'\rho'}z_{\rho'}-A^{-1}_{\mu'\lambda'}\frac{\partial \Phi_{\lambda'}}{\partial t}\right)\\
&+ \frac{1}{3}\frac{\partial \alpha^z_{\alpha'\beta'\gamma'}}{\partial t}H_{\alpha'\beta'\gamma'}+\frac{1}{4!}\frac{\partial \beta^z_{\alpha'\beta'\gamma'\delta'}}{\partial t}H_{\alpha'\beta'\gamma'\delta'}\Bigg] \qquad (2.112)
\end{aligned}$$

We can use the property (2.100) to rewrite this solely in terms of Hermite polynomials. Doing this and cancelling some terms, the final expression for the evolution of the pdf is

$$\begin{aligned}
\frac{\partial P}{\partial t} &= P_g\Bigg[-\frac{1}{2}\Sigma^{-1}_{\mu'\nu'}\frac{\partial \Sigma_{\mu'\nu'}}{\partial t}\left(1+\frac{\alpha^z_{\alpha'\beta'\gamma'}}{3!}H_{\alpha'\beta'\gamma'}+\frac{\beta^z_{\alpha'\beta'\gamma'\delta'}}{4!}H_{\alpha'\beta'\gamma'\delta'}\right)\\
&- H_{\mu'\rho'}\frac{\partial A^{-1}_{\mu'\nu'}}{\partial t}A_{\nu'\rho'}-\frac{\partial A^{-1}_{\mu'\nu'}}{\partial t}A_{\nu'\mu'}+H_{\mu'}A^{-1}_{\mu'\nu'}\frac{\partial \Phi}{\partial t}+\frac{1}{4!}H_{\alpha'\beta'\gamma'\delta'}\frac{\partial \beta^z_{\alpha'\beta'\gamma'\delta'}}{\partial t}\\
&- \frac{\alpha^z_{\alpha'\beta'\gamma'}}{3!}\frac{\partial A^{-1}_{\mu'\nu'}}{\partial t}A_{\nu'\rho'}(H_{\alpha'\beta'\gamma'\mu'\rho'}+\delta_{\alpha'\rho'}H_{\beta'\gamma'\mu'}+\delta_{\beta'\rho'}H_{\alpha'\gamma'\mu'}+\delta_{\gamma'\rho'}H_{\alpha'\beta'\mu'}\\
&\quad+\delta_{\mu'\rho'}H_{\alpha'\beta'\gamma'})\\
&- \frac{\beta^z_{\alpha'\beta'\gamma'\delta'}}{4!}\frac{\partial A^{-1}_{\mu'\nu'}}{\partial t}A_{\nu'\rho'}(H_{\alpha'\beta'\gamma'\delta'\mu'\rho'}+\delta_{\alpha'\rho'}H_{\beta'\gamma'\delta'\mu'}+\delta_{\beta'\rho'}H_{\alpha'\gamma'\delta'\mu'}+\delta_{\gamma'\rho'}H_{\alpha'\beta'\delta'\mu'}\\
&+ \delta_{\delta'\rho'}H_{\alpha'\beta'\gamma'\mu'}+\delta_{\mu'\rho'}H_{\alpha'\beta'\gamma'\delta'})\\
&+ \frac{\alpha^z_{\alpha'\beta'\gamma'}}{3!}A^{-1}_{\mu'\nu'}\frac{\partial \Phi_{\nu'}}{\partial t}H_{\alpha'\beta'\gamma'\mu'}+\frac{\beta^z_{\alpha'\beta'\gamma'\delta'}}{4!}A^{-1}_{\mu'\nu'}\frac{\partial \Phi_{\nu'}}{\partial t}H_{\alpha'\beta'\gamma'\delta'\mu'}\\
&+ \frac{1}{3!}H_{\alpha'\beta'\gamma'}\frac{\partial \alpha^z_{\alpha'\beta'\gamma'}}{\partial t}\Bigg] \qquad (2.113)
\end{aligned}$$

2.B.4 Calculating $\frac{\partial}{\partial \varphi_{\alpha'}}(u_{\alpha'}P)$

The next step is to calculate the second term in (2.106), namely

$$\frac{\partial}{\partial \varphi_{\alpha'}}(u_{\alpha'}P)=\frac{\partial u_{\alpha'}}{\partial \varphi_{\alpha'}}P+u_{\alpha'}\frac{\partial P}{\partial \varphi_{\alpha'}} \qquad (2.114)$$

Differentiating both $u_{\alpha'}$ and P with respect to $\varphi_{\alpha'}$ we get

$$\begin{aligned}
\frac{\partial u_{\alpha'}}{\partial \varphi_{\alpha'}} &= u_{\alpha'\alpha'}+u_{\alpha'\alpha'\beta'}A_{\beta'\kappa'}z_{\kappa'}+\frac{1}{2!}u_{\alpha'\alpha'\beta'\gamma'}A_{\beta'\kappa'}A_{\gamma'\lambda'}z_{\kappa'}z_{\lambda'}\\
&\quad+\frac{1}{3!}u_{\alpha'\alpha'\beta'\gamma'\delta'}A_{\beta'\kappa'}A_{\gamma'\lambda'}A_{\delta'\rho'}z_{\kappa'}z_{\lambda'}z_{\rho'} \qquad (2.115)
\end{aligned}$$

$$\begin{aligned}\frac{\partial P}{\partial \varphi_{\alpha'}} &= P_g\Bigg[- z_{\tau'} A^{-1}_{\tau'\alpha'}\left(1 + \frac{\alpha^z_{\kappa'\lambda'\rho'}}{3!}H_{\kappa'\lambda'\rho'} + \frac{\beta^z_{\kappa'\lambda'\rho'\sigma'}}{4!}H_{\kappa'\lambda'\rho'\sigma'}\right)\\ &+ \frac{\alpha^z_{\kappa'\lambda'\rho'}}{3!}A^{-1}_{\tau'\alpha'}\left(\delta_{\tau'\kappa'}H_{\lambda'\rho'} + \delta_{\tau'\lambda'}H_{\kappa'\rho'} + \delta_{\tau'\rho'}H_{\kappa'\lambda'}\right)\\ &+ \frac{\beta^z_{\kappa'\lambda'\rho'\sigma'}}{4!}A^{-1}_{\tau'\alpha'}(\delta_{\tau'\kappa'}H_{\lambda'\rho'\sigma'} + \delta_{\tau'\lambda'}H_{\kappa'\rho'\sigma'} + \delta_{\tau'\rho'}H_{\kappa'\lambda'\sigma'}\\ &+ \delta_{\tau'\sigma'}H_{\kappa'\lambda'\rho'})\Bigg] \end{aligned} \tag{2.116}$$

where we have used the fact that $\partial z_{\tau'}/\partial\varphi_{\alpha'} = A^{-1}_{\tau'\alpha'}$. Using the identity (2.100) we can replace the $z_{\alpha'}$ using Hermite polynomials to give

$$\frac{\partial P}{\partial \varphi_{\alpha'}} = P_g\left[A^{-1}_{\tau'\alpha'}H_{\tau'} - \frac{\alpha^z_{\kappa'\lambda'\rho'}}{3!}A^{-1}_{\tau'\alpha'}H_{\kappa'\lambda'\rho'\tau'} - \frac{\beta^z_{\kappa'\lambda'\rho'\sigma'}}{4!}A^{-1}_{\tau'\alpha'}H_{\kappa'\lambda'\rho'\sigma'\tau'}\right] \tag{2.117}$$

We then need to multiplying this by $u_{\alpha'}$, replace all the $z_{\alpha'}$ using the trick (2.100) and adding on the $P\partial u_{\alpha'}/\partial\varphi_{\alpha'}$. Writing out the final contribution to $\frac{\partial}{\partial\varphi_{\alpha'}}(u_{\alpha'}P)$ in orders of $u_{\alpha'}$ we get

$$\mathrm{O}(u_{\alpha'0}) : -u_{\alpha'0}P_g\left(A^{-1}_{\tau'\alpha'}H_{\tau'} + \frac{\alpha^z_{\kappa'\lambda'\rho'}}{3!}A^{-1}_{\tau'\alpha'}H_{\kappa'\lambda'\rho'\tau'}\right) \tag{2.118}$$

$$\begin{aligned}\mathrm{O}(u_{\alpha'\beta'}) \;:\; & -u_{\alpha'\psi'}P_g\,(A_{\psi'\omega'}A^{-1}_{\tau'\alpha'}H_{\tau'\omega'} + \frac{\alpha^z_{\omega'\lambda'\rho'}}{2!}A_{\psi'\omega'}A^{-1}_{\tau'\alpha'}H_{\lambda'\rho'\tau'}\\ & + \frac{\beta^z_{\omega'\lambda'\rho'\sigma'}}{3!}A_{\psi'\omega'}A^{-1}_{\tau'\alpha'}H_{\lambda'\rho'\sigma'\tau'}) \end{aligned} \tag{2.119}$$

$$\begin{aligned}\mathrm{O}(u_{\alpha'\beta'\gamma'}) \;:\; & -\frac{1}{2}u_{\alpha'\psi'\phi'}P_g\,(A_{\psi'\omega'}A_{\phi'\chi'}A^{-1}_{\tau'\alpha'}H_{\tau'\omega'\chi'} + A_{\psi'\omega'}A_{\phi'\omega'}A^{-1}_{\tau'\alpha'}H_{\tau'} \qquad (2.120)\\ & + \alpha^z_{\omega'\lambda'\rho'}A_{\psi'\omega'}A_{\phi'\chi'}A^{-1}_{\tau'\alpha'}H_{\lambda'\rho'\tau'\chi'}\\ & + \alpha^z_{\omega'\chi'\rho'}A_{\psi'\omega'}A_{\phi'\chi'}A^{-1}_{\tau'\alpha'}H_{\rho'\tau'} + \frac{\alpha^z_{\kappa'\lambda'\rho'}}{3!}A_{\psi'\omega'}A_{\phi'\omega'}A^{-1}_{\tau'\alpha'}H_{\kappa'\lambda'\rho'\tau'}\\ & + \frac{\beta^z_{\omega'\chi'\rho'\sigma'}}{2!}A_{\psi'\omega'}A_{\phi'\chi'}A^{-1}_{\tau'\alpha'}H_{\rho'\sigma'\tau'}) \qquad (2.121)\end{aligned}$$

$$\begin{aligned}\mathrm{O}(u_{\alpha'\beta'\gamma'\delta'}) \;:\; & -\frac{1}{3!}u_{\alpha'\psi'\phi'\theta'}P_g\,(A_{\psi'\omega'}A_{\phi'\chi'}A_{\theta'\zeta'}A^{-1}_{\tau'\alpha'}H_{\tau'\omega'\chi'\zeta'} + 3A_{\psi'\omega'}A_{\phi'\omega'}A_{\theta'\zeta'}A^{-1}_{\tau'\alpha'}H_{\tau'\zeta'}\\ & + \frac{3}{2}\alpha^z_{\omega'\lambda'\rho'}A_{\psi'\omega'}A_{\phi'\chi'}A_{\theta'\chi'}A^{-1}_{\tau'\alpha'}H_{\lambda'\rho'\tau'}\\ & + 3\alpha^z_{\omega'\chi'\rho'}A_{\psi'\omega'}A_{\phi'\chi'}A_{\theta'\zeta'}A^{-1}_{\tau'\alpha'}H_{\rho'\tau'\zeta'} + \alpha^z_{\omega'\chi'\zeta'}A_{\psi'\omega'}A_{\phi'\chi'}A_{\theta'\zeta'}A^{-1}_{\tau'\alpha'}H_{\tau'}\\ & + \frac{\beta^z_{\omega'\lambda'\rho'\sigma'}}{2!}A_{\psi'\omega'}A_{\phi'\chi'}A_{\theta'\chi'}A^{-1}_{\tau'\alpha'}H_{\lambda'\rho'\sigma'\tau'} \qquad (2.122)\\ & + 3\frac{\beta^z_{\omega'\chi'\rho'\sigma'}}{2!}A_{a\omega'}A_{\phi'\chi'}A_{\theta'\zeta'}A^{-1}_{\tau'\alpha'}H_{\rho'\sigma'\tau'\zeta'}\\ & + \beta^z_{\omega'\chi'\zeta'\sigma'}A_{\psi'\omega'}A_{\phi'\chi'}A_{\theta'\zeta'}A^{-1}_{\tau'\alpha'}H_{\sigma'\tau'}) \qquad (2.123)\end{aligned}$$

where we have reduced the equations to Hermites of rank $\leqslant 4$. Using these equations and the result for the evolution of the pdf (2.113) we can extract the moment hierarchy order by order. The first order terms gives the evolution of the centroid

$$\frac{\partial \Phi_{\alpha'}}{\partial t} = u_{\alpha' 0} + \frac{1}{2!} u_{\alpha'\psi'\phi'} \Sigma_{\psi'\phi'} + \frac{1}{3!} u_{\alpha'\psi'\phi'\theta'} \alpha_{\psi'\phi'\theta'}. \tag{2.124}$$

The second order equation gives a transport equation for the two-point function

$$\begin{aligned} \frac{\partial \Sigma_{\kappa'\rho'}}{\partial t} &= u_{\kappa'\psi'} \Sigma_{\psi'\lambda'} + u_{\lambda'\psi'} \Sigma_{\psi'\kappa'} + \frac{1}{2} u_{\kappa'\psi'\phi'} \alpha_{\lambda'\psi'\phi'} + \frac{1}{2} u_{\lambda'\psi'\phi'} \alpha_{\kappa'\psi'\phi'} \\ &+ \frac{1}{2} u_{\kappa'\psi'\phi'\theta'} \Sigma_{\psi'\phi'} \Sigma_{\lambda'\theta'} + \frac{1}{2} u_{\lambda'\psi'\phi'\theta'} \Sigma_{\psi'\phi'} \Sigma_{\kappa'\theta'} \\ &+ \frac{1}{3!} u_{\kappa'\psi'\phi'\theta'} \beta_{\lambda'\psi'\phi'\theta'} + \frac{1}{3!} u_{\lambda'\psi'\phi'\theta'} \beta_{\kappa'\psi'\phi'\theta'}. \end{aligned} \tag{2.125}$$

The transport equation for the three-point function is

$$\begin{aligned} \frac{\partial \alpha_{\xi'\eta'\epsilon'}}{\partial t} &= u_{\xi'\psi'} \alpha_{\eta'\epsilon'\psi'} + \text{cyclic} \\ &+ u_{\xi'\psi'\phi'} \Sigma_{\psi'\eta'} \Sigma_{\phi'\epsilon'} + \text{cyclic} \\ &+ \frac{1}{2} u_{\xi'\psi'\phi'\theta'} \alpha_{\eta'\epsilon'\psi'} \Sigma_{\phi'\theta'} + \text{cyclic} \\ &+ \frac{1}{2} u_{d\psi'\phi'\theta'} \alpha_{\eta'\psi'\phi'} \Sigma_{\epsilon'\theta'} + \text{cyclic}. \end{aligned} \tag{2.126}$$

Finally, the new result that we have derived here using the Gauss–Hermite expansion method is the transport equation for the trispectrum

$$\begin{aligned} \frac{\partial \beta_{\xi'\eta'\epsilon'\pi'}}{\partial t} &= u_{\xi'\psi'} \beta_{\eta'\epsilon'\pi'\psi'} + \text{cyclic} \\ &+ u_{\xi'\psi'\phi'} \alpha_{\psi'\eta'\epsilon'} \Sigma_{\phi'\pi'} + \text{cyclic} \\ &+ u_{\xi'\psi'\phi'\theta'} \Sigma_{\psi'\eta'} \Sigma_{\phi'\epsilon'} \Sigma_{\theta'\pi'} + \text{cyclic}. \end{aligned} \tag{2.127}$$

We have checked that these equations match the results derived using the geometrical optics approach described in Seery, Mulryne et al. (2012).

REFERENCES

[1] Laila Alabidi and David H. Lyth. 'Inflation models and observation'. In: *JCAP* 0605 (2006), p. 016. arXiv: astro-ph/0510441 [astro-ph] (cit. on p. 104).

[2] L. Amendola. 'Non Gaussian likelihood function and COBE data'. In: *Mon.Not.Roy.Astron.Soc.* 283 (1996), pp. 983–989 (cit. on p. 131).

[3] Luca Amendola. 'The dependence of cosmological parameters estimated from the microwave background on non-gaussianity'. In: *Astrophys.J.* 569 (2002), pp. 595–599. arXiv: astro-ph/0107527 [astro-ph] (cit. on p. 131).

[4] M Andrews. 'Evolution of moments over quantum wavepackets or classical clusters'. In: *Journal of Physics A* 18 (1985), p. 37 (cit. on p. 108).

[5] Valentin Assassi, Daniel Baumann and Daniel Green. 'On Soft Limits of Inflationary Correlation Functions'. In: (2012). arXiv: 1204.4207 [hep-th] (cit. on pp. 104, 125).

[6] LE Ballentine. 'Moment equations for probability distributions in classical and quantum mechanics'. In: *Physical Review A* 58 (1998), pp. 1799–1809 (cit. on p. 108).

[7] Lotfi Boubekeur and David.H. Lyth. 'Detecting a small perturbation through its non-Gaussianity'. In: *Phys.Rev.* D73 (2006), p. 021301. arXiv: astro-ph/0504046 [astro-ph] (cit. on pp. 104, 108).

[8] F.R. Bouchet. 'Introductory overview of Eulerian and Lagrangian perturbation theories'. In: (1995). arXiv: astro-ph/9603013 [astro-ph] (cit. on p. 131).

[9] F.R. Bouchet and R. Juszkiewicz. 'Perturbation theory confronts observations: Implications for the 'initial' conditions and omega'. In: (1993). arXiv: astro-ph/9312007 [astro-ph] (cit. on p. 131).

[10] Christian T. Byrnes, Ki-Young Choi and Lisa M.H. Hall. 'Conditions for large non-Gaussianity in two-field slow-roll inflation'. In: *JCAP* 0810 (2008), p. 008. arXiv: 0807.1101 [astro-ph] (cit. on p. 125).

[11] Christian T. Byrnes, Misao Sasaki and David Wands. 'The primordial trispectrum from inflation'. In: *Phys.Rev.* D74 (2006), p. 123519. arXiv: astro-ph/0611075 [astro-ph] (cit. on pp. 104, 112, 117).

[12] C. DeWitt-Morette. 'The Semiclassical Expansion'. In: *Annals Phys.* 97 (1976), pp. 367–399 (cit. on p. 104).

[13] C. DeWitt-Morette and T.R. Zhang. 'PATH INTEGRALS AND CONSERVATION LAWS'. In: *Phys.Rev.* D28 (1983), pp. 2503–2516 (cit. on p. 104).

[14] C. DeWitt-Morette, T.R. Zhang and B. Nelson. 'CAUSTIC PROBLEMS IN QUANTUM MECHANICS WITH APPLICATIONS TO SCATTERING THEORY'. In: *Phys.Rev.* D28 (1983), pp. 2526–2546 (cit. on p. 104).

[15] Mafalda Dias, Jonathan Frazer and Andrew R. Liddle. 'Multifield consequences for D-brane inflation'. In: (2012). arXiv: 1203.3792 [astro-ph.CO] (cit. on pp. 106, 111, 119, 124, 128).

[16] Mafalda Dias and David Seery. 'Transport equations for the inflationary spectral index'. In: *Phys.Rev.* D85 (2012), p. 043519. arXiv: 1111.6544 [astro-ph.CO] (cit. on pp. 111, 128).

[17] Joseph Elliston, Laila Alabidi et al. 'Large trispectrum in two-field slow-roll inflation'. In: (2012). arXiv: 1203.6844 [astro-ph.CO] (cit. on p. 125).

[18] Joseph Elliston et al. 'Evolution of non-Gaussianity in multi-scalar field models'. In: *Int.J.Mod.Phys.* A26 (2011), pp. 3821–3832. arXiv: 1107.2270 [astro-ph.CO] (cit. on p. 125).

[19] Joseph Elliston et al. 'Evolution of $f_{\rm NL}$ to the adiabatic limit'. In: *JCAP* 1111 (2011), p. 005. arXiv: 1106.2153 [astro-ph.CO] (cit. on p. 125).

[20] P. Fosalba, E. Gaztanaga and E. Elizalde. 'Gravitational evolution of the large scale density distribution: the edgeworth & gamma expansions'. In: (1999). arXiv: astro-ph/9910308 [astro-ph] (cit. on p. 131).

[21] Juan Garcia-Bellido and David Wands. 'Metric perturbations in two field inflation'. In: *Phys.Rev.* D53 (1996), pp. 5437–5445. arXiv: astro-ph/9511029 [astro-ph] (cit. on p. 118).

[22] S.W. Hawking and G.F.R. Ellis. *The Large scale structure of space-time*. Cambridge University Press, 1973 (cit. on p. 104).

[23] Klaus Hepp. 'The classical limit for quantum mechanical correlation functions'. In: *Communications in Mathematical Physics* 35.4 (Dec. 1974), pp. 265–277 (cit. on p. 108).

[24] Ian Huston and Adam J. Christopherson. 'Calculating Non-adiabatic Pressure Perturbations during Multi-field Inflation'. In: *Phys.Rev.* D85 (2012), p. 063507. arXiv: 1111.6919 [astro-ph.CO] (cit. on p. 125).

[25] Ian Huston and Karim A. Malik. 'Second Order Perturbations During Inflation Beyond Slow-roll'. In: *JCAP* 1110 (2011), p. 029. arXiv: 1103.0912 [astro-ph.CO] (cit. on p. 110).

[26] C. J. Jacobi. In: *Journal für die reine und angewandte Mathematik* 17 (1837), pp. 68–82 (cit. on p. 104).

[27] Philip R. Jarnhus and Martin S. Sloth. 'de Sitter limit of inflation and nonlinear perturbation theory'. In: *JCAP* 0802 (2008), p. 013. arXiv: 0709.2708 [hep-th] (cit. on pp. 109, 114).

[28] Roman Juszkiewicz et al. 'Weakly nonlinear Gaussian fluctuations and the Edgeworth expansion'. In: *Astrophys.J.* 442 (1995), p. 39 (cit. on p. 131).

[29] Soo A. Kim, Andrew R. Liddle and David Seery. 'Non-gaussianity in axion Nflation models'. In: *Phys.Rev.Lett.* 105 (2010), p. 181302. arXiv: 1005.4410 [astro-ph.CO] (cit. on pp. 125, 126).

[30] Komatsu and Spergel. 'Acoustic signatures in the primary microwave background bispectrum'. In: *Phys.Rev.* D63 (2001), p. 063002. arXiv: astro-ph/0005036 [astro-ph] (cit. on p. 103).

[31] Tsz Yan Lam and Ravi K. Sheth. 'Halo abundances in the f_{NL} model'. In: *Mon.Not.Roy.Astron.Soc.* 398 (2009), pp. 2143–2151. arXiv: 0905.1702 [astro-ph.CO] (cit. on p. 131).

[32] Antony Lewis. 'The full squeezed CMB bispectrum from inflation'. In: (2012). arXiv: 1204.5018 [astro-ph.CO] (cit. on p. 104).

[33] Antony Lewis and Anthony Challinor. 'Weak gravitational lensing of the CMB'. In: *Phys.Rept.* 429 (2006), pp. 1–65. arXiv: astro-ph/0601594 [astro-ph] (cit. on p. 104).

[34] Marilena LoVerde et al. 'Effects of Scale-Dependent Non-Gaussianity on Cosmological Structures'. In: *JCAP* 0804 (2008), p. 014. arXiv: 0711.4126 [astro-ph] (cit. on p. 131).

[35] David H. Lyth and Yeinzon Rodriguez. 'The Inflationary prediction for primordial non-Gaussianity'. In: *Phys.Rev.Lett.* 95 (2005), p. 121302. arXiv: astro-ph/0504045 [astro-ph] (cit. on pp. 103, 104, 113, 115, 129).

[36] David H. Lyth and David Seery. 'Classicality of the primordial perturbations'. In: *Phys.Lett.* B662 (2008), pp. 309–313. arXiv: astro-ph/0607647 [astro-ph] (cit. on p. 108).

[37] David H. Lyth and Ignacio Zaballa. 'A Bound concerning primordial non-Gaussianity'. In: *JCAP* 0510 (2005), p. 005. arXiv: astro-ph/0507608 [astro-ph] (cit. on pp. 111, 129).

[38] Juan Martin Maldacena. 'Non-Gaussian features of primordial fluctuations in single field inflationary models'. In: *JHEP* 05 (2003), p. 013. arXiv: astro-ph/0210603 (cit. on pp. 103, 118).

[39] Karim A. Malik and David Wands. 'Cosmological perturbations'. In: *Phys.Rept.* 475 (2009), pp. 1–51. arXiv: 0809.4944 [astro-ph] (cit. on p. 118).

[40] Sabino Matarrese, Licia Verde and Raul Jimenez. 'The Abundance of high-redshift objects as a probe of non-Gaussian initial conditions'. In: *Astrophys.J.* 541 (2000), p. 10. arXiv: astro-ph/0001366 [astro-ph] (cit. on p. 131).

[41] Anupam Mazumdar and Lingfei Wang. 'Separable and non-separable multi-field inflation and large non-Gaussianity'. In: (2012). arXiv: 1203.3558 [astro-ph.CO] (cit. on p. 123).

[42] David J. Mulryne, David Seery and Daniel Wesley. 'Moment transport equations for non-Gaussianity'. In: *JCAP* 1001 (2010), p. 024. arXiv: 0909.2256 [astro-ph.CO] (cit. on pp. 105, 106, 109, 118, 119, 131).

[43] David J. Mulryne, David Seery and Daniel Wesley. 'Moment transport equations for the primordial curvature perturbation'. In: *JCAP* 1104 (2011). * Temporary entry *, p. 030. arXiv: 1008.3159 [astro-ph.CO] (cit. on pp. 105, 106, 109, 131).

[44] David Mulryne, Stefano Orani and Arttu Rajantie. 'Non-Gaussianity from the hybrid potential'. In: *Phys.Rev.* D84 (2011). 9 pages, 7 figures, p. 123527. arXiv: 1107.4739 [hep-th] (cit. on p. 126).

[45] Sebastien Renaux-Petel. 'Combined local and equilateral non-Gaussianities from multi-field DBI inflation'. In: *JCAP* 0910 (2009), p. 012. arXiv: 0907.2476 [hep-th] (cit. on p. 113).

[46] Misao Sasaki and Ewan D. Stewart. 'A General analytic formula for the spectral index of the density perturbations produced during inflation'. In: *Prog.Theor.Phys.* 95 (1996), pp. 71–78. arXiv: astro-ph/9507001 [astro-ph] (cit. on pp. 103, 104).

[47] Misao Sasaki, Jussi Väliviita and David Wands. 'Non-Gaussianity of the primordial perturbation in the curvaton model'. In: *Phys.Rev.* D74 (2006), p. 103003. arXiv: astro-ph/0607627 [astro-ph] (cit. on pp. 103, 104).

[48] David Seery. 'Infrared effects in inflationary correlation functions'. In: *Class.Quant.Grav.* 27 (2010), p. 124005. arXiv: 1005.1649 [astro-ph.CO] (cit. on p. 108).

[49] David Seery and J. Carlos Hidalgo. 'Non-Gaussian corrections to the probability distribution of the curvature perturbation from inflation'. In: *JCAP* 0607 (2006), p. 008. arXiv: astro-ph/0604579 [astro-ph] (cit. on p. 131).

[50] David Seery and James E. Lidsey. 'Primordial non-gaussianities from multiple-field inflation'. In: *JCAP* 0509 (2005), p. 011. arXiv: astro-ph/0506056 (cit. on pp. 103, 111, 130).

[51] David Seery and James E. Lidsey. 'Non-Gaussianity from the inflationary trispectrum'. In: *JCAP* 0701 (2007), p. 008. arXiv: astro-ph/0611034 [astro-ph] (cit. on pp. 103, 104).

[52] David Seery, James E. Lidsey and Martin S. Sloth. 'The inflationary trispectrum'. In: *JCAP* 0701 (2007), p. 027. arXiv: astro-ph/0610210 [astro-ph] (cit. on pp. 103, 115, 117, 129).

[53] David Seery, David J. Mulryne et al. 'Inflationary perturbation theory is geometrical optics in phase space'. In: (2012). arXiv: 1203.2635 [astro-ph.CO] (cit. on pp. 104–107, 109, 111, 113, 117, 118, 122, 123, 128, 137).

[54] David Seery, Martin S. Sloth and Filippo Vernizzi. 'Inflationary trispectrum from graviton exchange'. In: *JCAP* 0903 (2009), p. 018. arXiv: 0811.3934 [astro-ph] (cit. on pp. 103, 115, 129).

[55] Joseph Smidt et al. 'CMB Constraints on Primordial non-Gaussianity from the Bispectrum (f_{NL}) and Trispectrum (g_{NL} and τ_{NL}) and a New Consistency Test of Single-Field Inflation'. In: *Phys.Rev.* D81 (2010), p. 123007. arXiv: 1004.1409 [astro-ph.CO] (cit. on p. 124).

[56] Kendrick M. Smith, Marilena LoVerde and Matias Zaldarriaga. 'A universal bound on N-point correlations from inflation'. In: *Phys.Rev.Lett.* 107 (2011), p. 191301. arXiv: 1108.1805 [astro-ph.CO] (cit. on pp. 104, 124).

[57] Alexei A. Starobinsky. 'Multicomponent de Sitter (Inflationary) Stages and the Generation of Perturbations'. In: *JETP Lett.* 42 (1985), pp. 152–155 (cit. on pp. 103, 104).

[58] Teruaki Suyama and Masahide Yamaguchi. 'Non-Gaussianity in the modulated reheating scenario'. In: *Phys.Rev.* D77 (2008), p. 023505. arXiv: 0709.2545 [astro-ph] (cit. on pp. 104, 124).

[59] Andrew Taylor and Peter Watts. 'Evolution of the cosmological density distribution function'. In: (2000). arXiv: astro-ph/0001118 [astro-ph] (cit. on p. 131).

[60] Licia Verde et al. 'Large scale structure, the cosmic microwave background, and primordial non-gaussianity'. In: *Mon.Not.Roy.Astron.Soc.* 313 (2000), pp. L141–L147. arXiv: astro-ph/9906301 [astro-ph] (cit. on p. 103).

[61] Filippo Vernizzi and David Wands. 'Non-gaussianities in two-field inflation'. In: *JCAP* 0605 (2006), p. 019. arXiv: astro-ph/0603799 [astro-ph] (cit. on pp. 111, 118, 129).

[62] Matt Visser. 'van Vleck determinants: Geodesic focusing and defocusing in Lorentzian space-times'. In: *Phys.Rev.* D47 (1993), pp. 2395–2402. arXiv: hep-th/9303020 [hep-th] (cit. on p. 104).

[63] Peter Watts and Peter Coles. 'Statistical cosmology with quadratic density fields'. In: *Mon.Not.Roy.Astron.Soc.* 338 (2003), p. 806. arXiv: astro-ph/0208295 [astro-ph] (cit. on p. 131).

[64] Shuichiro Yokoyama, Teruaki Suyama and Takahiro Tanaka. 'Primordial Non-Gaussianity in Multi-Scalar Slow-Roll Inflation'. In: *JCAP* 0707 (2007), p. 013. arXiv: 0705.3178 [astro-ph] (cit. on pp. 105, 122, 123).

[65] Shuichiro Yokoyama, Teruaki Suyama and Takahiro Tanaka. 'Primordial Non-Gaussianity in Multi-Scalar Inflation'. In: *Phys.Rev.* D77 (2008), p. 083511. arXiv: 0711.2920 [astro-ph] (cit. on pp. 105, 122, 123).

[66] Shuichiro Yokoyama, Teruaki Suyama and Takahiro Tanaka. 'Efficient diagrammatic computation method for higher order correlation functions of local type primordial curvature perturbations'. In: *JCAP* 0902 (2009), p. 012. arXiv: 0810.3053 [astro-ph] (cit. on p. 122).

Conclusion

2.3 Summary of this work

There are many models of inflation in the literature, each involving their own set of interactions and predictions. Our goal is to use the inflationary signatures observed in the CMB to distinguish between them, with the ultimate goal of understanding the microphysics behind inflation. The signatures correspond to a handful of statistical observables, most recently measured to a high degree of precision by the *Planck* satellite.

In order to test these models in a systematic way and discriminate between them requires substantial effort on the interface of theory and observation. This is where the work in this thesis makes its contribution. With such a large number of existing inflationary models and more appearing every day, it is imperative that we have efficient ways of computing their observable predictions and find ways to utilize the data as effectively as possible. This task of constraining models is still very a much a "work-in-progress", making it a very exciting time for early universe cosmology. The goal of the work presented in this thesis has been to develop efficient methods to constrain models of inflation using non-Gaussian observables. Here we will list the key outcomes for each of the papers.

Optimal bispectrum constraints on single-field models of inflation.— In the first part of this thesis we obtained optimal constraints on the parameter space of single-field inflation using WMAP9 bispectrum data. We performed a partial-wave decomposition of the CMB bispectrum data, then used this to construct a maximum likelihood estimate for the mass parameters that characterize the amplitude of particular interactions in the most general single-field model, given by the effective field theory for inflation. This is the first time this systematic approach has been used and it offers many benefits over more traditional methods for constraining models. For example, it is common for the amplitude of non-Gaussianity to be quoted only for a handful of templates, leaving vast regions of the data effectively unexplored. The partial-wave method uses a large number of shape configurations and therefore enables us to explore these regions. Moreover, by considering the

most general single-field Lagrangian compatible with the underlying inflationary spacetime in our analysis, we were able to probe a very large region of inflationary parameter space. Specifically, not restricting ourselves to a particular model meant that we could remain entirely agnostic to the physical mechanism that may have generated the perturbations. The only assumption is that a single scalar degree of freedom was active during inflation. The key difference with this approach over more common methods is that we are working *backwards* from the data and asking the question "*what is the most likely combination of mass parameters given the data?*". Therefore we are using the data to directly probe the dynamics of inflation. Our results can be summarized as follows:

- We found that there was no significant non-Gaussianity in the regions probed by the effective field theory Lagrangian. Constraints still allow for these terms to generate some non-Gaussian signal, however the consistency with zero suggests that higher-order derivative terms may not have played an important role in the generation of the perturbations during inflation.

- Degeneracies amongst the bispectrum shapes generated from the EFT operators meant that only 4 linear combinations of the original 11 shapes could be constrained. These are the principal components, which are effectively the shapes that are 'chosen' by the data. This implies that we are only able to use the data to constrain models of inflation with up to four mass parameters.

- As examples, we have provided the most accurate constraints on DBI inflation and Ghost inflation using the WMAP9 dataset.

- We also conducted a Bayesian model comparison, finding that models with a larger number of mass parameters appear to be disfavoured by the data.

Though it won't change our conclusions a great deal, we will be able to achieve marginally better constraints using *Planck* data. The full release is expected in the Summer. We aim to use our pipeline to constrain inflation in a similar fashion when the underlying theory is thought to be described by a Galileon model. The EFT Lagrangian we used in this paper does not incorporate models with sharp features. Therefore including these models in our analysis would be an obvious extension to this work.

TRANSPORT EQUATIONS FOR THE INFLATIONARY TRISPECTRUM.— Many of the high-energy physics inspired models of inflation involve multiple scalar fields that can predict a large non-Gaussianity in some cases. Therefore it is crucial that we have efficient ways of computing the non-Gaussian

prediction for these models in order to confront them with the observed constraints. The transport formalism provides a numerically efficient method to track the superhorizon evolution of the correlation functions to the adiabatic limit, where they take on a constant value. In the second part of this thesis we extended the transport formalism to compute the local trispectrum non-linearity parameters. The main conclusions of the paper are:

- We derived a transport equation for the four-point function of the field perturbations using a Gauss–Hermite expansion approach.
- This transport equation was separated into separate evolution equations for the "squeezed" and "collapsed" trispectrum configurations.
- The transport method was compared with other approaches in the literature and we demonstrated their equivalence.
- We then perform a gauge transformation from the field perturbations to the curvature perturbation in order to find expressions for $\tau_{\rm NL}$ and $g_{\rm NL}$, the local non-linearity parameters for the trispectrum.

Though the constraints on the trispectrum are currently weak, it is still an observable that may help break the degeneracies between models, especially in the future with more data arriving from LSS surveys. With very few observables, it is important that we consider all possible ways to place constraints on the inflationary epoch.

The transport approach has been extended a great deal and now is able to compute many of the inflationary observables for a wide variety of models. Work is ongoing at Sussex to provide a complete "toolbox" to calculate the observables for a given model of inflation.

2.4 OUTLOOK FOR THE FUTURE

With the recent hint of a "smoking gun" detection of primordial B-modes in the CMB polarization, inflation has prevailed as the leading candidate for the origin of structure in the Universe. No other theory has come close to providing such a successful mechanism to generate the primordial curvature perturbation ζ.

From a theoretical perspective, a successful inflationary model would be one that is embedded within a UV complete theory, such as string theory. There is currently a huge theoretical effort

underway to create new models of this sort that produce signatures that are consistent with observations. Finding such models presents one of the key outstanding challenges in inflationary cosmology.

With upcoming LSS surveys providing us with even more observational data, it will be important to find even more systematic ways to constrain the plethora of inflationary models in order to probe the physics of the very early Universe.